AN INVESTIGATION OF HELICOPTER TRANSMISSION NOISE REDUCTION BY VIBRATION ABSORBERS AND DAMPING

H. Sternfeld, et al

Boeing Company

Prepared for:

Army Air Mobility Research and Development Laboratory

August 1972

AD

USAAMRDL TECHNICAL REPORT 72-34

INVESTIGATION OF HELICOPTER TRANSMISSION NOISE REDUCTION BY VIBRATION ABSORBERS AND DAMPING

By

H. Sternfeld

J. Schairer

R. Spencer

August 1972

EUSTIS DIRECTORATE

U. S. ARMY AIR MOBILITY RESEARCH AND DEVELOPMENT LABORATORY

FORT EUSTIS, VIRGINIA

CONTRACT DAAJ02-71-C-0020

THE BOEING COMPANY, VERTOL DIVISION

PHILADELPHIA, PENNSYLVANIA

DISCLAIMERS

The findings in this report are not to be construed as an official Department of the Army position unless so designated by other authorized documents.

When Government drawings, specifications, or other data are used for any purpose other than in connection with a definitely related Government procurement operation, the United States Government thereby incurs no responsibility nor any obligation whatsoever; and the fact that the Government may have formulated, furnished, or in any way supplied the said drawings, specifications, or other data is not to be regarded by implication or otherwise as in any manner licensing the holder or any other person or corporation, or conveying any rights or permission, to manufacture, use, or sell any patented invention that may in any way be related thereto.

Trade names cited in this report do not constitute an official endorsement or approval of the use of such commercial hardware or software.

DISPOSITION INSTRUCTIONS

Destroy this report when no longer needed. Do not return it to the originator.

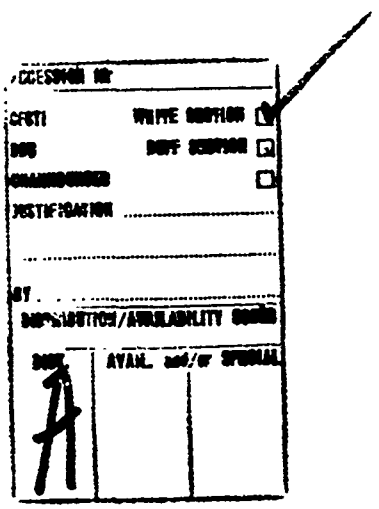

DEPARTMENT OF THE ARMY
U. S. ARMY AIR MOBILITY RESEARCH & DEVELOPMENT LABORATORY
EUSTIS DIRECTORATE
FORT EUSTIS, VIRGINIA 23604

The research described herein was conducted by the Boeing Company, Vertol Division, under the terms of Contract DAAJ02-71-C-0020. The work was performed under the technical management of Mr. E. R. Givens, Propulsion Division, Eustis Directorate, U.S. Army Air Mobility Research and Development Laboratory.

This report presents a part of a continuing effort to understand and ultimately control the noise produced by helicopter transmissions. The objective of this effort was to determine through design studies and tests the relative effectiveness of different methods of noise attenuation as they apply to the CH-47 helicopter forward transmission noise.

Appropriate technical personnel of this Division have reviewed this report and concur with the conclusions contained herein.

I-C

Project 1F162204A142
Contract DAAJ02-71-C-0020
USAAMRDL Technical Report 72-34
August 1972

AN INVESTIGATION OF HELICOPTER TRANSMISSION NOISE REDUCTION BY VIBRATION ABSORBERS AND DAMPING

Final Report

Prepared by

H. Sternfeld
J. Schairer
R. Spencer

The Boeing Company, Vertol Division
Philadelphia, Pennsylvania

for

EUSTIS DIRECTORATE
U. S. ARMY AIR MOBILITY RESEARCH AND DEVELOPMENT LABORATORY
FORT EUSTIS, VIRGINIA

I-D

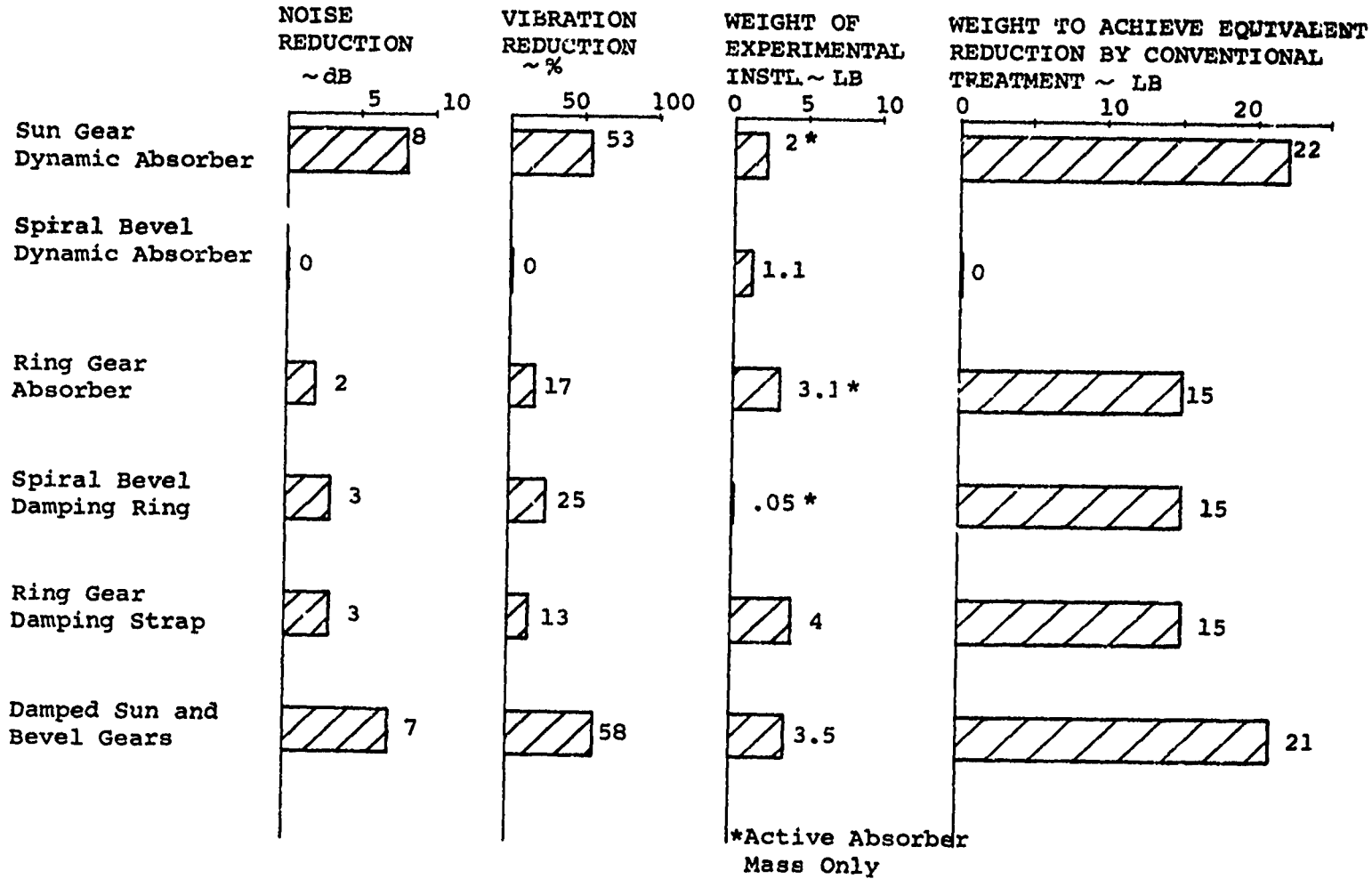

Figure 1. Summary of Test Results.

Unclassified

Security Classification

DOCUMENT CONTROL DATA - R & D

(Security classification of title, body of abstract and indexing annotation must be entered when the overall report is classified)

1. ORIGINATING ACTIVITY *(Corporate author)*
The Boeing Company, Vertol Division
Philadelphia, Pennsylvania

2a. REPORT SECURITY CLASSIFICATION
Unclassified

2b. GROUP

3. REPORT TITLE
AN INVESTIGATION OF HELICOPTER TRANSMISSION NOISE REDUCTION BY VIBRATION ABSORBERS AND DAMPING

4. DESCRIPTIVE NOTES *(Type of report and inclusive dates)*
Final Report

5. AUTHOR(S) *(First name, middle initial, last name)*
H. Sternfeld
J. Schairer
R. Spencer

6. REPORT DATE	7a. TOTAL NO. OF PAGES	7b. NO. OF REFS
August 1972	~~169~~ 171	10

8a. CONTRACT OR GRANT NO.	9a. ORIGINATOR'S REPORT NUMBER(S)
DAAJ02-71-C-0020	USAAMRDL Technical Report 72-34
b. PROJECT NO. 1F162204A142	
c.	9b. OTHER REPORT NO(S) *(Any other numbers that may be assigned this report)*
d.	

10. DISTRIBUTION STATEMENT
Approved for public release; distribution unlimited.

Details of illustrations in this document may be better studied on microfiche.

11. SUPPLEMENTARY NOTES	12. SPONSORING MILITARY ACTIVITY
	Eustis Directorate U.S. Army Air Mobility R&D Laboratory Fort Eustis, Virginia

13. ABSTRACT

A test program was conducted to evaluate the effect of dynamic absorbers and damping on the noise generated by a CH-47 rotor transmission. Comparison was made between predicted and measured results, and a method for comparing the efficiency of various methods of transmission noise reduction was developed.

Figure 1 summarizes the measured reduction in gear case vibration and radiated noise along with a comparison of the weight of each device and the weight required to achieve a similar reduction by conventional airframe acoustical treatment. Figure 2 illustrates the effect of the sun gear absorber.

Lack of similar effects in the spiral bevel system is attributed to the axial components of the tooth contact loads which may have been relatively unaffected by the torsional absorbers.

It was found that the fundamental gear mesh frequencies were accompanied by very strong sidebands due to planetary gear passage. Since the planet system was not treated, this limited the noise reduction that could be realized.

Gear damping was achieved by filling the gear shafts with Viton, and by a ring of Viton on the spiral bevel ring gear. Constrained layer damping was also used on the outside of the planetary ring gear.

Each of the above methods provided some noise reduction; however, none of them provided a large enough general reduction to be immediately applicable for use on aircraft in flight. It is felt that more work is required with any of these methods combined with a program to define case vibration and radiation before they can become effective helicopter noise-reduction techniques.

DD FORM 1 NOV 68 1473 REPLACES DD FORM 1473, 1 JAN 64, WHICH IS OBSOLETE FOR ARMY USE.

IA

Unclassified

Security Classification

Unclassified
Security Classification

14. KEY WORDS	LINK A		LINK B		LINK C	
	ROLE	WT	ROLE	WT	ROLE	WT
Transmission Noise Reduction Vibration Absorbers Gear Damping						

I-B

9163-72

Unclassified
Security Classification

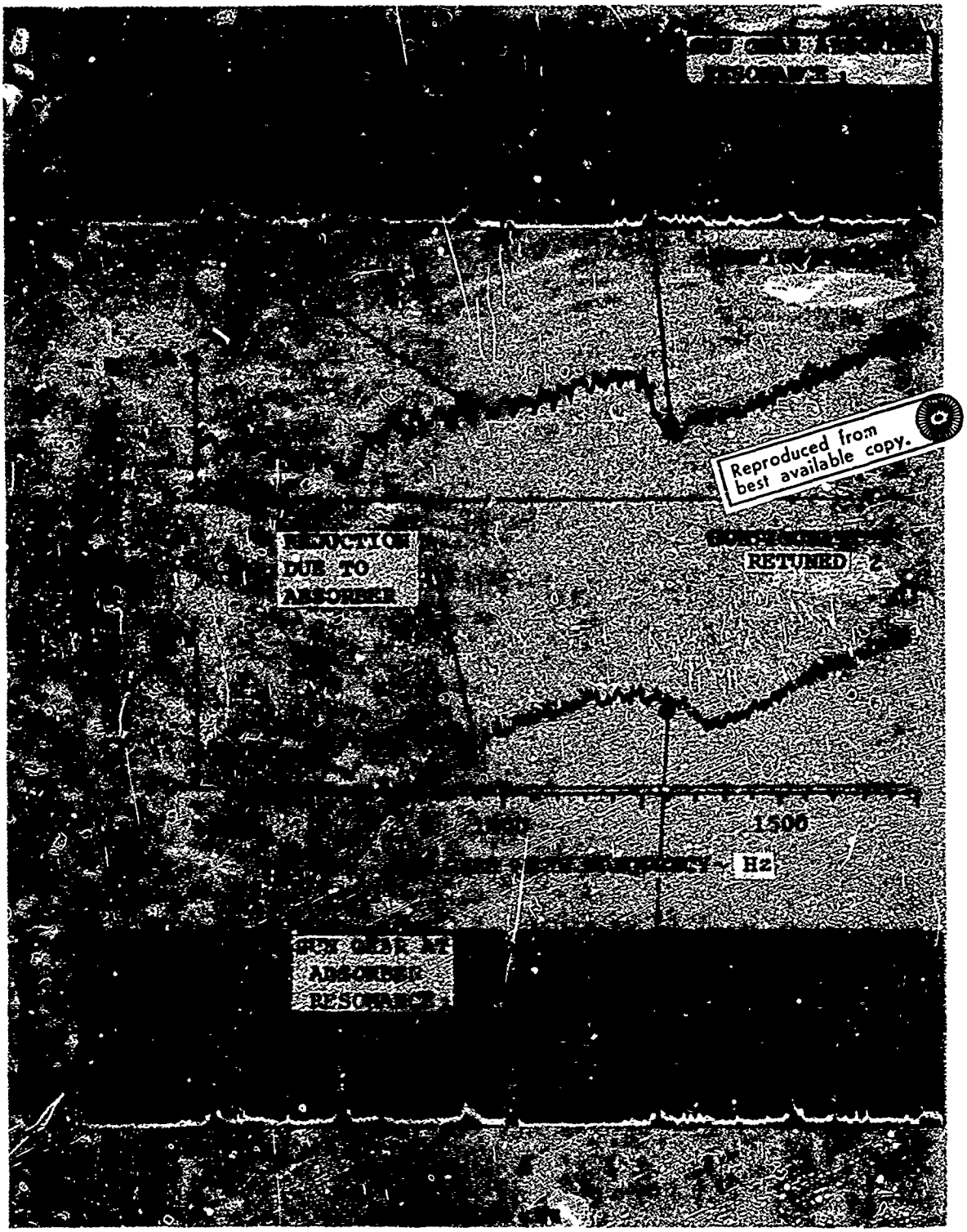

Figure 2. Effect of Retuning the Sun Gear Absorber.

FOREWORD

The work reported herein was performed by The Boeing Company, Vertol Division under Contract DAAJ02-71-C-0020, Project 1F162204A142, for the Eustis Directorate, U. S. Army Air Mobility Research and Development Laboratory, Fort Eustis, Virginia. The work was carried out by the Boeing-Vertol Acoustics Staff under the technical cognizance of Mr. Rouzee Givens of the USAAMRDL staff.

TABLE OF CONTENTS

TABLE OF CONTENTS

LIST OF ILLUSTRATIONS

LIST OF ILLUSTRATIONS

LIST OF ILLUSTRATIONS

LIST OF ILLUSTRATIONS

LIST OF ILLUSTRATIONS

LIST OF SYMBOLS

A	amplitude
a	vibration amplitude on the ring gear
e	gear pitch-line excitation amplitude, μ in.
F	dynamic response force amplitude, lb
$(FM)_{ac}$	figure of merit of acoustical treatments
f_m	natural frequency of machine
f_o	gear tooth mesh frequency
f_p	planet passage frequency
K_a	spring constant for absorber, lb/ft
K_m	spring constant for machine, lb/ft
M_a	mass of absorber, lb_m
M_m	mass of machine, lb_m
m	number of frequency bands
NRC	noise reduction coefficient
n_i	attenuation greater than mass law in the i^{th} frequency band, dB
r	radial distance to center of radiating surface, ft
W	surface weight of the treatment, lb/ft
α	energy conversion factor
β	gear housing factor
ips	inches per second
Ω	forcing frequency - Hz

LIST OF SYMBOLS

ω	resonant frequency - Hz
SB	spiral bevel gear
S	sun gear
R	ring gear
TL	transmission loss

1.0 INTRODUCTION

The arguments for reasonably low noise levels in military aircraft are generally well understood and encompass requirements for an environment which will:

1. not be medically damaging to hearing
2. not cause undue fatigue
3. permit reliable communication

In order to ensure compliance with the above requirements, the Military Services generally include MIL-A-8806A as part of the specification for procurement of production aircraft. Even this specification, however, represents a compromise between an optimum acoustical environment and the penalties imposed on an aircraft by inclusion of sound-reducing treatments.

However, the MIL specification criterion is often exceeded by negotiated deviation or is not realized in actual military usage for one or more of the following reasons:

1. Weight: In most aircraft, the material installed for noise control constitutes a pound-for-pound reduction in payload, or at a constant payload, means a reduction in aircraft performance. Since payload and performance are the primary objectives of most military aircraft designs, contractor and customer are reluctant to impose operational penalties in order to gain a more favorable acoustical environment.

2. Cost Effectiveness: Here, again, acoustical treatments show up as a complete liability because there has, to date, been no dollar value assigned to sound pressure level (dollars per dB), while weight and speed are main parameters which determine cost effectiveness of a given aircraft.

3. Maintenance: A study conducted by Vertol for the Navy,[1] which led to a revision of Specification MIL-S-6144, investigated the problems which were experienced in the Fleet with regard to the maintenance of acoustical treatments. A brief summary of results indicates that many acoustical blankets are prone to damage and/or difficult to

install. It is obvious that installations, no matter how perfect when delivered, either will be removed from the aircraft or will not provide the noise reduction for which they were designed after relatively short periods in service.

4. Incompatibility With Other Requirements: Certain elements of the acoustical treatments are often removed from the aircraft because they conceal items which require frequent inspection; because they become oil soaked and therefore hazardous; because they interfere with equipment cooling requirements; and for a multitude of similar reasons. In all these cases, the flight crew is not afforded the noise level environment which was designed into the aircraft. The contractor, on the other hand, is reluctant to take paper performance penalties, in the competition and design stages of an aircraft development program, for weight which he knows will not actually be there in service.

In considering approaches to the solution of these problems, it must be kept in mind that the acoustical sources and paths to the occupant in a helicopter are quite different from those in an airplane. The fundamental difference lies in the fact that the primary sources of noise in most airplanes occur externally to the fuselage shell, and arise from powerplants, propellers, or aerodynamic noise on the skin itself. Helicopter noise, on the other hand, generally arises from sources contained within the fuselage or mounted directly on the skin. The major sources are generally rotor and engine transmissions, powerplants, and accessories.

Of the various sources of internal noise, the highest levels, in most helicopters, arise from the rotor transmissions. Unfortunately, these highly loaded gearboxes are generally located near or over the flight crew and/or passenger compartments; and if no treatment is applied, this will result in an environment which will not permit any reliable speech communication, will result in temporary hearing threshold shifts after relatively short exposure, and will probably result in permanent hearing loss after repeated extended exposure of unprotected ears.

Therefore, the question regarding acoustical treatment of helicopter rotor transmissions is not if it shall be done, but rather how much and in what manner.

In a helicopter, noise can be transmitted from rotor transmission to the flight crew or observer through various paths:

1. Airborne waves radiated directly to the observer.

2. Airborne waves reflected to the observer.

3. Airborne waves impinging on the structure resulting in bending waves transmitted by the structure and then radiated as airborne waves.

4. Mechanical motion of dynamic components inducing bending waves in the structure and traveling along the structure and then radiated as airborne waves.

The intensity of the transmitted sound depends on many things, such as frequency, intensity, and angles of incidence (on the surrounding structure) of the incident waves, the fuselage dimension, stiffness, materials, and the presence of damping. In addition, the influence of any one or more of these paths on a resulting noise environment at the receiver depends on the physical relationship between the receiver and the source. For example, a somewhat exposed rotor transmission case in proximity to a flight crew station might result in airborne noise radiation paths 1 and 2 being the dominating factor in producing adverse noise environments, whereas gearboxes buried within existing structure or compartments at a considerable distance from the crew could result in structure-borne waves in the fuselage paths 3 and 4 being the dominating paths.

Many existing noise-control principles and techniques can be applied for acoustical control of each path; however, it is complicated by the fact that there are generally many sources, many paths, and many receivers or occupied areas all interconnected within an aircraft fuselage. Therefore, any treatment applied that significantly controls only one or two paths may not be the optimum overall solution for successful noise control of the rotor transmission.

The experimental program reported herein tested two possible source reduction techniques: dynamic gear absorbers and gear damping. These techniques have the advantage that they treat the noise before it enters any of these paths, thus effectively treating all of them.

2.0 RELATIVE EFFICIENCY OF TRANSMISSION NOISE REDUCTION METHODS

The noise from helicopter transmissions can be controlled by two fundamental approaches. The first is reduction and control of the acoustical energy at, or within, the gearbox itself; the second is acoustical treatment of the airframe to attenuate the noise after generation. The latter approach is the one that has been most frequently used in past designs.

In establishing trade-offs between source reduction and airframe treatment, however, many of the disadvantages of bases for comparison which were outlined in the introduction deal with intangibles, leaving weight as the optimum measurable trade-off parameter.

Appendix III to this report presents a general discussion of the principles involved in acoustical design for the reduction of transmission noise by airframe treatment. The analysis which follows develops a methodology for estimating the equivalent weight of airframe treatment which is required to achieve a stated reduction in gearbox noise. The technique employed is general in approach but will vary in detail application depending on the aircraft configuration.

The acoustical energy generated by the gearbox is transmitted through two paths. The first (Figure 3(a)) is airborne noise which is radiated from the vibrating case. An enclosure, which may be composed of aircraft structure and acoustical materials, provides attenuation of the sound pressure level, which then radiates into the cabin area. The resulting level then becomes a function of the acoustical absorption of the cabin lining.

The second path which the energy can follow is that shown in Figure 3(b). Case vibration is transmitted through the mounting structure to the aircraft skin and along the structure, whose vibrations reradiate the energy as airborne noise. The controls in this path can consist of one or more of the following: isolation of the transmission, damping of the structure, attenuation of the cabin lining, and absorption of the receiving space. Appendix III presents information required for determining the effect of each of these elements of the airborne and structure-borne treatments.

(a) AIRBORNE NOISE

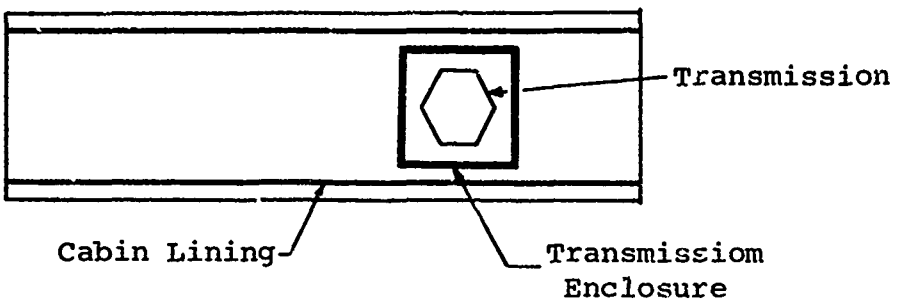

(b) STRUCTURE-BORNE NOISE

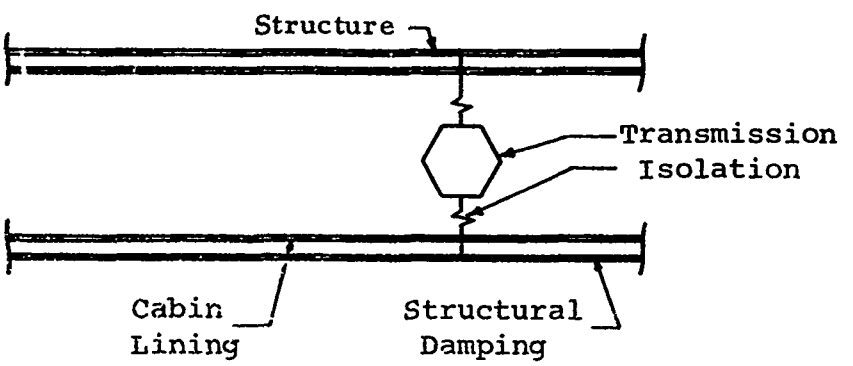

Figure 3. Model of Transmission Noise Trade-off Analysis.

The general approach is based on the concept of noise reduction as a function of attenuation and absorption, which is presented in Figure 79 of Appendix III as a plot in the format shown in Figure 4.

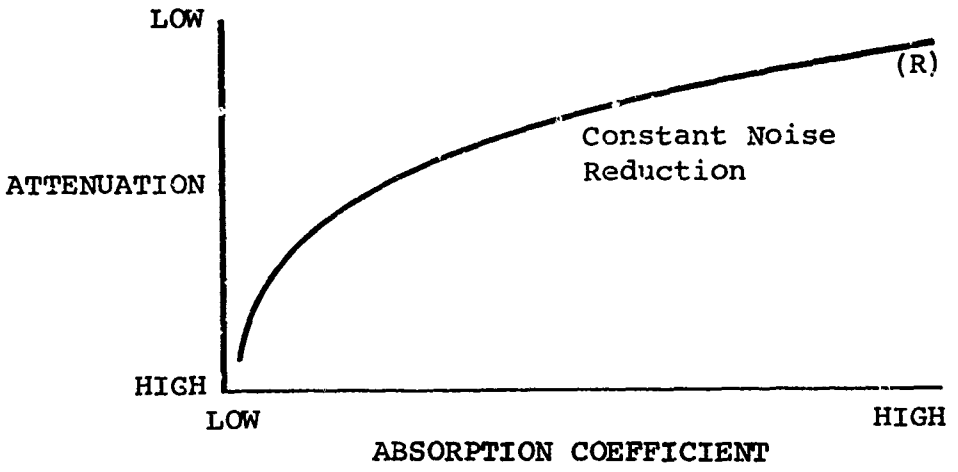

Figure 4. Reduction of Noise in Enclosed Spaces.

In the case under question, the attenuation is due to the transmission enclosure and the absorption is due to the cabin lining. Having selected candidate materials for each treatment, and through a knowledge of their variation in acoustical properties with surface weight, Figure 4 can be replotted as shown in Figure 5.

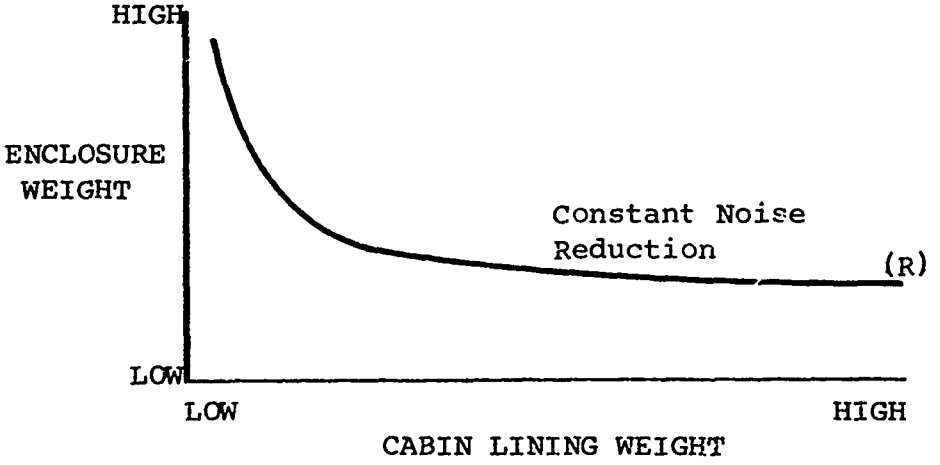

Figure 5. Weight of Noise Reduction.

The optimum weight can be found by summing the two weights at several points along the course and replotting as shown in Figure 6.

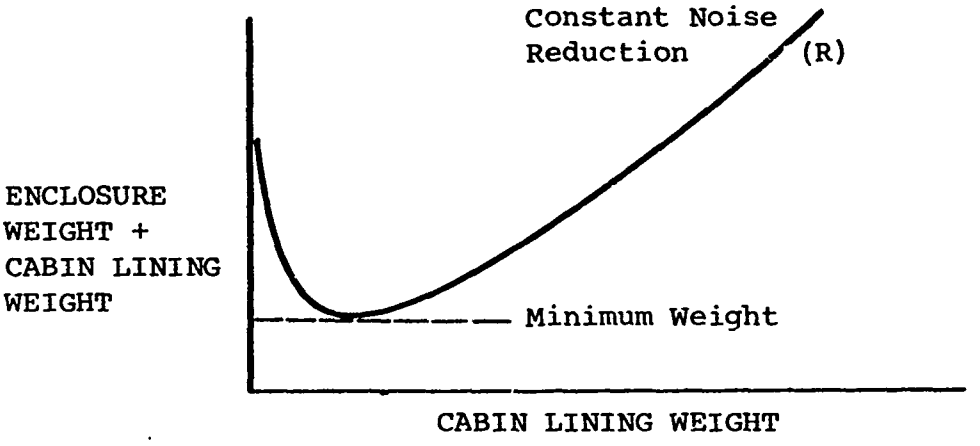

Figure 6. Determination of Minimum-Weight Acoustical Treatment.

The weight involved in achieving a given noise reduction can then be compared with the weight involved in achieving the same reduction by other methods.

In applying the analysis to the CH-47C helicopter, the aircraft is divided into the elements illustrated in Figure 7. The transmission enclosure consists of the entire area bounded by the bulkhead at Station 95, the frame at Station 120, the butt line beams, and drip pan. This surface area is 110ft^2. The cabin lining includes the side walls and ceiling (less windows) from Station 120 to 440 and has an area of 530ft^2.

Airborne Noise

Figure 8(a), derived from Boeing test data, shows the relationship between cabin lining weight and absorption coefficient for the same two frequencies.

Figure 8(b), which is obtained from Figure 78 of Appendix III, presents the optimum weight treatments for attenuating spiral bevel and lower stage planetary gear noise as it passes through the enclosure and into the cabin receiving space.

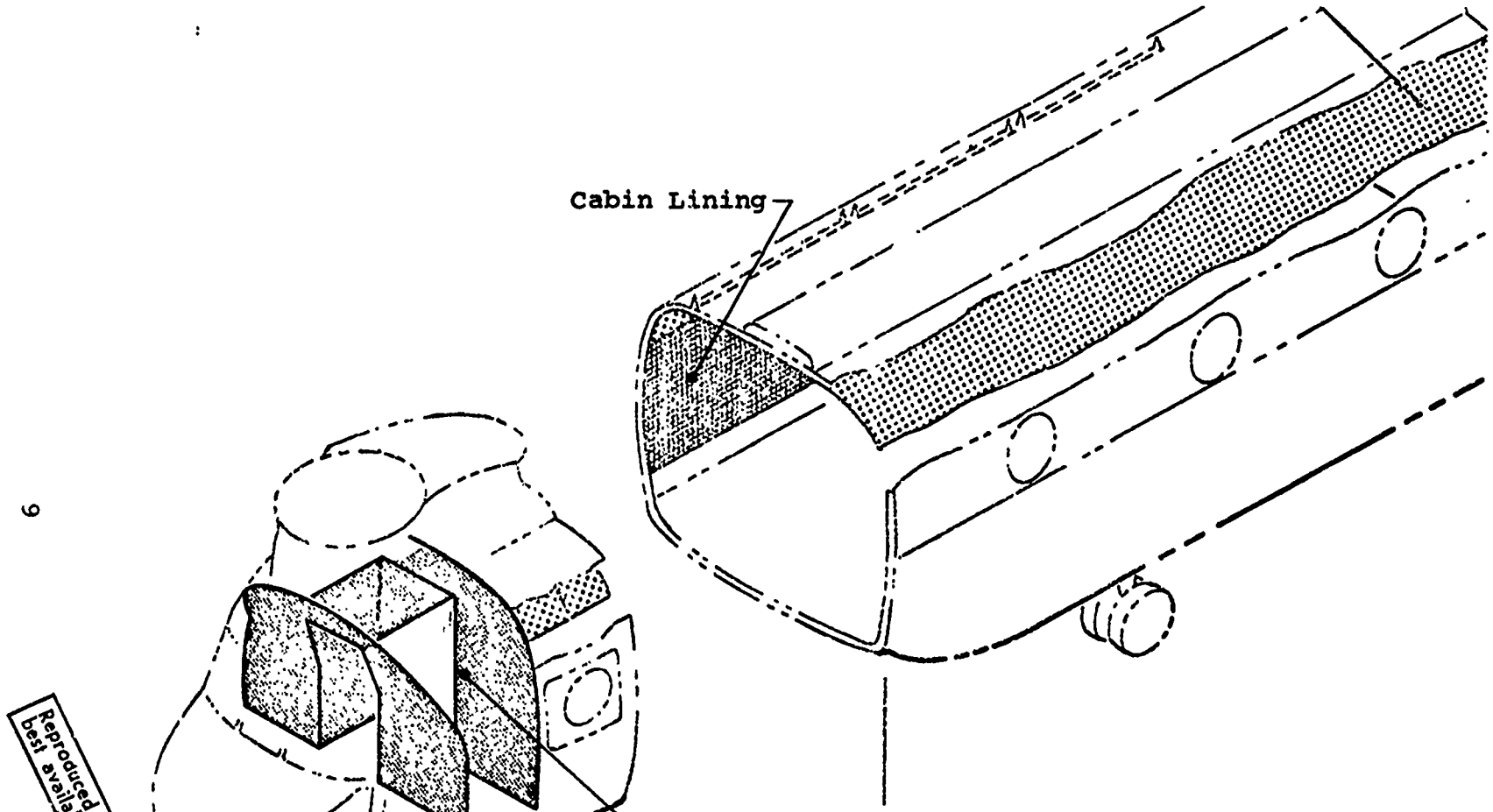

Figure 7. Acoustical Treatment - CH-47C.

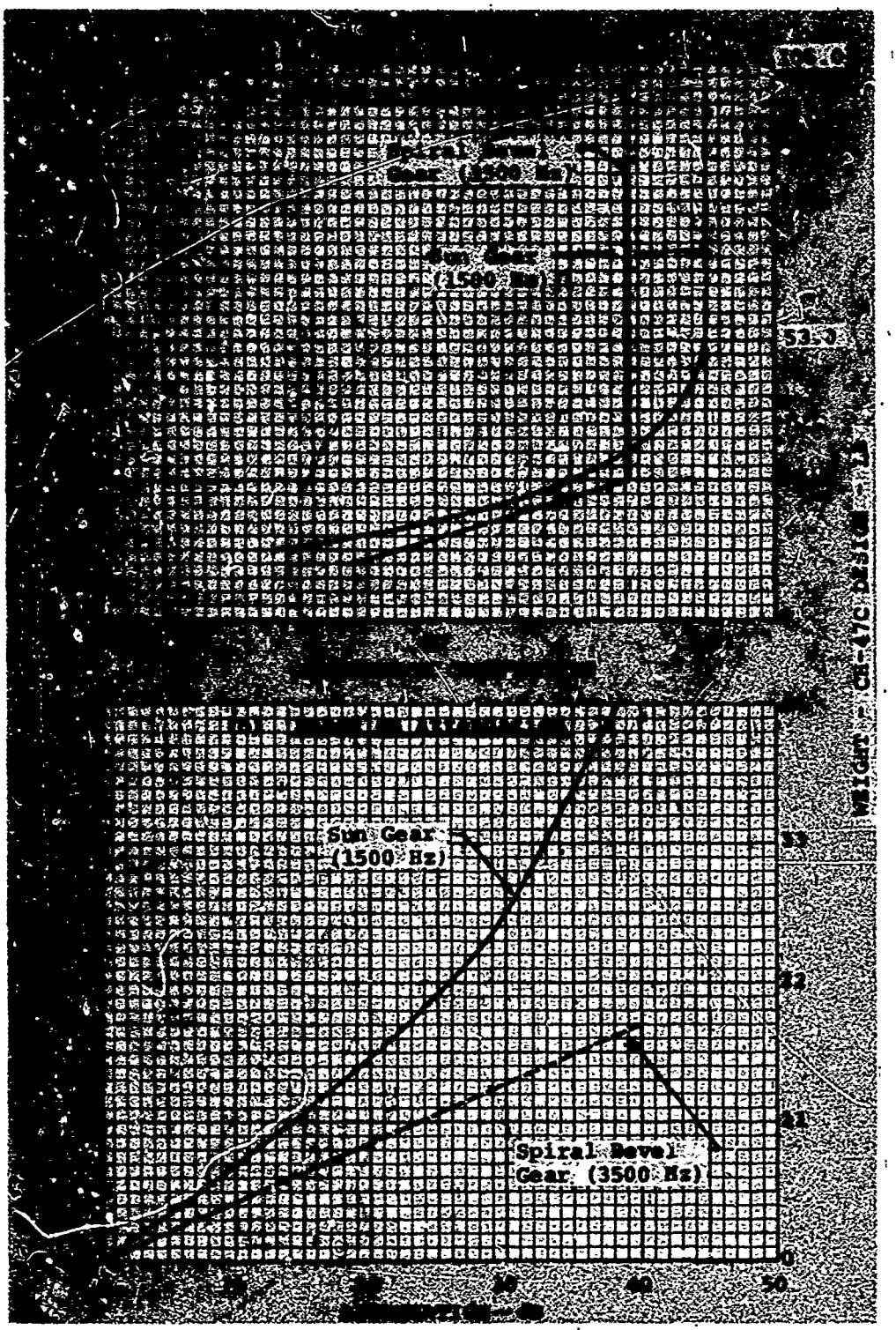

Figure 8. Weight of Acoustical Treatment, CH-47C Helicopter.

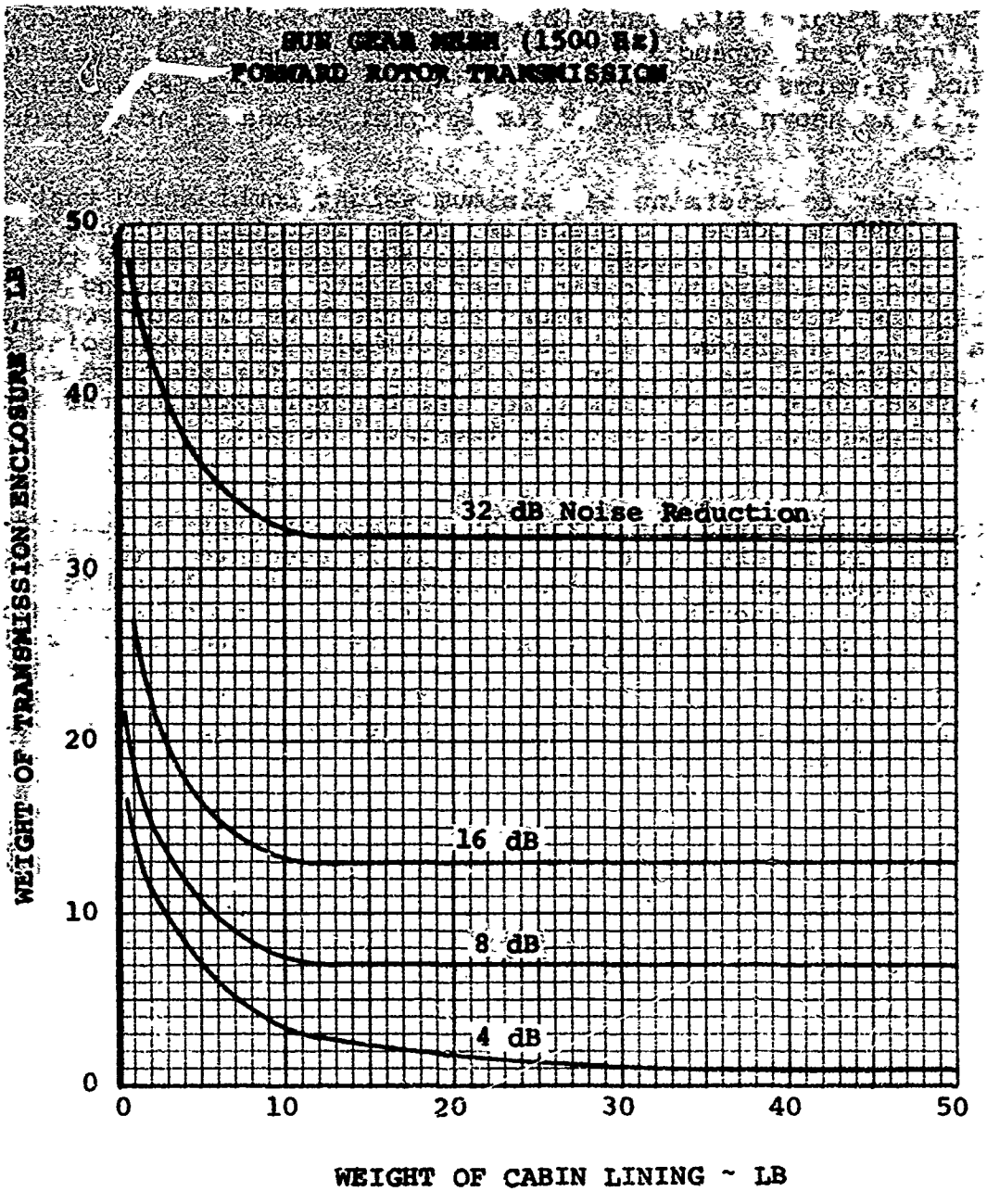

Figure 9. Weight Required To Achieve Noise Reduction, CH-47C Helicopter.

Using Figures 8(a) and 8(b), it is now possible to replot Figure 79 of Appendix III so that the ordinate and abscissa are now in terms of weights rather than acoustical parameters. This is shown in Figure 9 for several values of noise reduction.

In order to determine the minimum weight combination that is required to achieve a specified noise reduction, Figure 9 is reconstructed as Figure 10, where the ordinate is now the sum of the enclosure and cabin liner weights. In applying these results, however, it is found that the true minimum requires a lining thickness which is impractical from a standpoint of manufacturing process and durability and, for the case examined, that the minimum practical blanket dictates the amount of absorption, and hence the treatment weight.

Once having sized the lining by optimum absorption requirements, it remains to ensure that it is adequate with respect to attenuation of the noise radiated from the structure. Since the prescribed lining will provide 17 dB of attenuation at 1500 Hz (Figure 8(a)), while Figures 75a and 75b show that the noise radiated from the structure is about 36 dB below the airborne level, it can be concluded that the 1/2-inch blanket will be adequate unless noise reduction of the order of 40 dB or more is required.

A similar analysis could be carried out for the spiral bevel gear (3500 Hz), but due to the greater attenuation of the enclosure at the higher frequency, it will be found that the sun gear mesh is the more critical in establishing the design weight.

The above example was idealized for illustration but specific in application to a particular aircraft. The general methodology can, however, be applied to any particular design and materials.

Some of the assumptions were:

1. No leakage of the enclosure was considered. If desired, the attenuation of Figure 8b could have been adjusted by application of Figure 77 of Appendix III.

2. No surface trim was considered on the cabin lining. The weight and effect of trim on absorption coefficient can be included in Figure 8a.

3. Weight of attaching hardware was considered to be independent of weight of treatment and, therefore,was not included as a parameter.

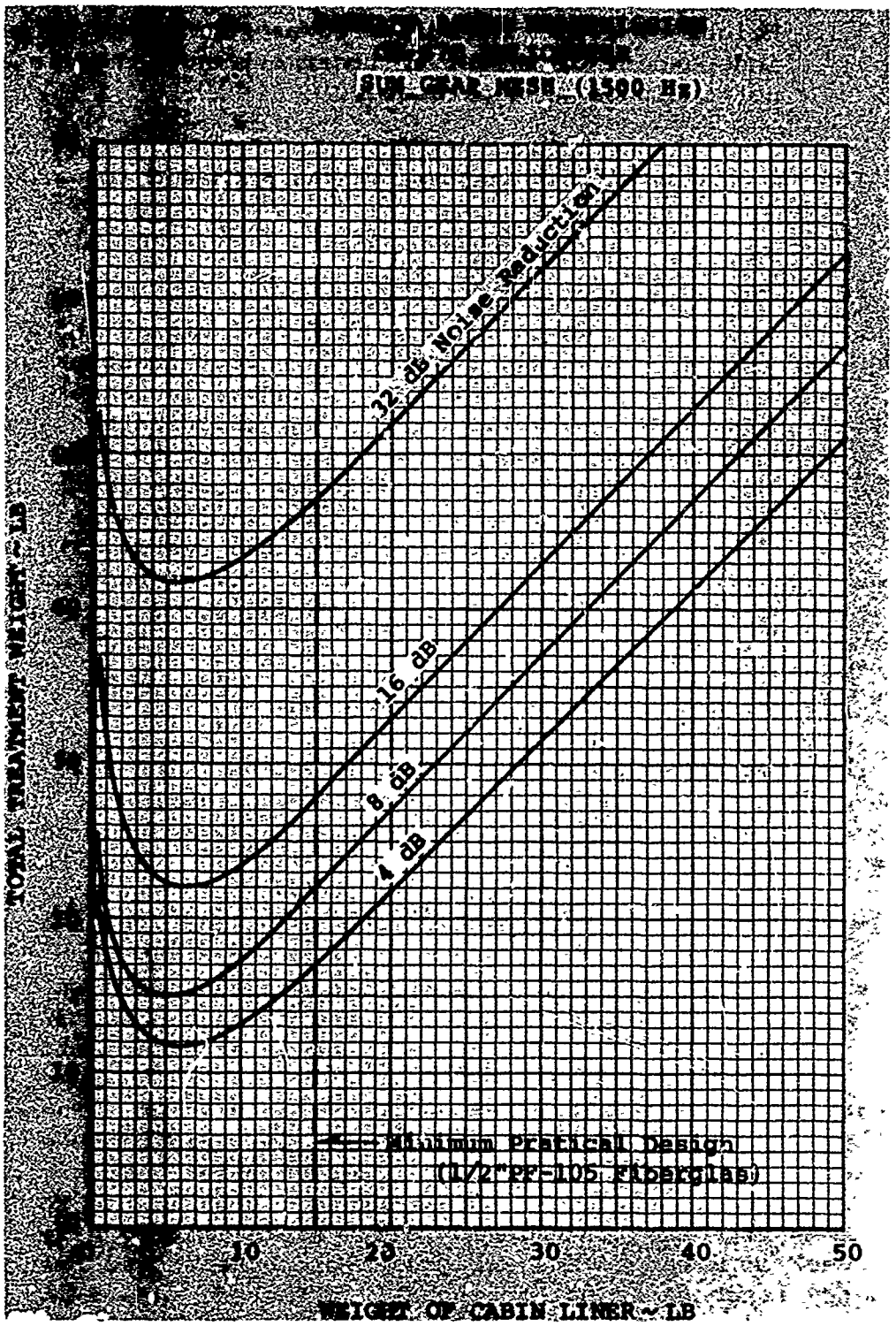

Figure 10. Total Weight of Acoustical Treatment.

3.0 DESCRIPTION OF TEST PROGRAM

3.1 TEST SETUP

3.1.1 Transmission

The transmission used in this program was a CH-47C forward rotor transmission.

3.1.2 Test Stand

The transmission was run in the Boeing-Vertol closed-loop test stand (see Figure 11). This stand employs four components to close the loop. First, a set of helical gears increases the output or rotor shaft speed to input or synchronization shaft speed. A torque device connects this gear shaft to a bevel gearbox. The bevel gearbox closes the loop to the input shaft of the transmission and also connects to a variable-speed clutch and an electric motor which drives the system. This closed-loop test stand provides the capability of running a transmission over its full design torque and speed range under controlled conditions.

3.1.3 Instrumentation

Six accelerometers were mounted on the transmission case as shown in Figure 12. A block of aluminum was epoxied to the transmission at each of the desired locations, and the accelerometers were attached to these blocks using Endevco studs.

Preliminary data were obtained at many locations with a hand-held accelerometer. From these data, six locations were chosen which showed strong and relatively clean peaks at gear mesh frequencies, and which also had the highest possibility of demonstrating a reduction due to dynamic absorber action.

Six microphones were placed around the transmission. These were B&K 4131 microphone cartridges with B&K 2613 cathode followers and B&K 2801 microphone power supplies. Each microphone was loosely covered with a very thin plastic bag to protect it from the transmission oil. A preliminary side-by-side check of a bagged and unbagged microphone showed that the frequency response is not appreciably affected.

The microphone locations are shown in Figure 13. They were chosen using preliminary data in the same way the accelerome-

ters were chosen. Four of the microphones, Locations 2, 3, 4 and 6, were placed about 2 inches away from the transmission case to pick up the locally generated noise. The other two were placed in the far field (about 10 ft away and 3 ft above and below the transmission) to estimate the overall noise level.

The microphones were supported on wooden 2 x 4s clamped to the transmission stand structure. The boards and the stand were constructed so that the microphones could be removed and replaced to within 1/2 inch of their original position.

In order to minimize microphonics from the vibration of the test stand, the microphones were wrapped in foam before being clamped in position (Figure 14).

The microphone and accelerometer data were recorded on an Ampex AR-200 1-inch, 14 channel, wide-band FM tape recorder at 30 ips. Figures 15 and 16 show the data acquisition system. This has a frequency response which is essentially flat from 0 Hz to 10 kHz. Typical system response curves are shown in Figure 17.

Before recording, the accelerometer data was amplified using Unholtz-Dickie accelerometer amplifiers.

A 60/rev signal from the input shaft, used for speed indication, was also recorded on one channel. This signal was produced with a 60-toothed wheel and a magnetic pickup.

The remaining channel on the tape was used for voice identification.

3.2 ABSORBER DESIGN

3.2.1 Dynamic Vibration Absorbers

The concept of dynamic vibration absorbers is that at the resonant frequency of the absorber, the machinery it is attached to stops moving. This can be most easily seen in the idealized system shown in Figure 18. A large spring-mass system is shown to represent the machinery. It has a sinusoidal force applied to it; $F = F_0 \sin 2\pi\Omega t$. With no absorber attached, the machinery vibrates with an amplitude determined by the resonant frequency of the system, $\omega = \frac{1}{2\pi}\sqrt{\frac{K_m}{M_m}}$, and the

frequency of excitation, Ω. The addition of the absorber, however, changes the situation. Now the system has two resonant modes: the one with the lower frequency where the two masses (absorber and machine) vibrate together against the larger spring, K_m, and the other at a higher frequency where the masses vibrate against each other. The force applied to the machinery can excite either of these modes. Somewhere between them, however, exists a condition where the absorber moves and the machine does not. At this frequency, the force excited by the absorber on the machine exactly cancels the driving force, F.

Since the machinery is not moving, the absorber acts as if it were attached to a solid wall. This frequency is thus the resonant frequency of the absorber alone. Therefore, to design a dynamic vibration absorber, it is only necessary to establish that the uncoupled natural frequency of the absorber is equal to the frequency of excitation. For more detail and derivations of the equations, see Reference 7.

Two types of absorbers were used in this program as illustrated in Figure 19. The bending absorbers were placed on the ring gear in order to stop the motion and thus the sound radiation of that part of the case. Torsional absorbers were placed inside the sun gear and spiral bevel pinion. These absorbers then stopped the torsional motion of those gears at their tuned frequency. The forces on the gear teeth were also reduced at a slightly different frequency when the absorber made the gear move just enough to eliminate the excitation.

The reduction of the dynamic forces on the gear teeth then reduces the forces transmitted through the bearings to the casing and then to noise. The torsional absorbers were tuned to the spiral bevel and sun gear mesh frequencies to correspond to the gears where they were placed. The bending absorbers were tuned at the planet ring mesh frequency where the torsional absorbers reduced the noise. An additional calculation was made to ensure that the absorbers would be strong enough to sustain resonance without mechanical failure.

In order to study the frequency effects of dynamic absorbers, two sets of torsional absorbers were designed and fabricated. Each absorber was tuned to the frequencies shown in Table II.

TABLE II. ABSORBER RESONANT FREQUENCIES		
Absorber Location	Configuration I	Configuration II
Spiral Bevel Pinion Gear, Hz	3410	3239
Sun Gear, Hz	1501	1420
Ring Gear, Hz	1463	-
Equivalent Rotor Speed, approx.	230	220

The torsional absorbers were designed with simple cylindrical sections (see Figures 20 and 21). The absorber was a shrink fit of the larger diameter disc into the gear. This provided a well balanced and very strong fit inside the gear; an axial force of 5-10 tons was required to force them out of the gears.

The bending absorbers used on the ring gear were simple cantilevered beams bolted to the ring gear. Figure 22 shows this design. A round rod was installed in each of the three directions. Since these absorbers were tunable, they were tuned after installation on the transmission.

3.2.2 Design Analysis

In order to obtain the best prediction of the effects of these absorbers, noise levels were predicted using the method developed at Mechanical Technology Incorporated (Reference 9).

This analysis starts by evaluating the gear tooth bending when subjected to the force from a mating gear tooth. As the gears rotate, sometimes two teeth and sometimes only one tooth carries the loads. The deviations from true conjugate action caused by this tooth bending excite torsional vibration modes which, in turn, amplify the oscillatory forces on the teeth. These forces are then transmitted through the bearings into the case and then radiated as noise.

Detailed explanations of the above procedures can be found in References 2 and 9.

Predictions made using this method are shown in Figures 23 and 24. Figure 23 indicates that noise amplitude at the spiral bevel mesh frequency should show a substantial noise amplification followed by a substantial attenuation at the tuned absorber frequency. It should be noted that this prediction method uses a spur gear equivalent of the spiral bevel gear. The sun gear prediction, Figure 24, also indicates a reduction, although not as large. The absorber acts on the sun-planet mesh but not on the planet-ring gear mesh. Thus a lower limit is set on the possible noise reduction by the noise produced by the planet-ring mesh alone.

Using the torsional response portion of the prediction method, the amplitude of the torsional oscillation of the absorbers can be calculated. This is shown in Figure 25 for the spiral bevel absorber configuration for comparison with test data (see Test Results, Figure 40). This shows that the response to the spiral bevel mesh frequency should be small except at the tuned frequency of the absorber, 3410 Hz.

3.3 TEST CONFIGURATIONS

3.3.1 Dynamic Absorber Configurations

The test data were obtained for the absorber configurations listed in Table III.

TABLE III. DYNAMIC ABSORBER TEST CONFIGURATIONS

Test No.	Spiral Bevel Absorber Config. 1	Sun Gear Absorber Config. 1	Ring Gear Absorbers	Spiral Bevel Absorber Config. 2	Sun Gear Absorber Config.2
1					
2	X				
3	X	X			
4	X	X	X		
5				X	X

3.3.2 Damping Configurations

a) Spiral Bevel Snap Ring

The standard CH-47C forward transmission has a snap ring installed in the spiral bevel pinion gear (see Figure 20). This snap ring provides frictional damping for ring modes of the gear. Test data were obtained with it in place. The baseline runs were made with the snap ring removed.

b) Ring Gear Damping Strap

Figure 26 shows a cross section of the constrained layer damping strap used on the outside of the ring gear. This strap covered the entire circumference of the ring gear. It consists of a 6-ft by 2-3/4-in. metal strap 1/16 in. thick with a .040-in.-thick layer of an experimental viscoelastic material bonded to it. The viscoelastic material was epoxied to the outside of the ring gear.

c) Internal Gear Damping

For this configuration, the sun gear, the spiral bevel pinion and the spiral bevel ring gear were treated with Viton as shown in Figure 27. The sun gear and the spiral bevel pinion were filled with sponge Viton. The ends were then capped with solid Viton to keep the sponge from absorbing the hot transmission oil. The back of the spiral bevel ring gear was filled with solid Viton. This configuration was run with the ring gear damping strap also in place.

3.3.3 Test Conditions

For each of the above configurations, data were taken at three torques.

TABLE II. TEST TORQUES

40%	$.422 \times 10^6$	in.-lb at output shaft
60%	.633	in.-lb at output shaft
80%	.844	in.-lb at output shaft
where 100%=	1.06×10^6	in.-lb at output shaft

For each of these torques, two RPM sweeps were made from 0 to 243 rotor shaft RPM (0-7460 input shaft RPM) and two from 243 rotor RPM to 0 RPM.

In addition, a minimum of ten stabilized RPM data points were obtained at each torque. The definition of these points was, in each configuration, based on examination of the sweep data. These data points are shown in Figure 28.

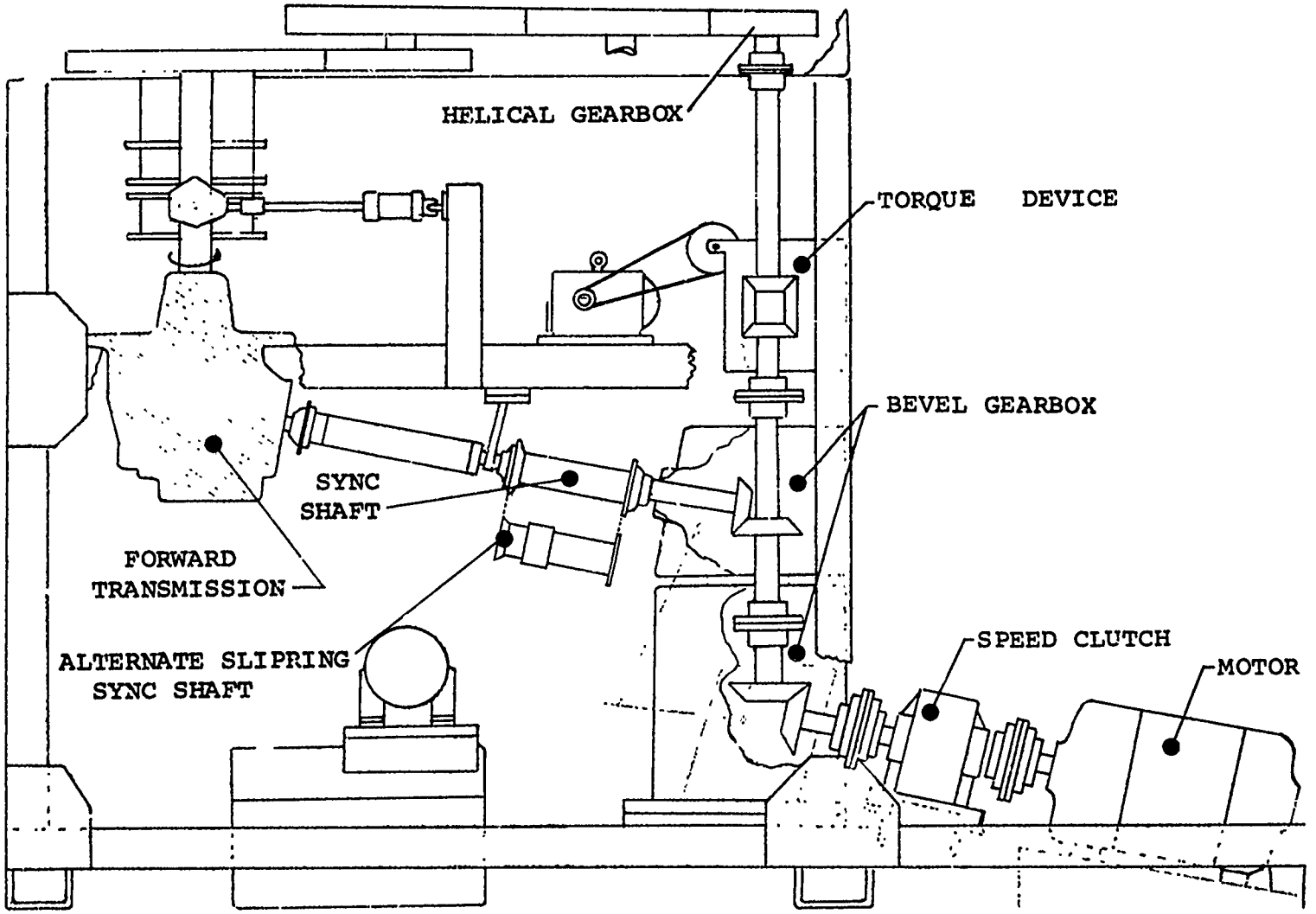

Figure 11. Closed-Loop Test Stand.

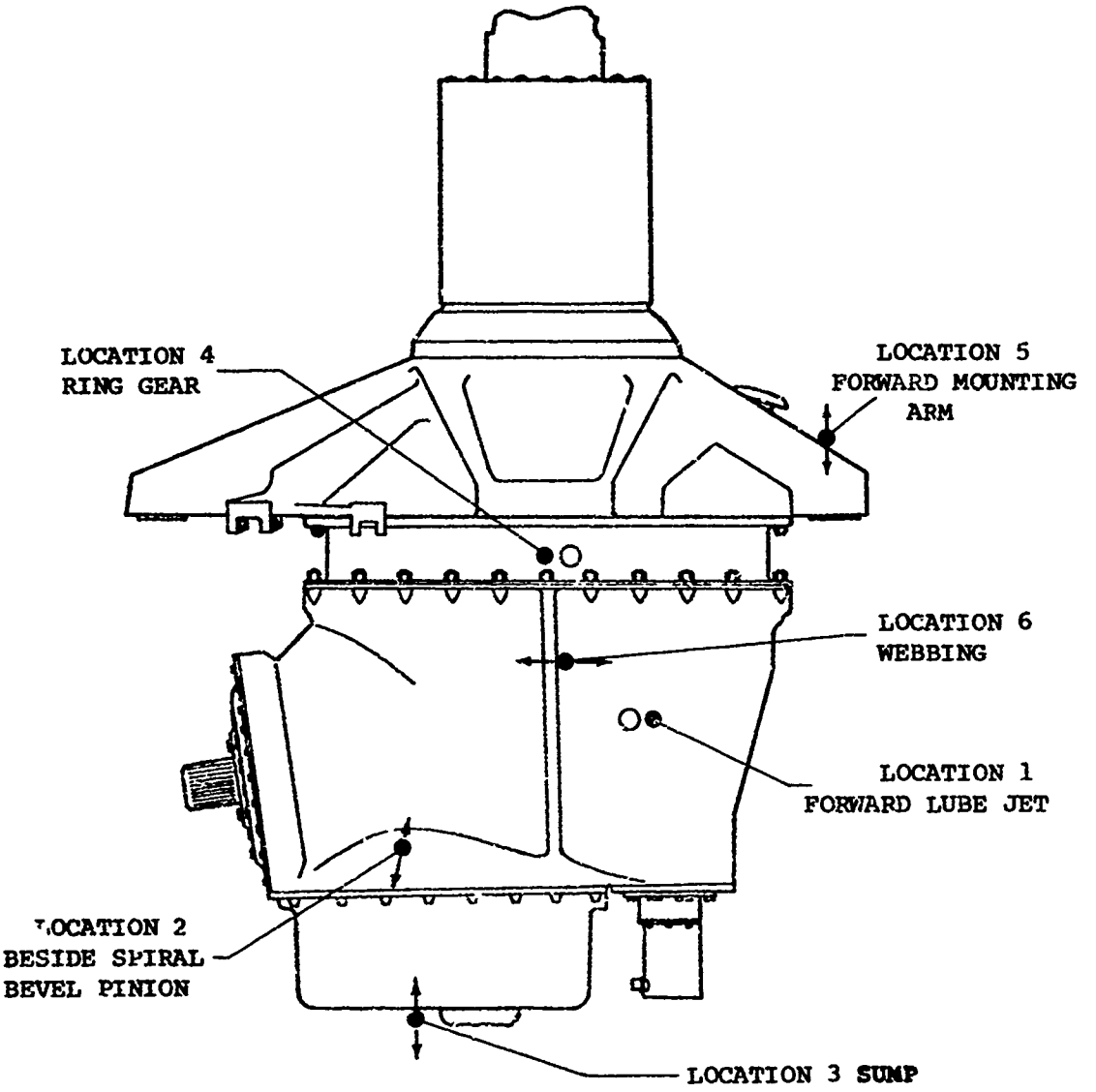

Figure 12. Accelerometer Locations.

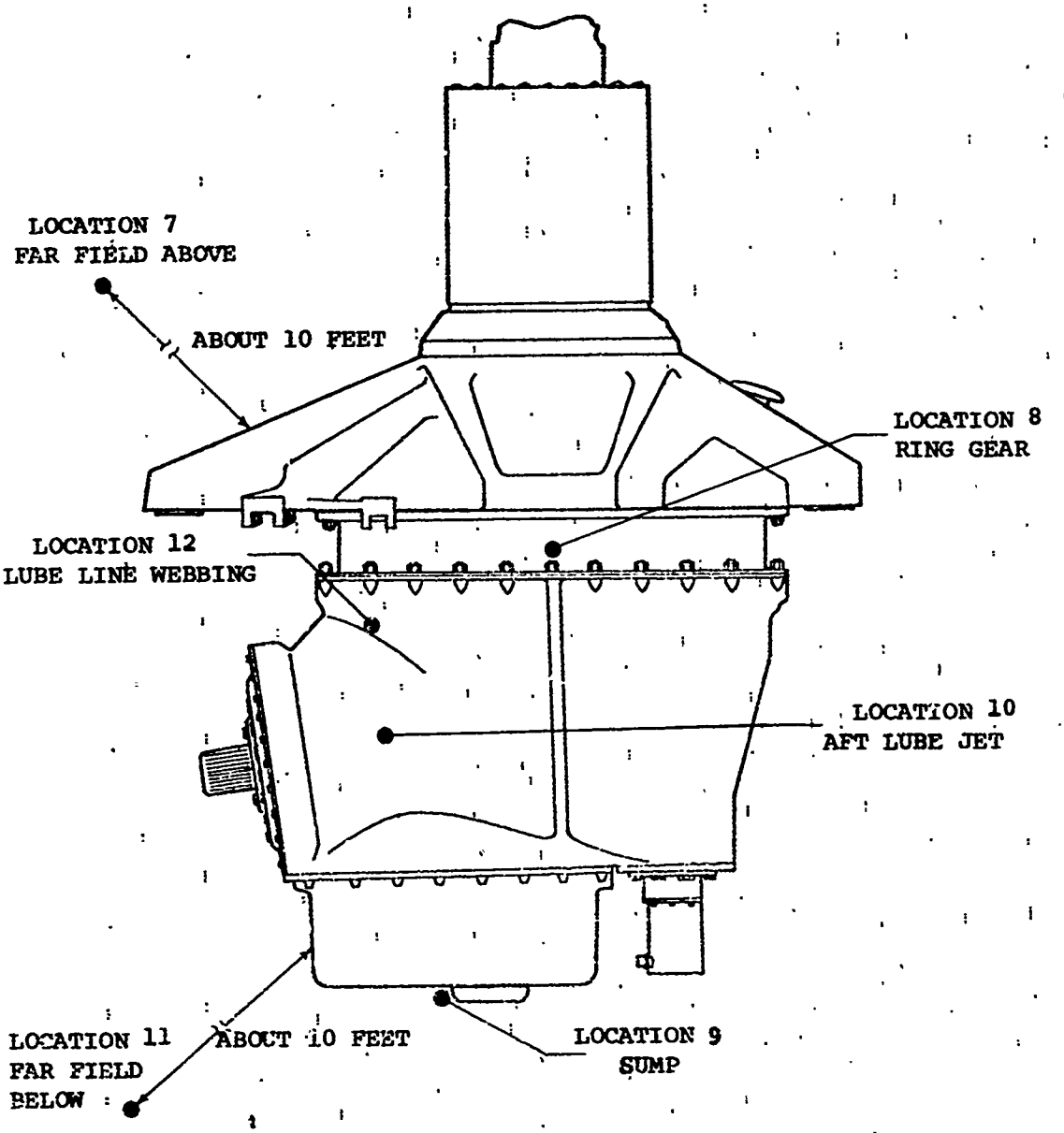

Figure 13. Microphone Locations.

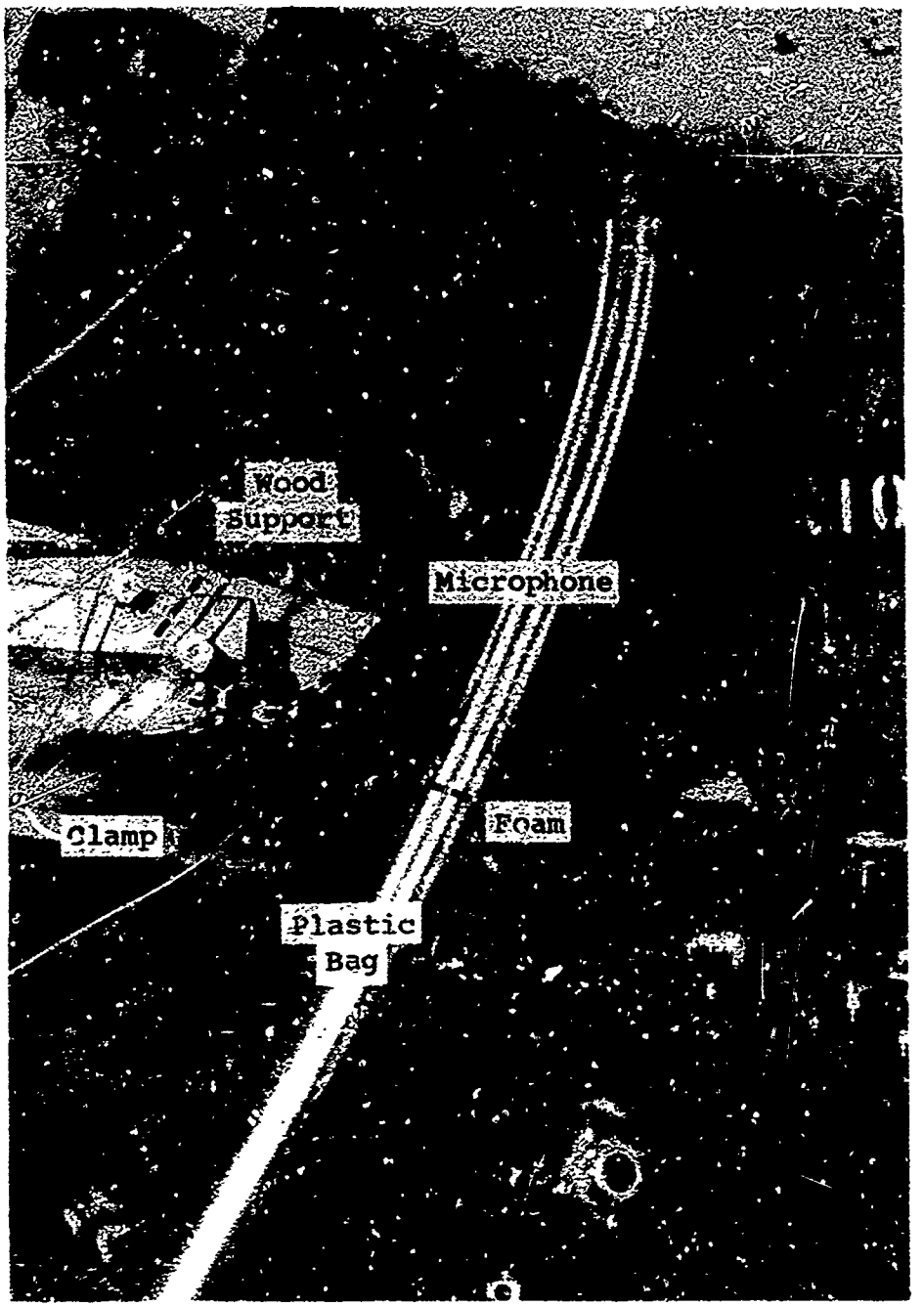

Figure 14. Microphone in Position.

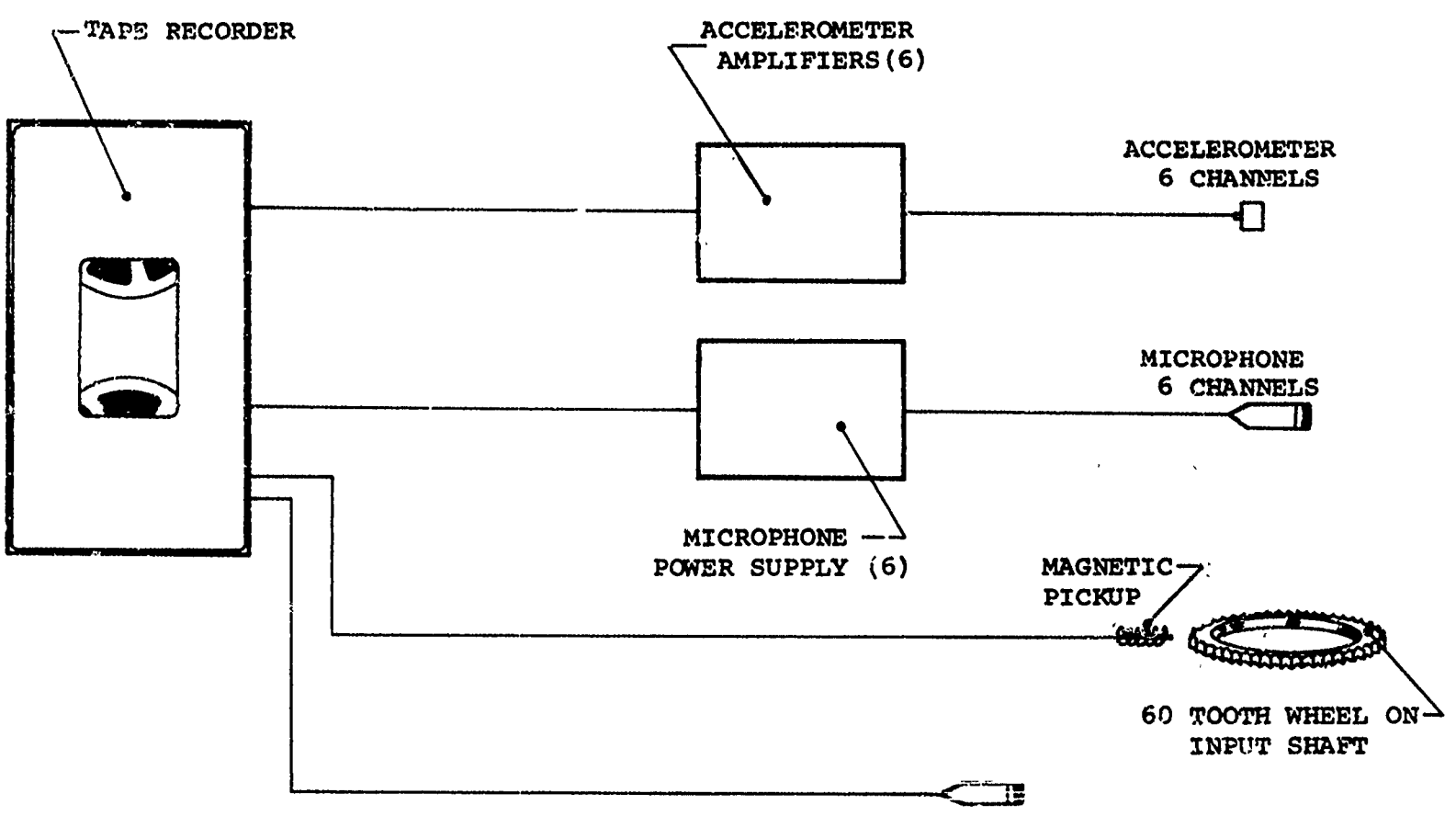

Figure 15. Data Acquisition System.

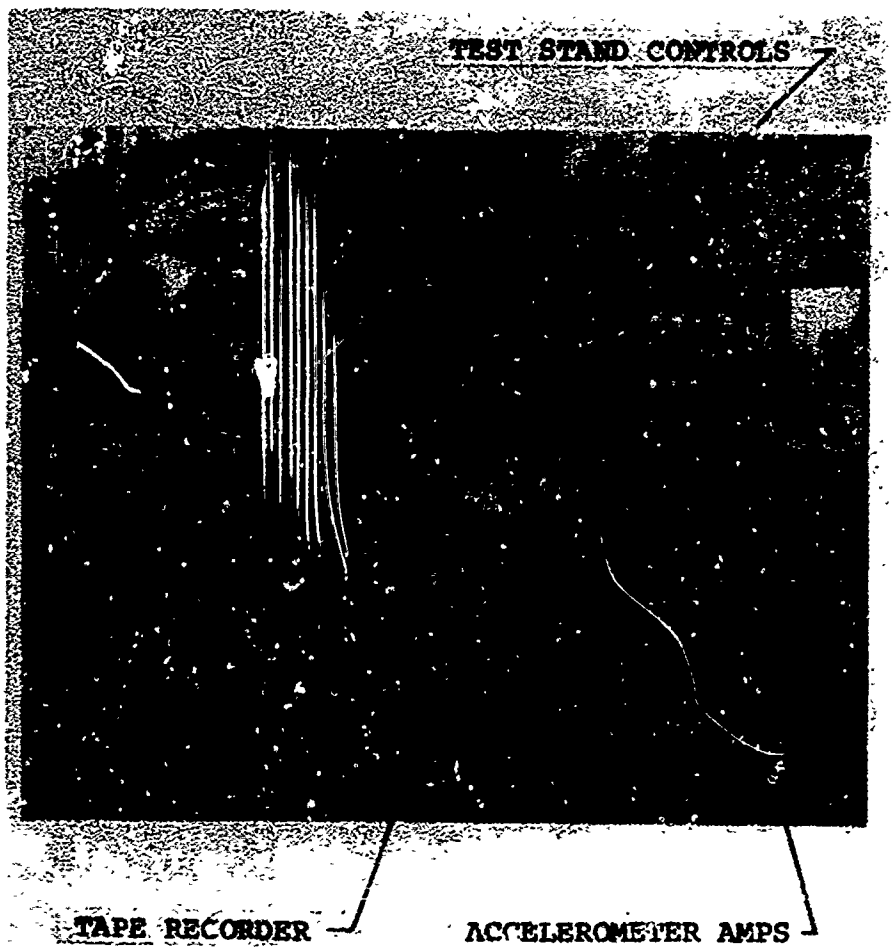

Figure 16. Test Stand and Data Acquisition Controls.

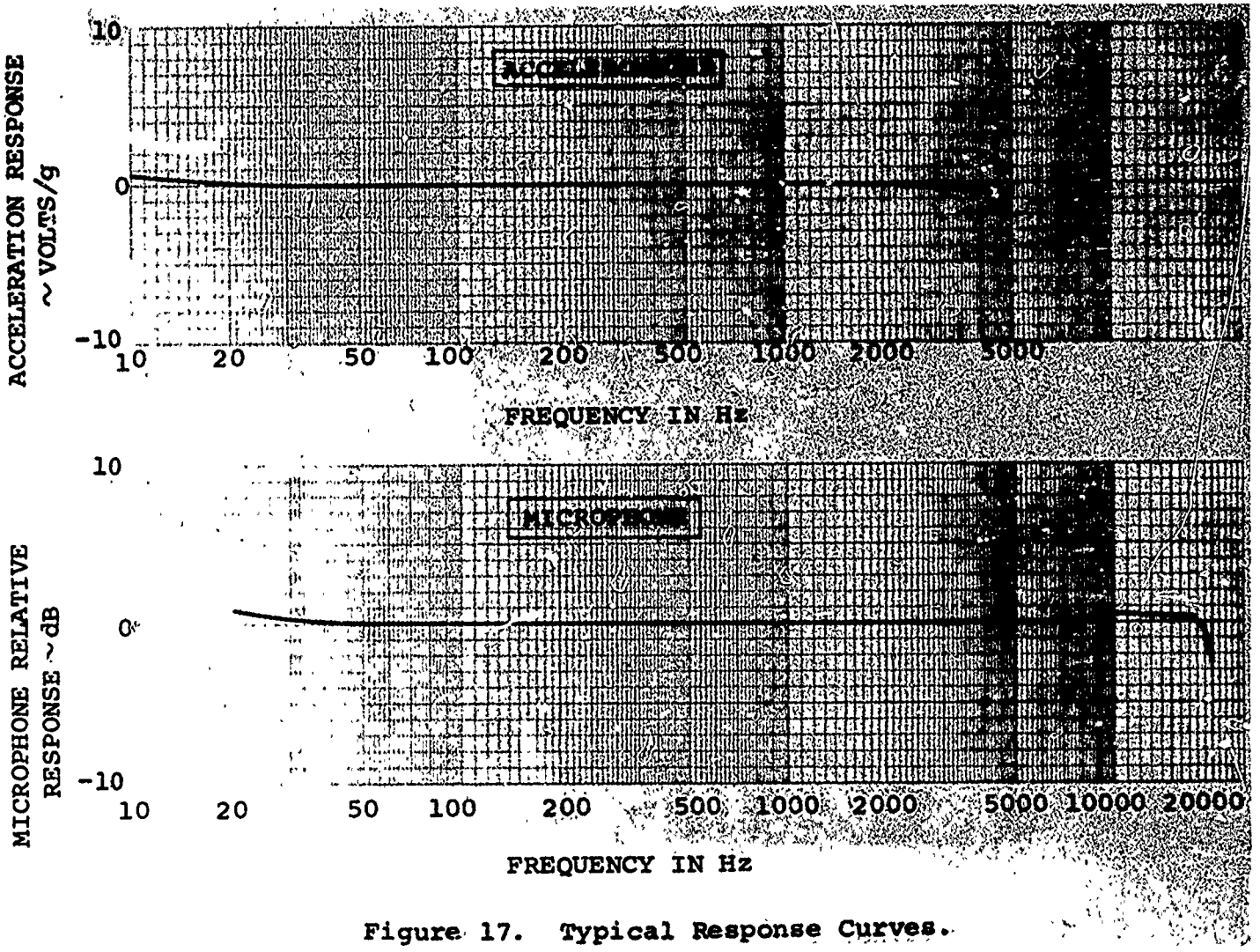

Figure 17. Typical Response Curves.

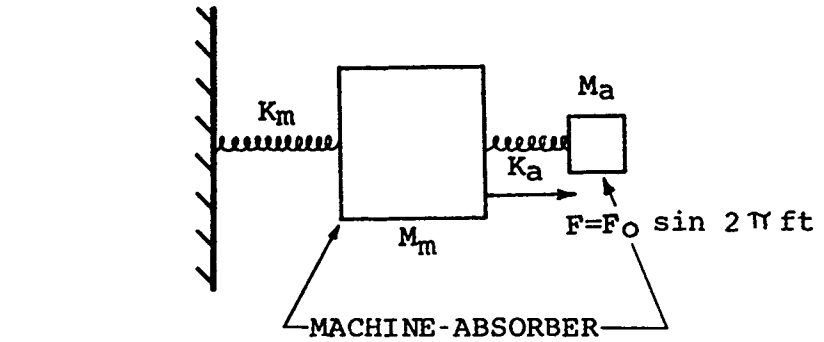

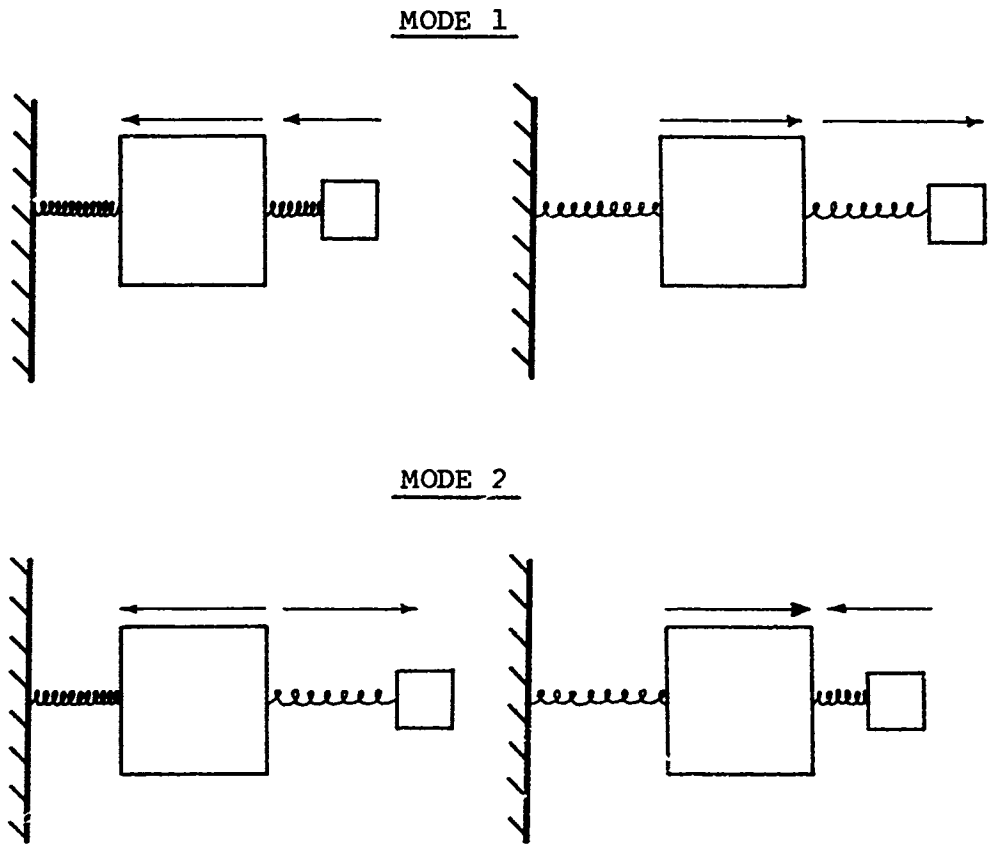

Figure 18. Concept of the Dynamic Vibration Absorber.

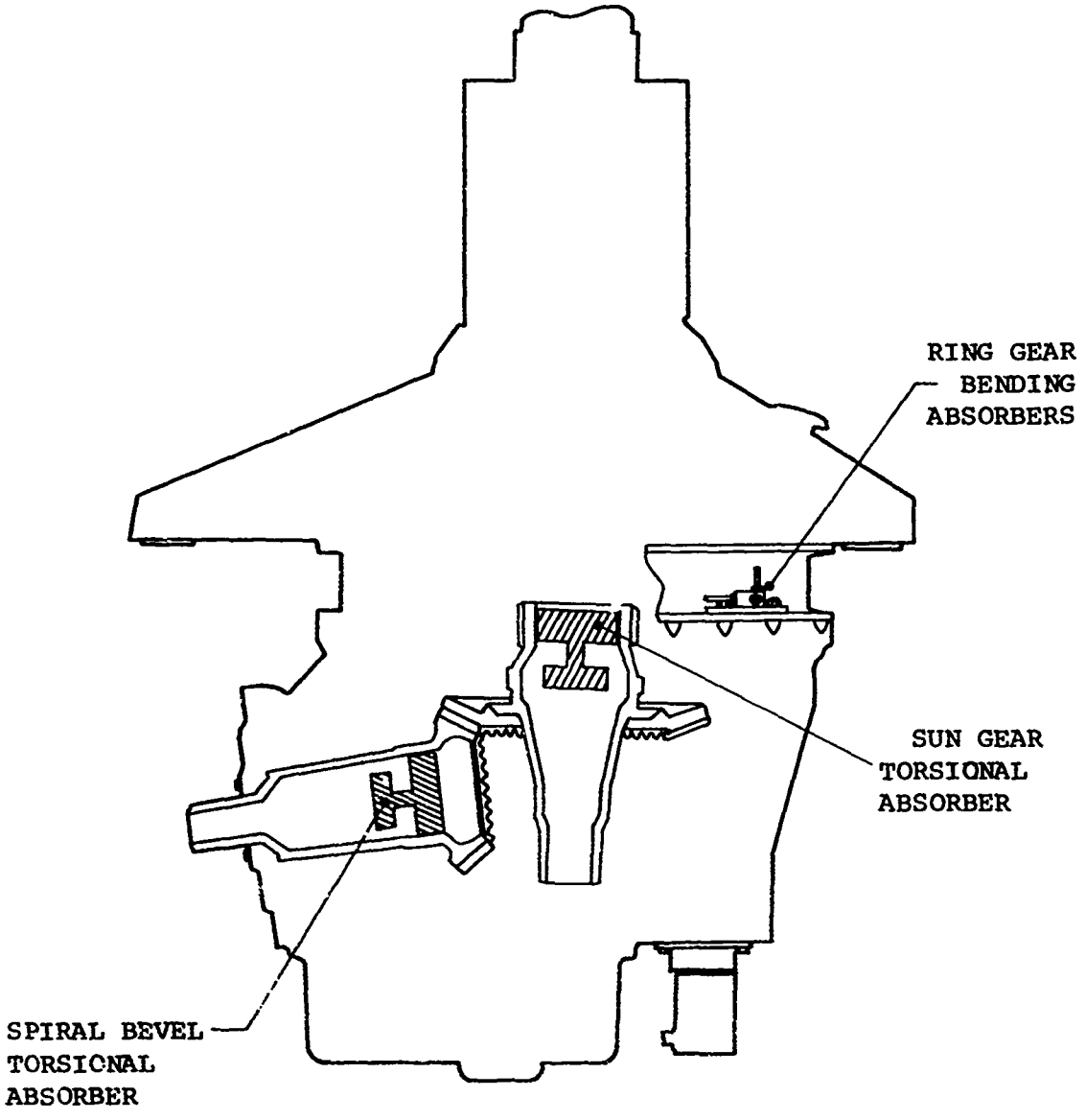

Figure 19. Absorber Locations.

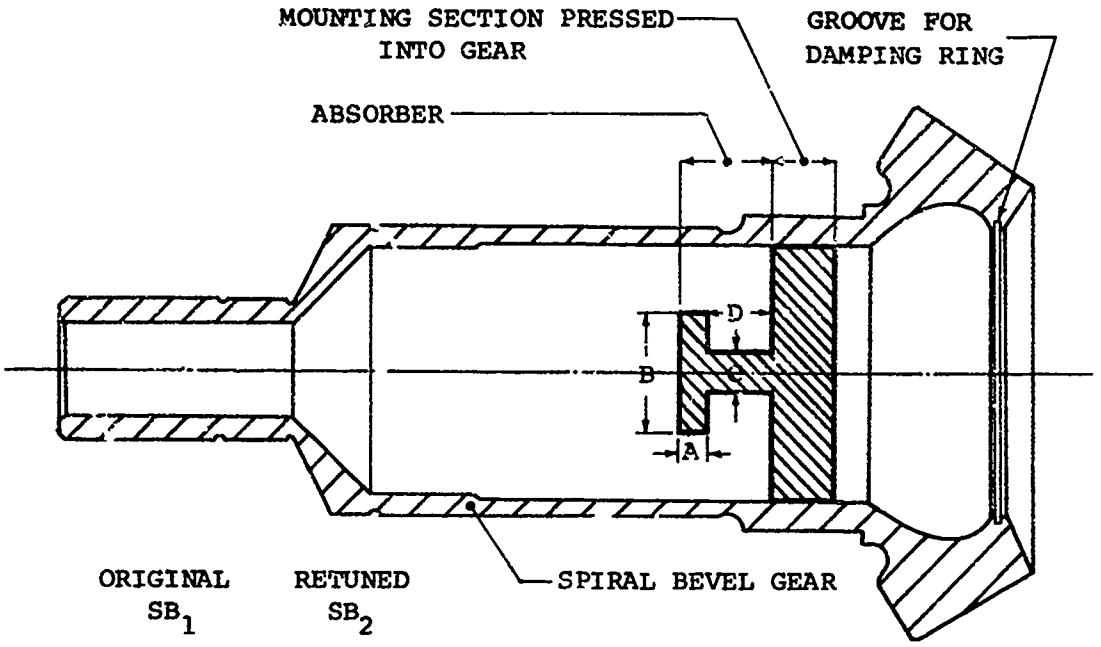

	ORIGINAL SB_1	RETUNED SB_2
A	.40"	.4035"
B	1.30"	1.802"
C	.60"	.585"
D	1.00"	.9895"
FREQ.	3410 Hz	3239 Hz

Figure 20. Spiral Bevel Absorber.

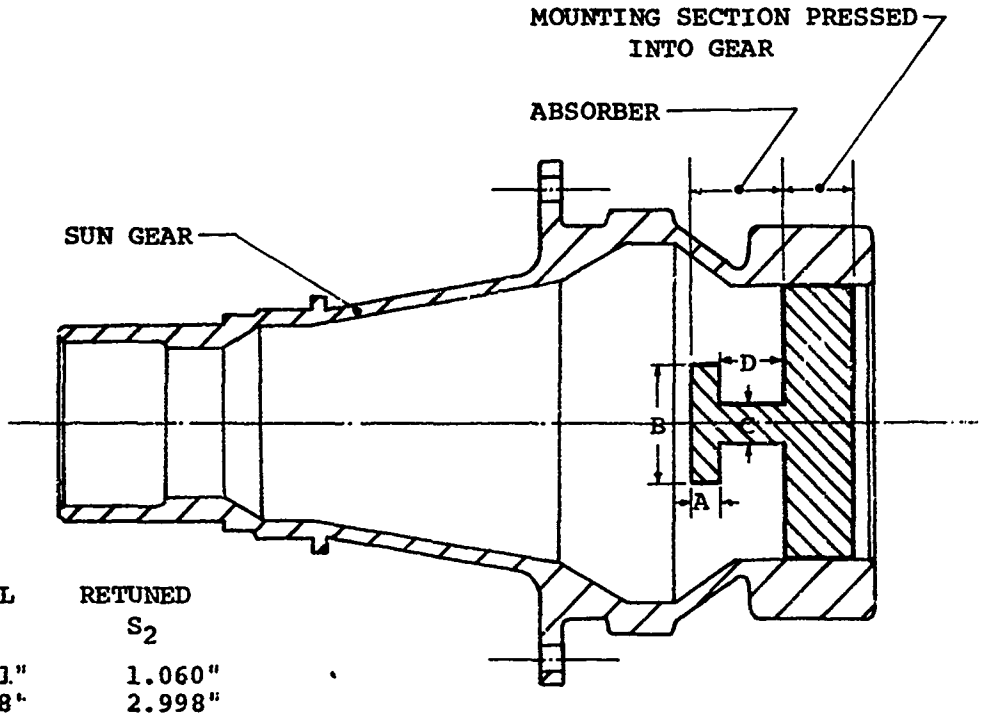

	ORIGINAL S_1	RETUNED S_2
A	1.061"	1.060"
B	2.998"	2.998"
C	1.004"	.9762"
D	1.987"	1.9875"
FREQ.	1501. Hz	1420. Hz

Figure 21. Sun Gear Absorber.

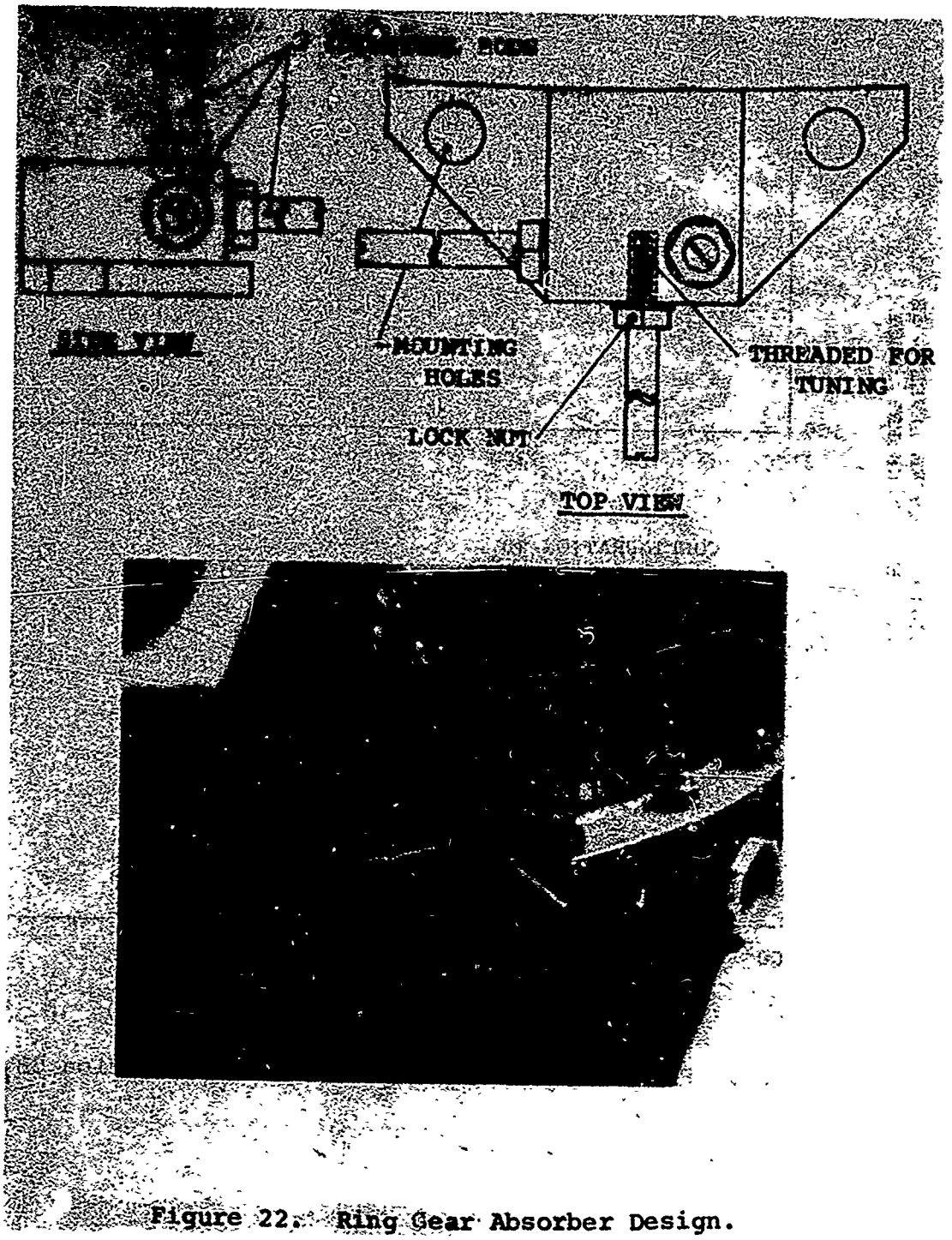

Figure 22. Ring Gear Absorber Design.

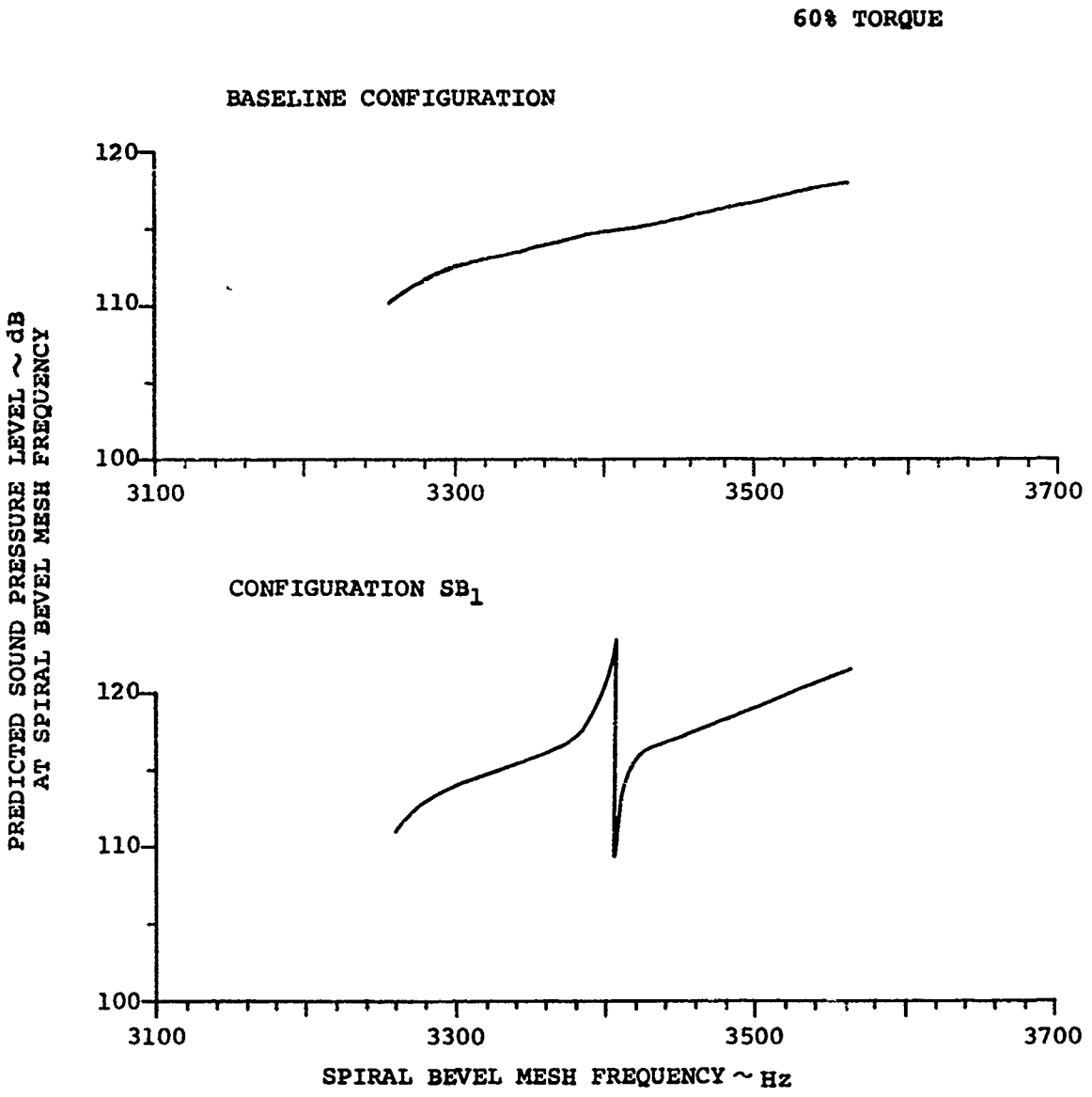

Figure 23. Predicted Noise Reduction - Configuration SB_1.

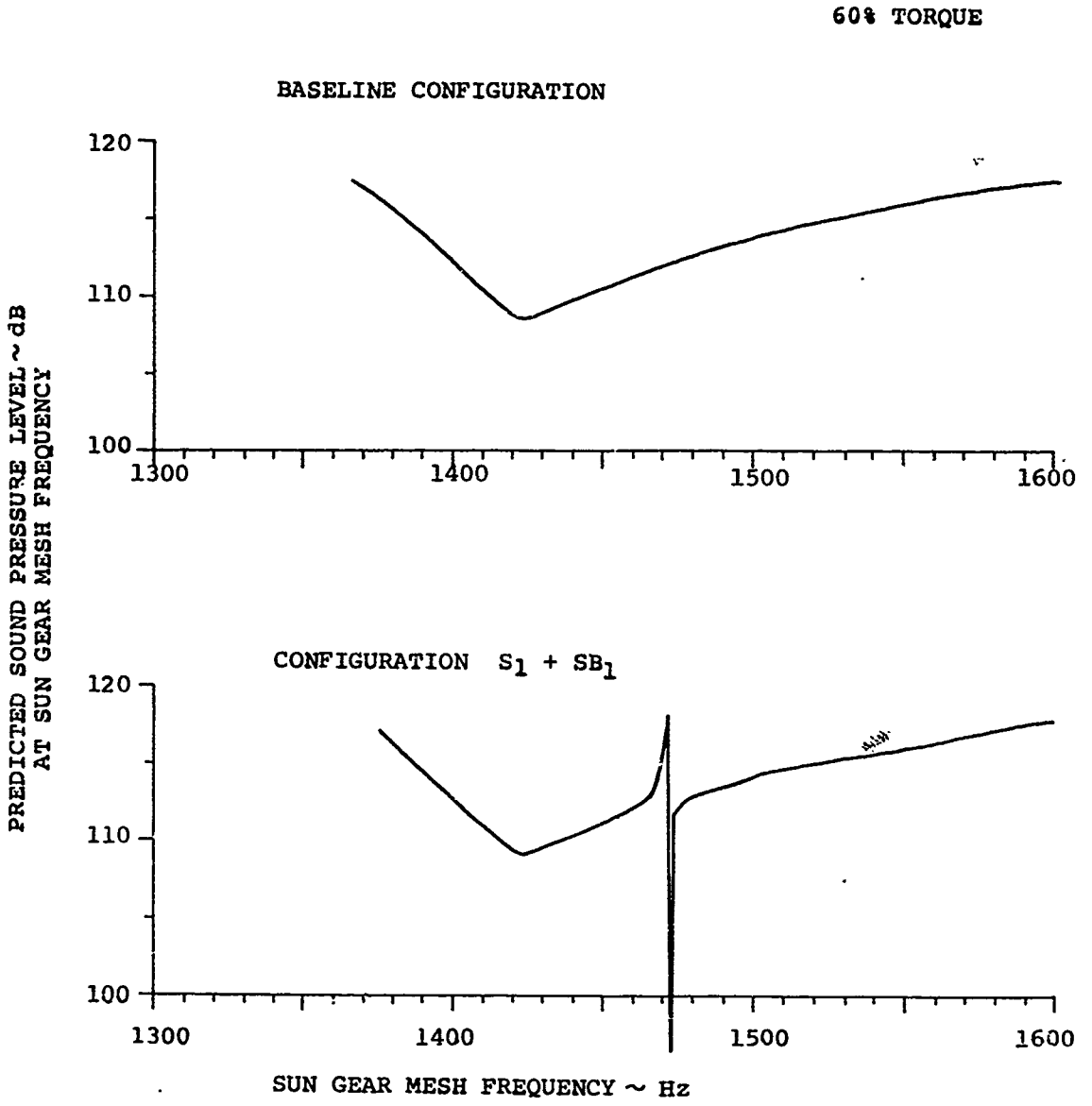

Figure 24. Predicted Noise Reduction - Configuration S_1 + SB_1.

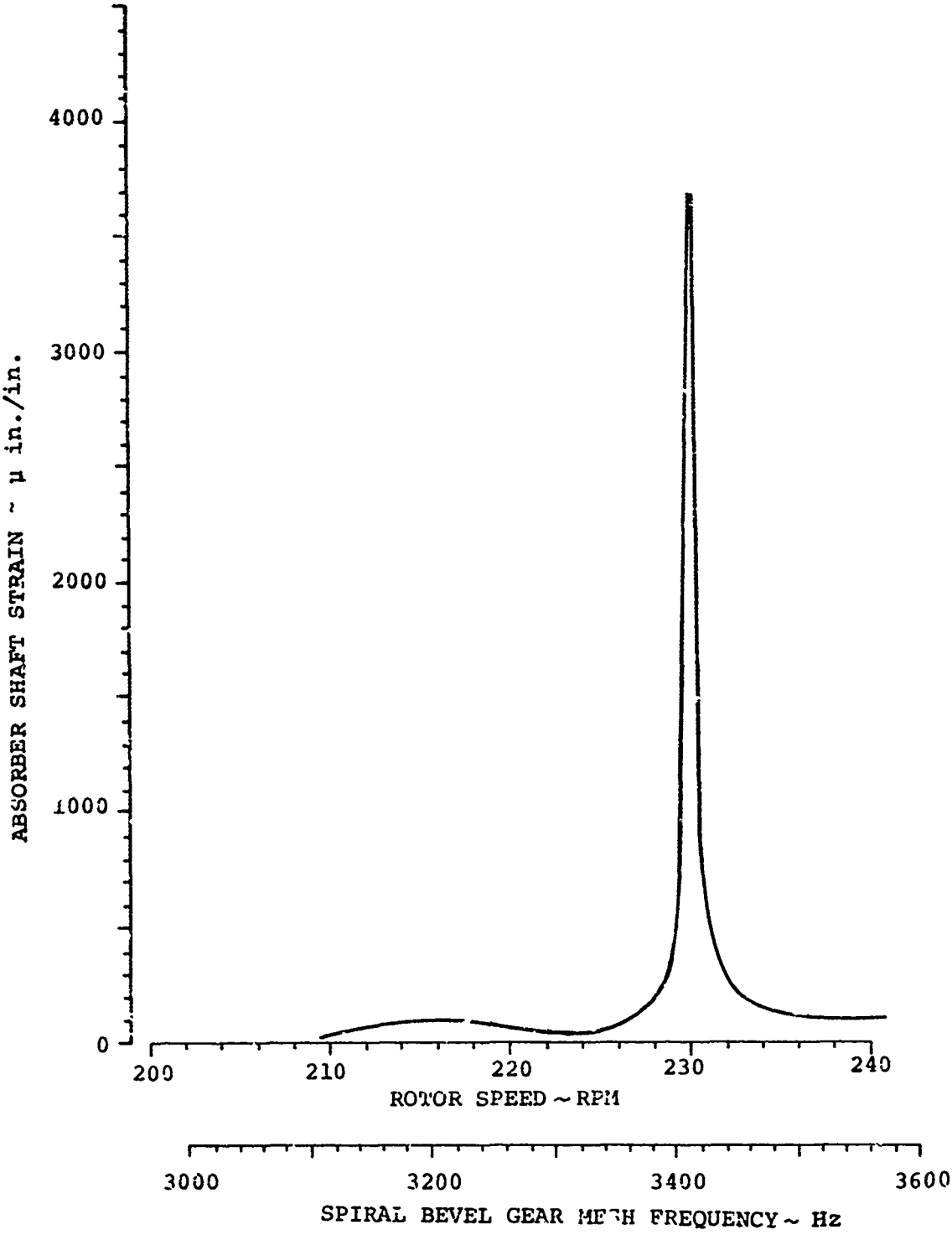

Figure 25. Predicted Spiral Bevel Absorber Response.

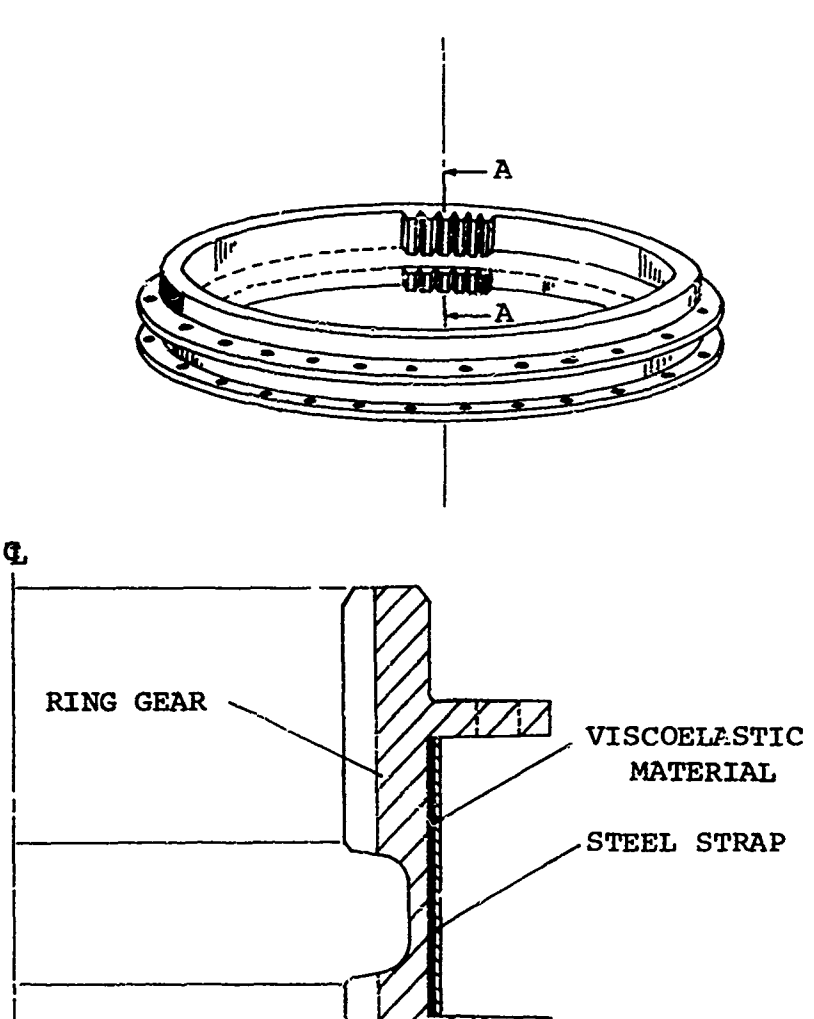

Figure 26. Cross Section of Damping Strap.

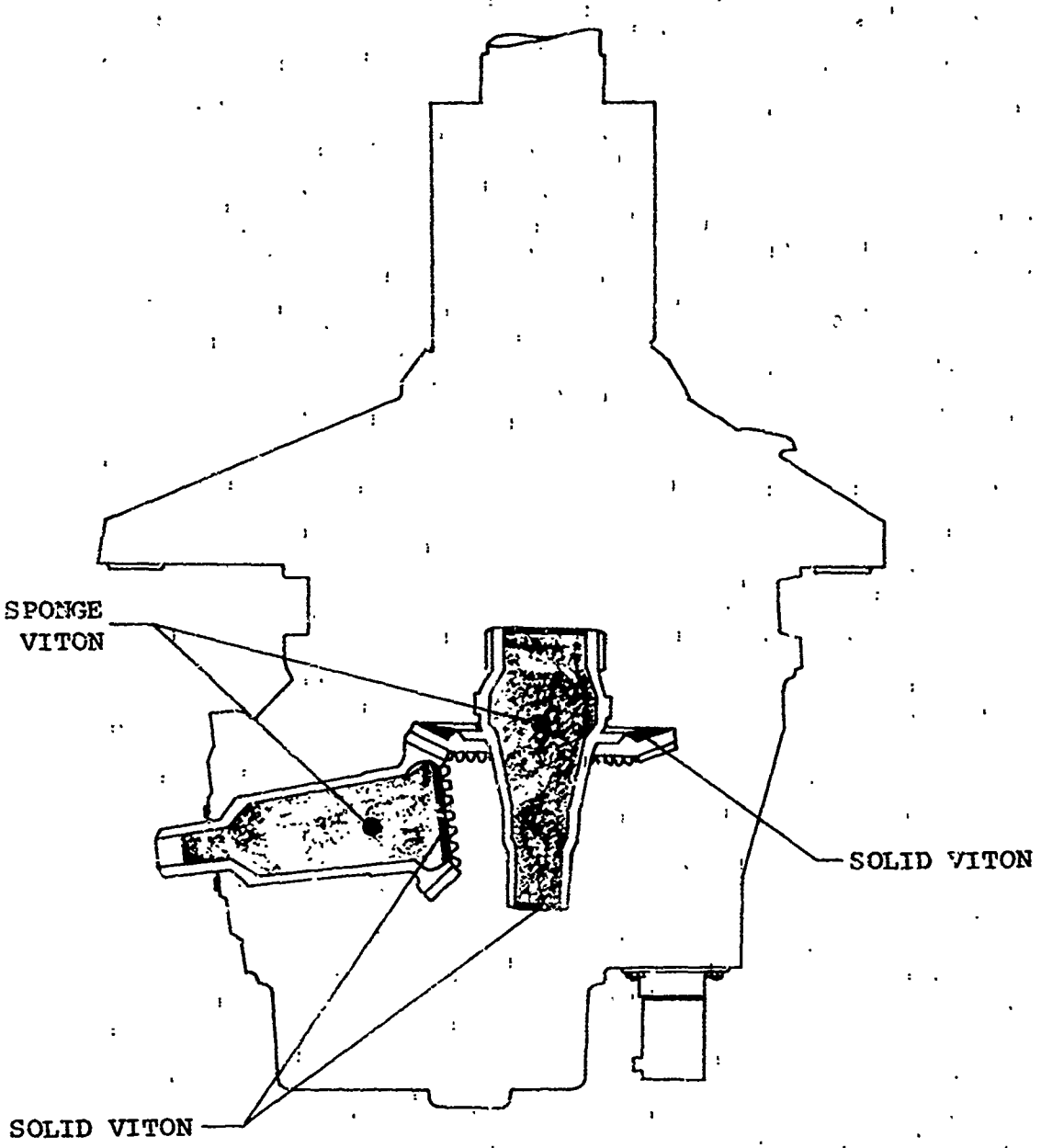

Figure 27. Gear Damping Treatment.

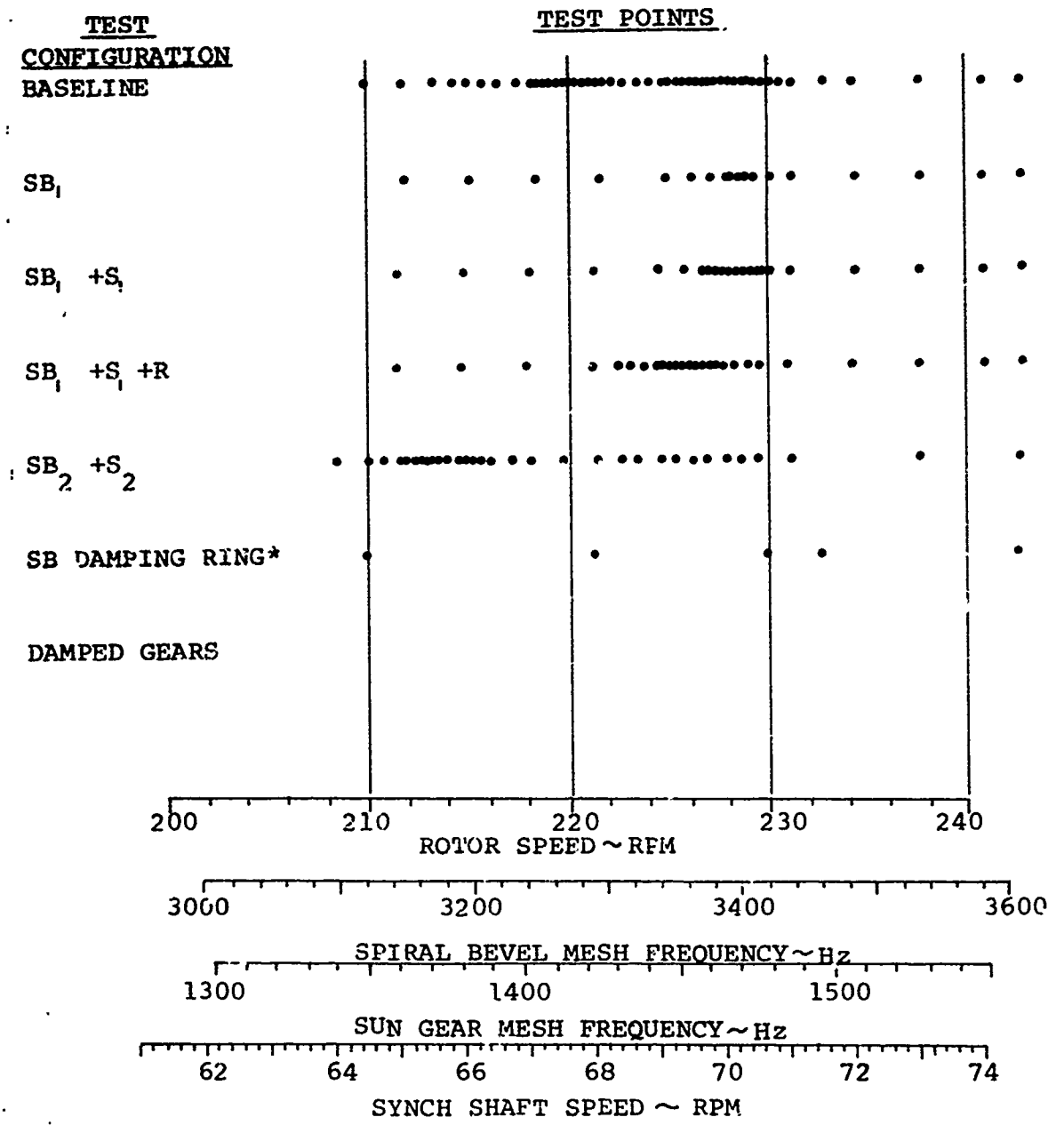

*ADDITIONAL POINTS AT: 4700, 5050, 5400, 5750, 6100 SYNCH SHAFT RPM

Figure 28. Matrix of Stabilized Points.

4.0 DISCUSSION OF RESULTS

4.1 DATA ANALYSIS

4.1.1 Stabilized Data

In order to properly interpret transmission noise data, narrow band analysis techniques are required. The data on this program were analyzed using a Federal Scientific UA-6 Ubiquitous Spectrum Analyzer (Figure 29(a)). This analyzer was used in a mode which gives a constant bandwidth of 10 Hz over the range of 0 to 5000 Hz.

4.1.2 Transmission Data Interpretation

A typical spectrum of the transmission vibration is shown in Figure 30. This data was taken from the ring gear accelerometer. The spectrum is dominated largely by pure tones which stand well above the background noise. These pure tones, as noted on the figure, are at tooth passage frequencies and their multiples.

It can be seen that not just one frequency is present for each tooth mesh, but many sidebands are also there. These sidebands are due to modulation of the center frequency. For instance, the sidebands in Figure 30 around the sun gear fundamental and second harmonic and spiral bevel gear are all separated from their center frequencies by 56 Hz. This is exactly the planet passage frequency (= rotational speed of the planet carrier in cycles/sec times the number of planets).

Since most of the vibrations at the ring gear are due to the planet ring mesh, each frequency is modulated by the planet's passing. The vibration signal is strong when the planet is close to the accelerometer and weaker when the planet goes away. Thus a sine wave of the planet-ring tooth mesh frequency will be amplitude modulated at the planet passage frequency:

$$A = (A \sin 2\pi f_p t) \cdot \sin 2\pi f_o t$$

where A = vibration amplitude on the ring gear

a = amplitude

f_p = planet passage frequency

f_o = tooth mesh frequency

Applying a standard trigonometry formula:

$$a = \frac{A}{2}\left\{\cos 2\pi (f_o - f_p)t - \cos 2\pi (f_o + f_p)t\right\}$$

Thus, when this is Fourier analyzed, the two sidebands appear at $f_o - f_p$ and $f_o + f_p$.

The vibration at another location is shown in Figure 31. This accelerometer was on the side of the transmission at location 2, near the spiral bevel gear. The sidebands on the spiral bevel mesh frequency are separated by 118 Hz rather than the planet passage period, 56 Hz. This is the frequency of rotation of the input pinion. Due to runout, the spiral bevel tooth forces are modulated at the rotational frequency, thus producing sidebands.

Note the low level of the sidebands at the planet passage period in Figure 31. Different locations on the transmission are excited by different mechanisms. The ring gear is closely excited by the planet-ring mesh and the lower case near location 2 by the spiral bevel bearings. Figure 32 shows spectra from all the accelerometer locations.

4.1.3 Speed Sweeps

Another method of looking at the data was to track a mesh frequency as the speed of the transmission was changed. The UA-6 analyzer was used as a tracking filter. The output was plotted on the vertical axis, and the tracking frequency was plotted on the horizontal axis (see Figure 29b). Figure 33 shows a typical plot produced with this method. In addition, several full spectra for points on the curve are shown. This illustrates how the sweep data was reduced.

4.1.4 Band-Pass Filter

In order to evaluate the effect of the damping treatments, it was necessary to obtain a measure of the energy included not only in the mesh frequency but also in the sidebands. For this purpose, a tunable, 500-Hz-wide, band-pass filter was used. With this filter simply centered near the desired mesh

frequency, it filtered out all but that frequency and the associated sidebands. This level was then simply read on a meter.

4.2 DYNAMIC ABSORBERS

4.2.1 Effect of the Spiral Bevel Absorber Only

During the initial portion of this test, a strain gauge on the smaller shaft of the spiral bevel absorber recorded the amplitude of the absorber. This curve is shown in Figure 34 along with the prediction copied from Figure 25. As predicted, the absorber goes into resonance at its pretuned frequency.

The noise and accelerometer data did not, however, demonstrate the predicted drop.

The data taken with the spiral bevel absorber installed are shown in comparison with the data with no absorber in Appendix II (spiral bevel mesh frequency). They show some differences probably due to the addition of the mass of the absorber but nothing that is as sharp as the tuned absorber spike.

4.2.2 Effect of Retuning the Spiral Bevel Gear Absorbers

In order to establish the dynamic effect of the absorbers as opposed to the mass and stiffness effects, the absorbers were retuned to a slightly different resonant frequency without appreciably altering the mass or the systems stiffness properties.

As can be seen from a comparison of the plots in Appendix II of the spiral bevel mesh frequency with the original absorbers ($SB_1 + S_1$) and the retuned absorbers ($SB_2 + S_2$), retuning the absorbers made no significant difference in the amplitude of the spiral bevel mesh frequency at any of the microphones or accelerometers. This may be due to the fact that the spiral bevel absorber reduces only the component of the force on the tooth acting circumferentially. If the gears were simple spur gears, then the noise levels would have been reduced. However, the spiral bevel gears have axial forces as well as circumferential forces, and the vibration from these axial forces transmitted through the thrust bearings to the case appears to be significant enough to override any reduction in the circumferential forces.

4.2.3 Effect of the Sun Gear Absorber

The effect of the sun gear absorber can be clearly seen in the data from accelerometer location 1. Figure 35 shows the comparison between the original and retuned absorber for this location. The dip in vibration is evident for both original and retuned absorbers. In examination of the data from all of the torques (see Appendix I), reductions from 20% to 55% in vibration levels are found. The closest microphone, location 10, is shown in Figure 36. The effect of the absorbers cannot be seen clearly. This is because the noise at location 10 is determined not only by the vibration of the transmission closest to it but also by the vibration from all the rest of the transmission.

Examination of the rest of the vibration data reveals that no other locations show the effect of the absorber as well as accelerometer 1, because the sun gear absorber only reduces the forces at the sun-planet mesh (see Figure 37). The planet-ring mesh forces are only slightly changed. Thus it would be expected that substantial reductions in vibration would be exhibited only at location where the vibration is determined by the sun gear bearings rather than by the ring gear. Thus the absorber effects are seen at location 1 of Figure 12, which is the most closely associated accelerometer with the sun gear bearings.

Examination of the noise data from location 10, Figure 13, indicates that the absorber produced from 2 to 8 dB reduction in noise. This is about what would be expected from the vibration data because 20% vibration reduction is about 2 dB and 55% is about 7 dB.

4.2.4 Effect of the Ring Gear Absorbers

The effect of the ring gear absorbers can be seen from a comparison of the ring gear absorber condition, SB_1+S_1+R, and the original torsional absorber condition, SB_1+S_1, in Appendix I, Figure63 . The effect is obscured by the presence of the sun gear absorber dip at the same frequency, as the ring gear absorbers were tuned to that frequency.

Comparison of the data from microphone location 8, the closest to the ring gear, shows from 0 to 2 dB reductions in noise.

4.3 DAMPING

4.3.1 Effect of the Spiral Bevel Snap Ring

The spiral bevel snap ring (Figure 20) produced a reduction in the spiral bevel mesh frequency of about 3 dB when the transmission was operating above 220 rotor RPM. Figure 38 shows this effect for the stabilized points. No effect was observed in the levels of the sun gear mesh frequency.

4.3.2 Effect of the Ring Gear Damping Strap

Figure 39 shows the only observed significant changes in the noise at the sun and spiral bevel frequencies due to adding the damping strap (Figure 26). Microphone location 8, the ring gear microphone, shows an average of 2.8 dB reduction at the spiral bevel mesh frequency. No significant reduction was observed at the ring gear microphone at the sun gear mesh frequency. This is consistent with the ring gear resonance modes calculated in Reference 9. A ring gear resonance was calculated to be between 4350 Hz and 2700 Hz depending on assumption of end fixity. The spiral bevel mesh frequency (between 3190 and 3600 Hz) is probably exciting that resonance. Because damping is more effective at or near resonance, the constrained layer damping strap was able to reduce the level of the noise at the spiral bevel mesh frequency and not at the sun gear frequency. However, the damping strap did reduce the noise at the sun gear mesh frequency at microphone location 10, near the side of the transmission (Figure 39). Although the planetary mesh noise was not reduced at the ring gear, it appears that the vibration which transmits through the transmission to the lower case is attenuated by the damping. The above results indicate the complexity of conduction and radiation of noise by a helicopter transmission case. The difficulty of interpreting these results indicates a need for further investigation in this area.

4.3.3 Effect of the Internal Gear Damping

Figure 40 shows the changes in the noise due to the addition inside the gears (Figure 27). The comparison shown is between the internal gear damping configuration and the ring gear strap configuration, since the ring gear strap was in place during both tests.

Noise reductions of up to 7 dB can be seen in the ring gear microphone (location 8) of the sun gear mesh frequency. However, an increase in the noise was observed in the spiral bevel frequency at microphone location 10. These contradictory results also indicate the need to investigate case vibration and radiation.

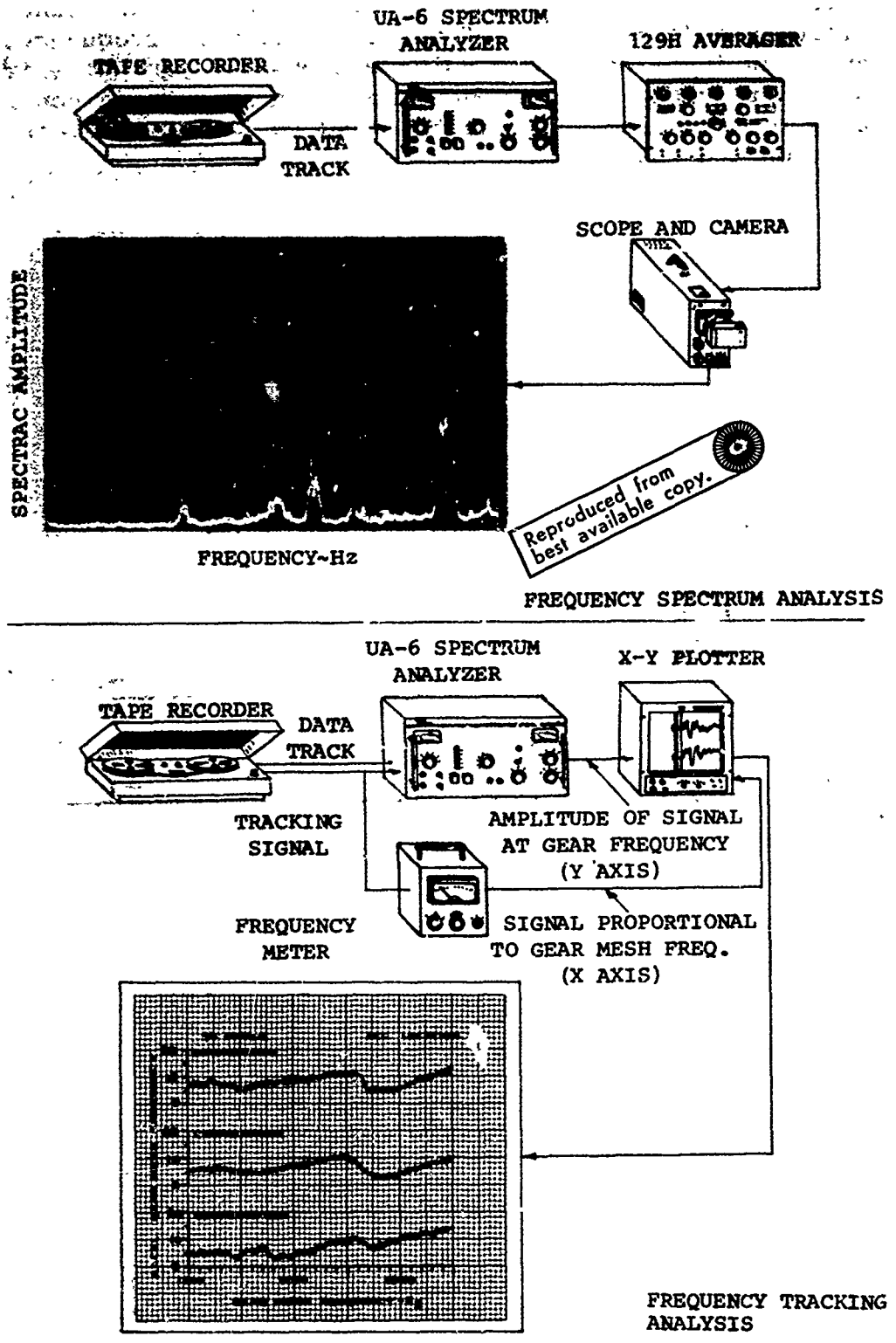

Figure 29. Frequency Spectrum and Tracking Analysis.

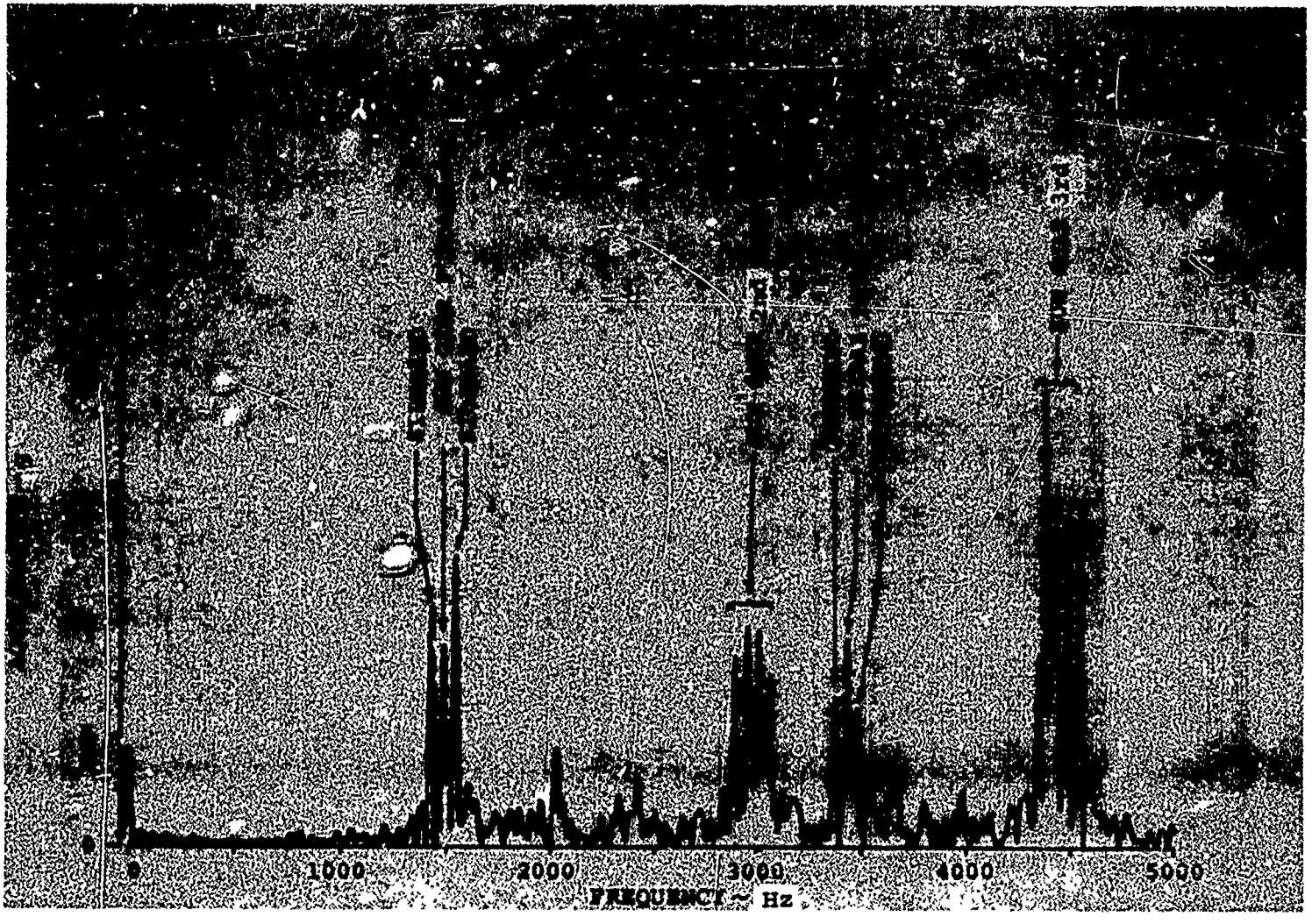

Figure 30. Typical Vibration Spectrum From Location 4.

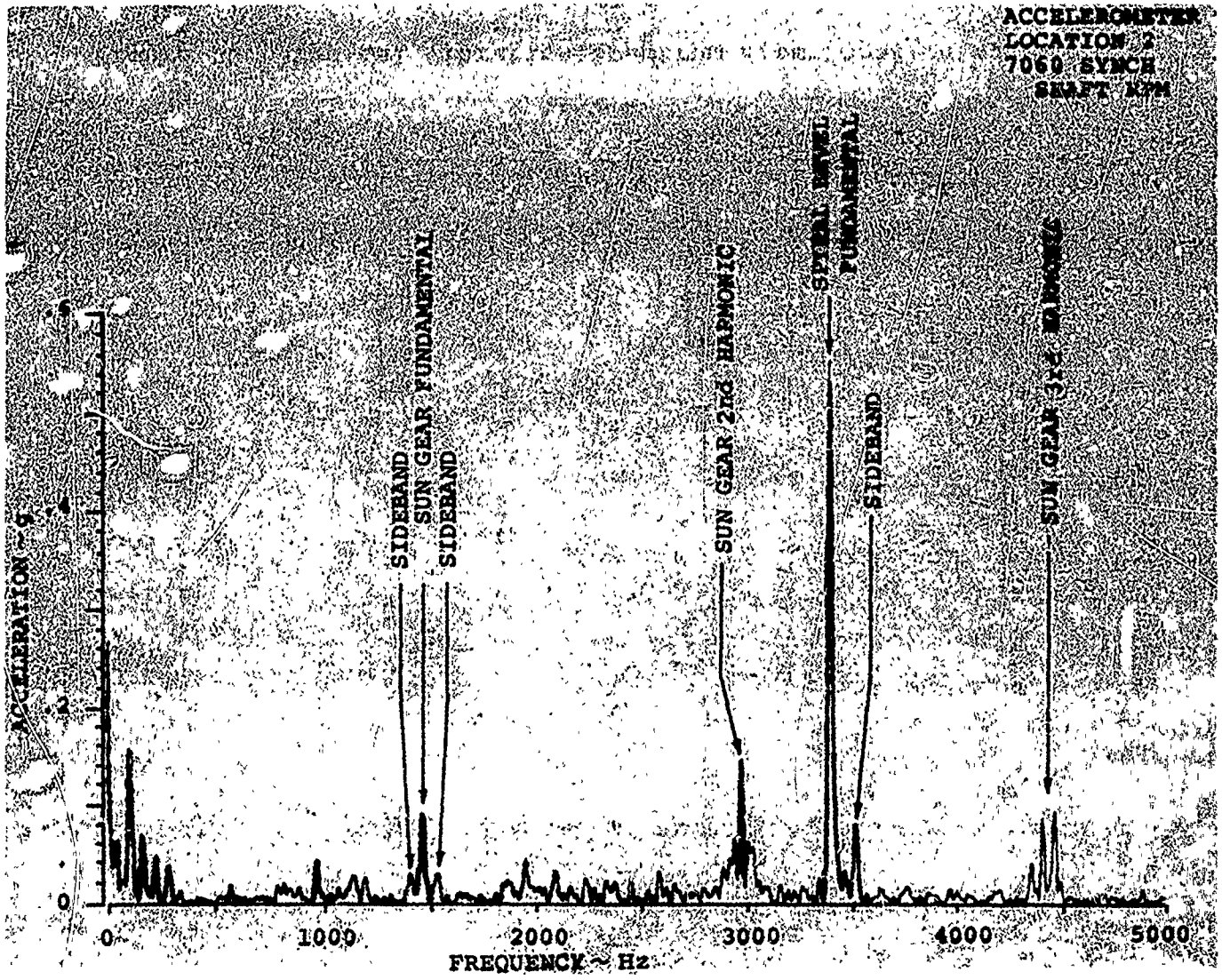

Figure 31. Typical Vibration Spectrum From Location 2.

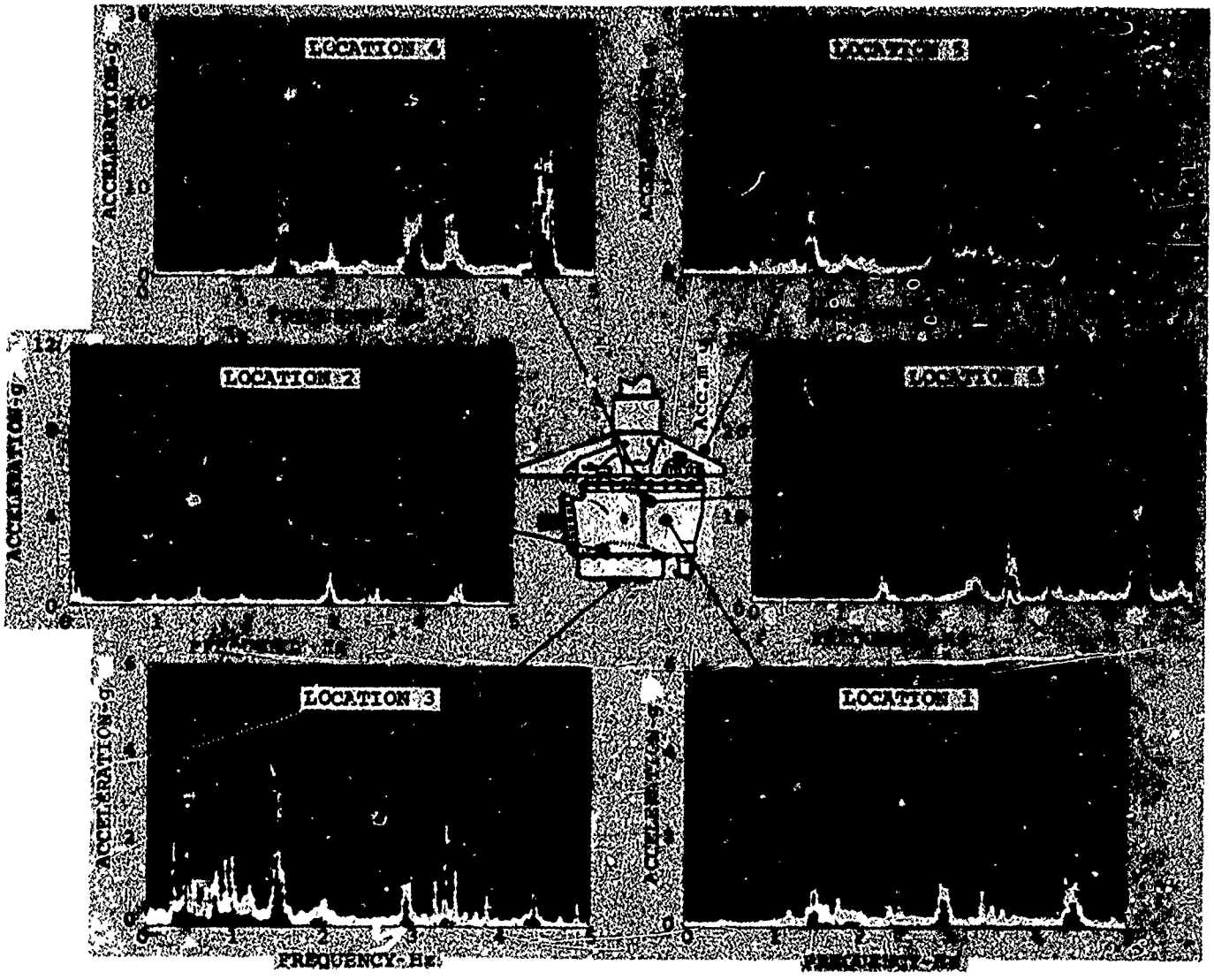

Figure 32. Vibration Spectra From All Locations.

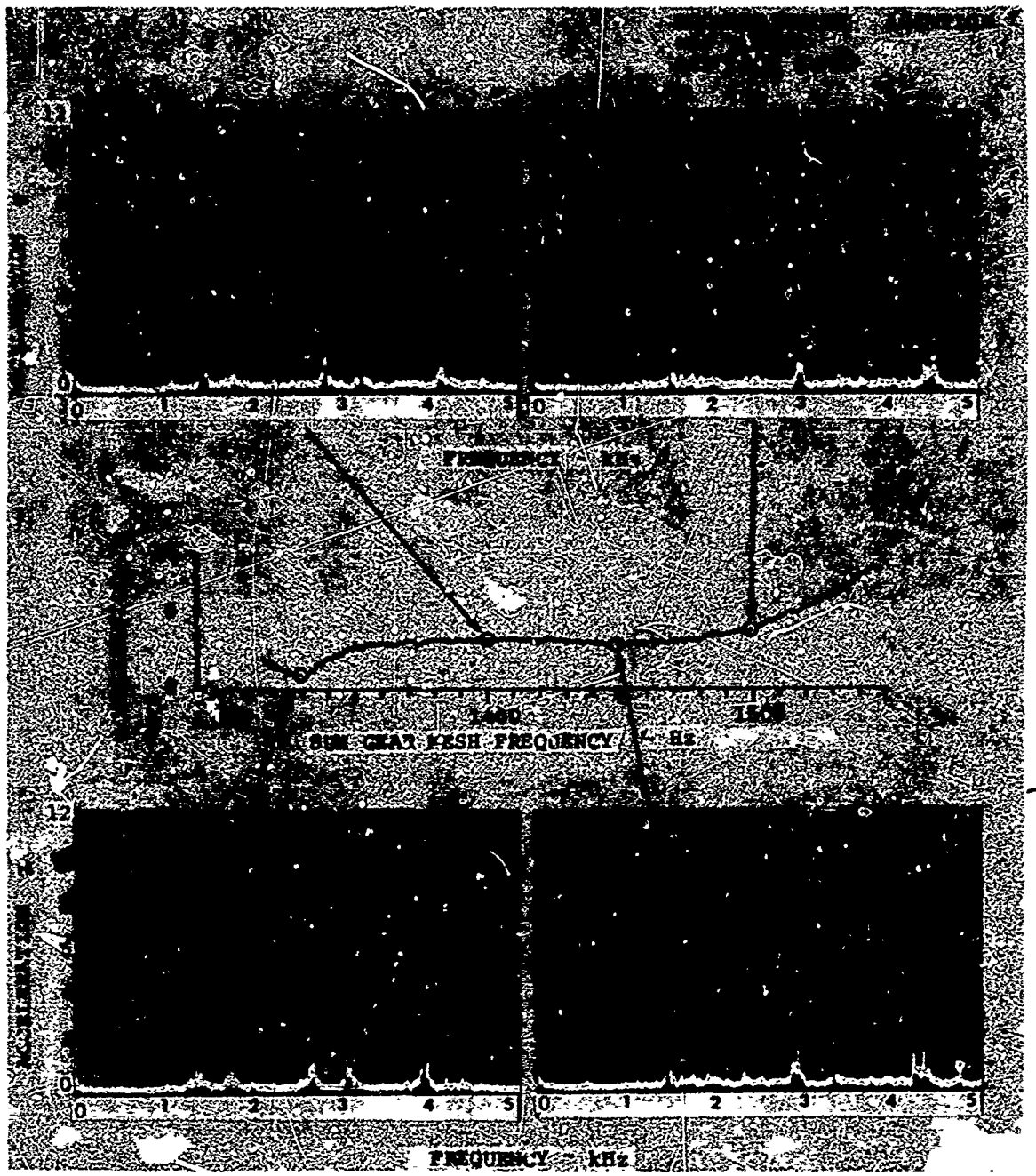

Figure 33. Baseline Sweep and Spectra.

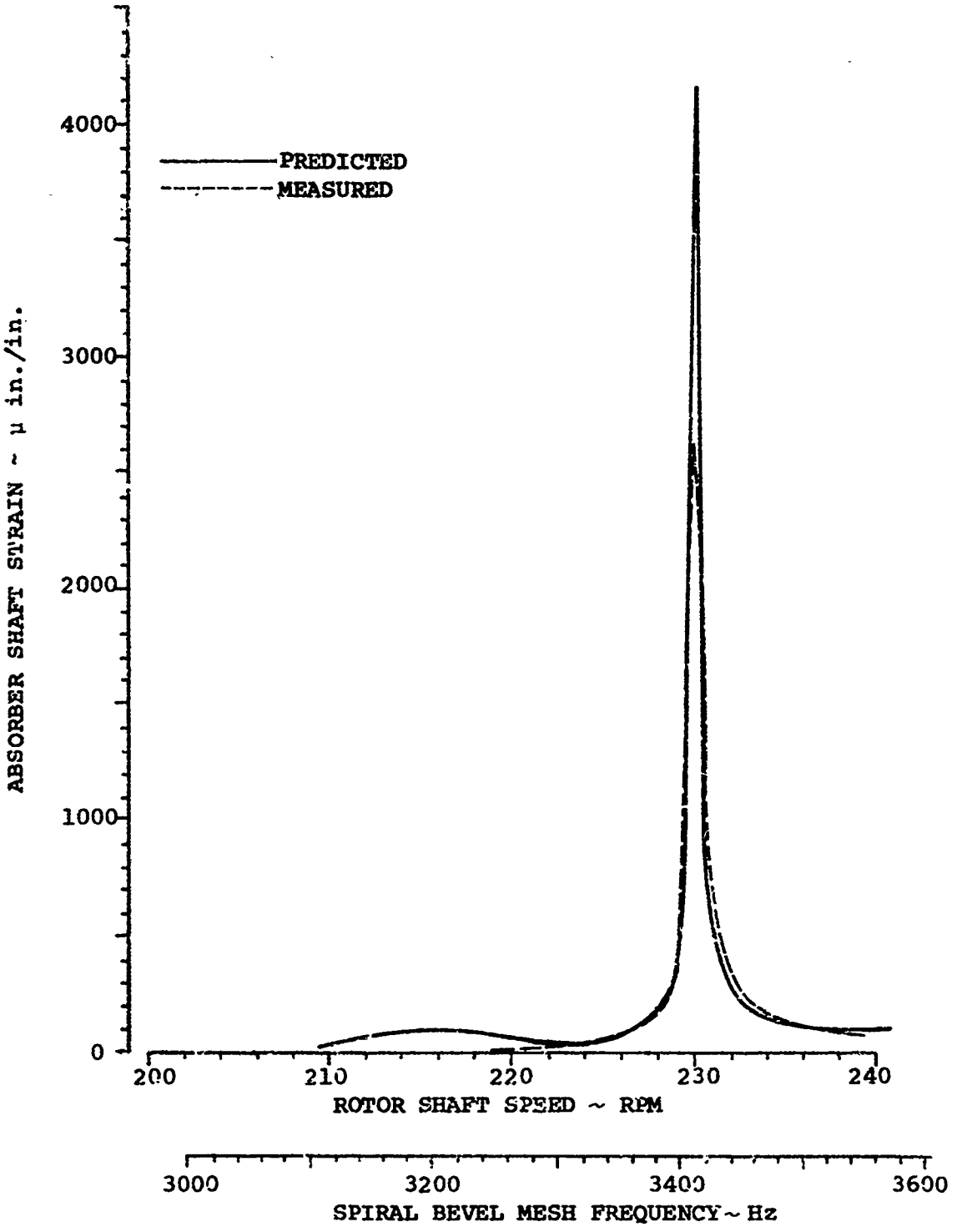

Figure 34. Comparison of Predicted and Measured Spiral Bevel Absorber Response.

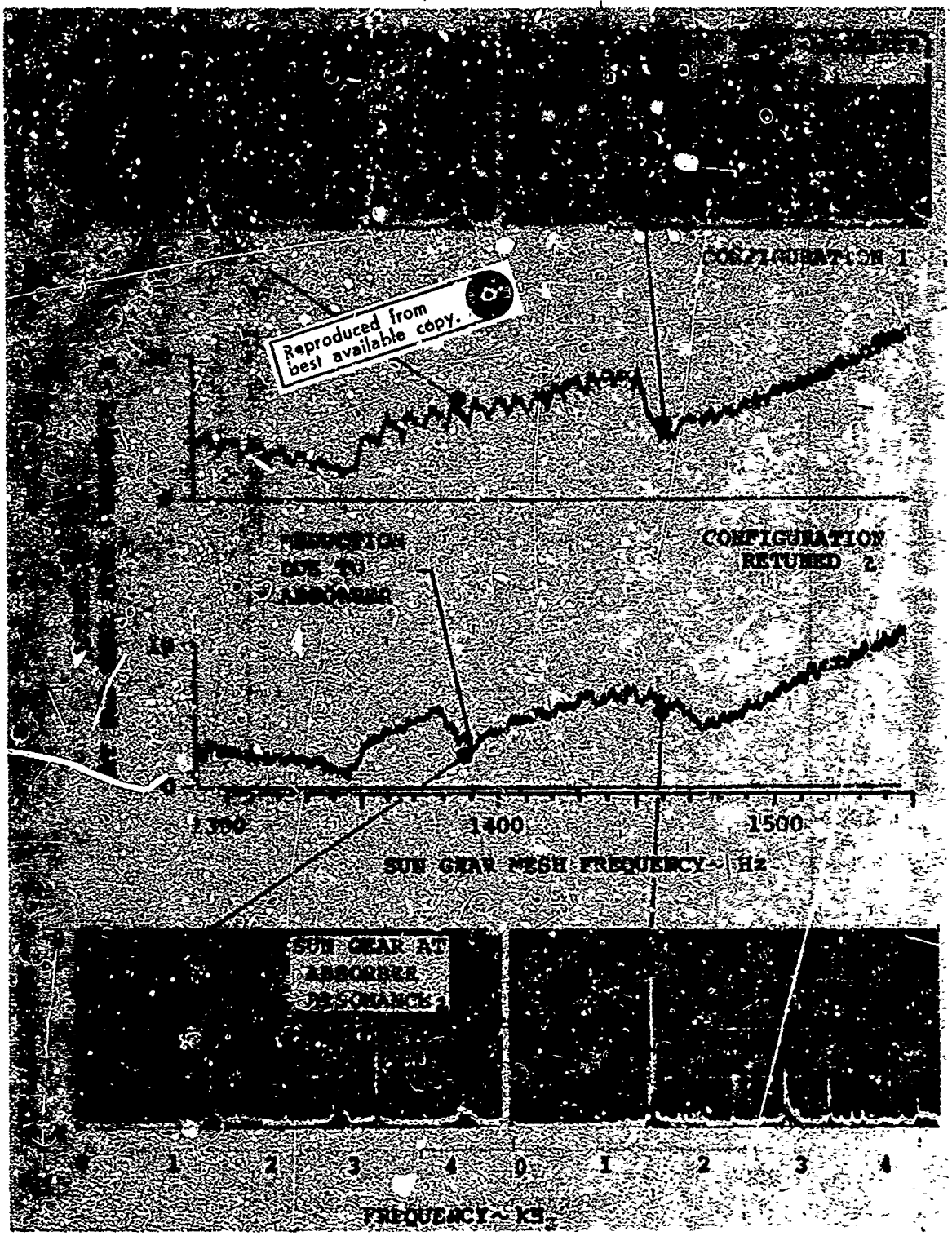

Figure 35. Effect of Retuning, the Sun Gear Absorber.

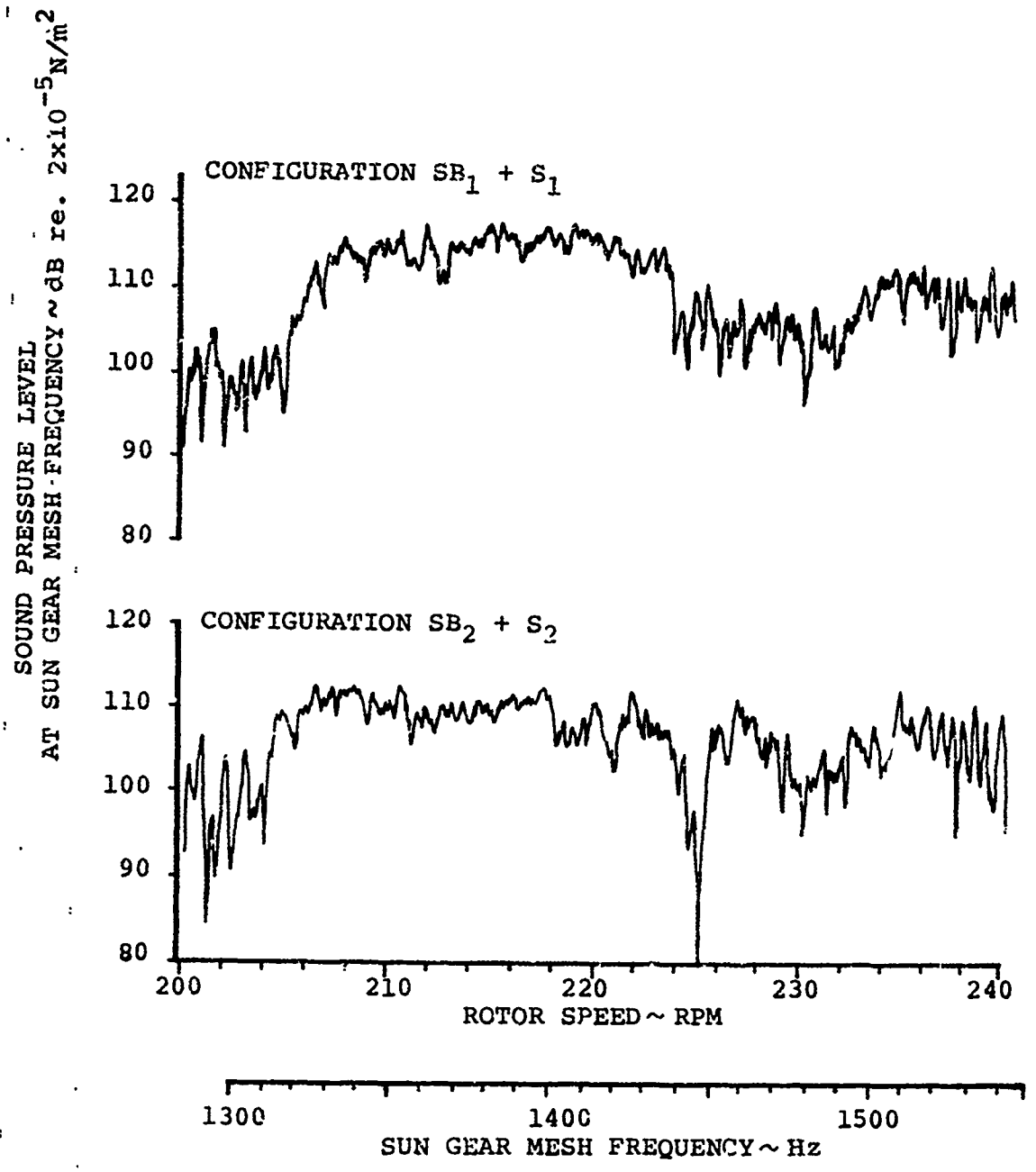

Figure 36. Effect on Noise of Retuning the Sun Gear Absorber.

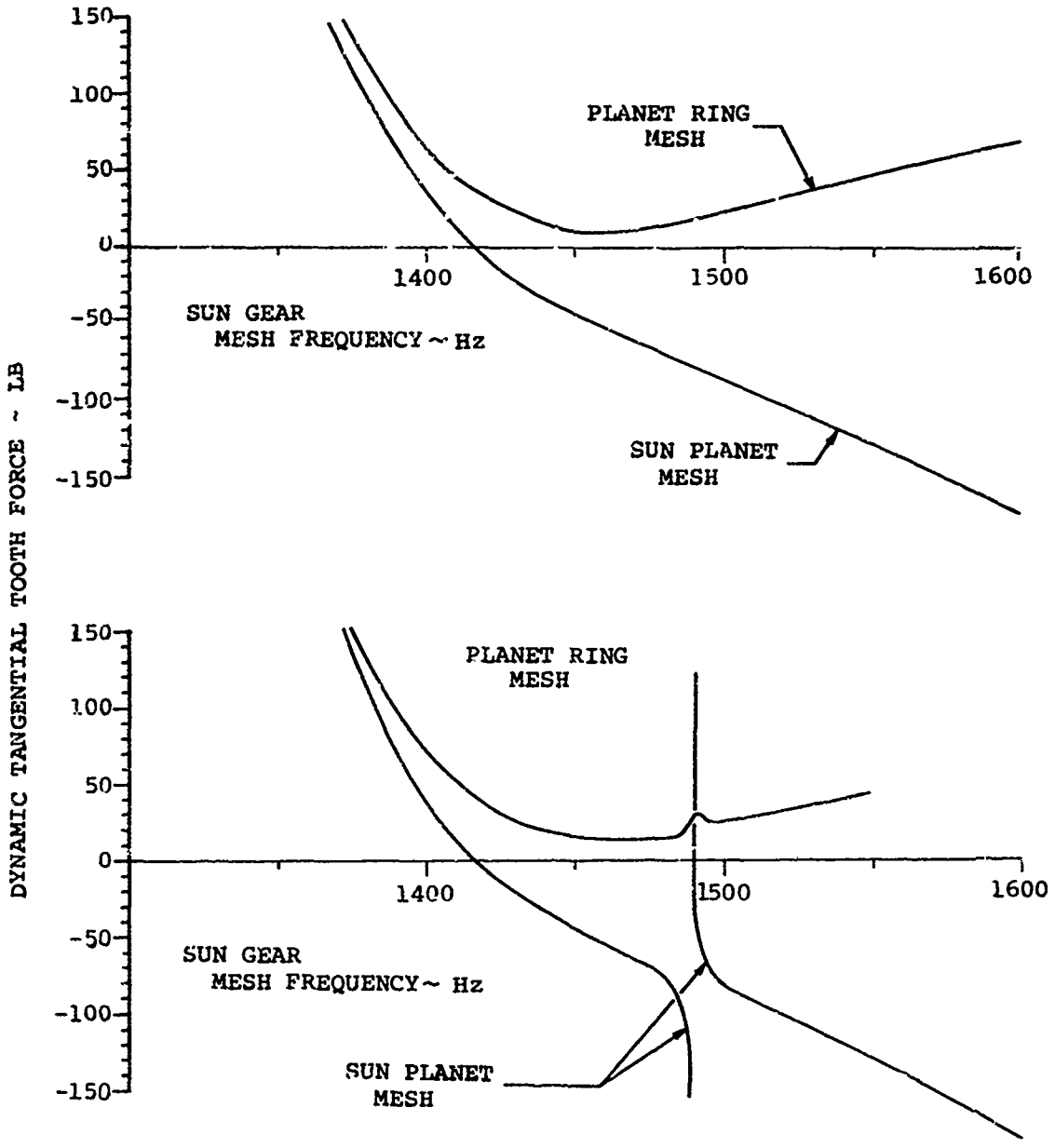

Figure 37. Prediction of Planetary System Mesh Forces.

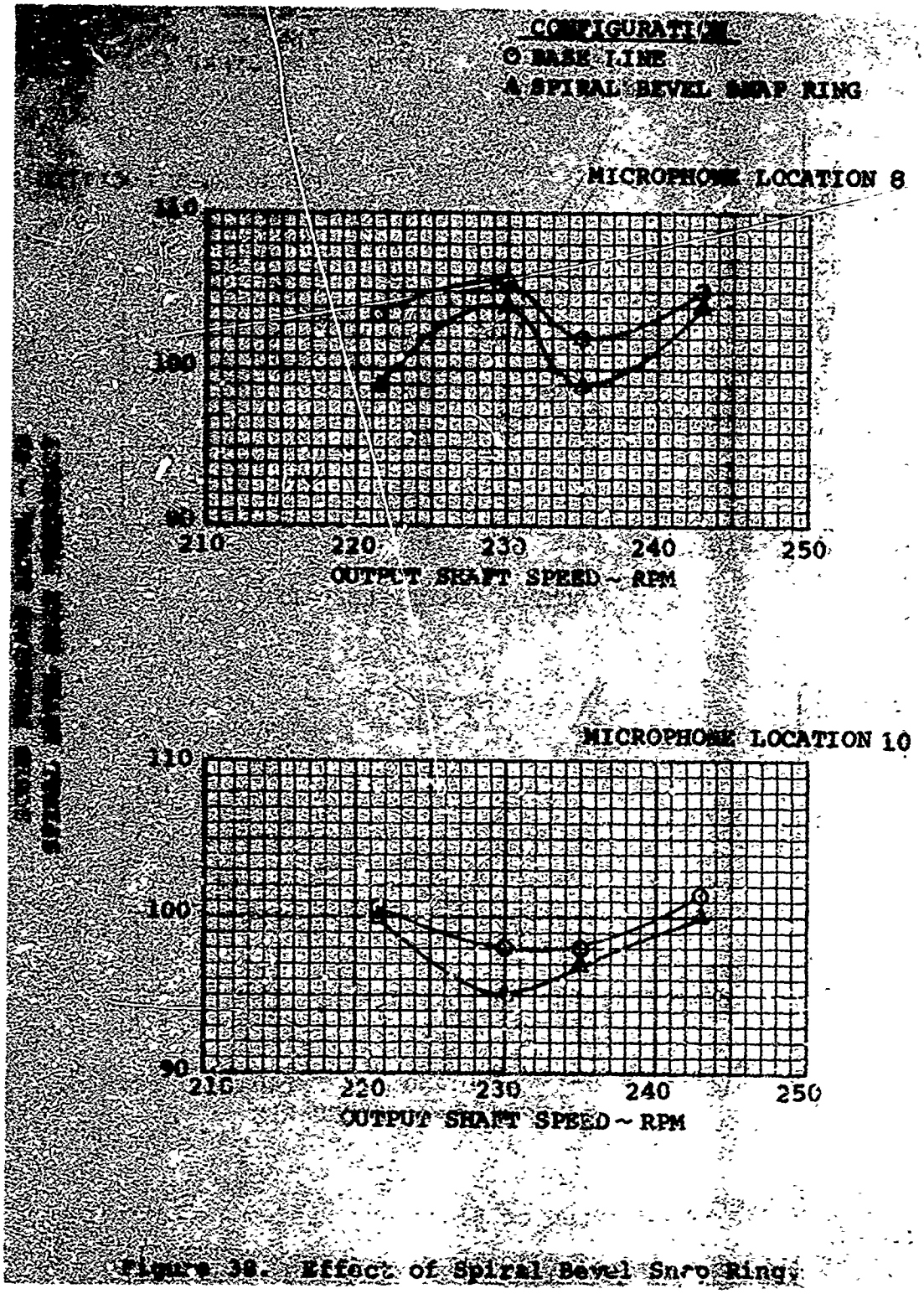

Figure 38. Effect of Spiral Bevel Snap Ring.

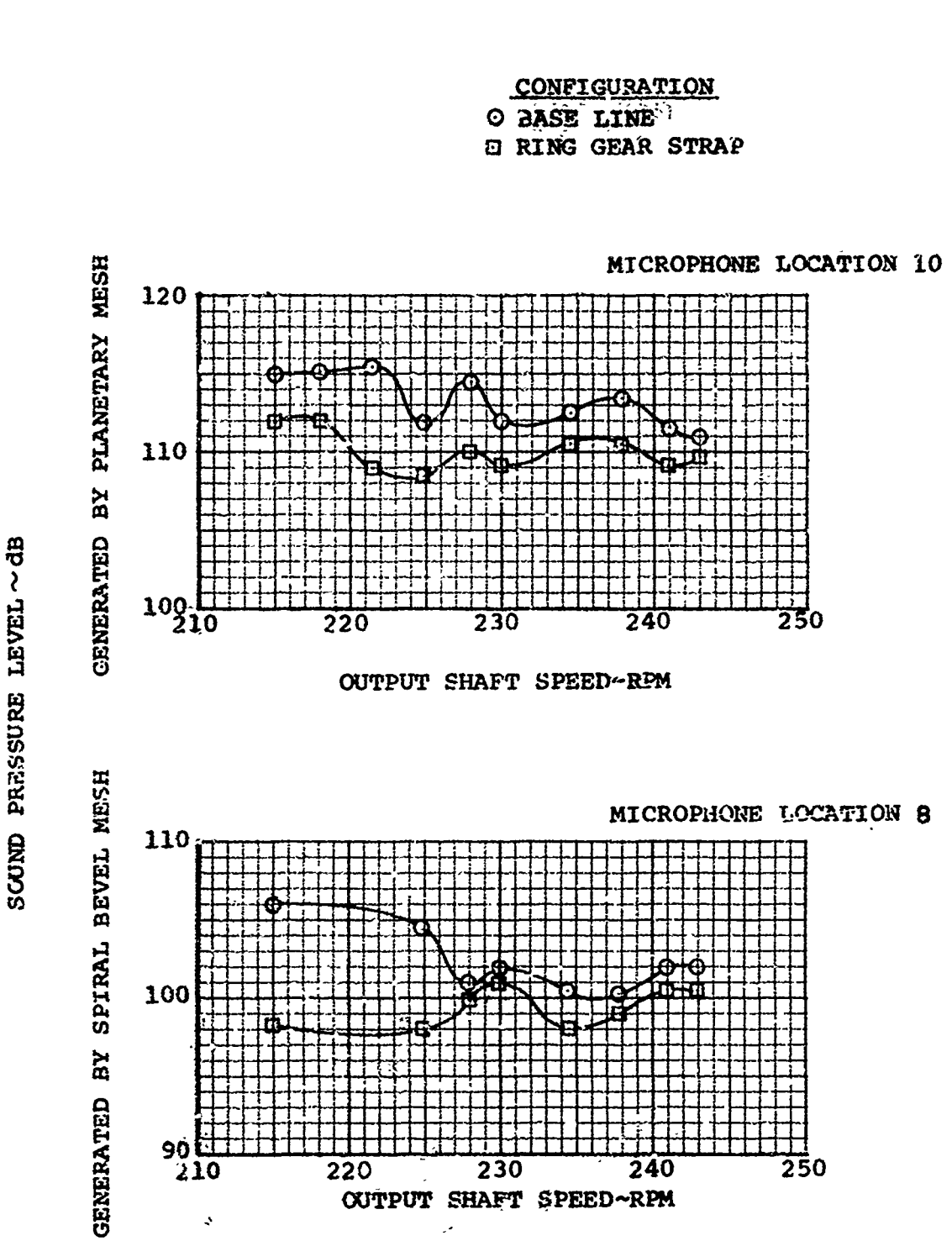

Figure 39. Effect of Ring Gear Strap.

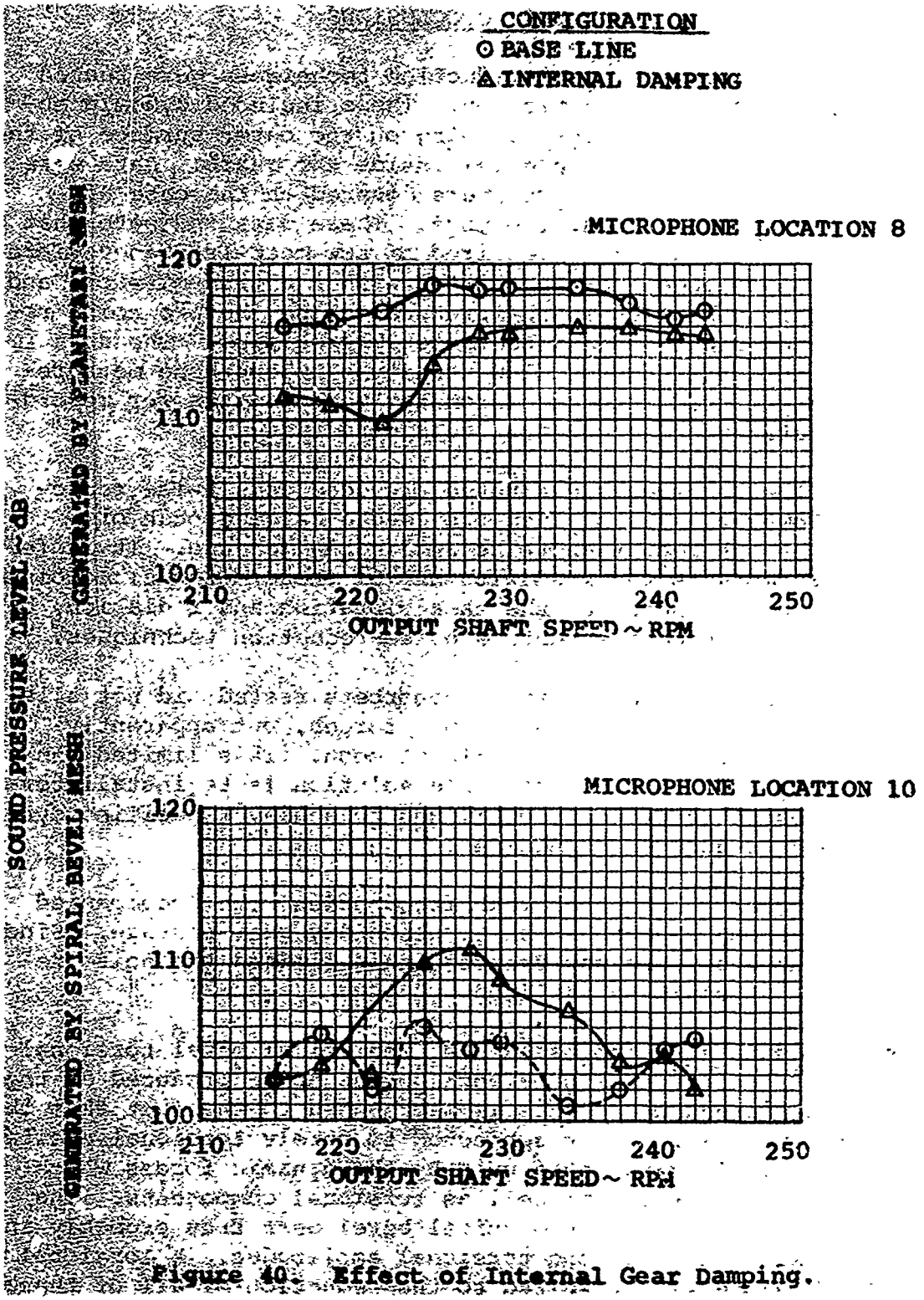

Figure 40. Effect of Internal Gear Damping.

5.0 CONCLUSIONS

Several transmission noise reduction techniques were tested in a CH-47 forward transmission. These included dynamic absorbers, constrained layer damping on the outer surface of the ring gear, and damping material inside the gears. Data were obtained both from accelerometers mounted on the case and microphones mounted near the case. These data indicate that a precise understanding is required of how mesh-frequency vibrations are produced and transmitted within a transmission, and of how this vibration energy produces noise, before noise reduction modifications can be properly specified. The data further indicate the very low utility of microphone measurements as compared with accelerometer measurements for recording of data under normal test cell conditions.

Each of the techniques evaluated provided some noise reduction. However, none of them provided a large enough or general enough reduction to be applicable for use. It is felt that more work is required with any of these methods, combined with an understanding of the case vibration and radiation, before they can become effective noise-reduction techniques.

The sun gear dynamic vibration absorbers tested did not alleviate the planet-ring mesh dynamic forces, but apparently only those forces at the sun-planet mesh. This limited the achievable reduction. A possible solution is to install torsional absorbers properly optimized to achieve specified dynamic force reduction objectives.

The ring gear fundamental mesh frequencies were accompanied by very strong sidebands due to planetary gear passage. Since these sidebands were not treated, this limited the noise reduction that could be realized.

The test data also indicated that the spiral bevel torsional absorber had little or no effect on the noise produced at the bevel mesh frequency. This is attributed to the fact that the spiral bevel gear is not subjected to purely torsional excitation, but is instead acted upon by the dynamic forces which have axial and radial as well as torsional components. The resulting vibration of the spiral bevel gear thus probably includes axial, radial, and torsional amplitudes. A torsional absorber alone is not suited to the reduction of all of these components.

Constrained layer damping used on the outside of the ring gear reduced the noise by 3 db at the spiral bevel mesh frequency for the microphone near the ring gear. This was attributed to a ring gear resonance near the spiral bevel frequency, but may be due to reduction of noise emitted directly for the ring-gear surface itself because of the presence of the damping material. Little or no reduction was noted in the ring-gear mesh frequency noise components, which are the most severe. This result indicates the importance of understanding case vibration modes in attempting to achieve noise reduction through case damping. Damping is more useful near resonances.

Because the case vibration and radiation properties affect the sound level measured at all locations, the internal gear damping treatment could not be evaluated. It produced both amplification and reduction of the noise depending upon microphone location, mesh frequency, and transmission speed. A program to evaluate the transmission case vibration and radiation properties must be conducted before these results can be properly interpreted. Such a program should incorporate direct measurements of the important gearbox component vibrations, by means of accelerometers, proximity probes, or strain gages.

6.0 LITERATURE CITED

1. Schaeffer, E. G., and Sternfeld, H., STUDY TO REVISE MIL-S-6144 GENERAL SPECIFICATION FOR INSTALLATION OF SOUNDPROOFING FOR AIRCRAFT, Vertol Division, The Boeing Company, R-346, Bureau of Naval Weapons, Department of the Navy, Airborne Equipment Division, Washington, D.C., March 1964.

2. Laskin, I., Orcutt, F.K., and Shipley, E. E., ANALYSIS OF NOISE GENERATED BY UH-1 HELICOPTER TRANSMISSION, Mechanical Technology Incorporated, USAAVLABS TR 68-41, U. S. Army Aviation Materiel Laboratories, Ft. Eustis, Va., June 1968, AD675457.

3. Sternfeld, H., Spencer, R.H., and Schaeffer, E.G., STUDY TO ESTABLISH REALISTIC ACOUSTIC DESIGN CRITERIA FOR FUTURE ARMY AIRCRAFT, Vertol Division, The Boeing Company, TREC TR 61-72, U. S. Army Transportation Research Command, Ft. Eustis, Va., June 1961.

4. Bolt, Beranek, and Newman, Inc., NOISE EVALUATION AND NOISE CONTROL RECOMMENDATIONS FOR PIASECKI H-21 HELICOPTER, BBN Report 355, January 1956.

5. Schaeffer, E.G., and Desaulniers, C., EFFECT OF DAMPING AND BLANKETING ON AIRFRAME RADIATED NOISE OF HELICOPTERS, The Boeing Company, Vertol Division Report D8-1031, December 1967.

6. Nichols, R.H., Sleeper, H.P., Wallace, R.L., and Ericson, H.L., ACOUSTICAL MATERIALS AND ACOUSTICAL TREATMENT FOR AIRCRAFT, J. Acoustical Soc. of Am., Vol. 19, Number 3, May 1947.

7. Federal Test Method Std. No. 406, Taber Abrasion Wear Test Method 1091, October 5, 1961.

8. Den Hartog, J.P., MECHANICAL VIBRATIONS, pg. 97-103, McGraw Hill Book Company, New York.

9. Badgley, R.H., and Laskin, I., PROGRAM FOR HELICOPTER GEARBOX NOISE PREDICTION AND REDUCTION, Mechanical Technology Incorporated, USAAVLABS TR 70-12, U. S. Army Aviation Materiel Laboratories, Ft. Eustis, Va., March 1970, AD869822.

10. Badgley, Robert H., and Chiang, Thomas, INVESTIGATION OF GEARBOX DESIGN MODIFICATIONS FOR REDUCING HELICOPTER GEARBOX NOISE, Mechanical Technology Incorporated, USAAMRDL TR 72-6, U. S. Army Air Mobility Research and Development Laboratory, Ft. Eustis, Va., March 1972.

APPENDIX I
SWEEP DATA FOR SUN GEAR MESH FREQUENCY

This appendix contains plots of the amplitude of the sun gear mesh frequency during transmission speed sweeps. These are presented for each transducer and absorber configuration at selected torque values.

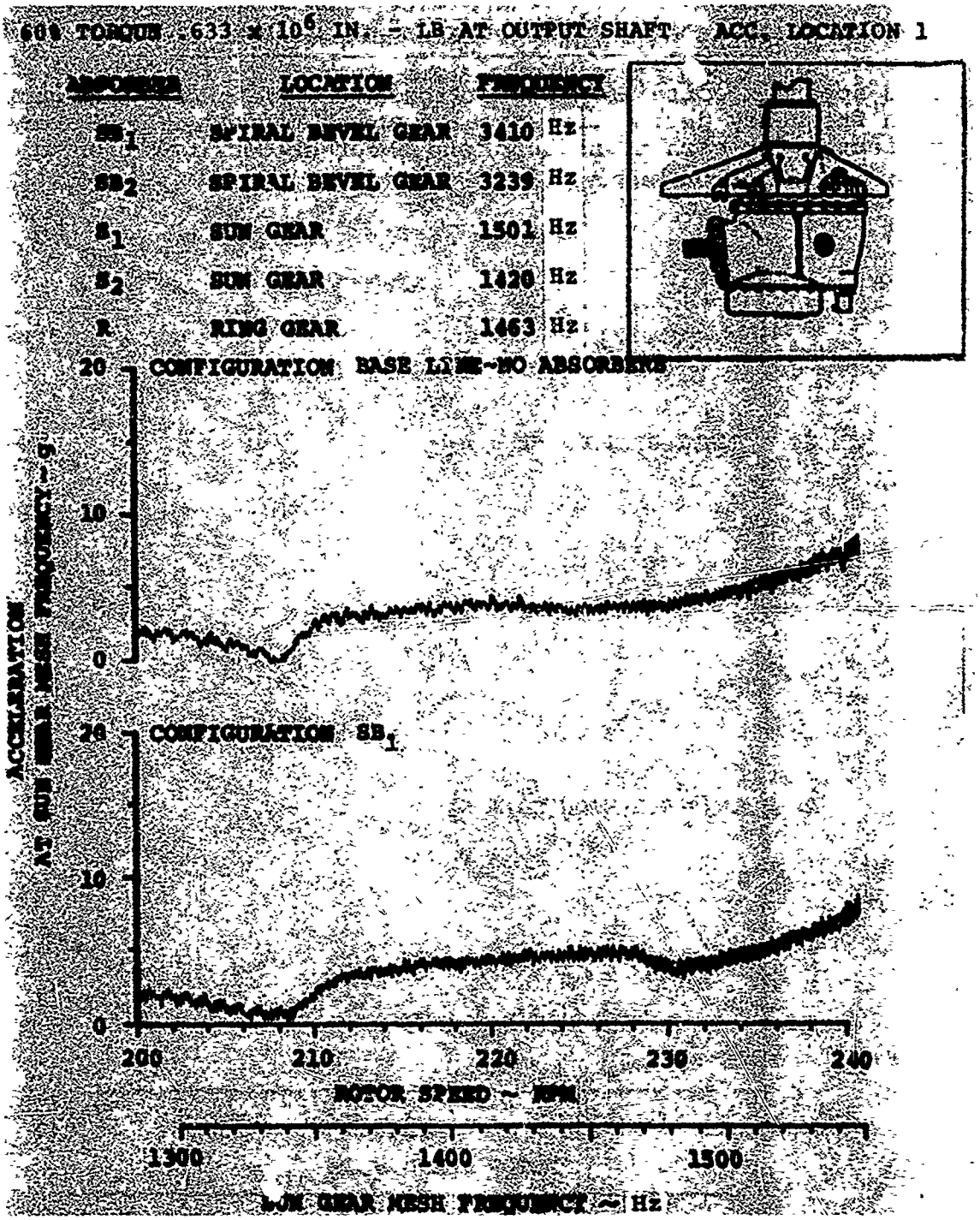

Figure 41. Sun Gear Sweep Data, Acc. Location 1, Torque 60%.

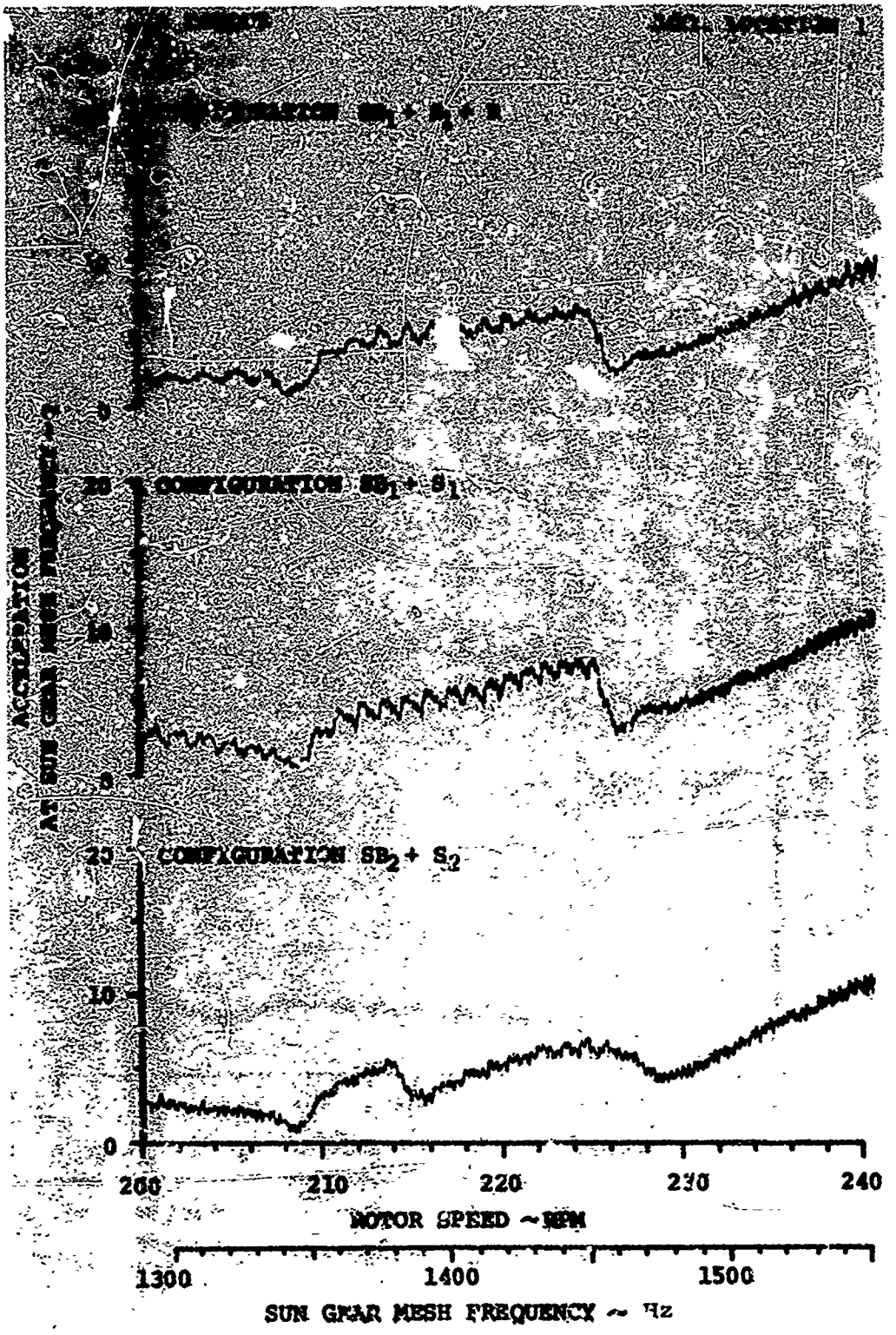

Figure 41. (Continued)

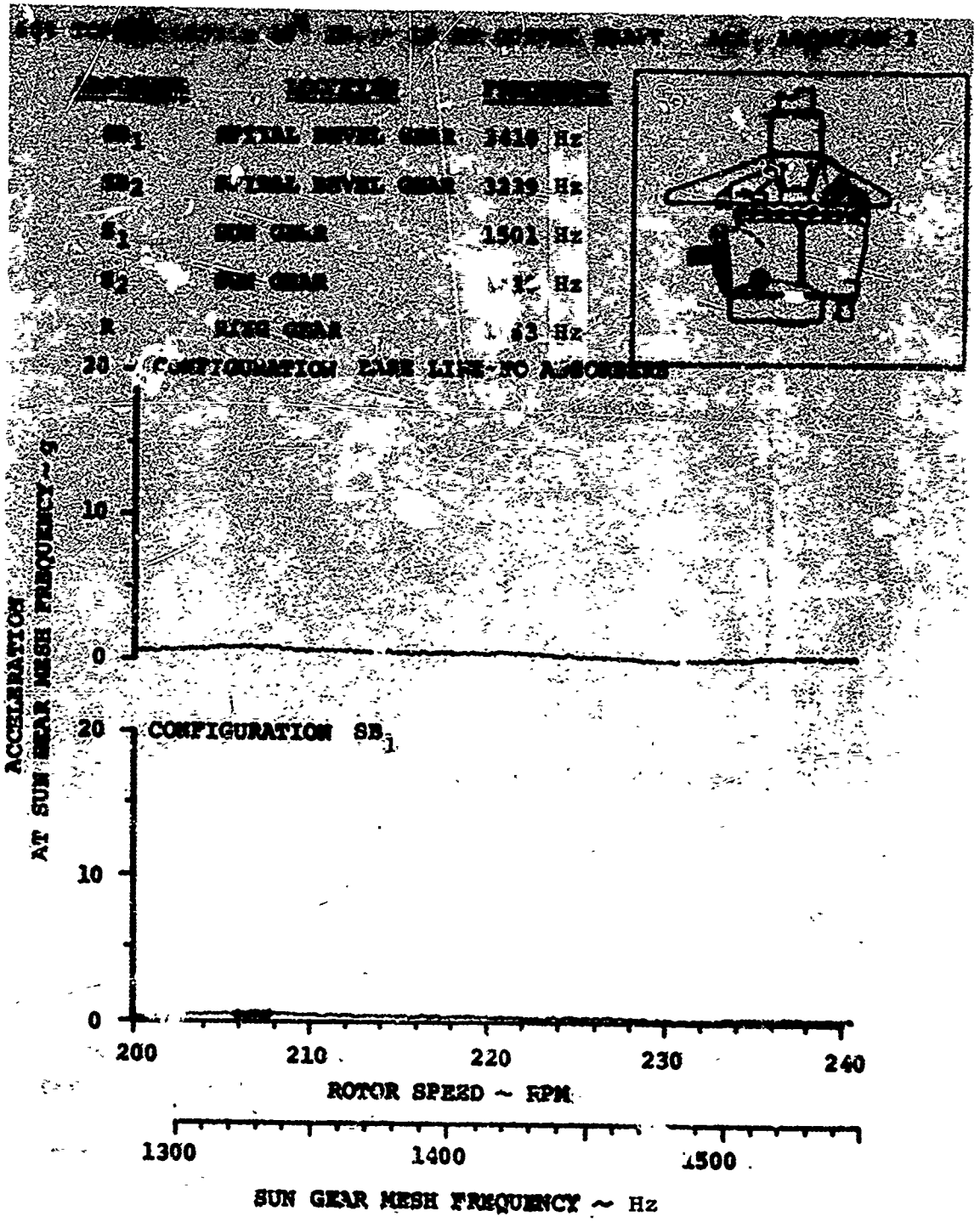

Figure 72. Sun Gear Sweep Data, Acc. Location 2, Torque 60%.

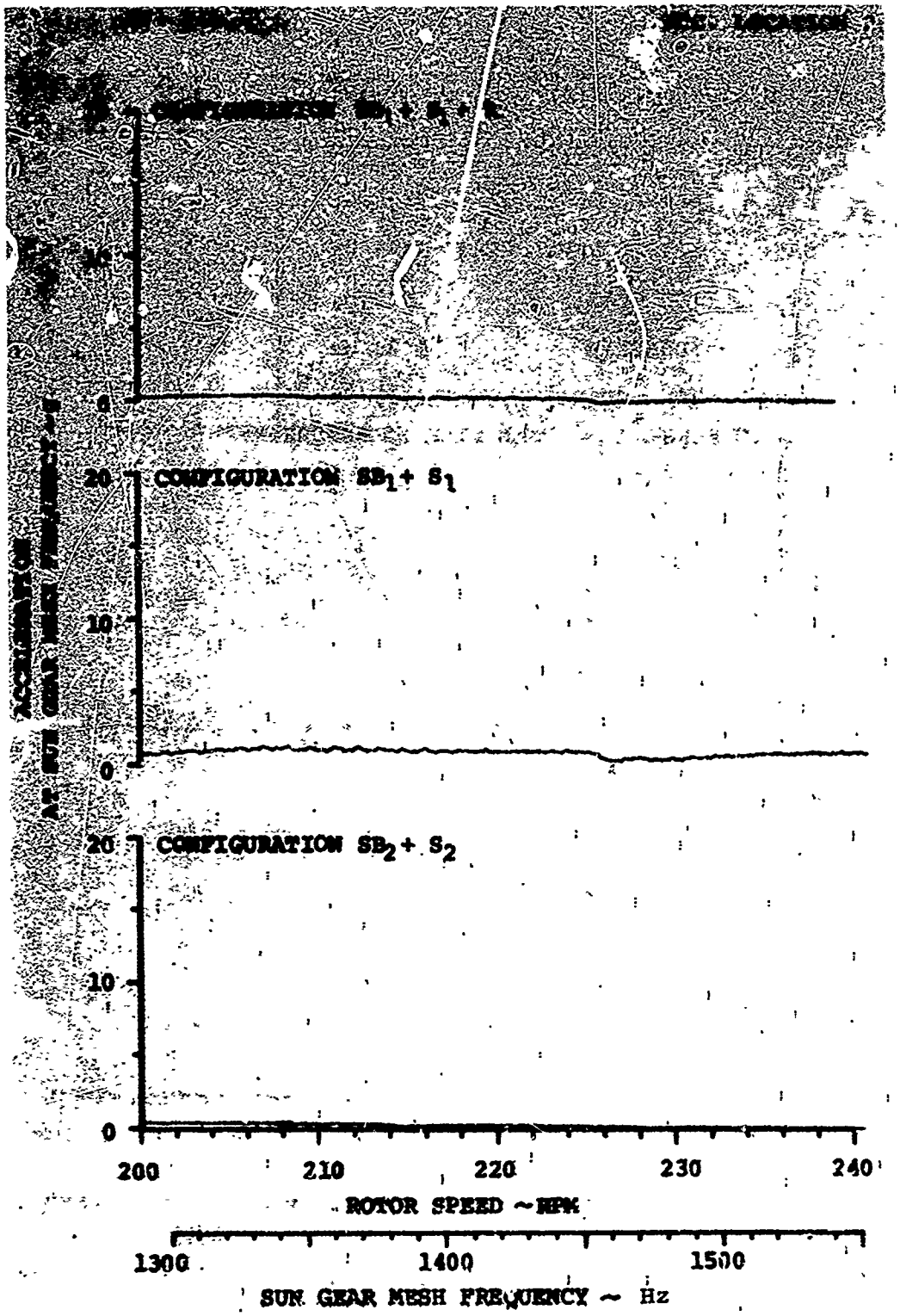

Figure 42. (Continued)

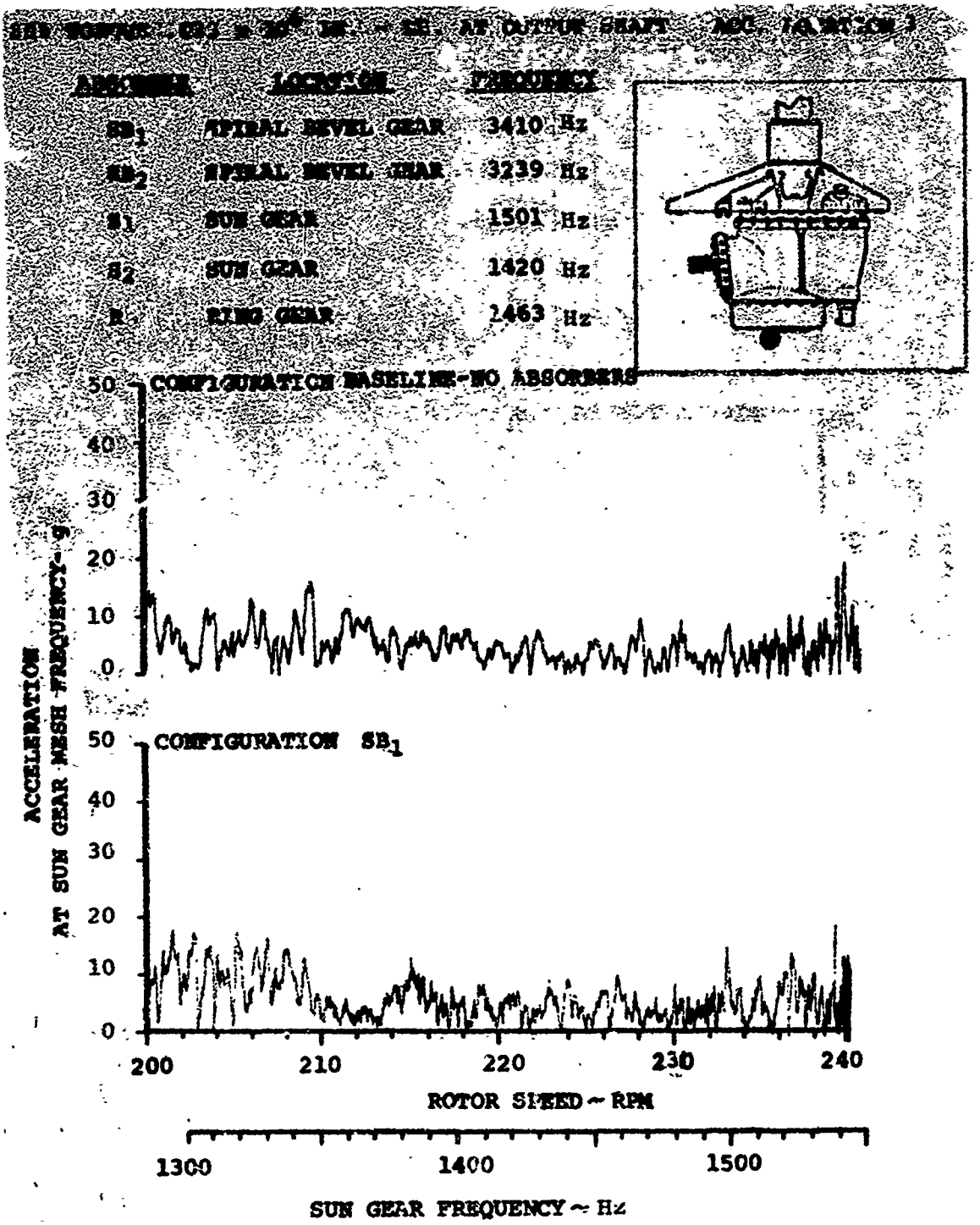

Figure 43. Sun Gear Sweep Data, Acc. Location 3, Torque 60%.

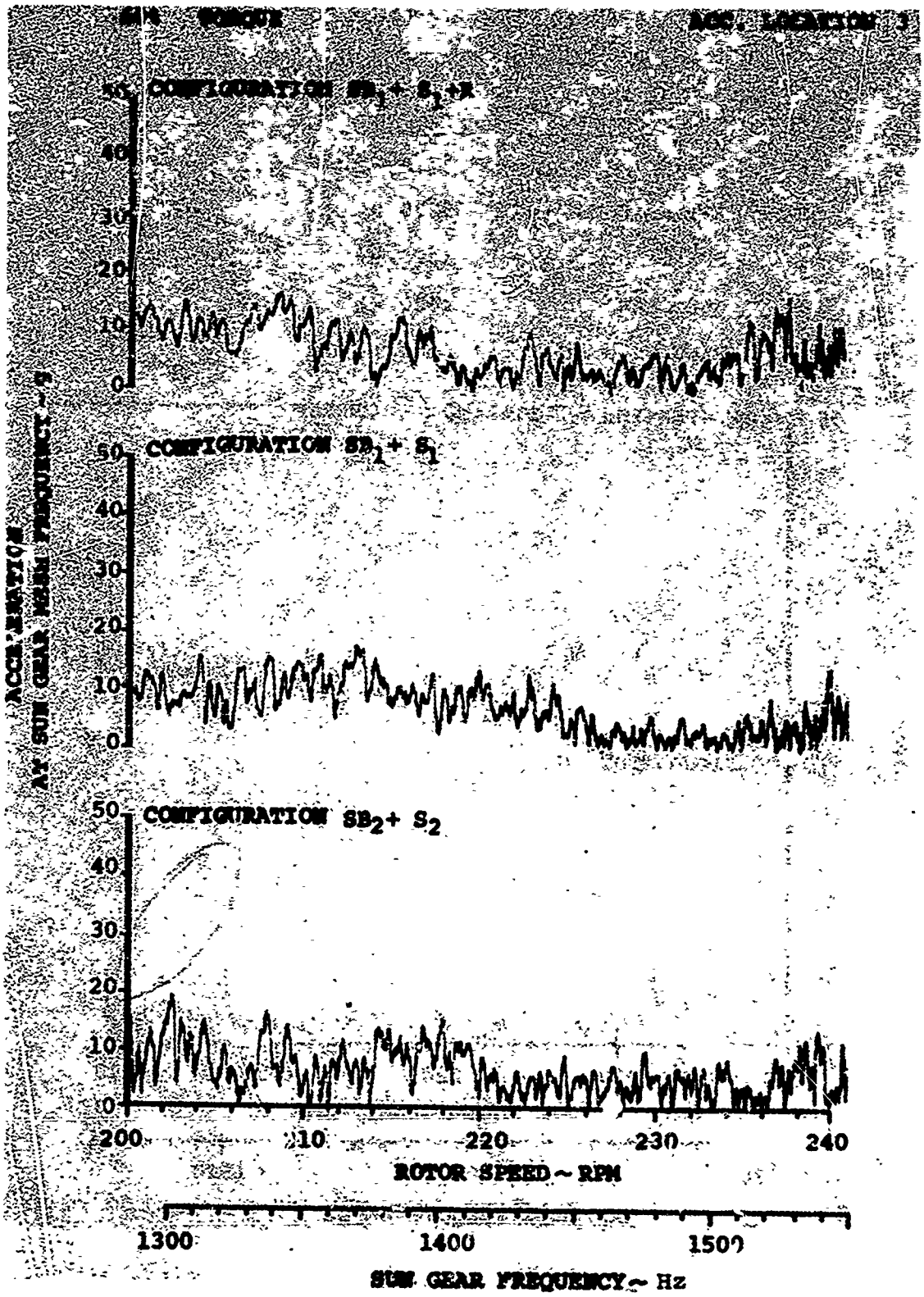

Figure 43. (Continued)

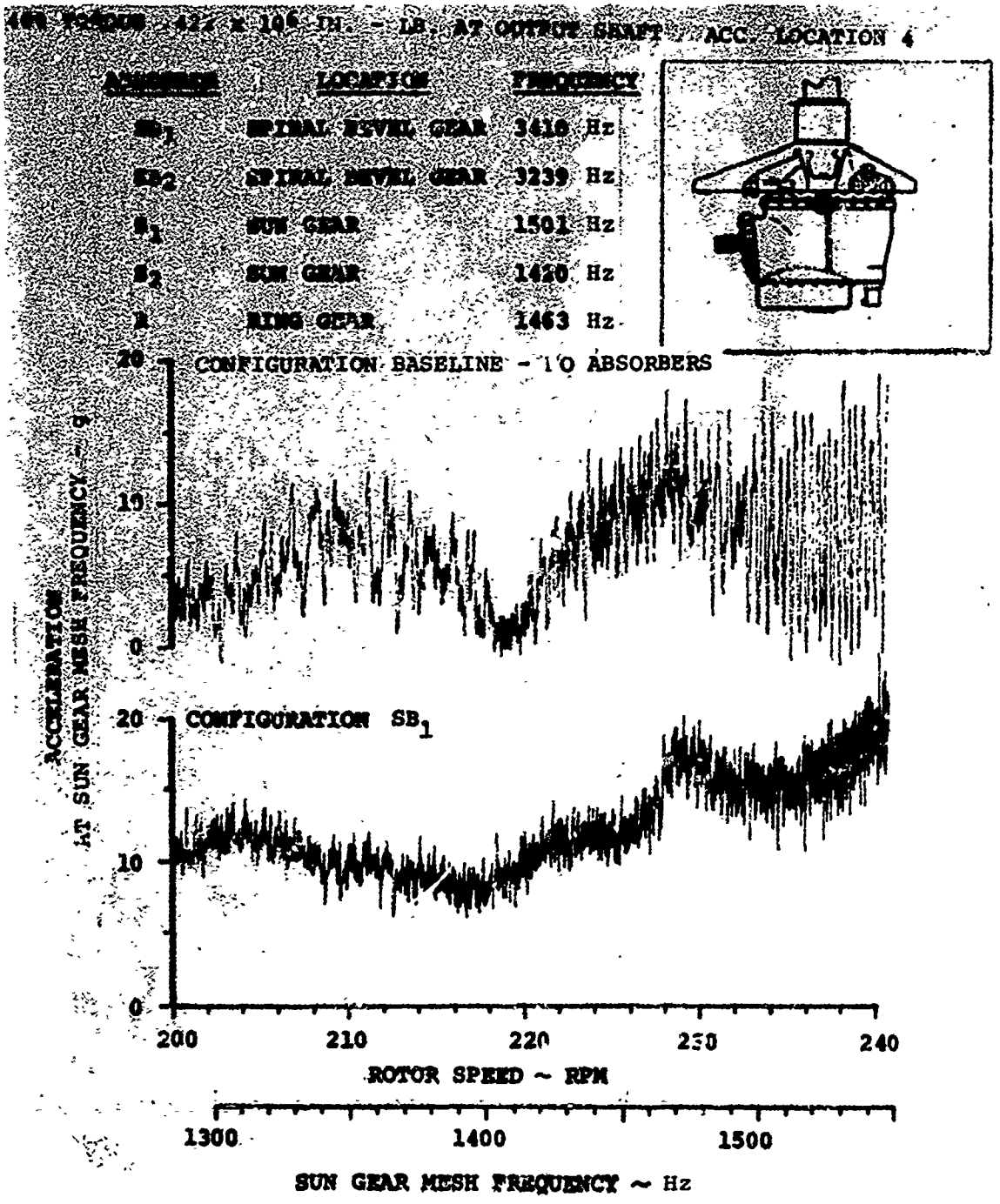

Figure 44. Sun Gear Sweep Data, Acc. Location 4, Torque 40%.

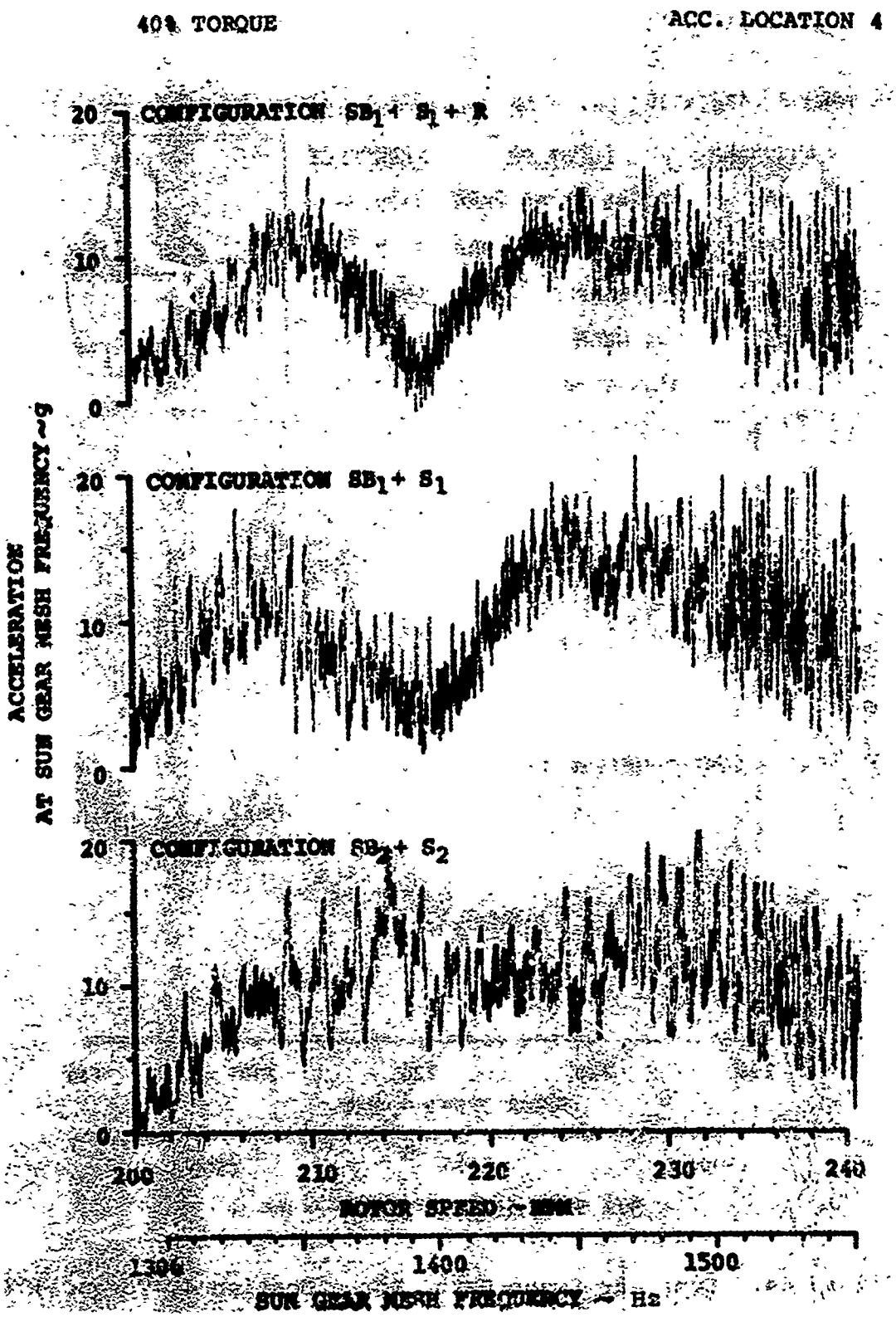

Figure 44. (Continued)

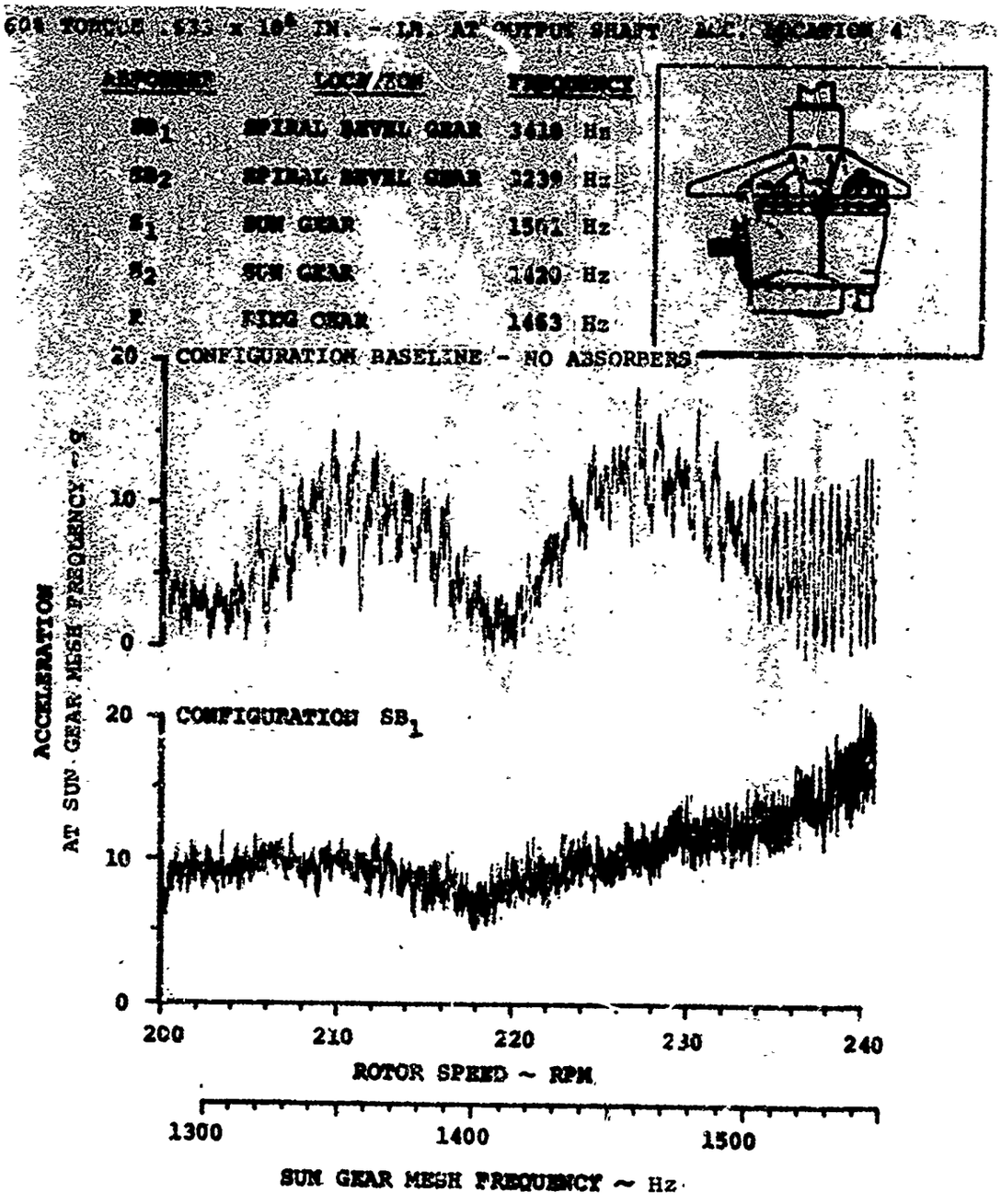

Figure 45. Sun Gear Sweep Data, Acc. Location 4, Torque 60%.

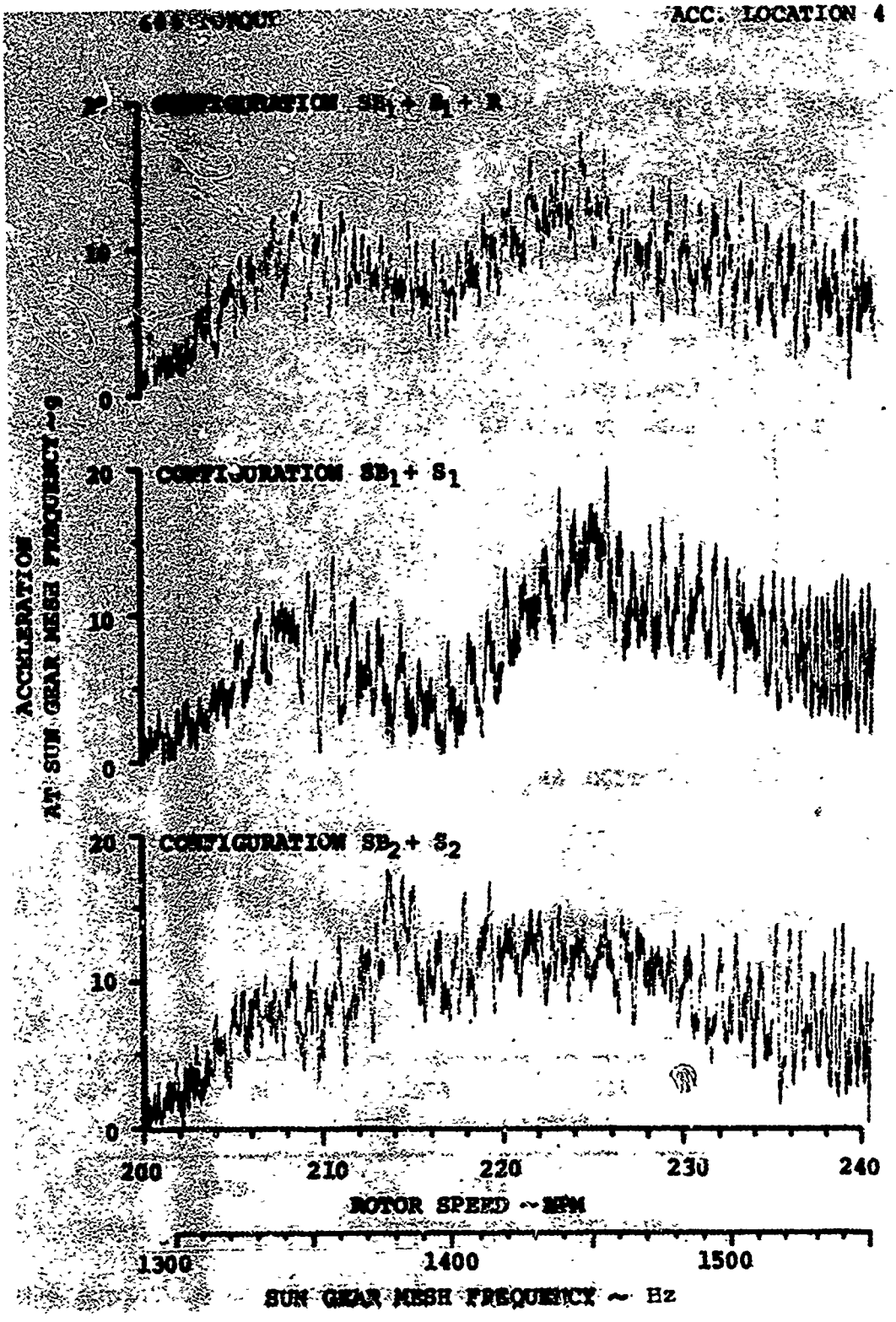

Figure 45. (Continued)

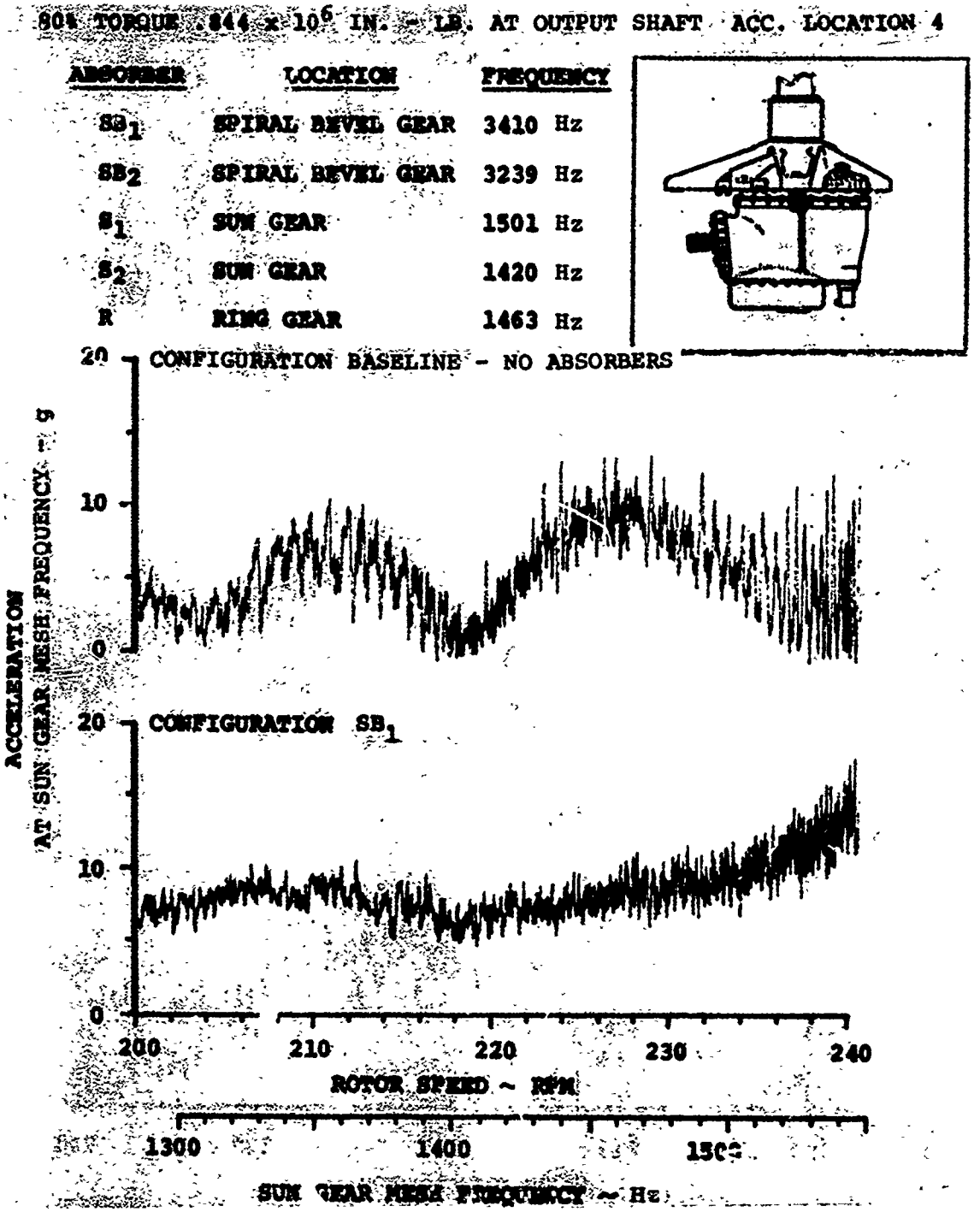

Figure 46. Sun Gear Sweep Data, Acc. Location 4, Torque 80%.

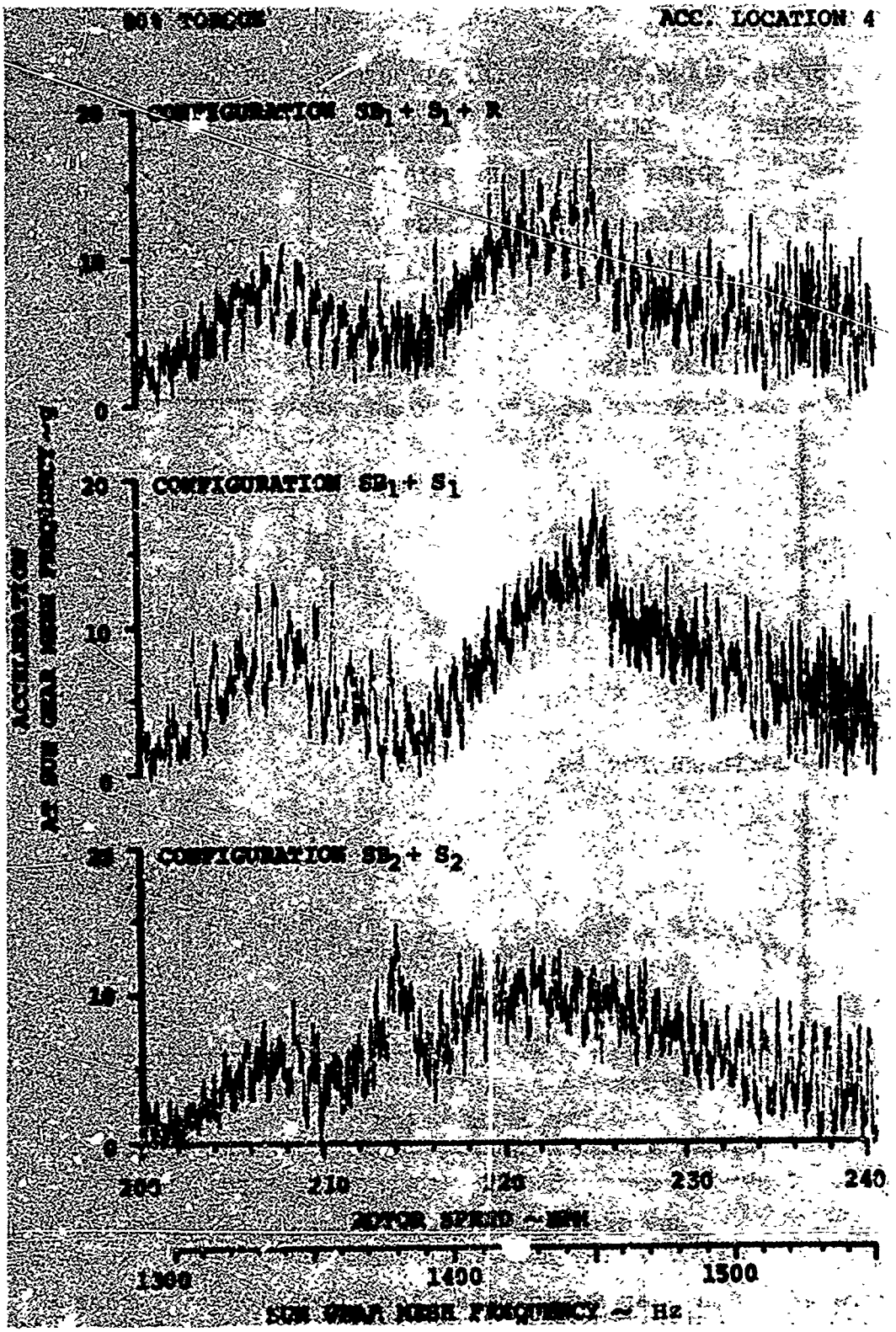

Figure 46. (Continued)

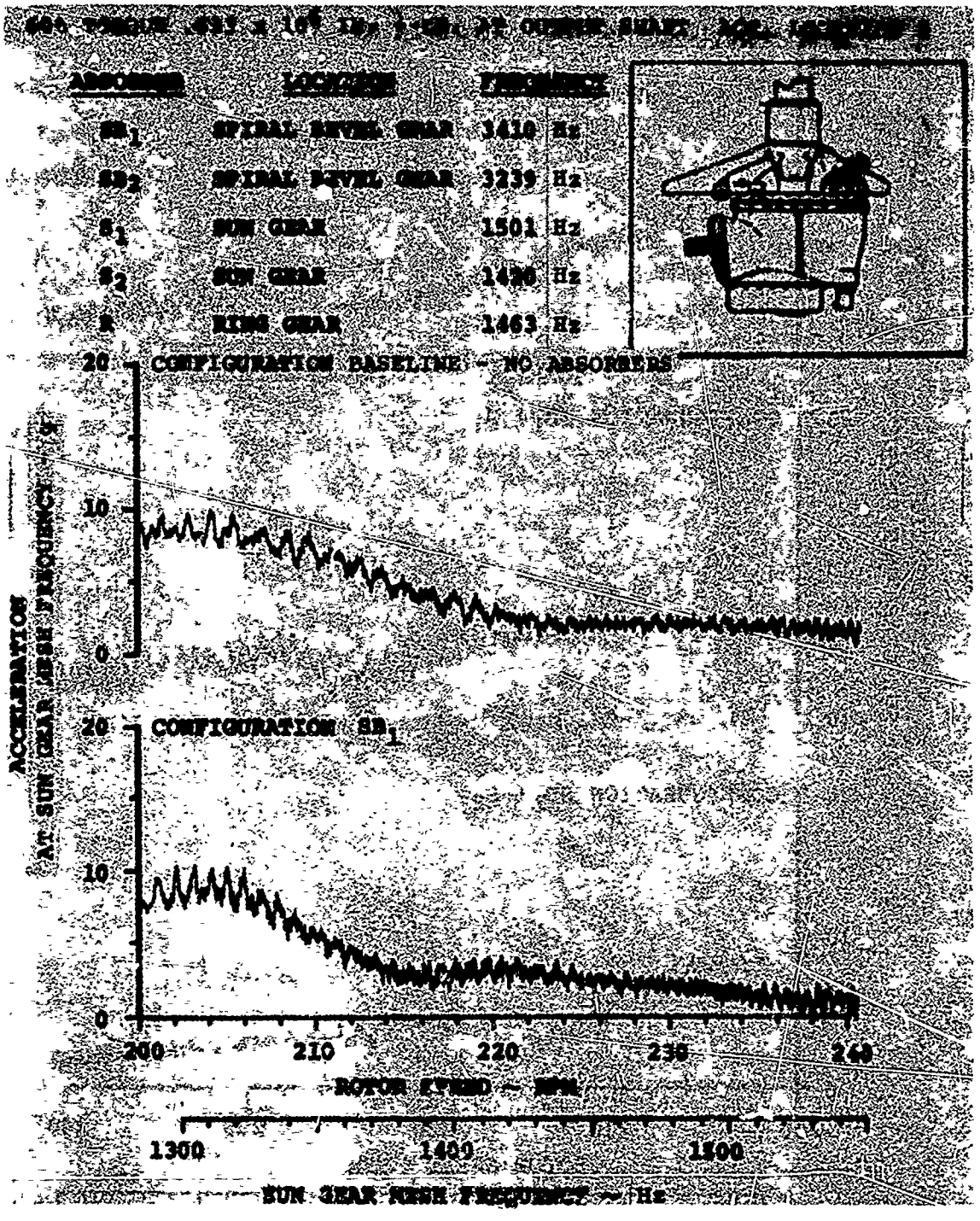

Figure 47. Sun Gear Sweep Data, Acc. Location 5, Torque 60%.

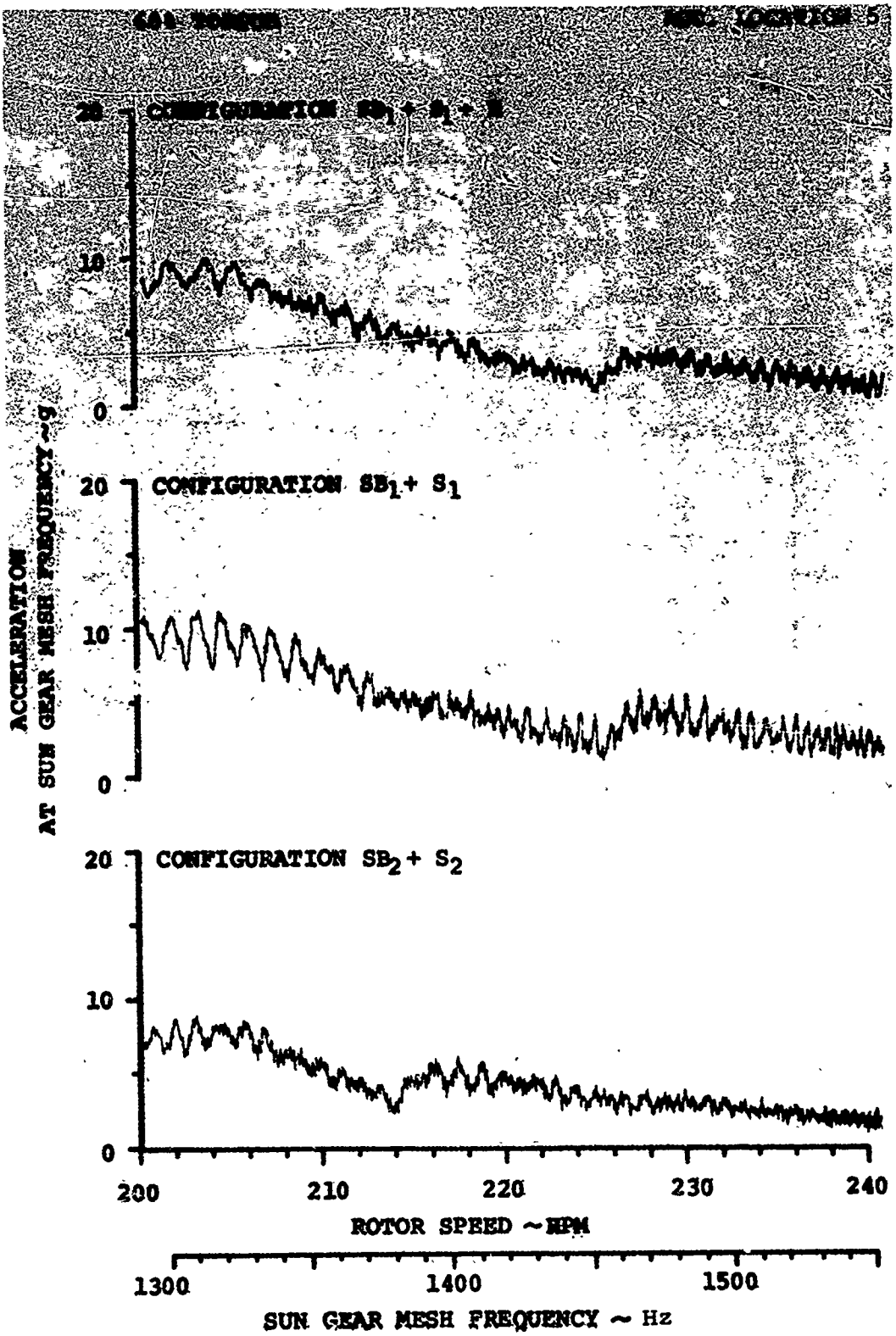

Figure 47. (Continued)

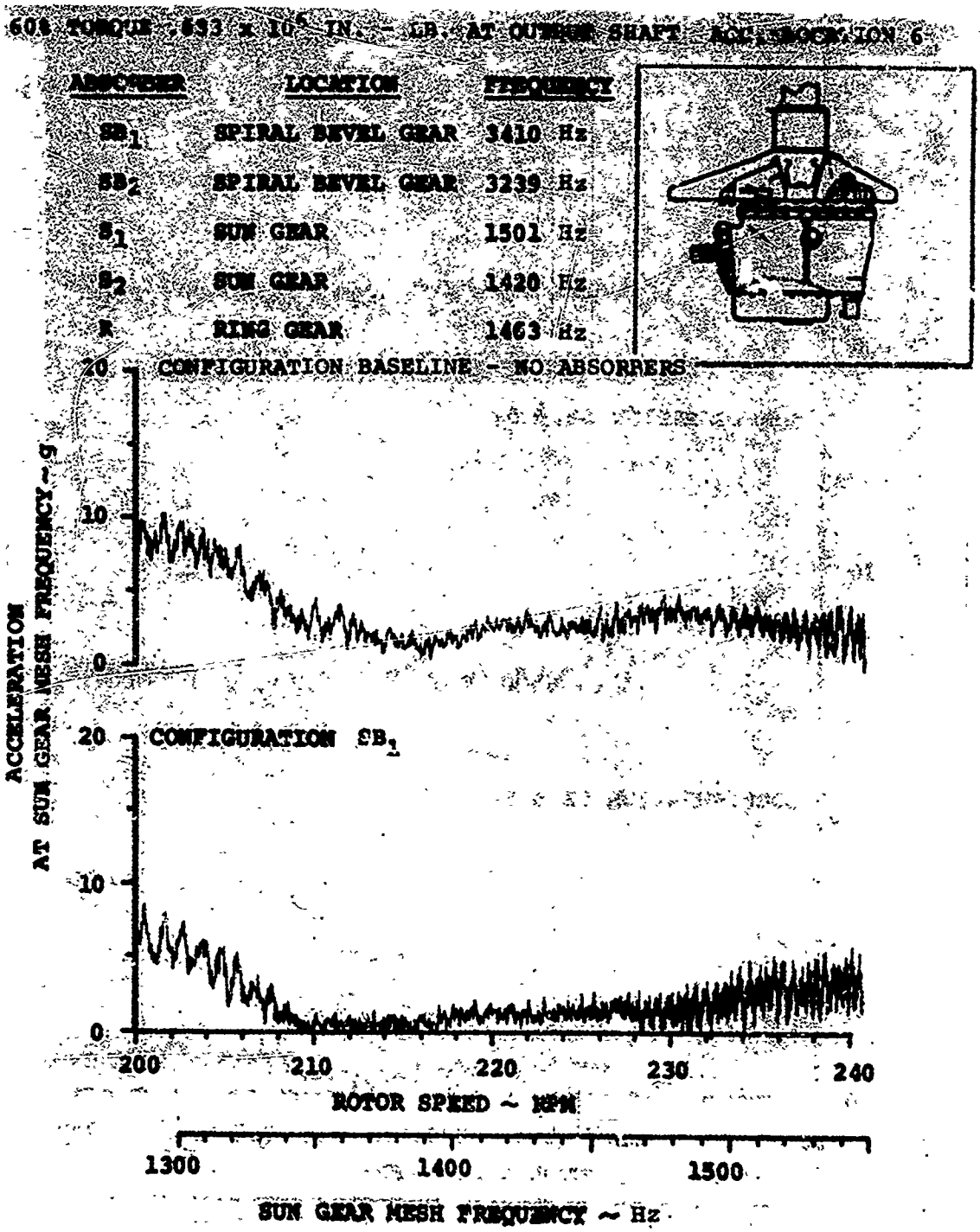

Figure 48. Sun Gear Sweep Data, Acc. Location 6, Torque 60%.

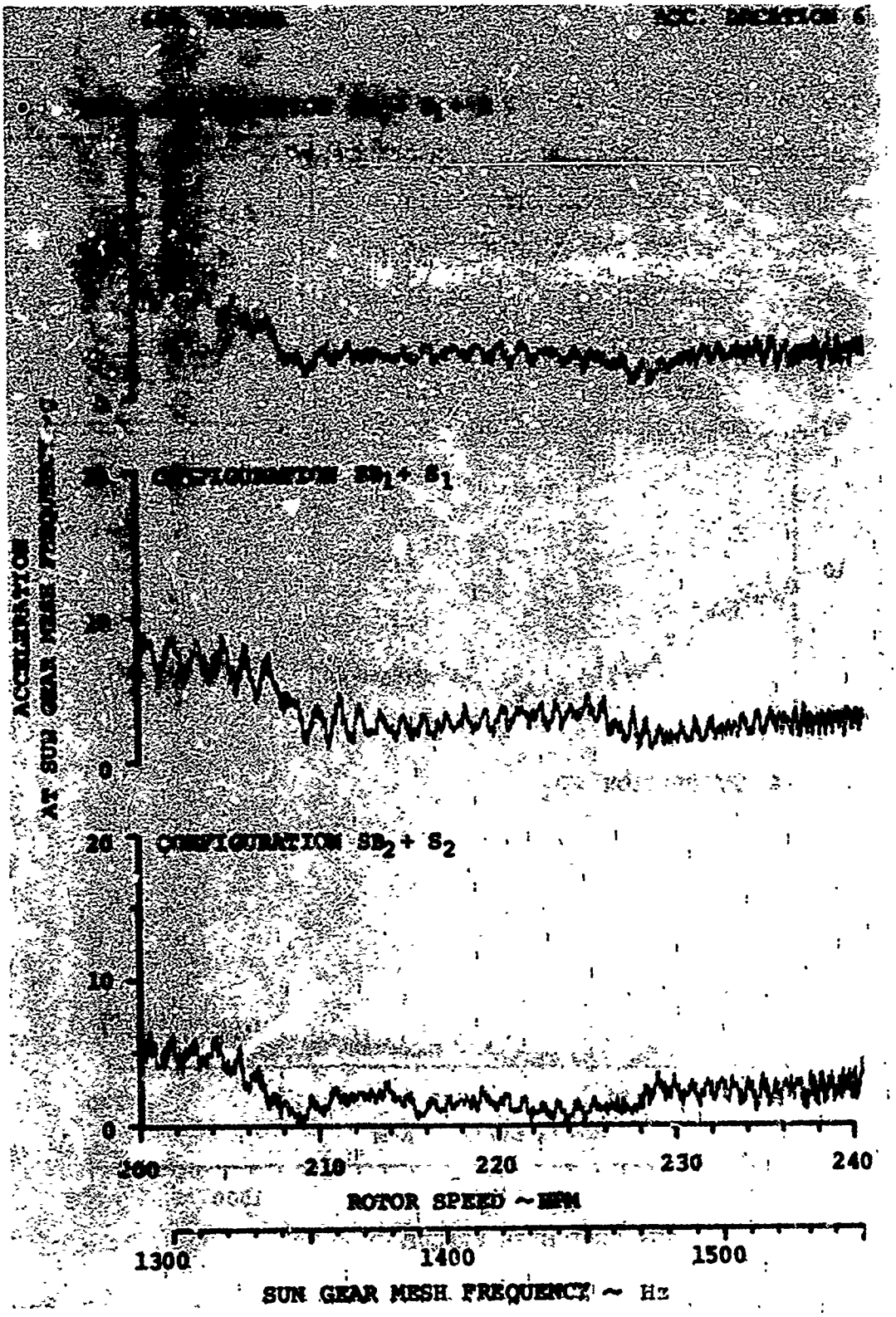

Figure 48. (Continued)

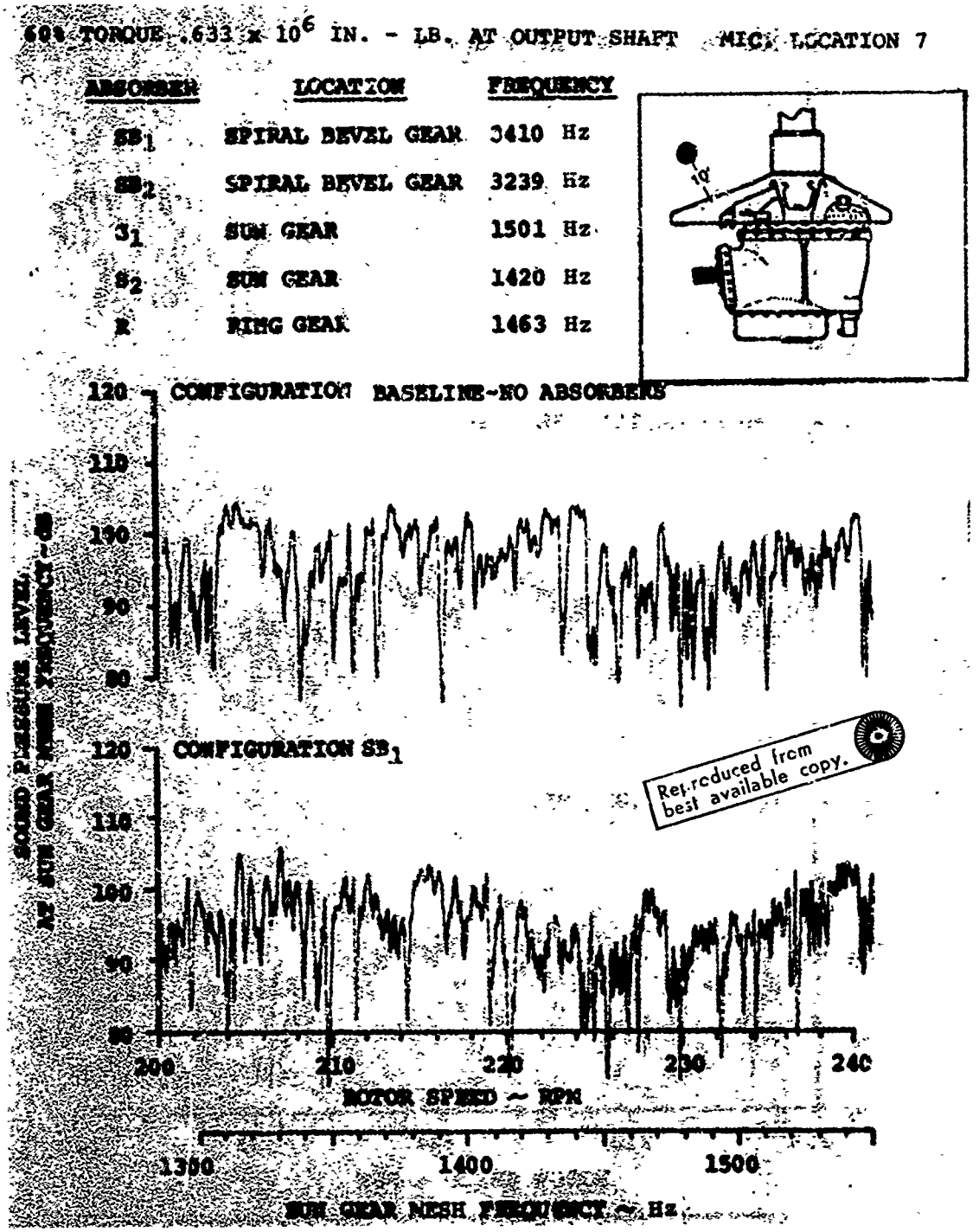

Figure 49. Sun Gear Sweep Data, Mic. Location 7, Torque 60%.

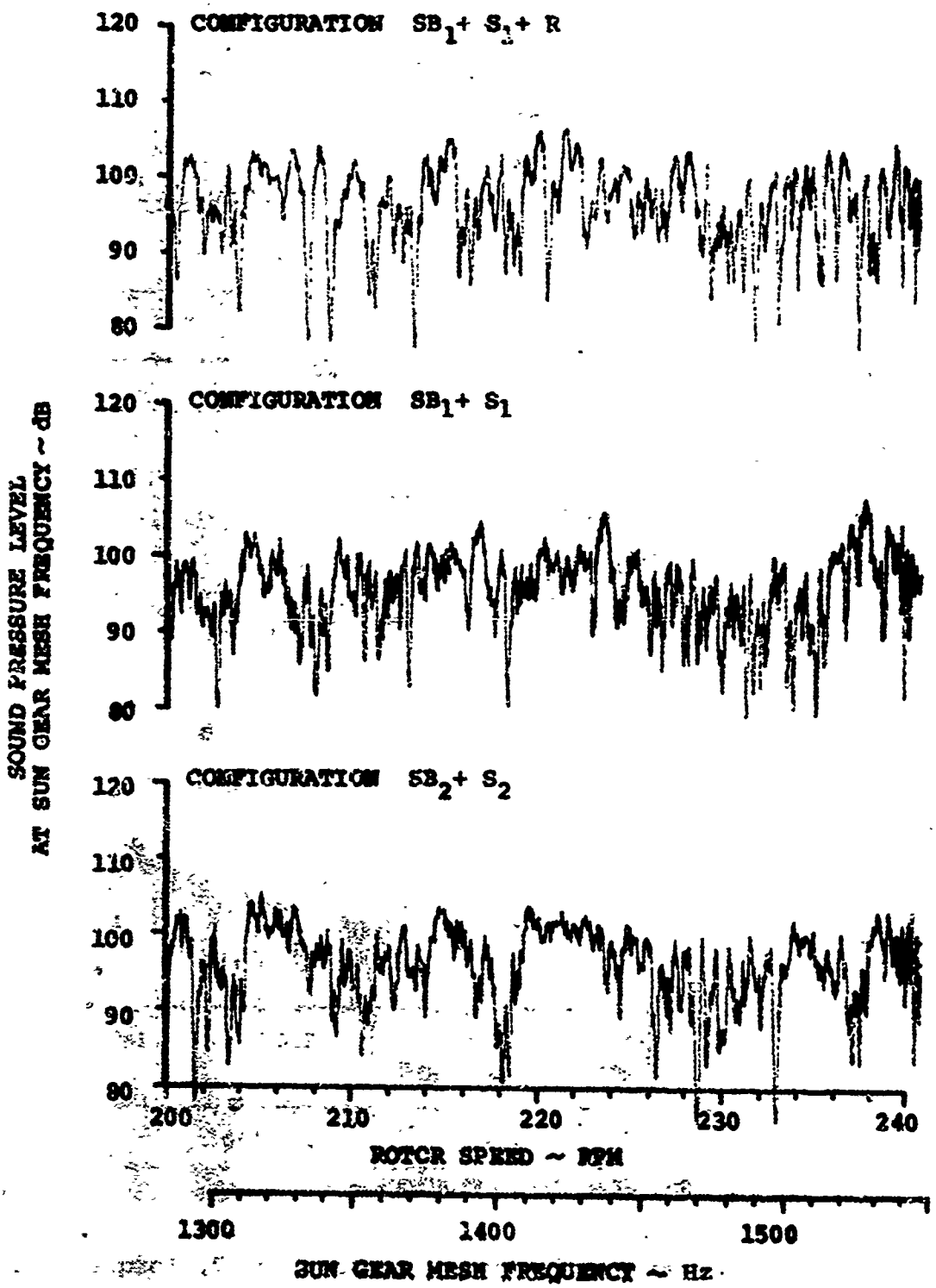

Figure 49. (Continued)

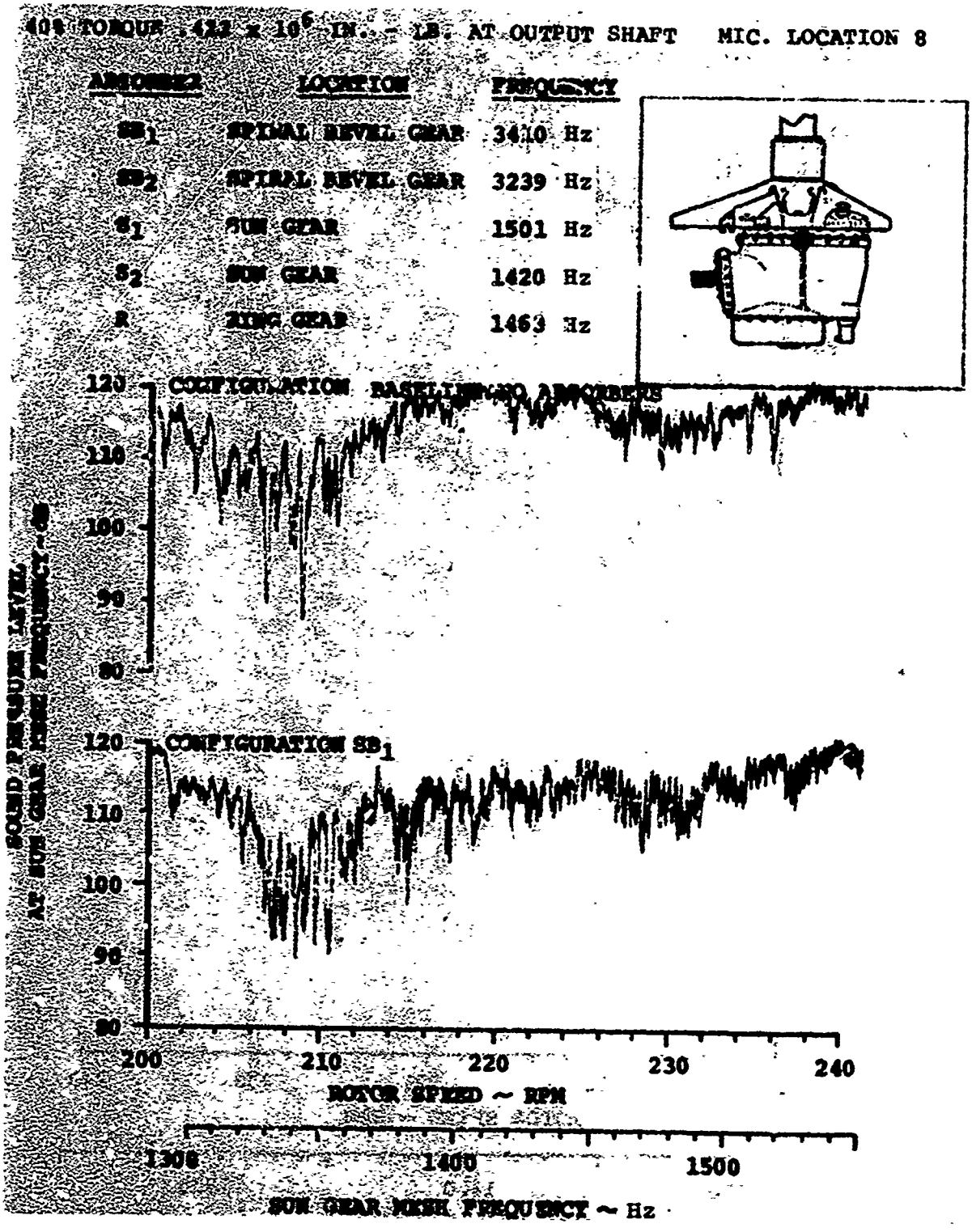

Figure 50. Sun Gear Sweep Data, Mic. Location 8, Torque 40%.

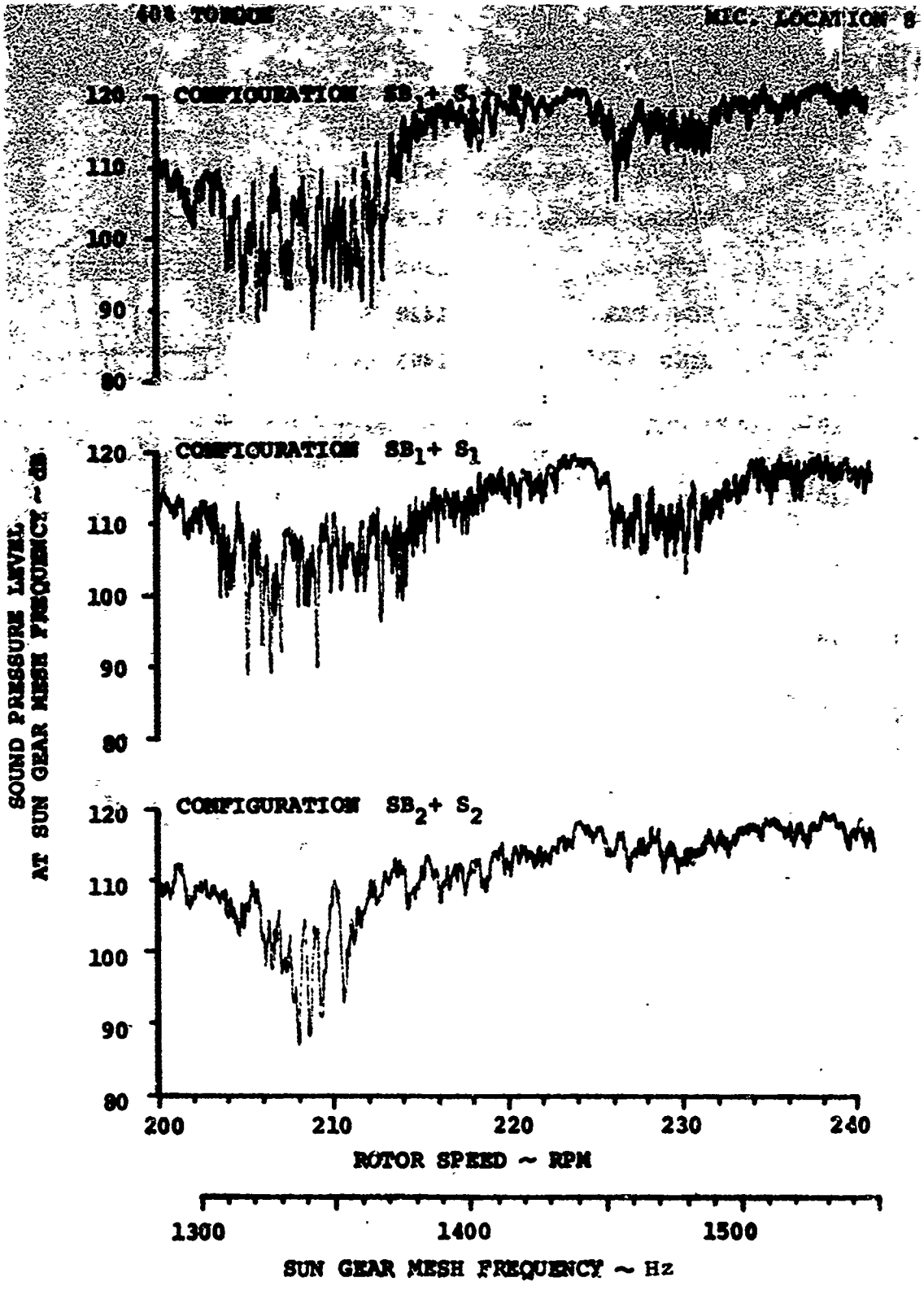

Figure 50. (Continued)

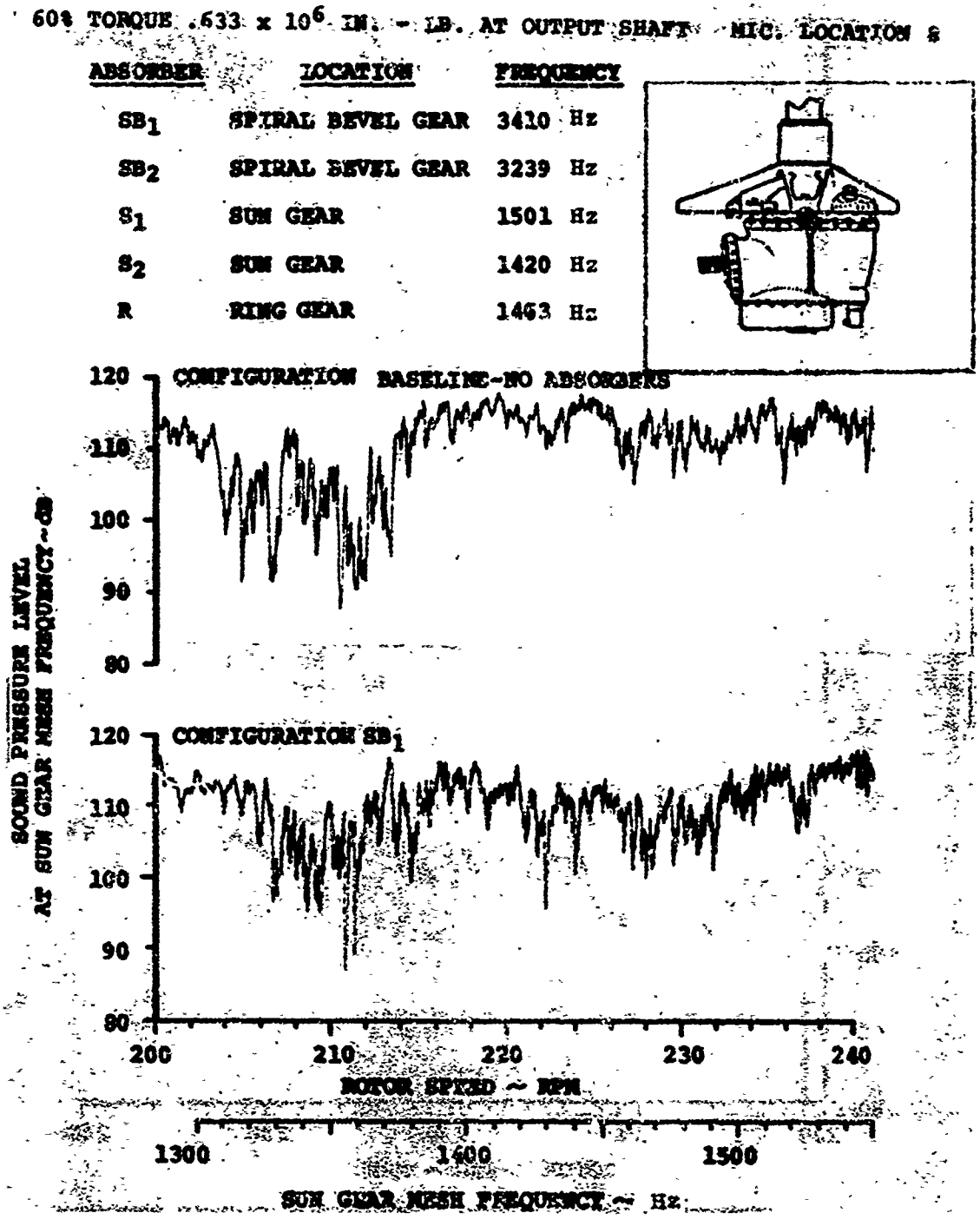

Figure 51. Sun Gear Sweep Data, Mic. Location 8, Torque 60%.

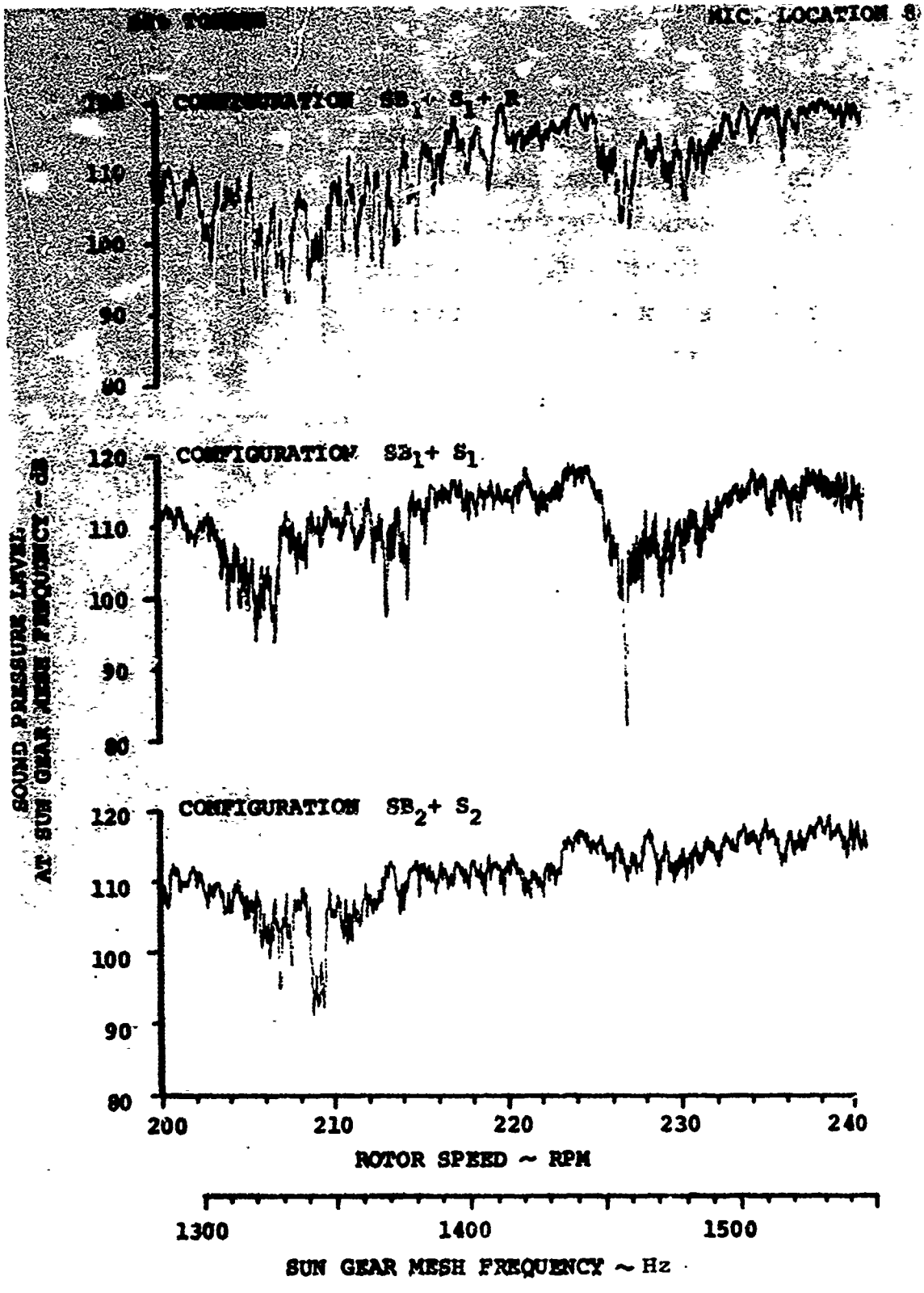

Figure 51. (Continued)

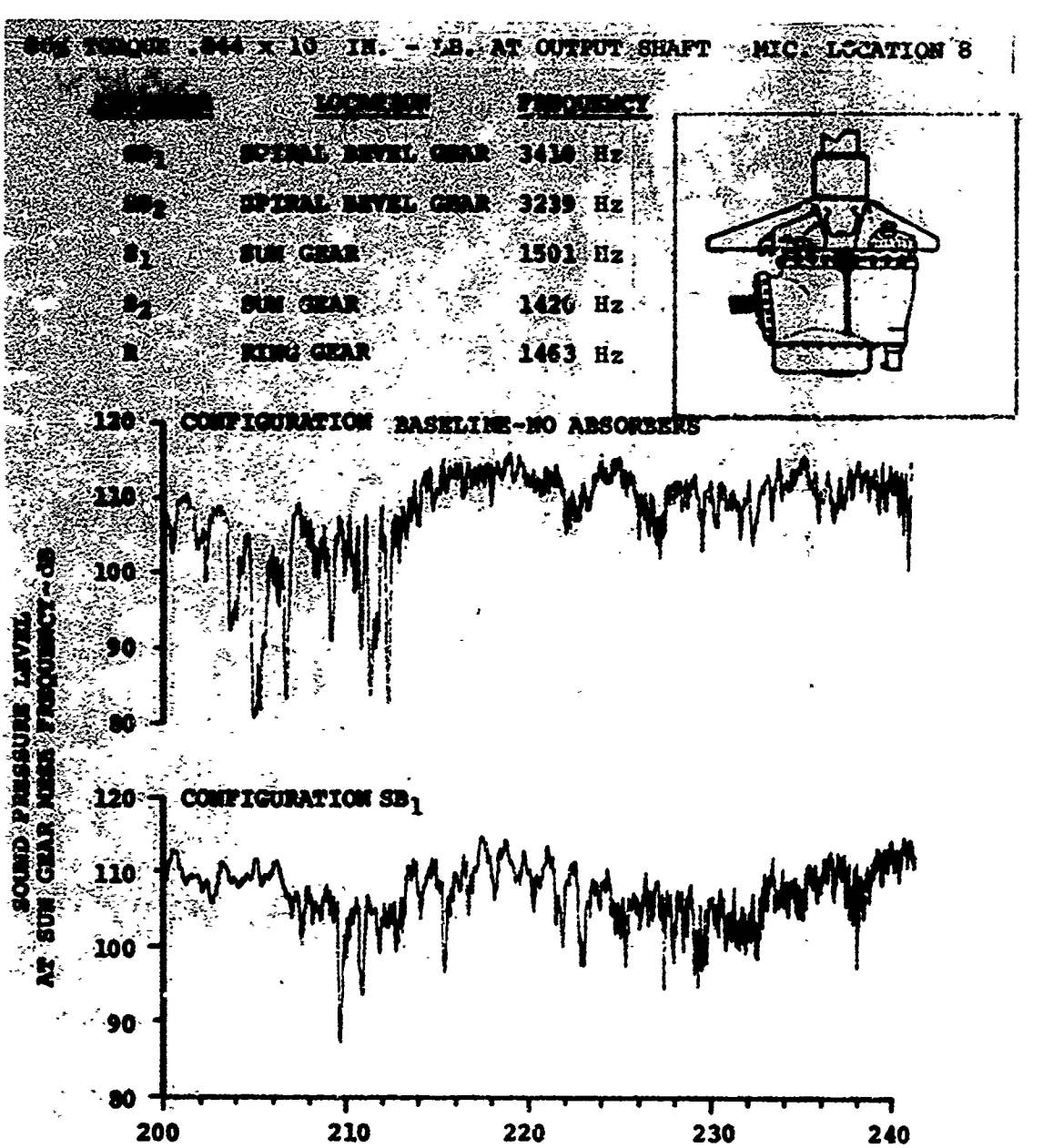

Figure 52. Sun Gear Sweep Data, Mic. Location 8, Torque 80%.

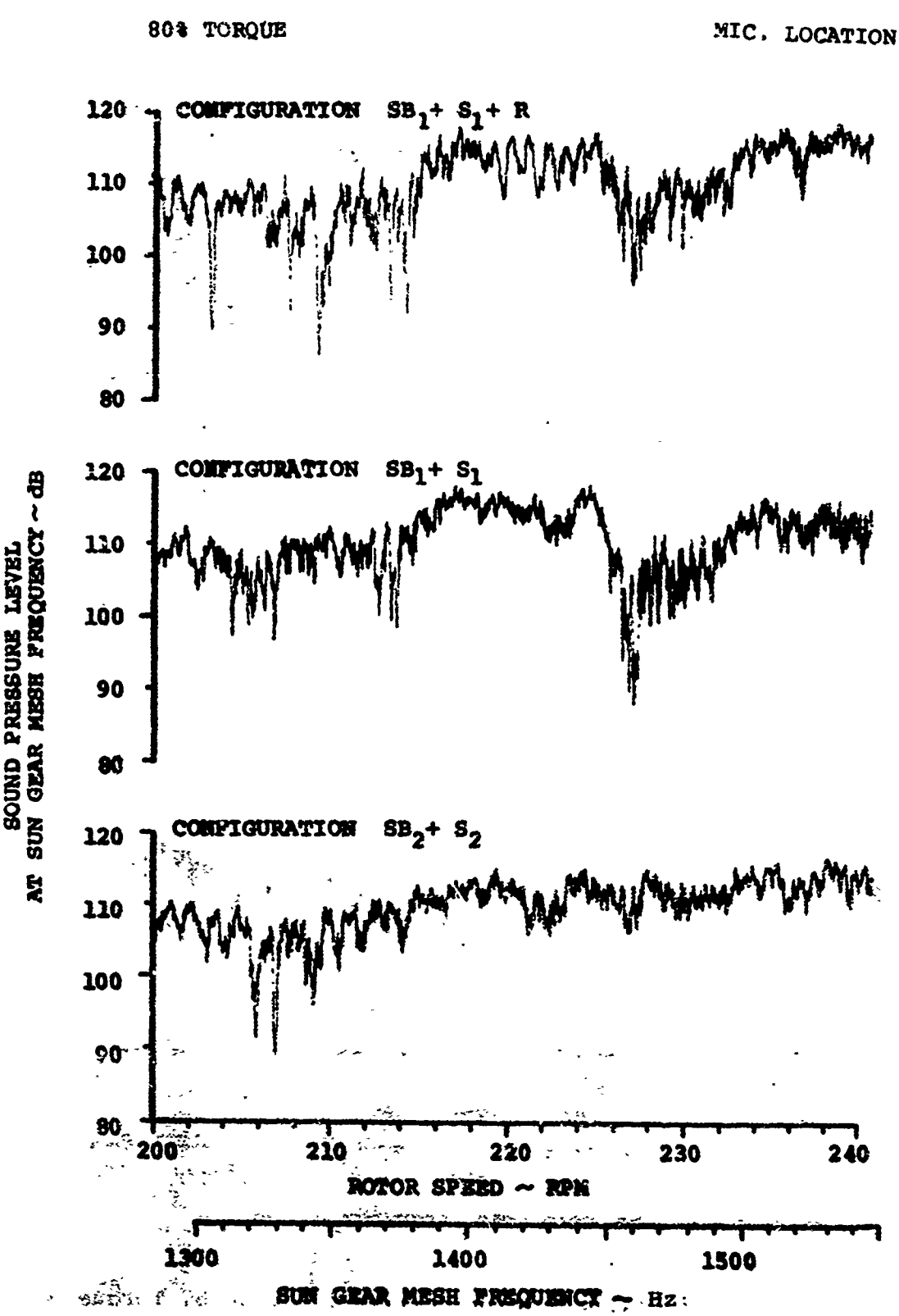

Figure 52. (Continued)

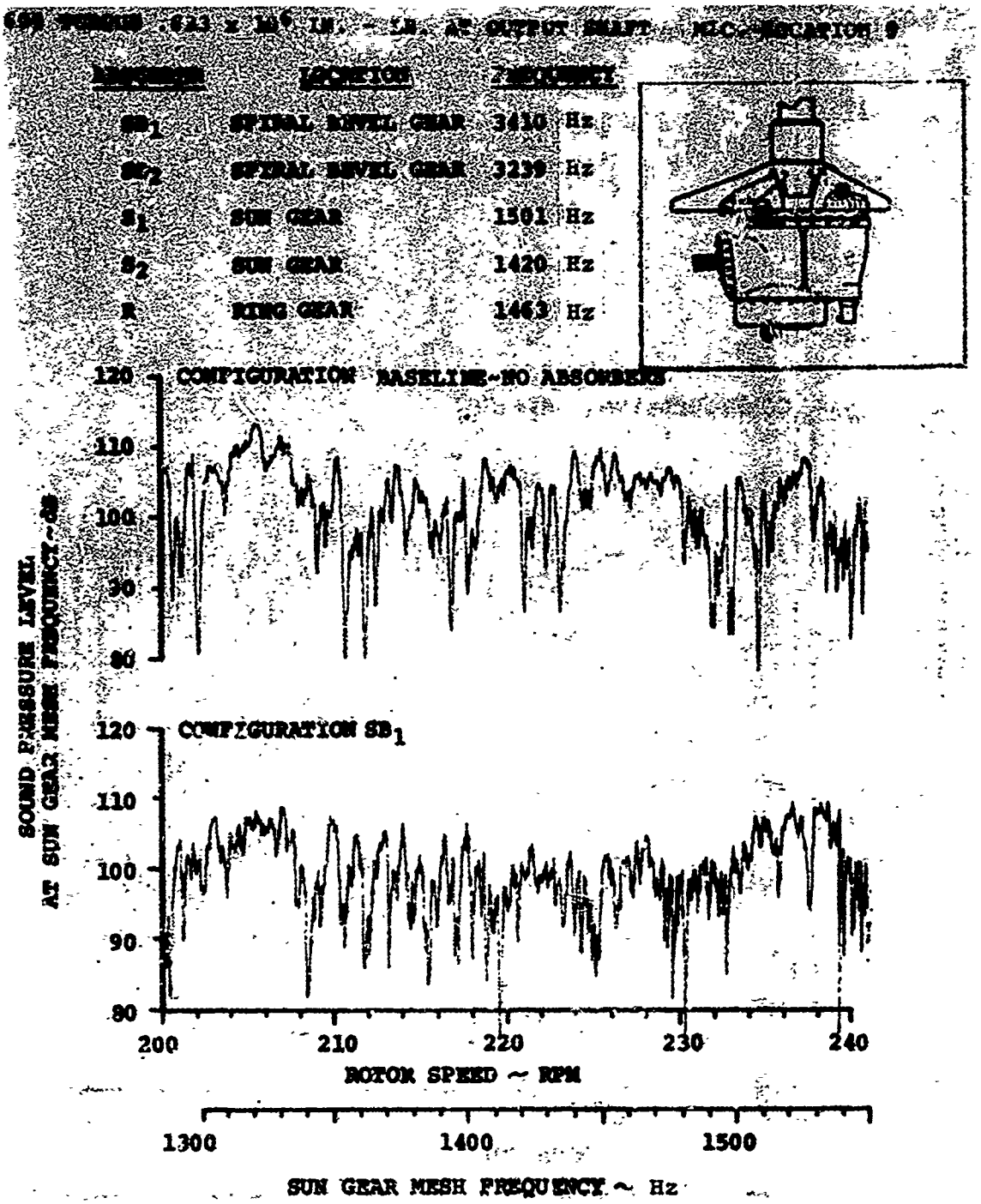

Figure 53. Sun Gear Sweep Data, Mic. Location 9, Torque 60%.

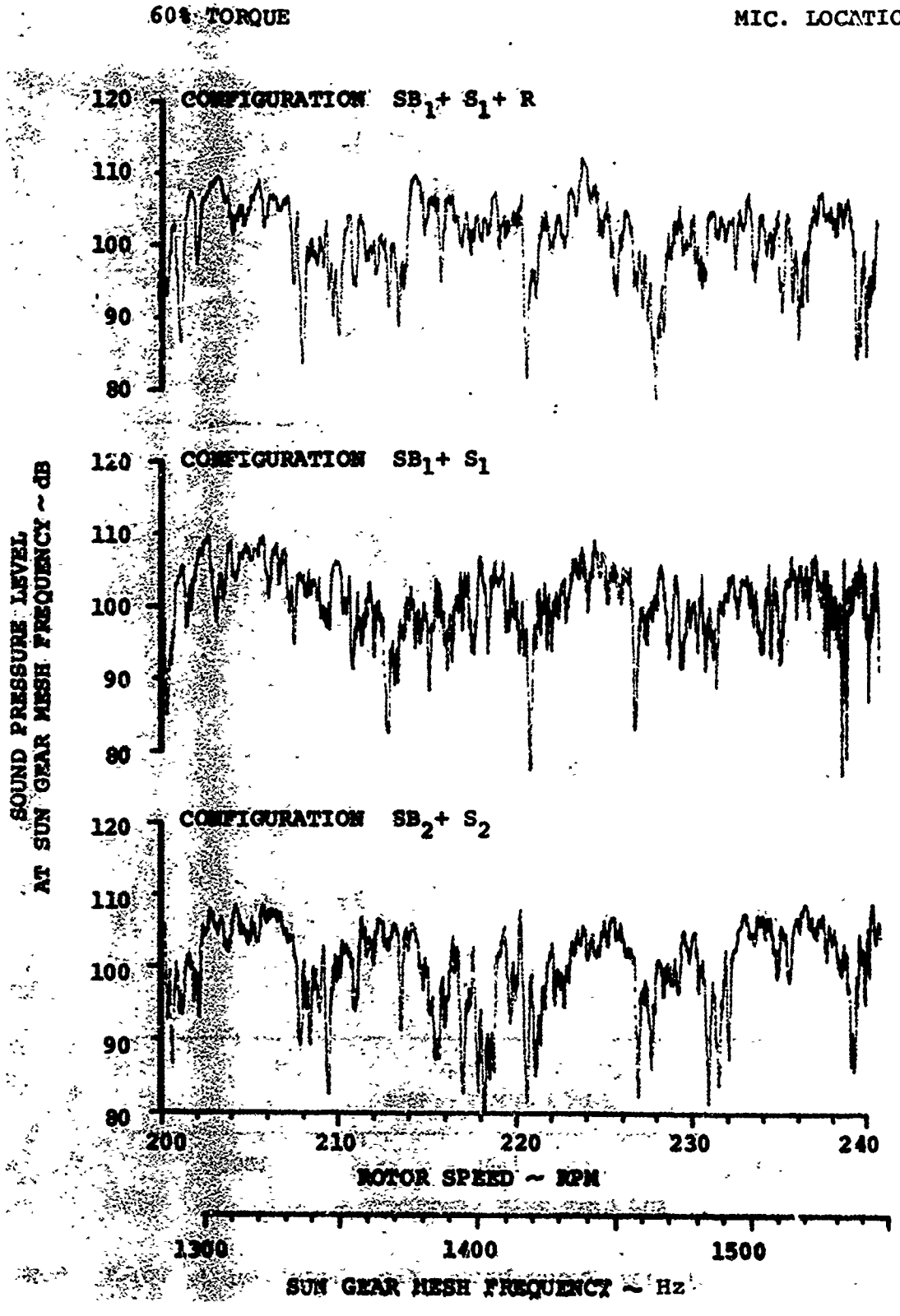

Figure 53. (Continued)

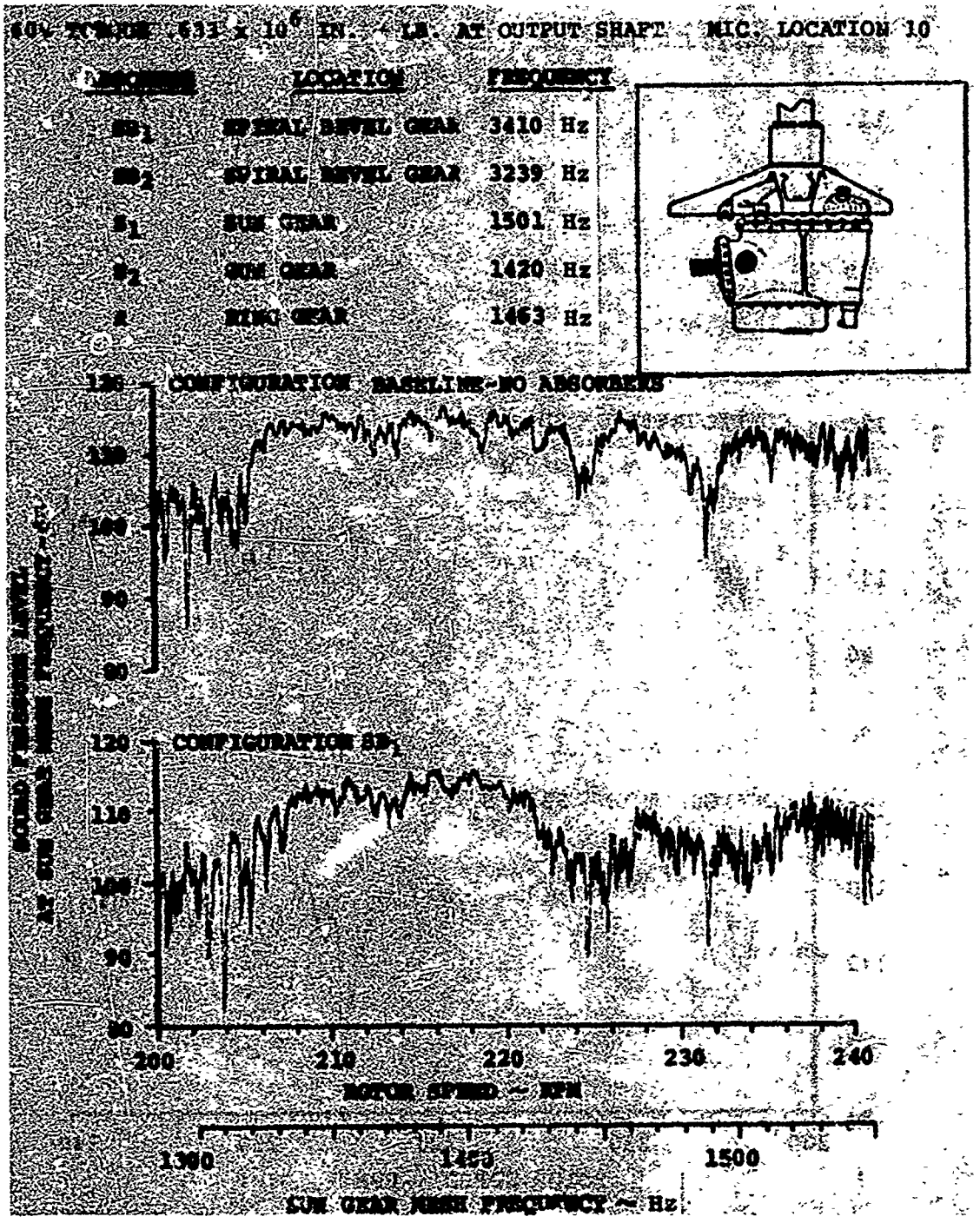

Figure 54. Sun Gear Sweep Data, Mic. Location 10, Torque 60%.

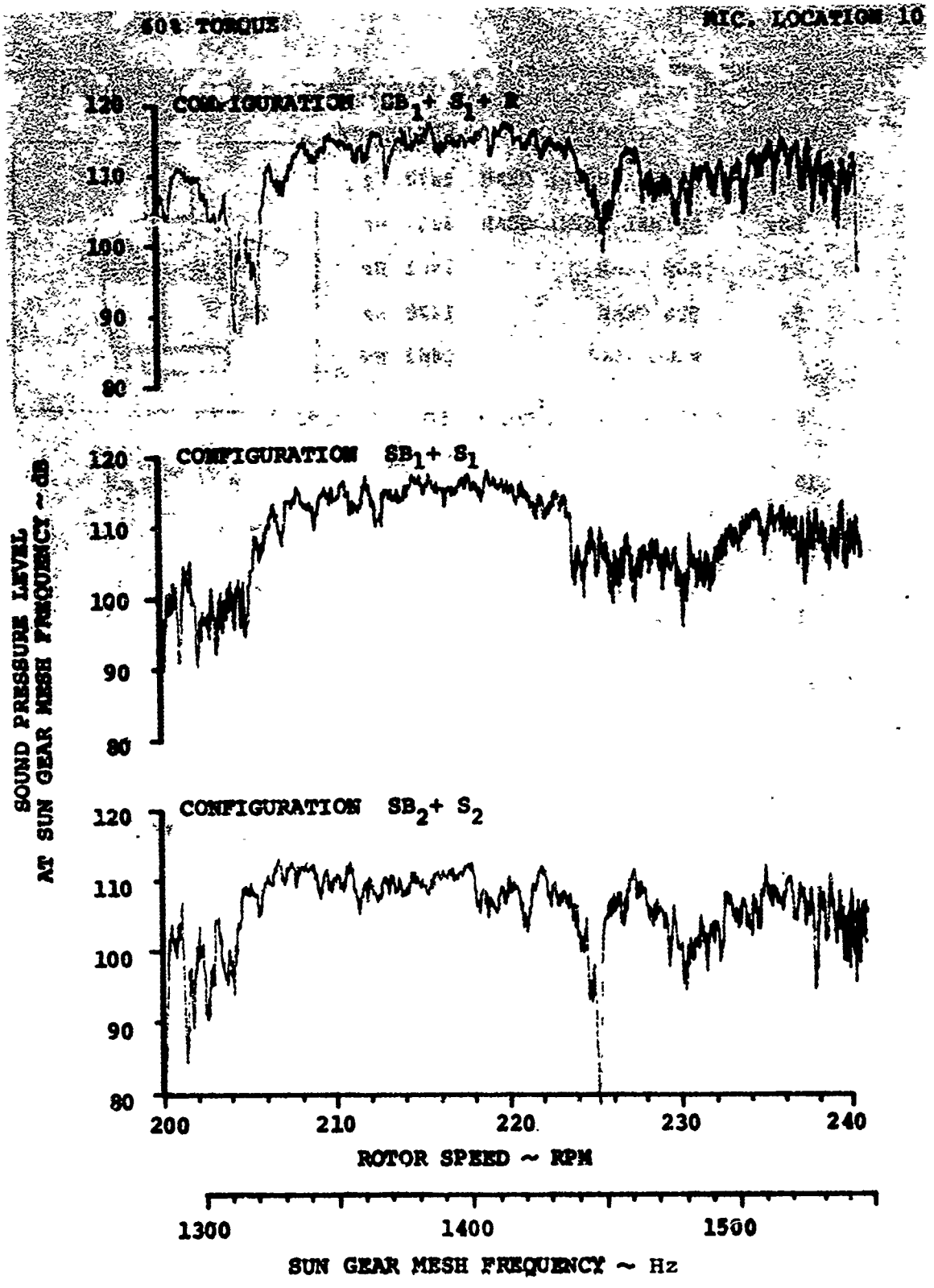

Figure 54. (Continued)

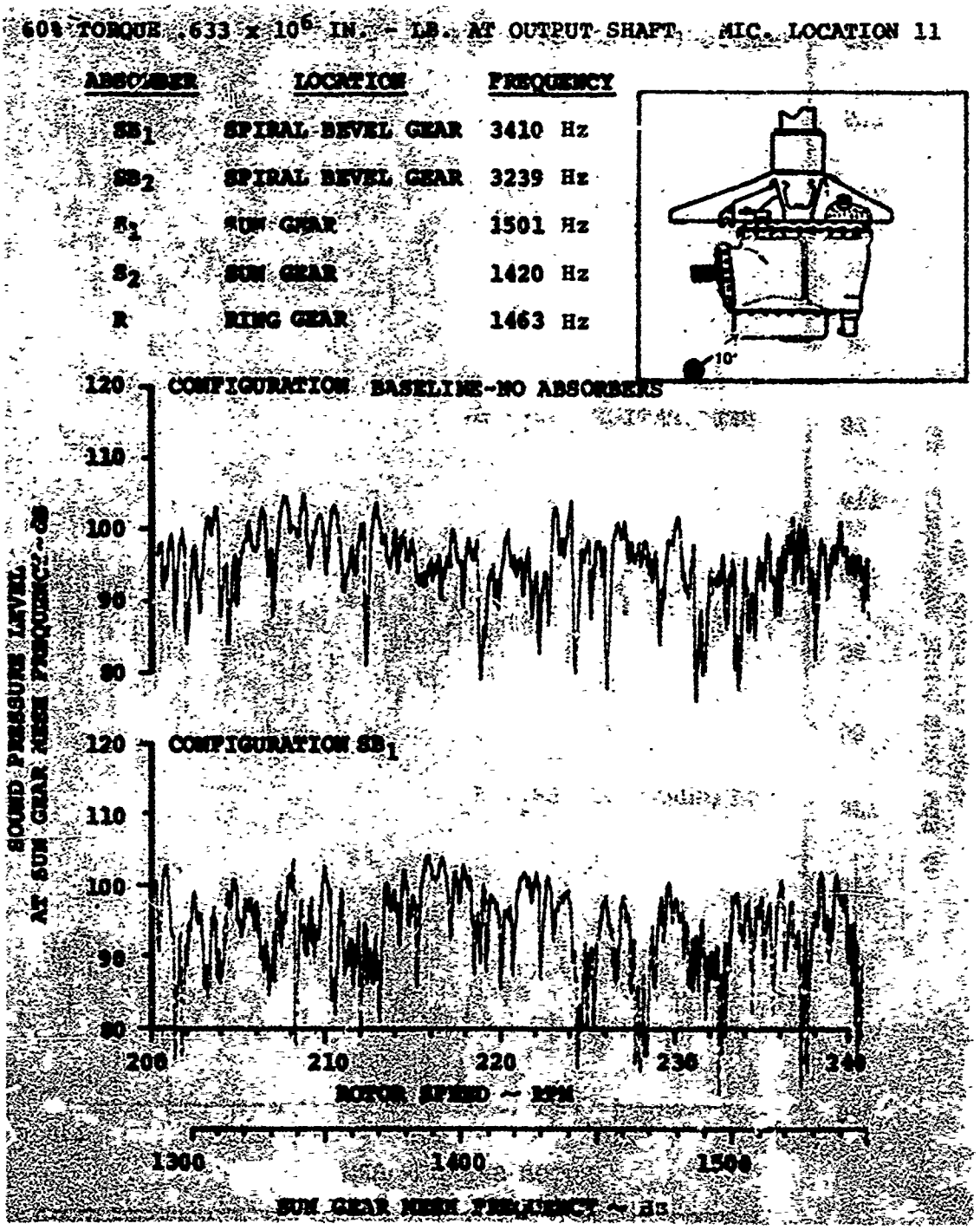

Figure 55. Sun Gear Sweep Data, Mic. Location 11, Torque 60%.

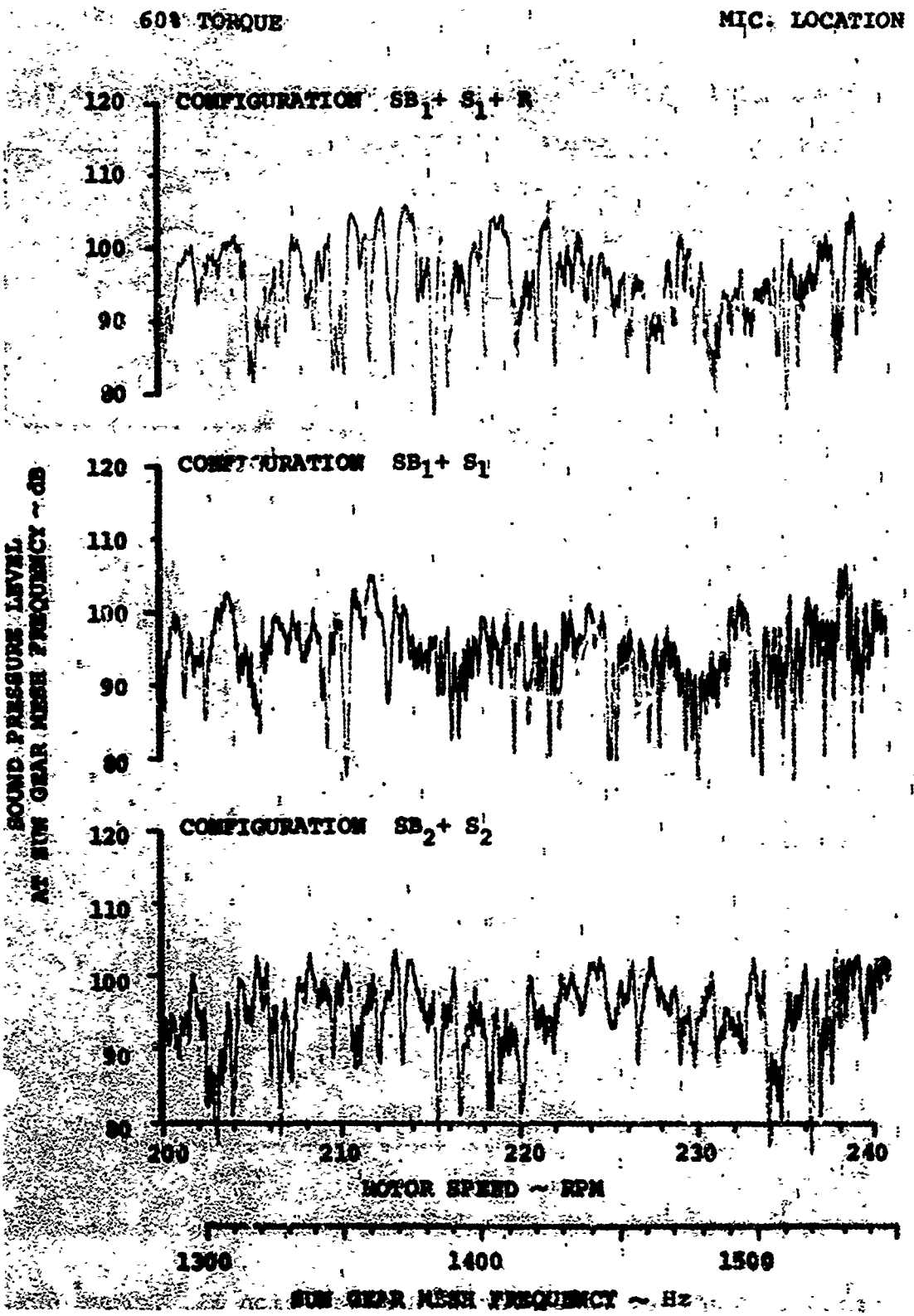

Figure 55. (Continued)

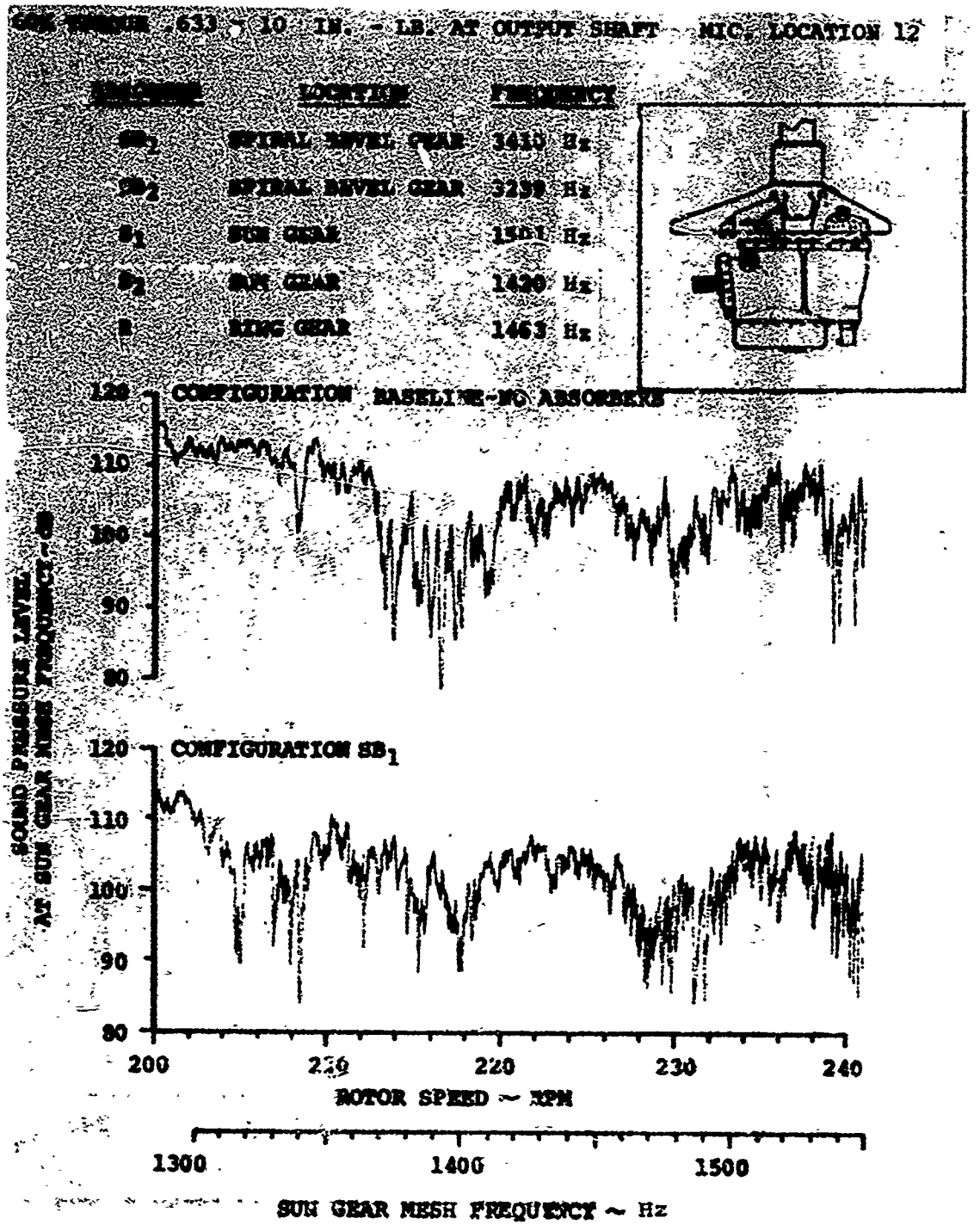

Figure 56. Sun Gear Sweep Data, Mic. Location 12, Torque 60%.

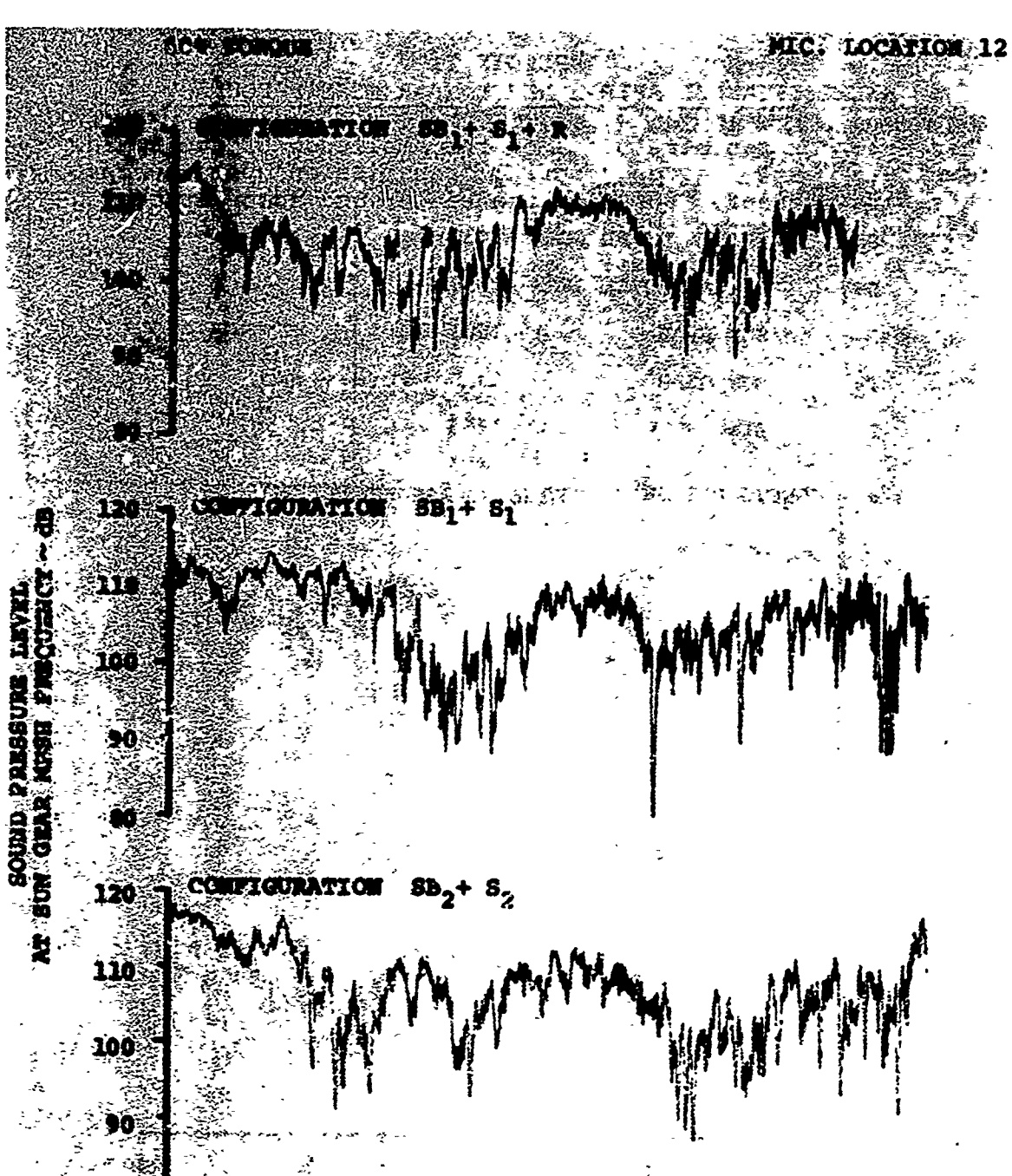

Figure 56. (Continued)

APPENDIX II
SWEEP DATA FOR SPIRAL BEVEL GEAR MESH FREQUENCY

This appendix contains plots of the amplitude of the spiral bevel gear mesh frequency during transmission speed sweeps. These are presented for each transducer and absorber configuration at selected torque values.

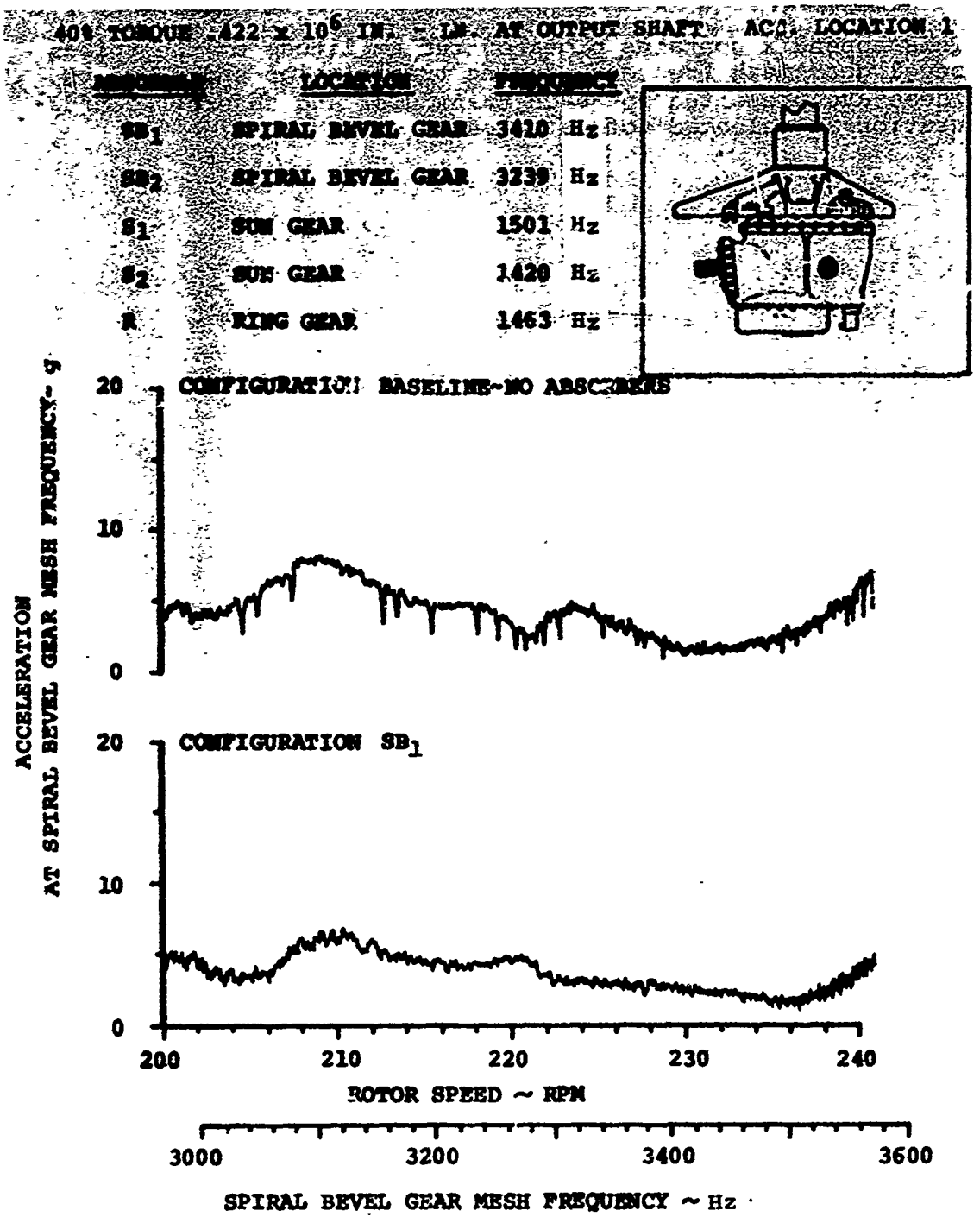

Figure 57. Spiral Bevel Sweep Data, Acc. Location,1, Torque 40%.

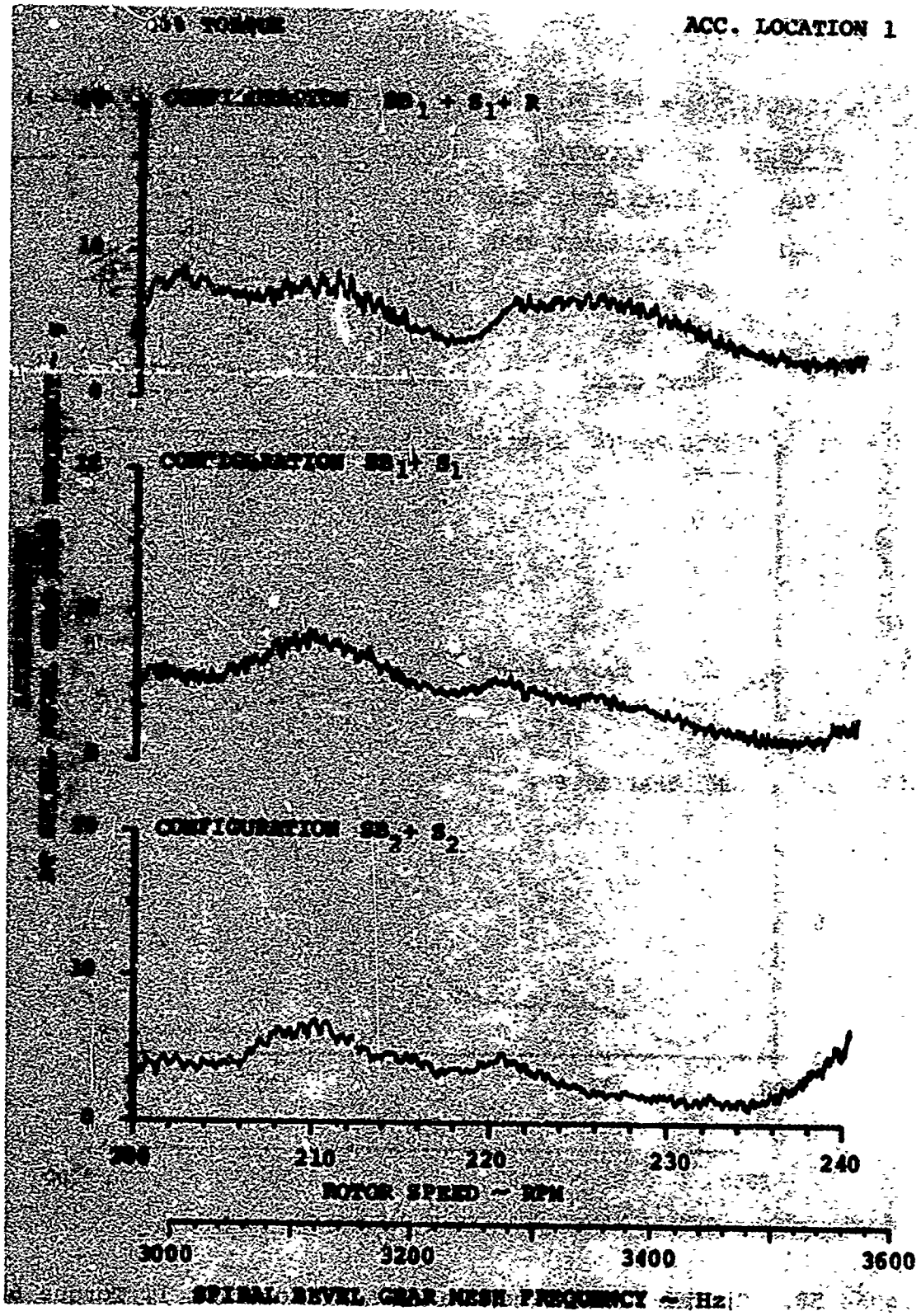

Figure 57. (Continued)

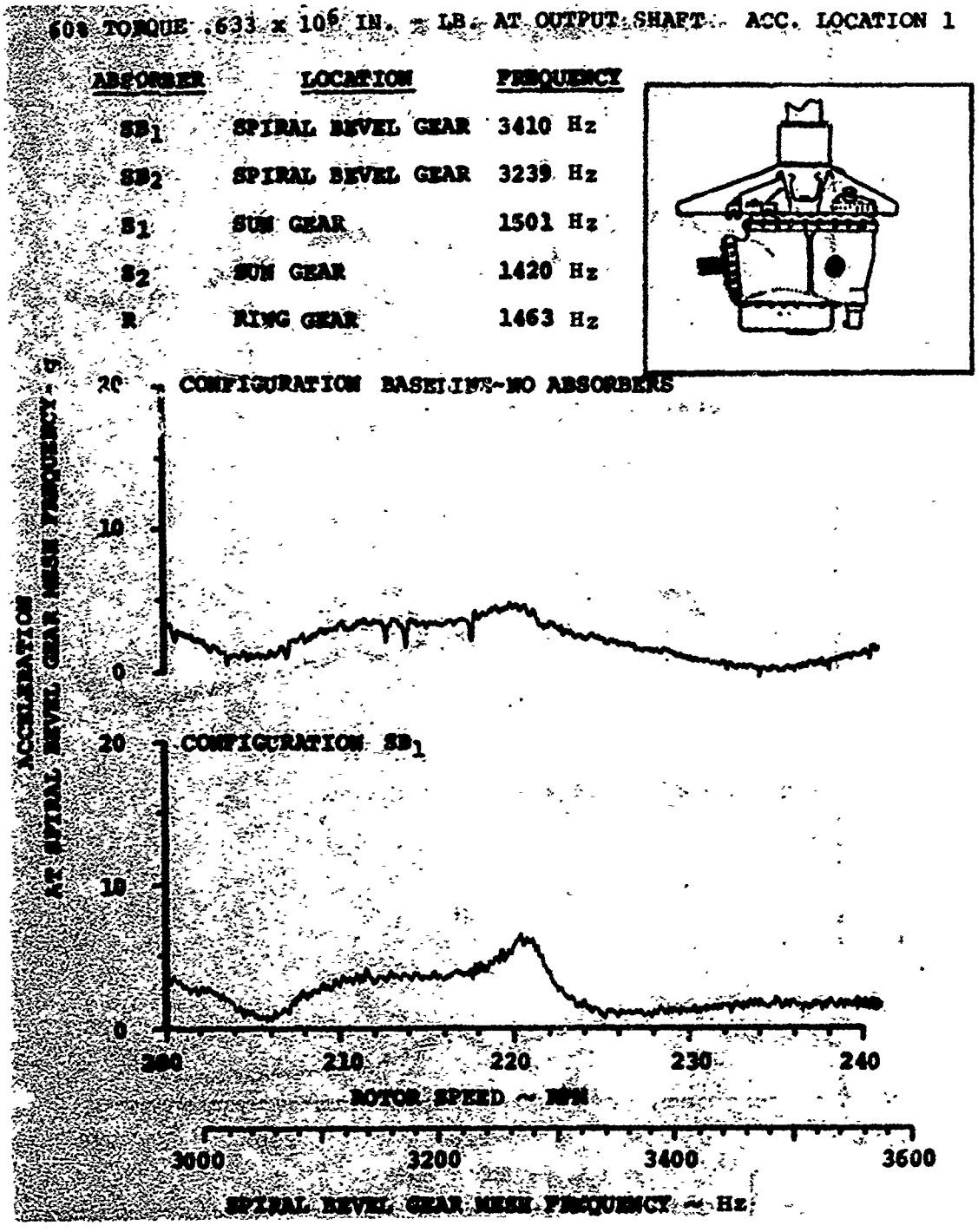

Figure 58. Spiral Bevel Sweep Data, Acc. Location 1, Torque 60%.

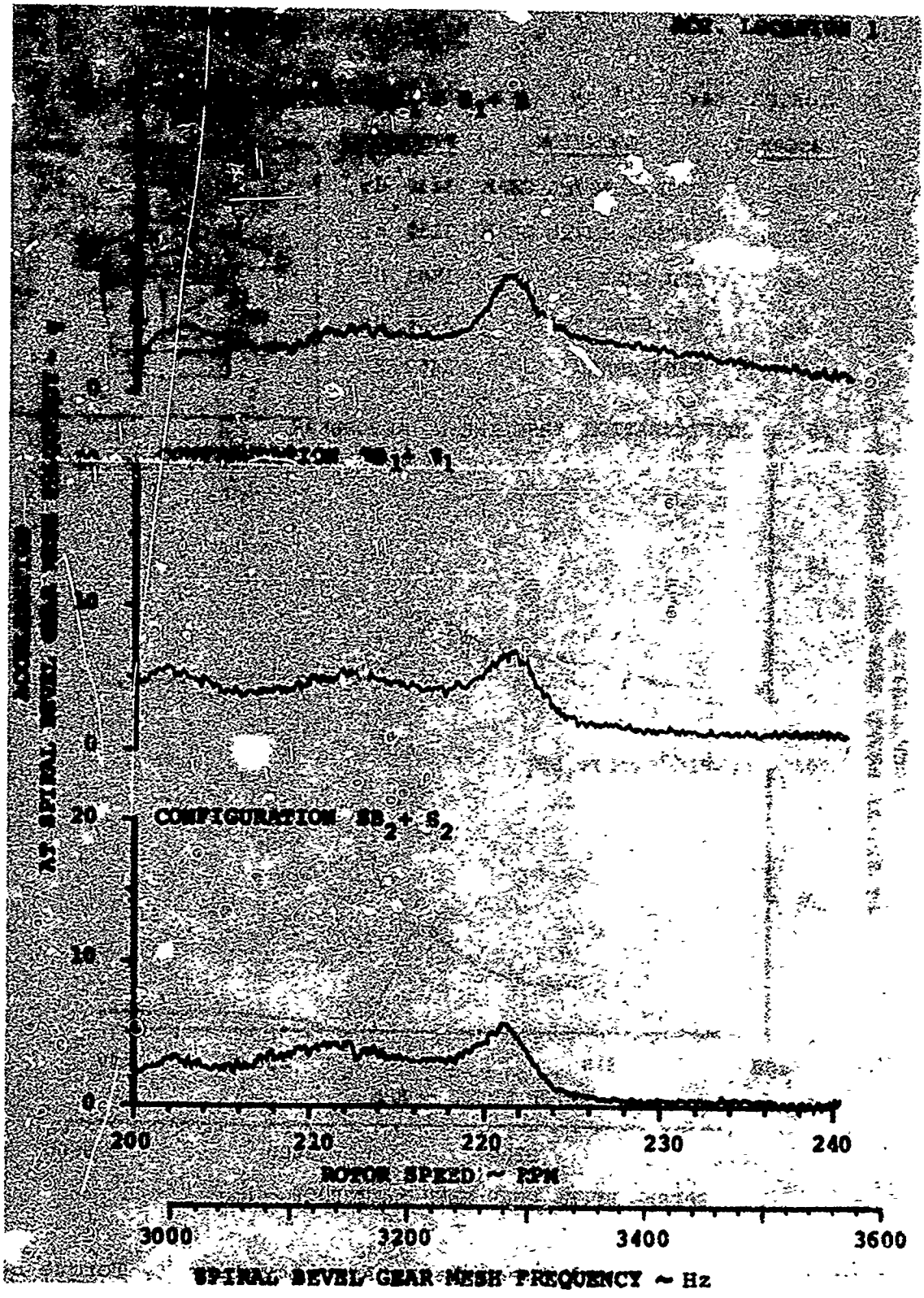

Figure 58. (Continued)

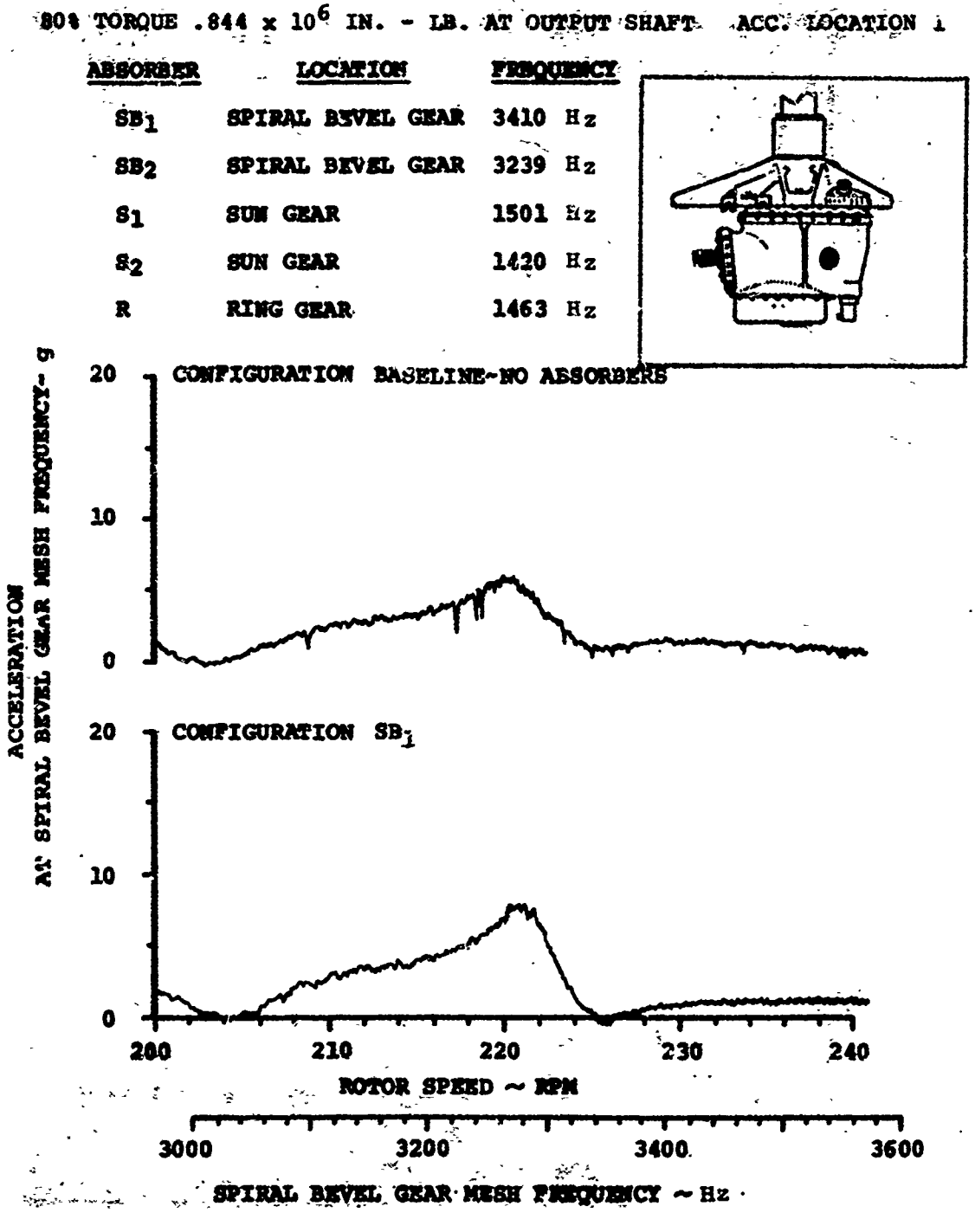

Figure 59. Spiral Bevel Sweep Data, Acc. Location 1, Torque 80%.

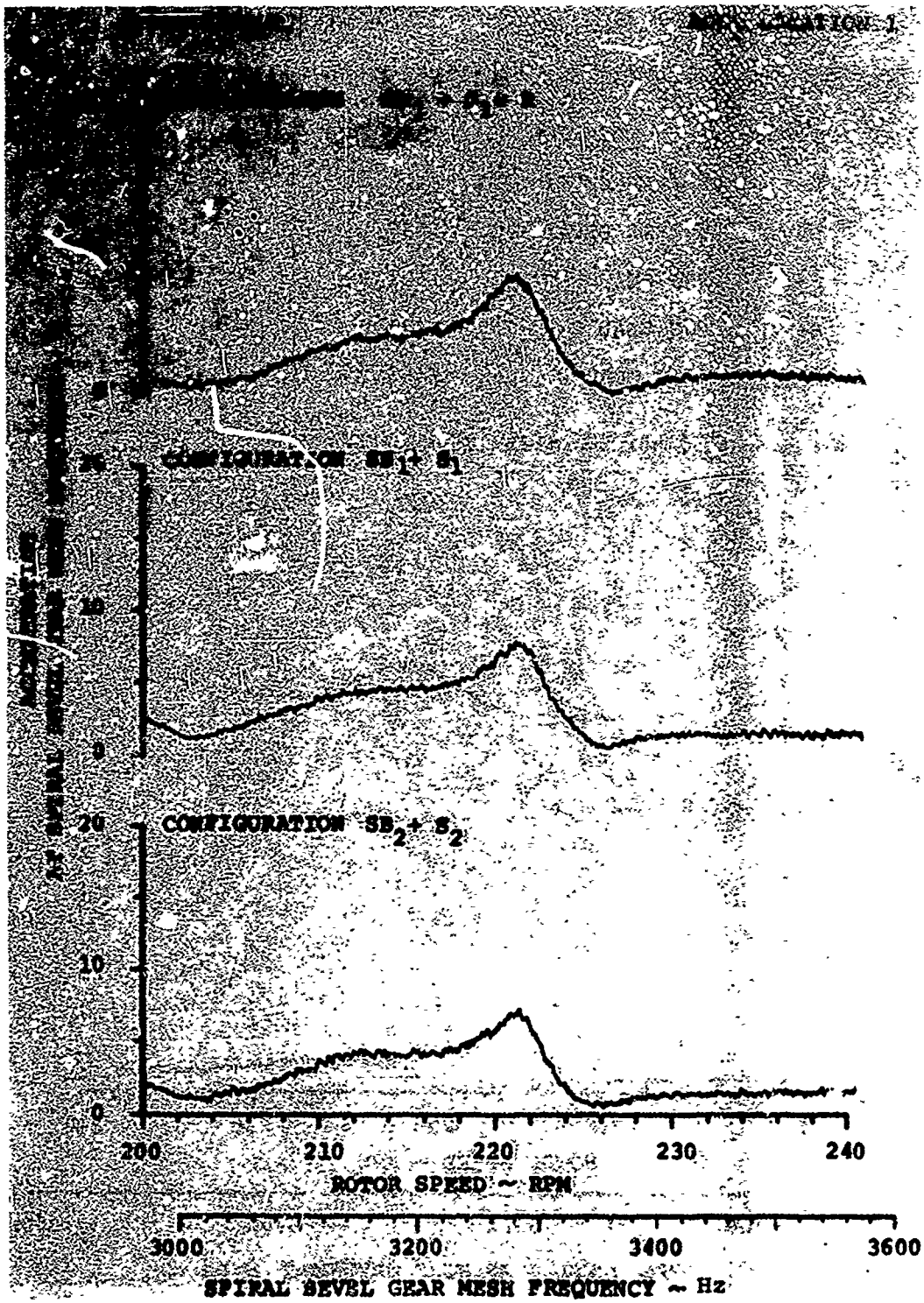

Figure 59. (Continued)

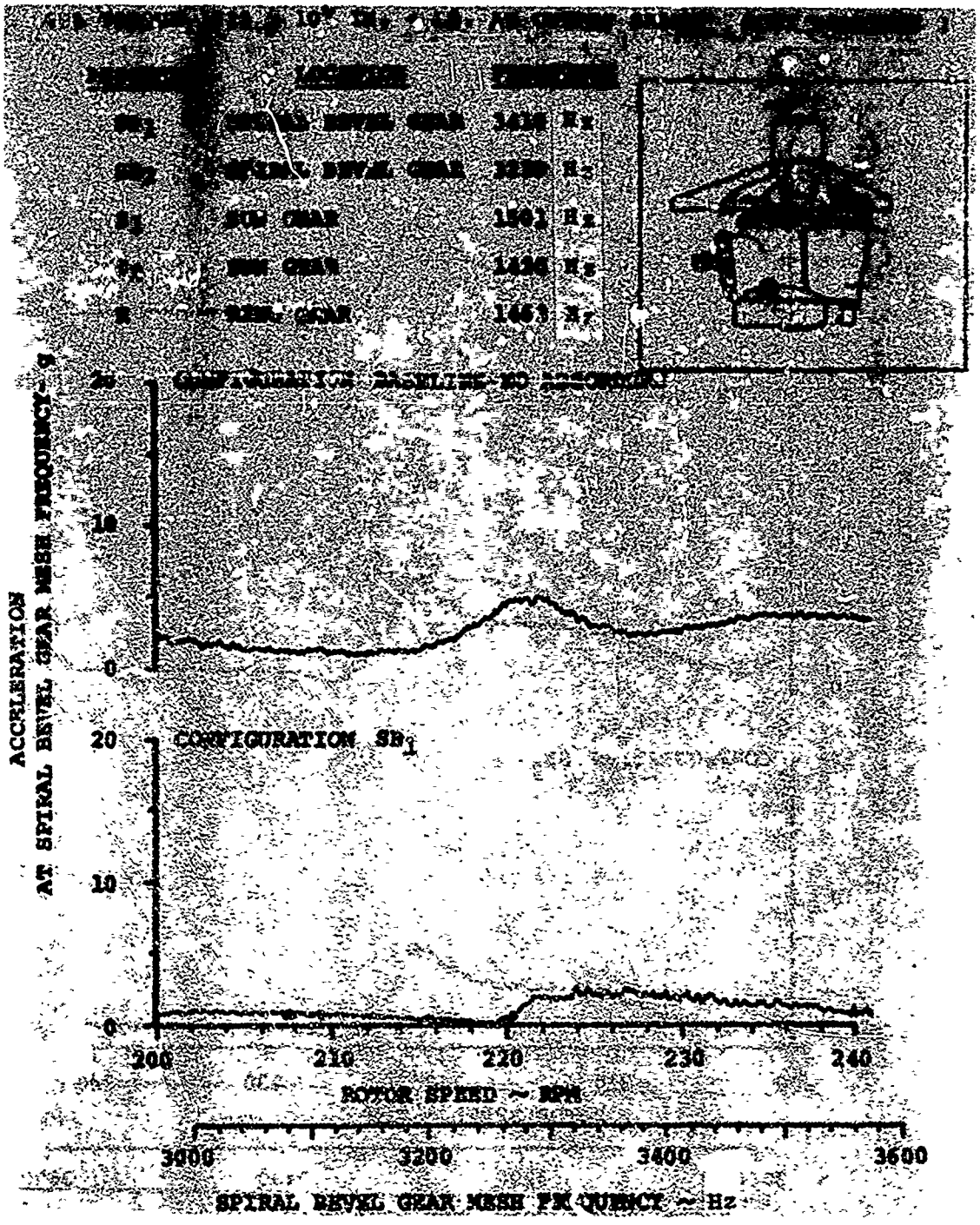

Figure 60. Spiral Bevel Sweep Data, Acc. Location 2, Torque 60%.

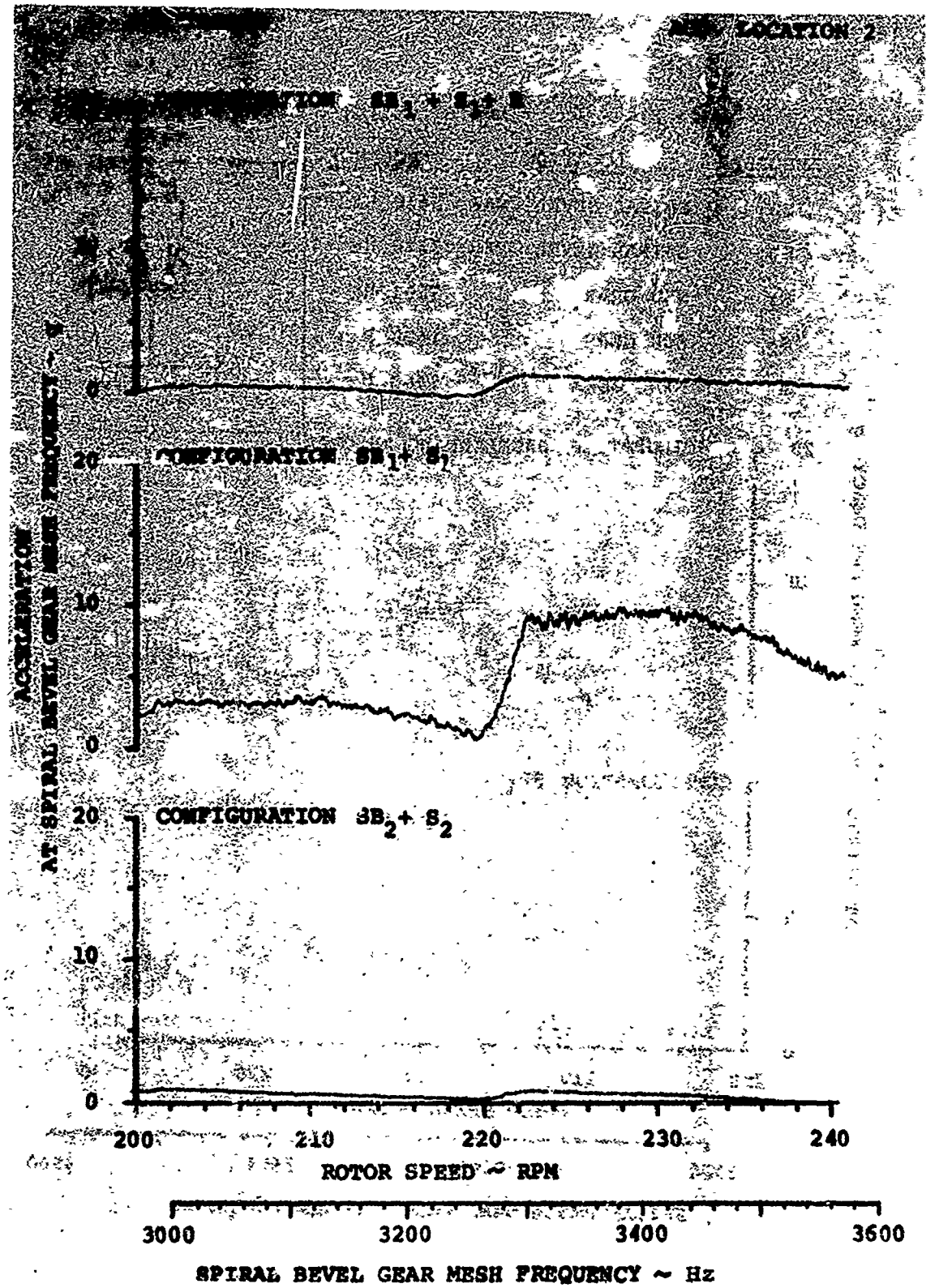

Figure 60. (Continued)

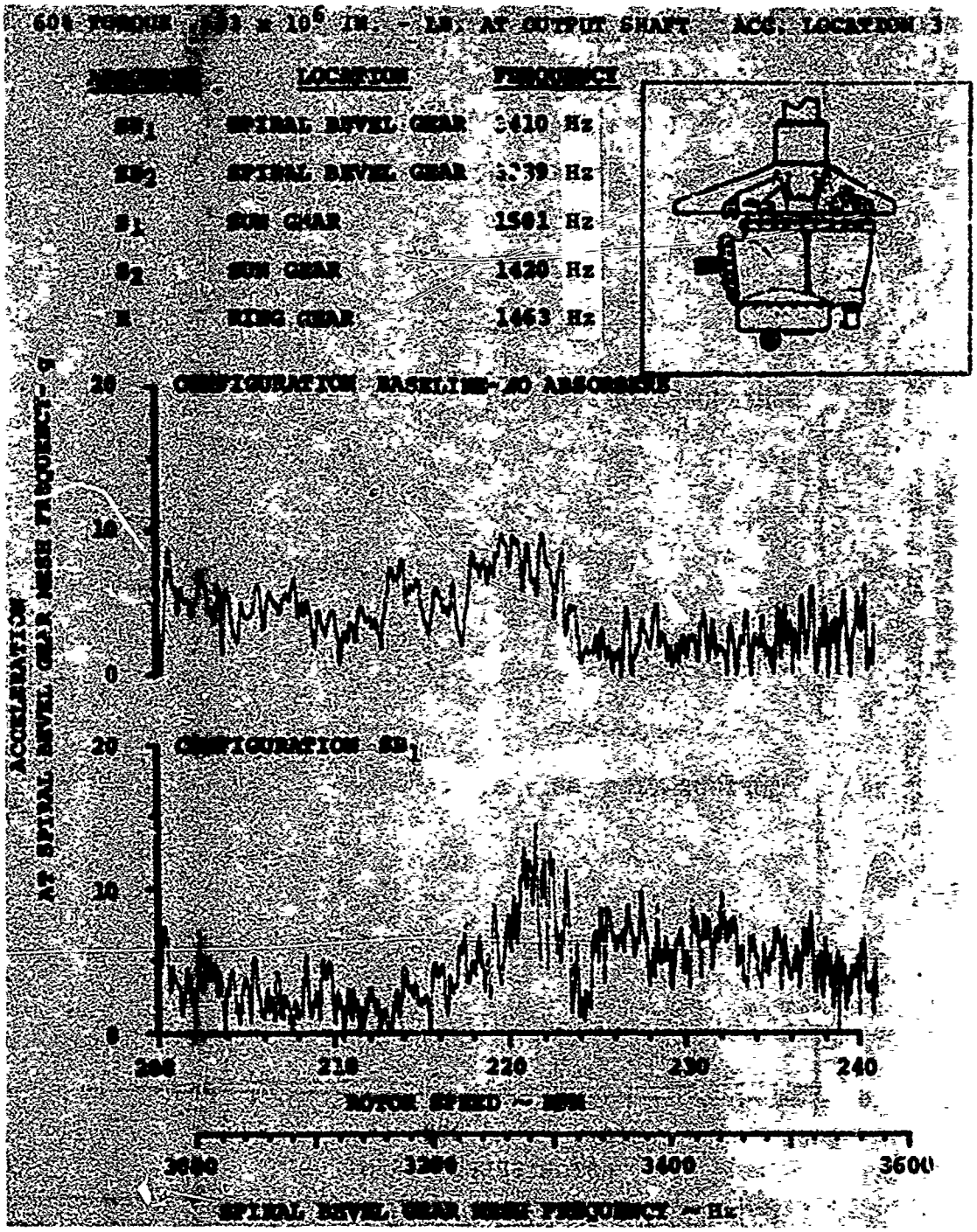

Figure 61. Spiral Bevel Sweep Data, Acc. Location 3, Torque 60%.

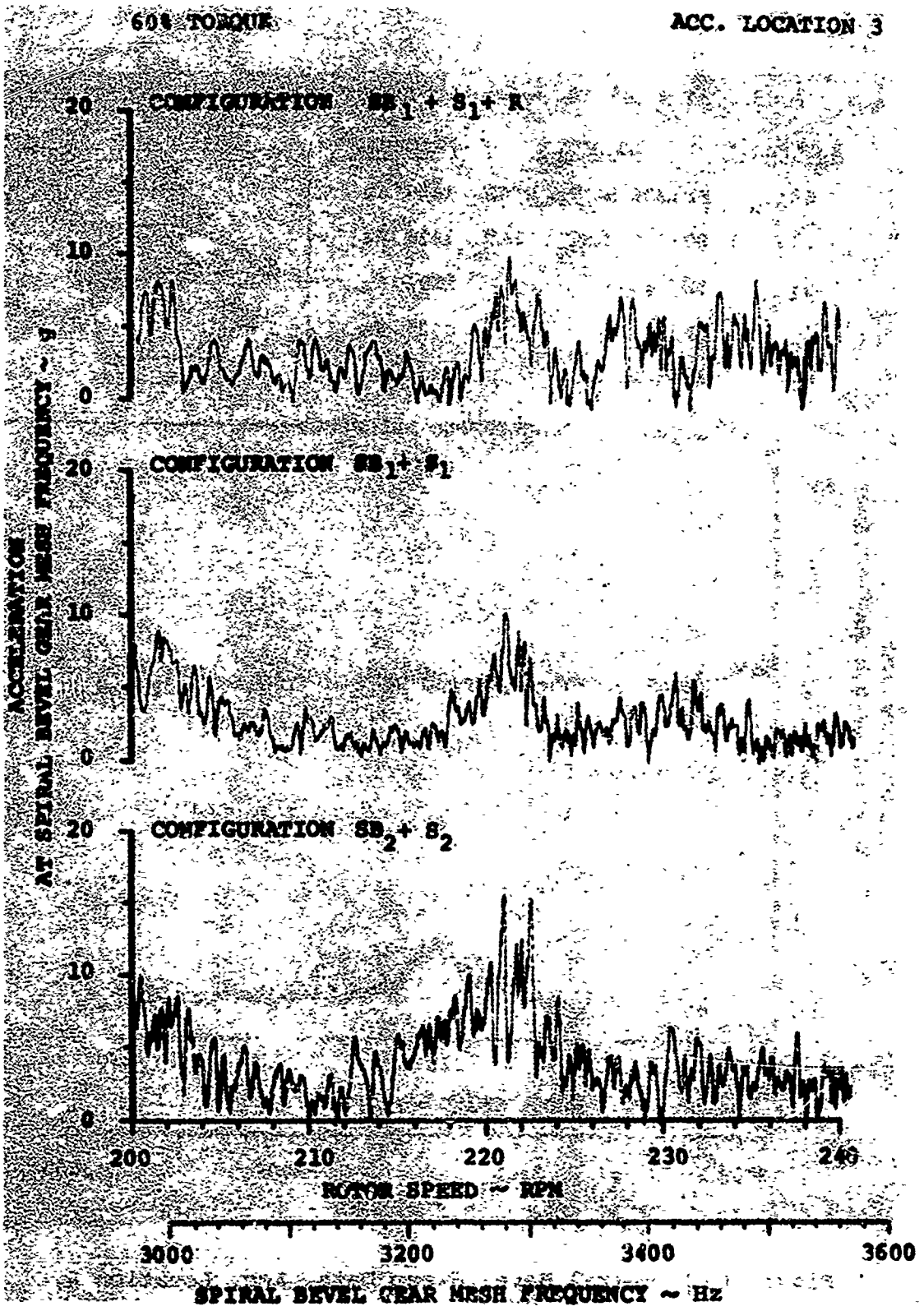

Figure 61. (Continued)

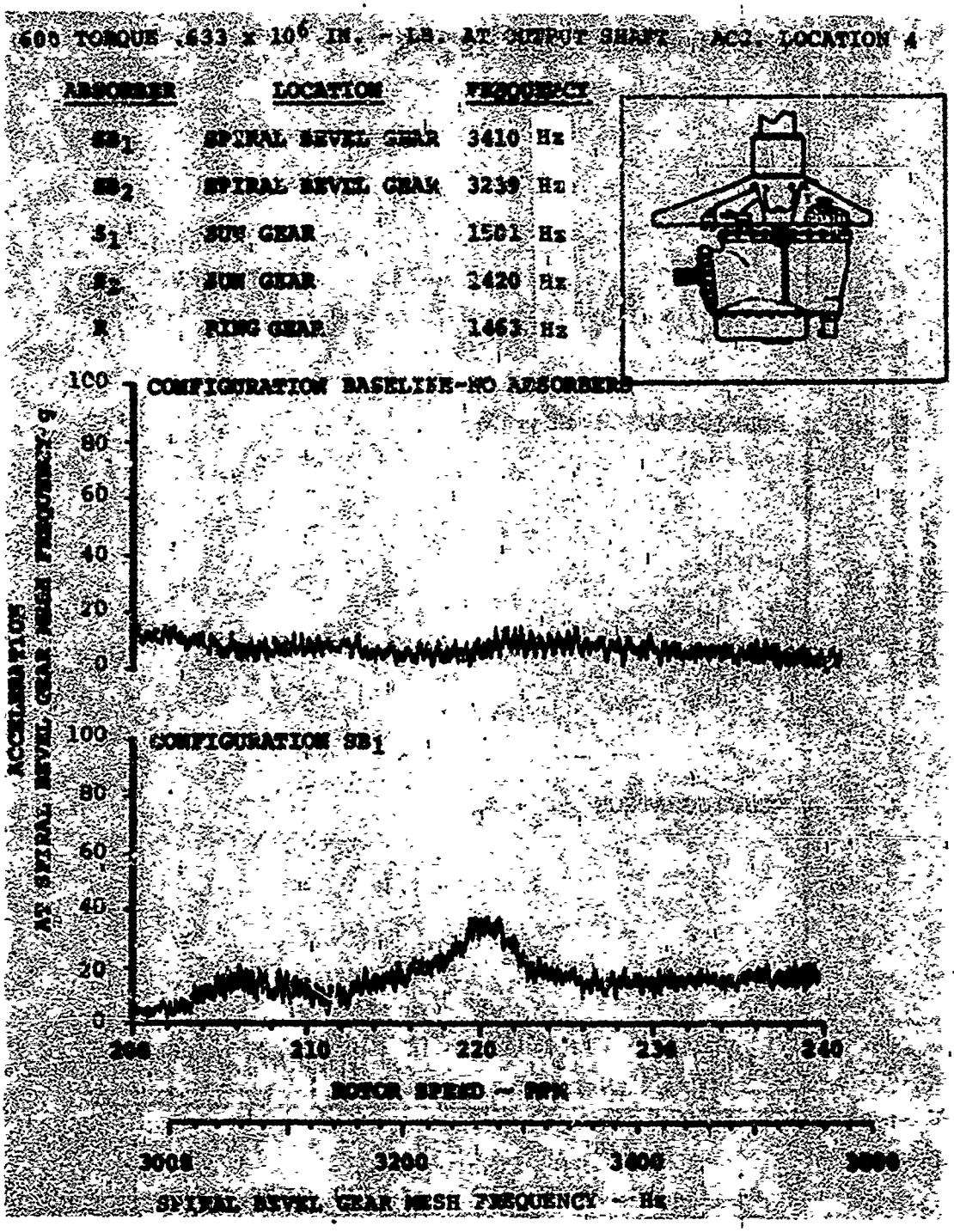

Figure 62. Spiral Bevel Sweep Data, Acc. Location 4, Torque 60%.

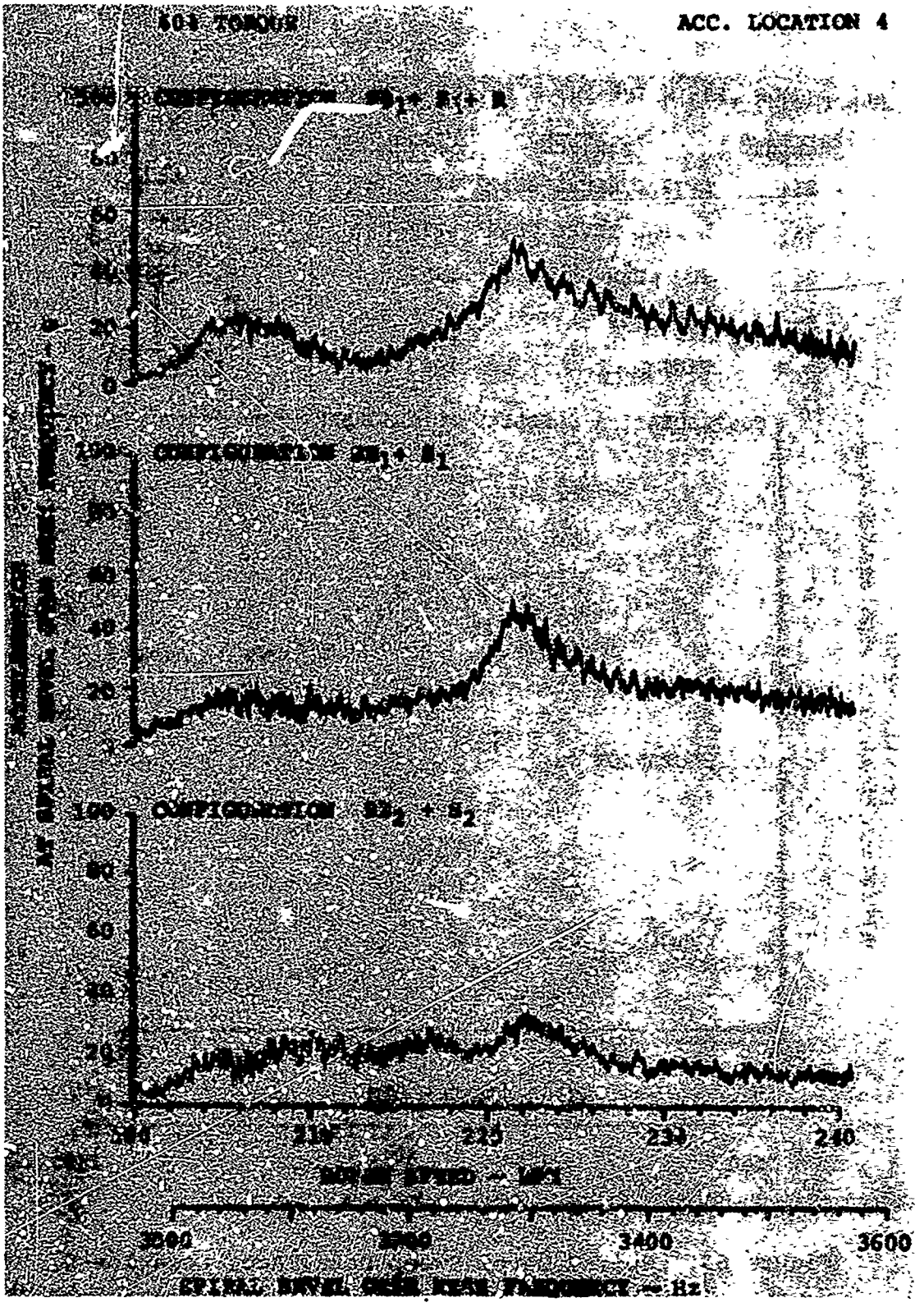

Figure 62. (Continued)

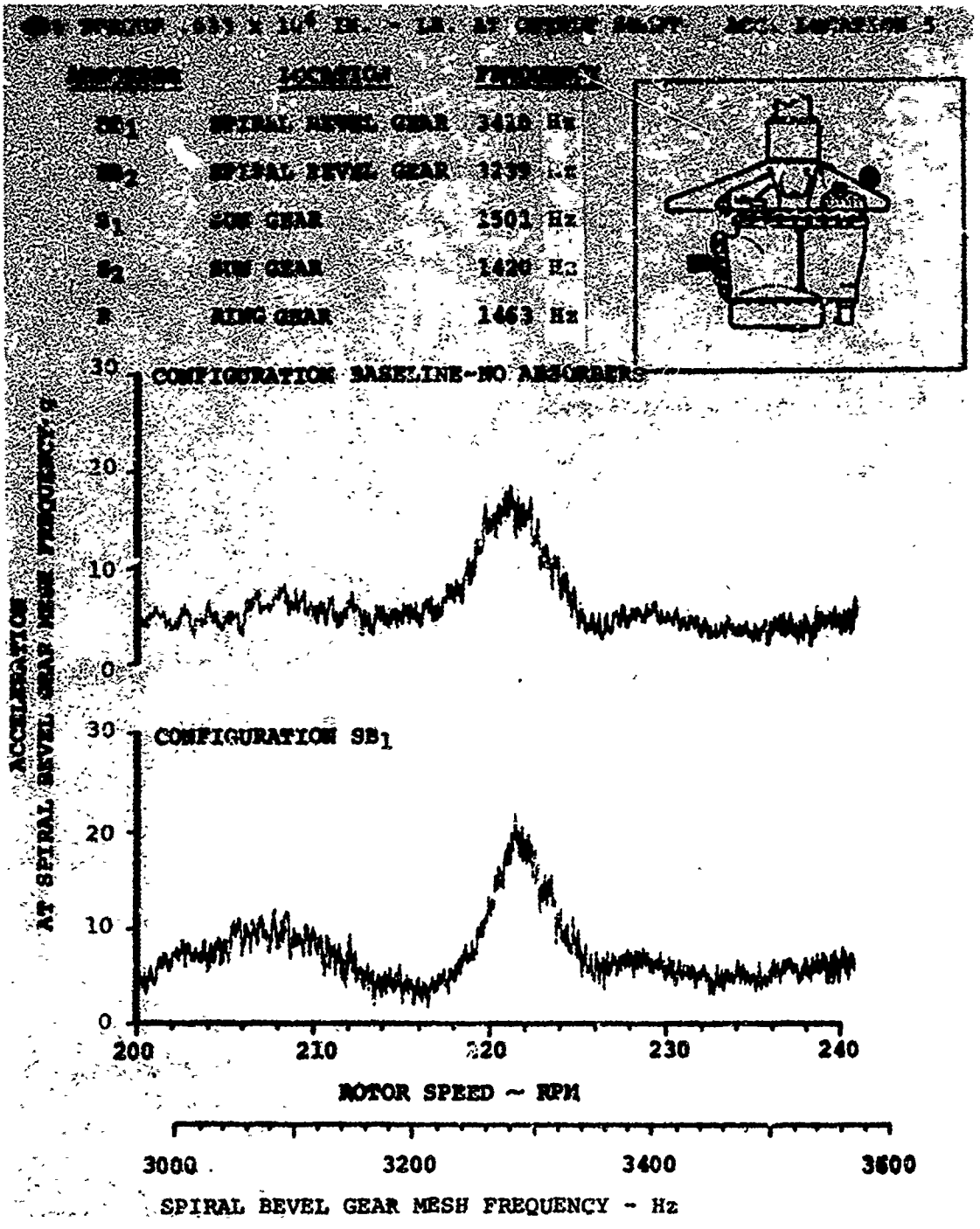

Figure 63. Spiral Bevel Sweep Data, Acc. Location 5, Torque 60%.

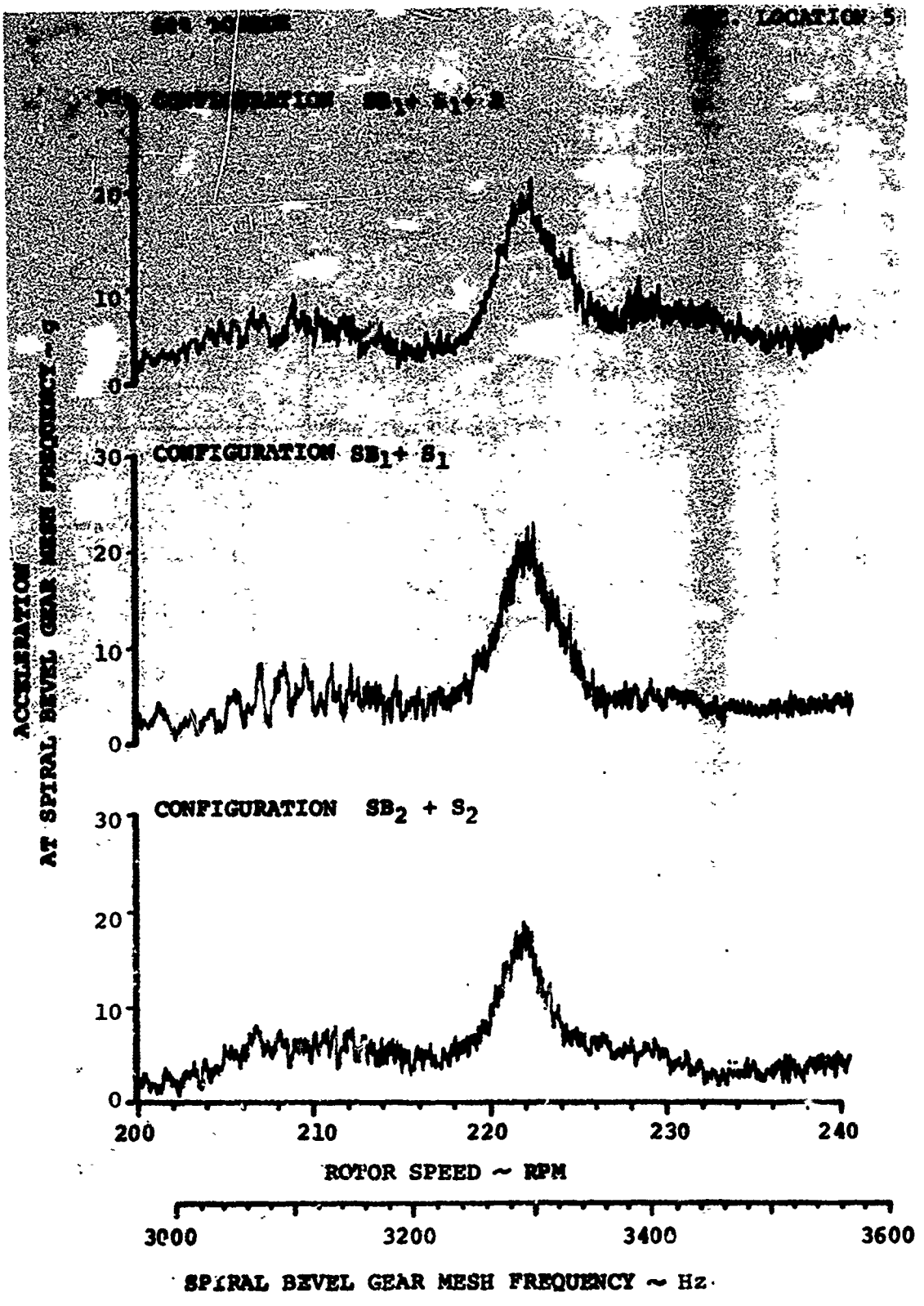

Figure 63. (Continued)

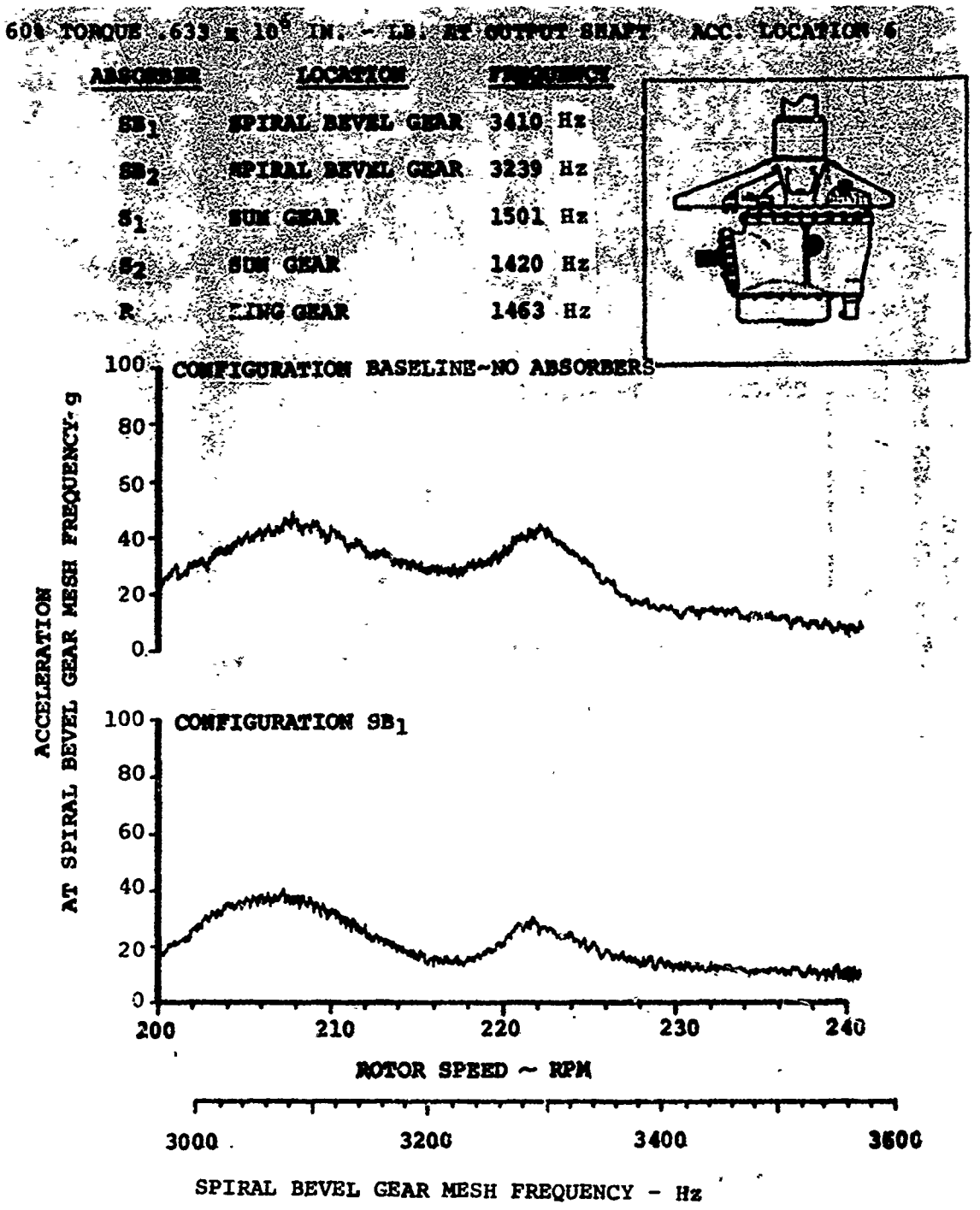

Figure 64. Spiral Bevel Sweep Data, Acc. Location 6, Torque 60%.

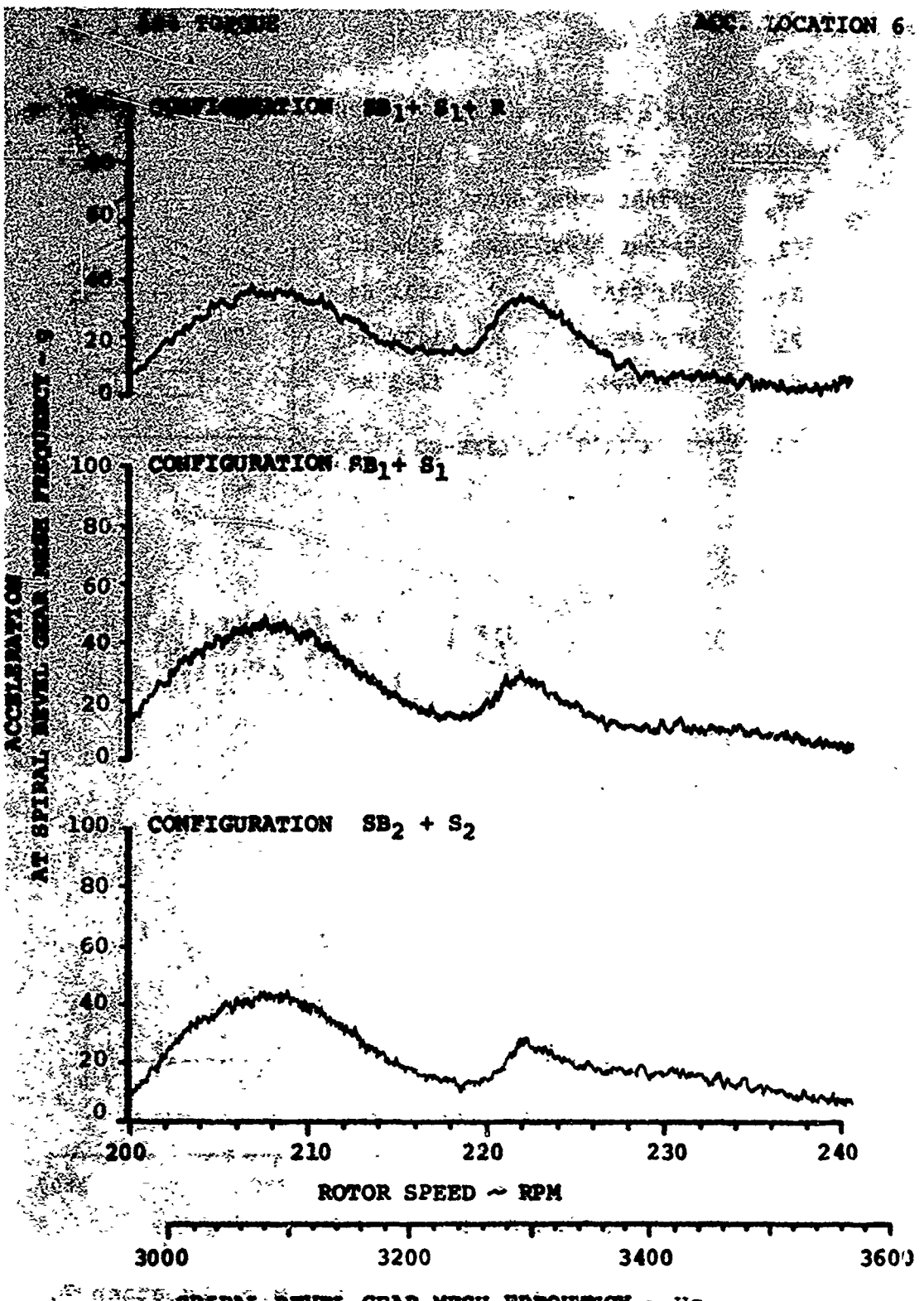

Figure 64. (Continued)

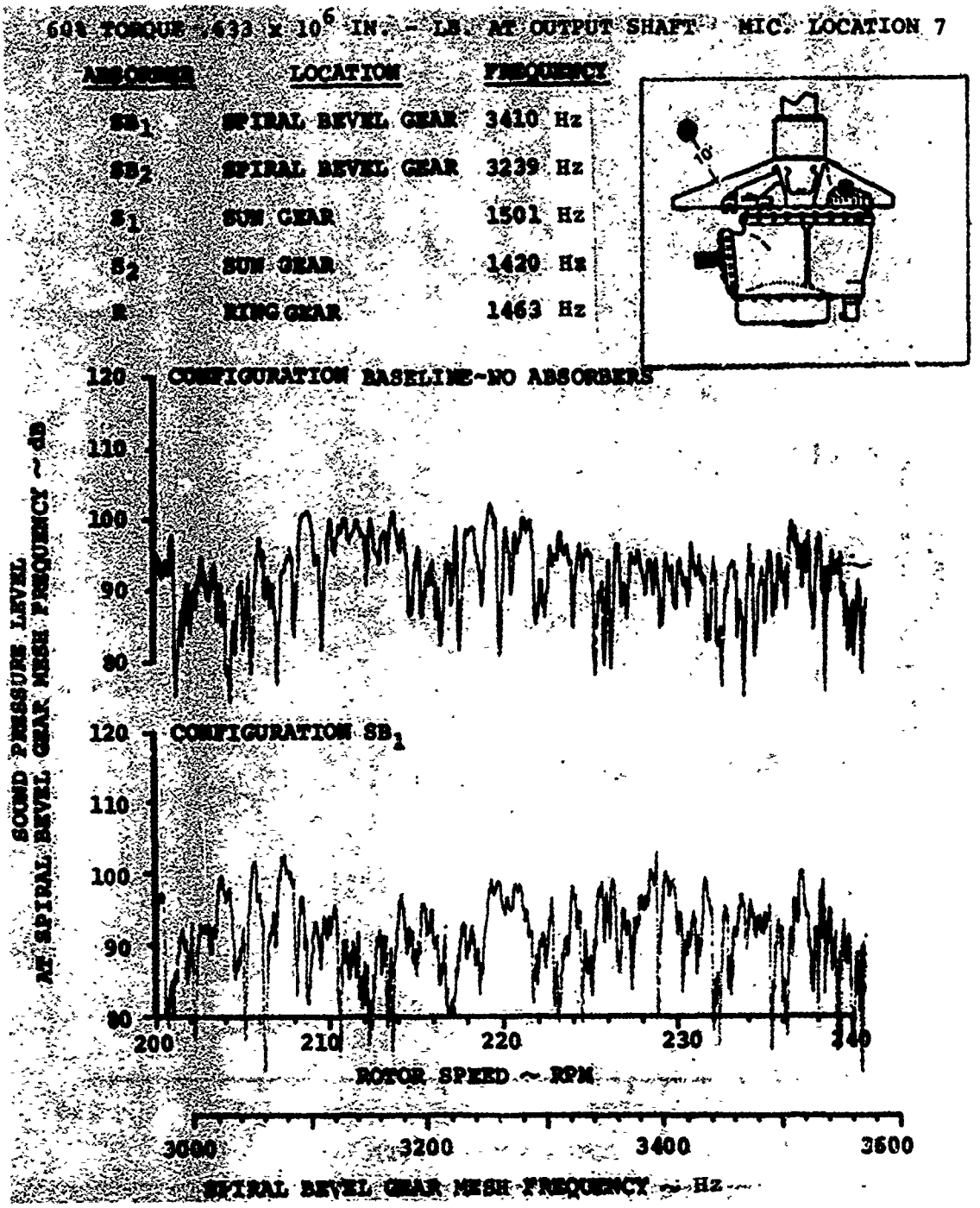

Figure 65. Spiral Bevel Sweep Data, Mic. Location 7, Torque 60%.

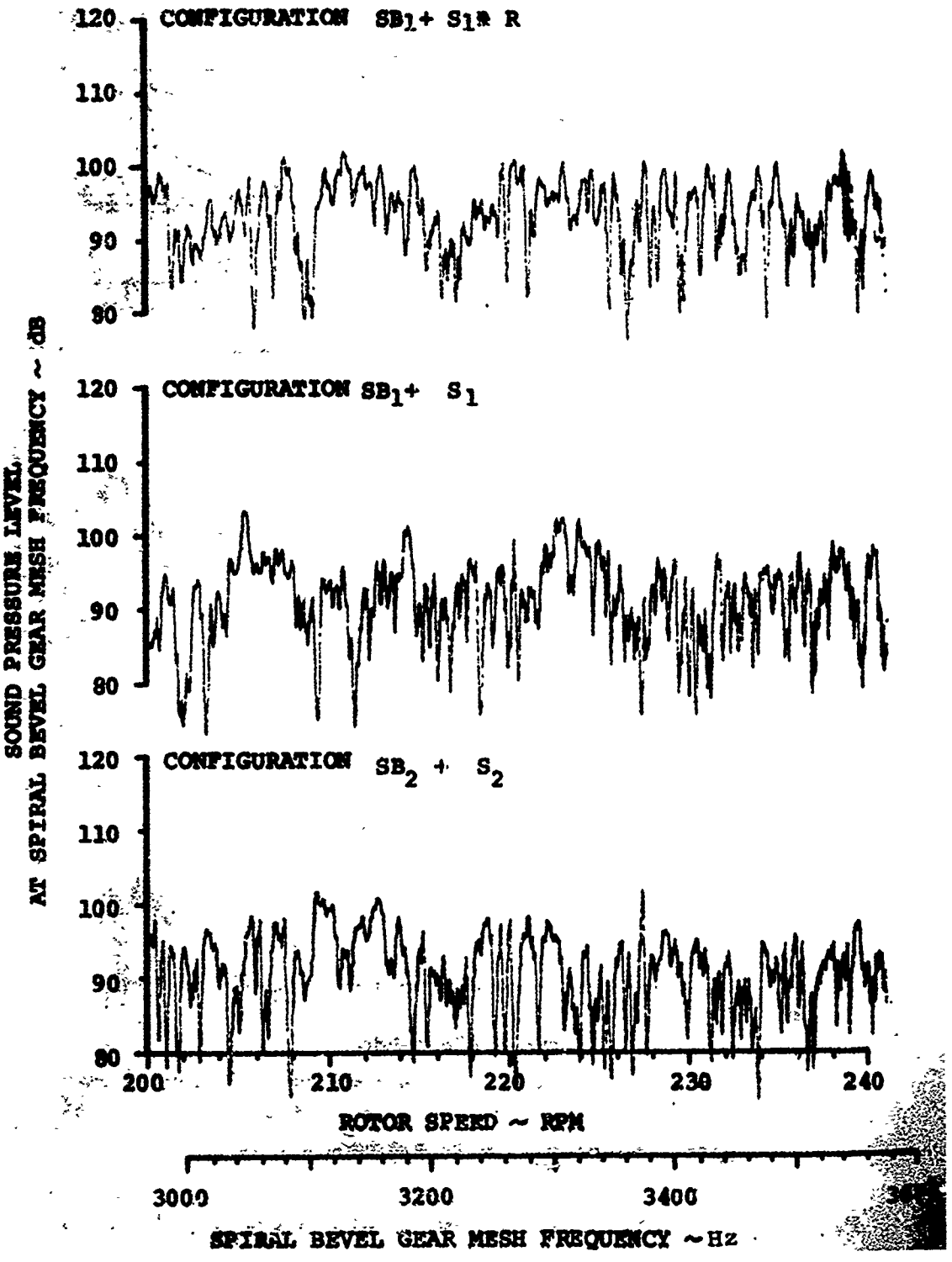

Figure 65. (Continued)

60% TORQUE .633 x 10^6 IN. - LB. AT OUTPUT SHAFT; MIC. LOCATION 8

ABSORBER	LOCATION	FREQUENCY
SB_1	SPIRAL BEVEL GEAR	3410 Hz
SB_2	SPIRAL BEVEL GEAR	3239 Hz
S_1	SUN GEAR	1501 Hz
S_2	SUN GEAR	1420 Hz
R	RING GEAR	1463 Hz

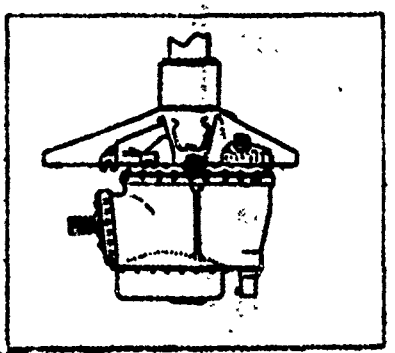

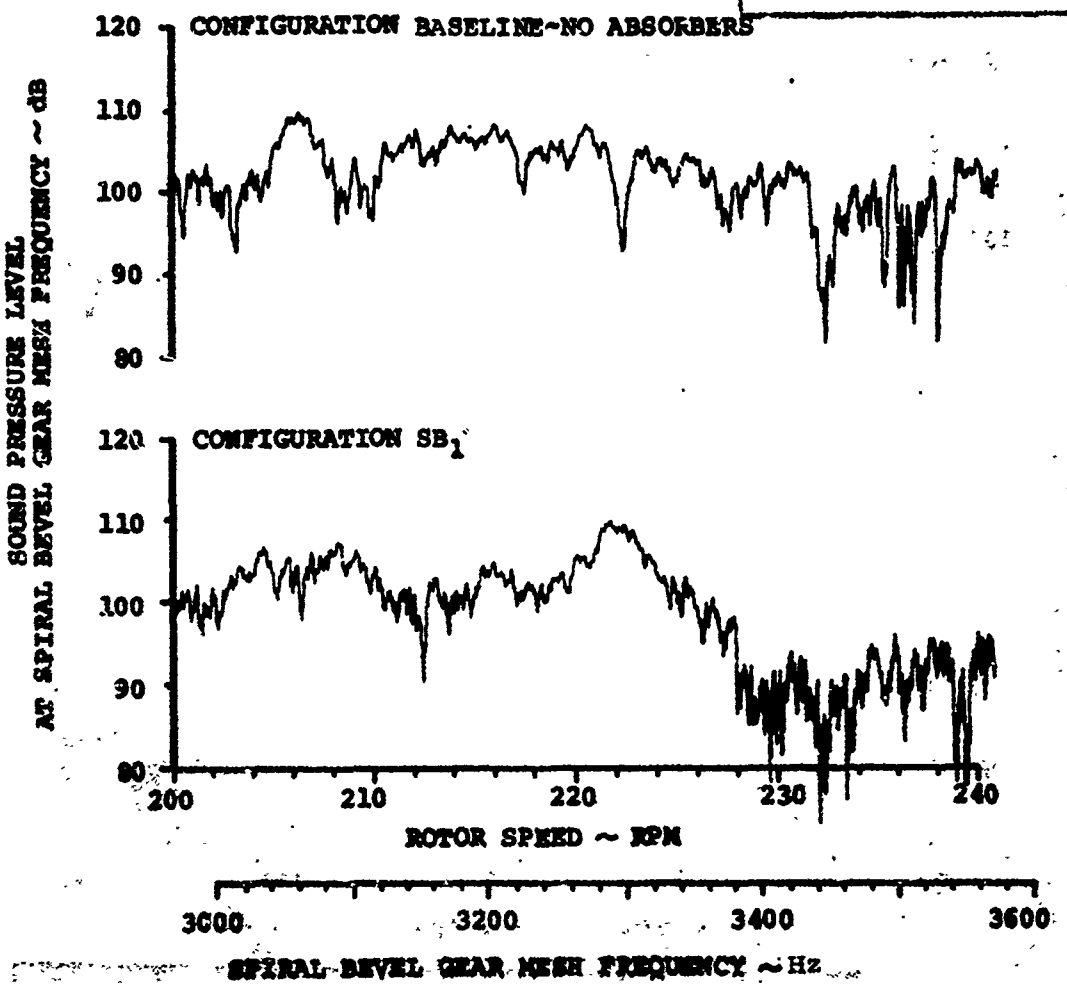

Figure 66. Spiral Bevel Sweep Data, Mic. Location 8, Torque 60%.

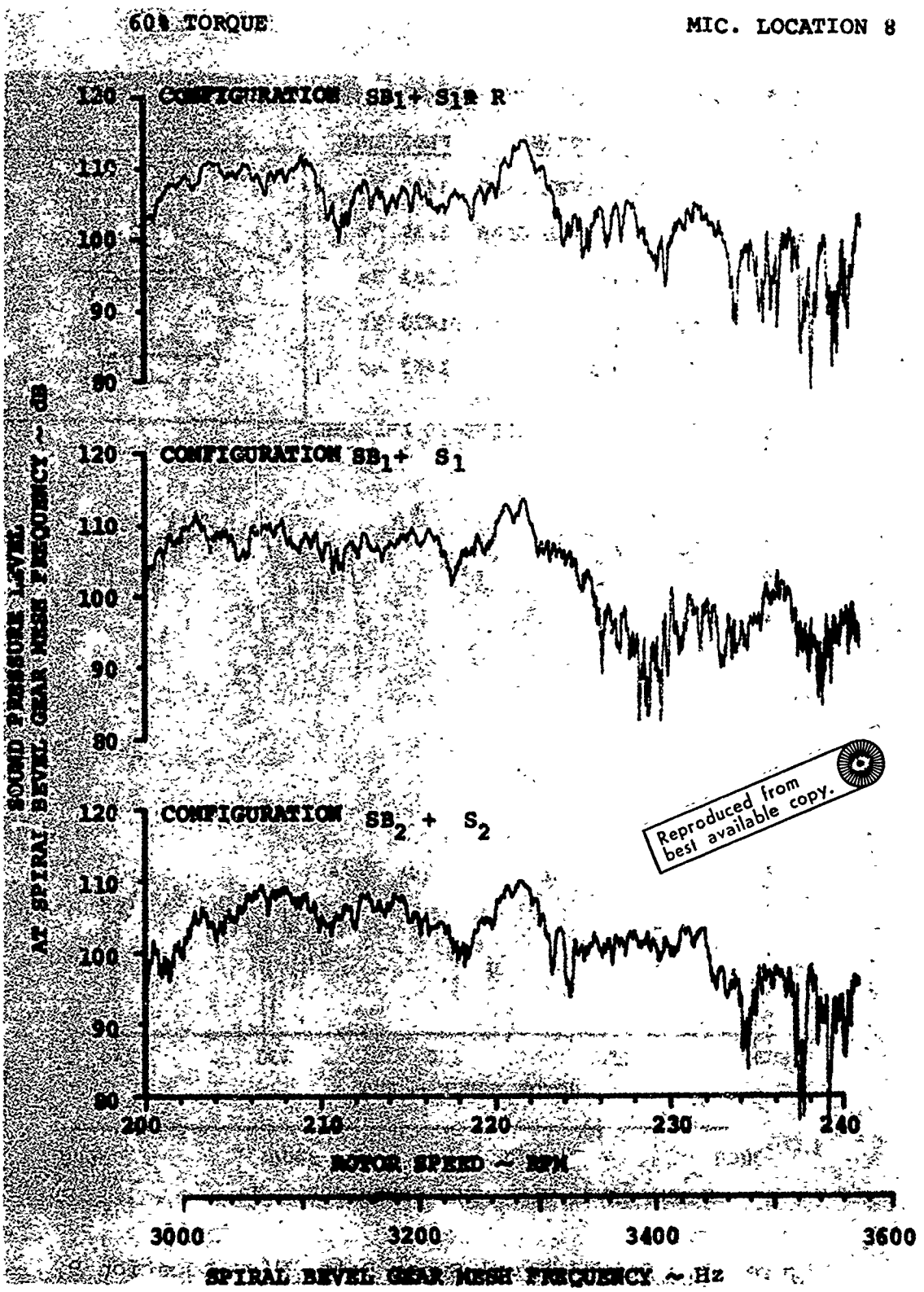

Figure 66. (Continued)

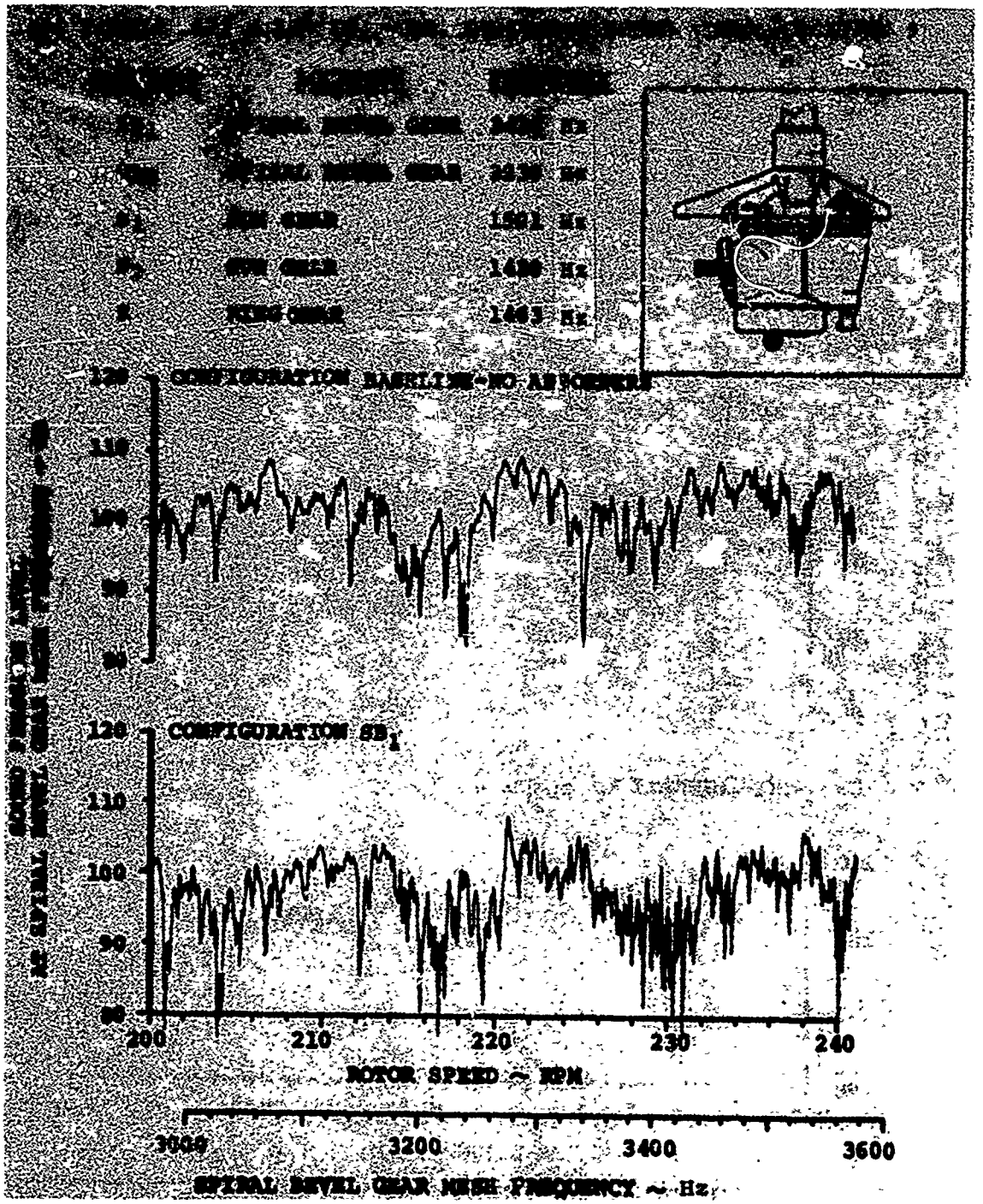

Figure 67. Spiral Bevel Sweep Data. Mic. Location 9, Torque 60%.

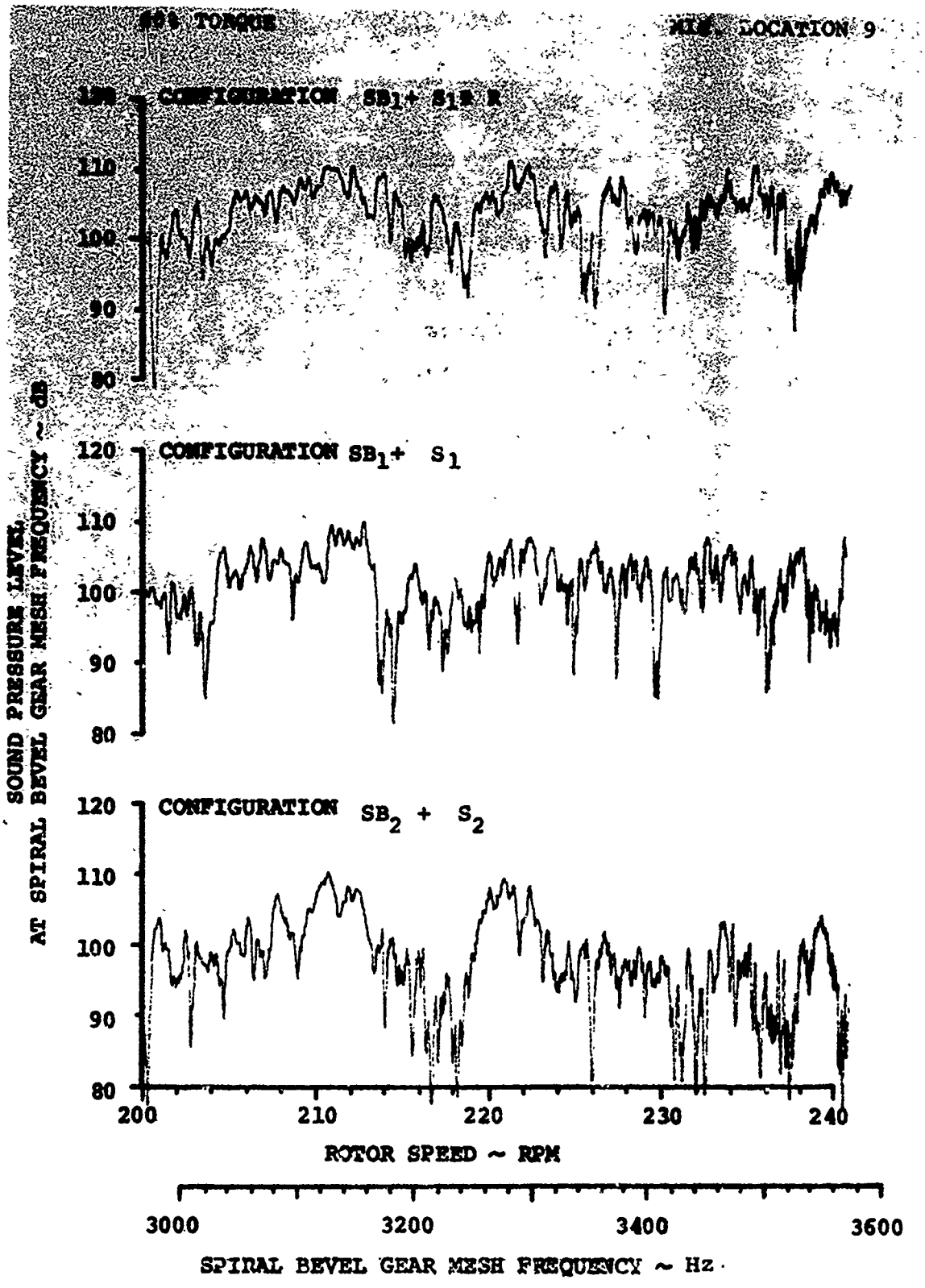

Figure 67. (Continued)

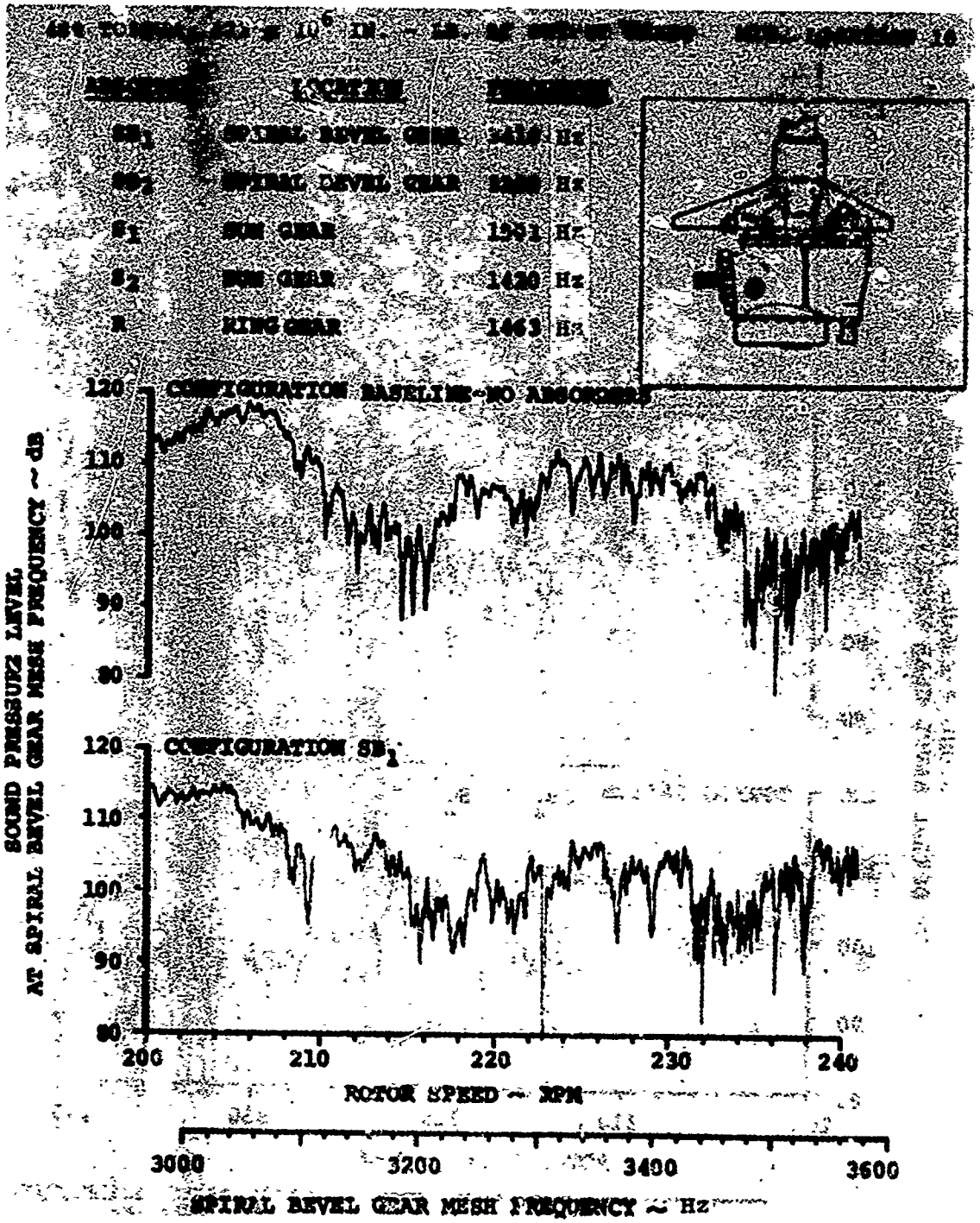

Figure 68. Spiral Bevel Sweep Data, Mic. Location 10, Torque 40%.

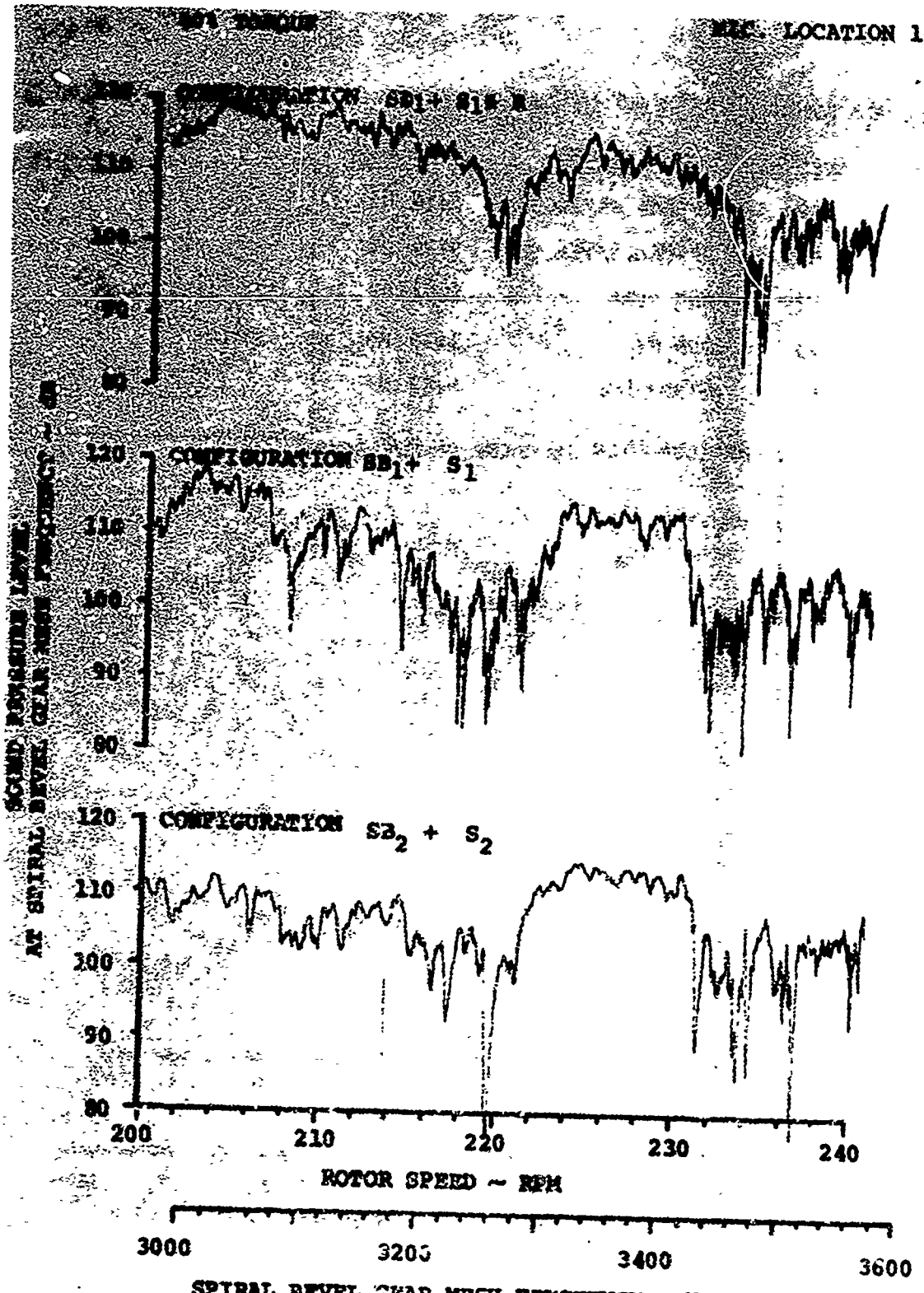

Figure 68. (Continued)

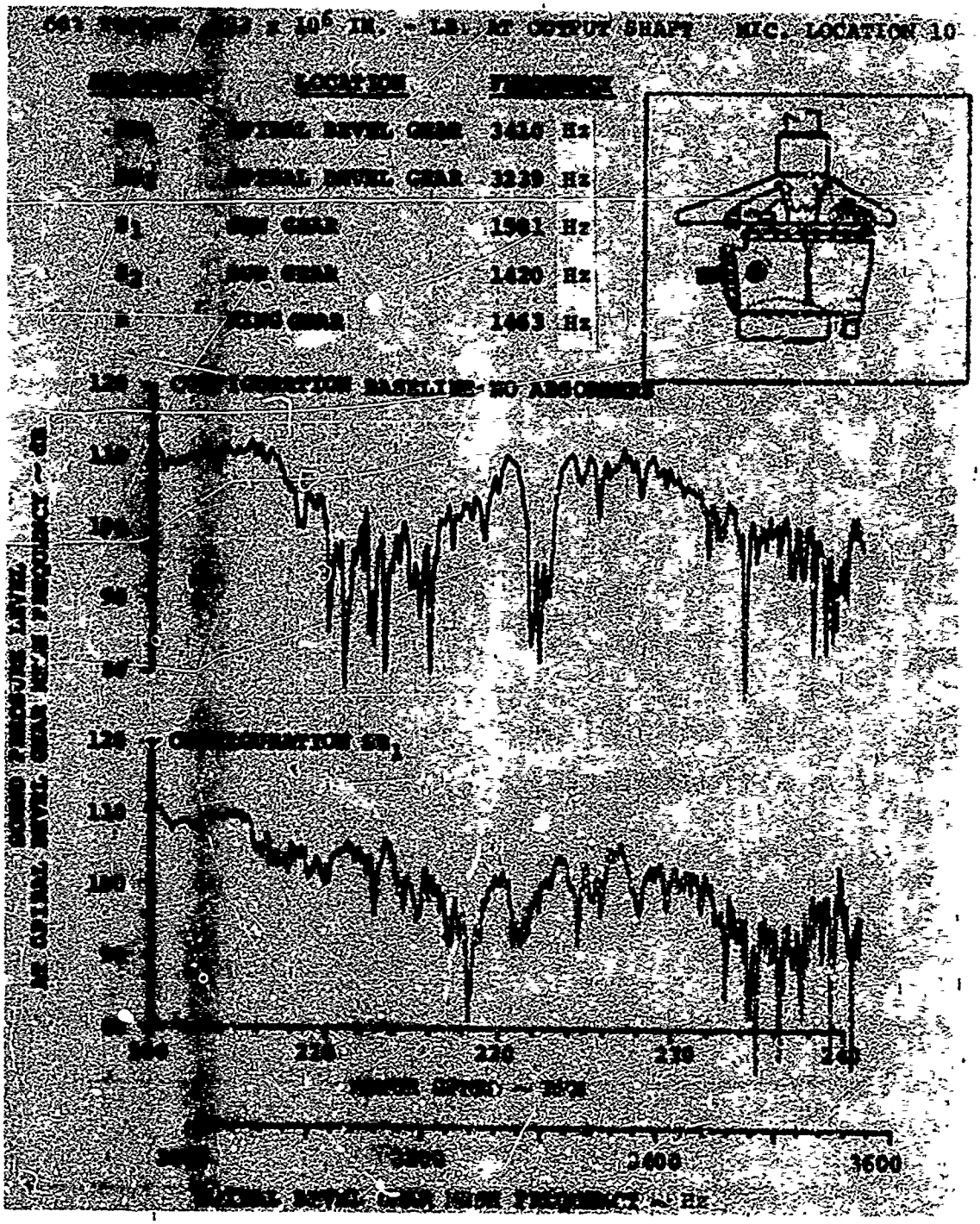

Figure 69. Spiral Bevel Sweep Data, Mic. Location 10, Torque 60%.

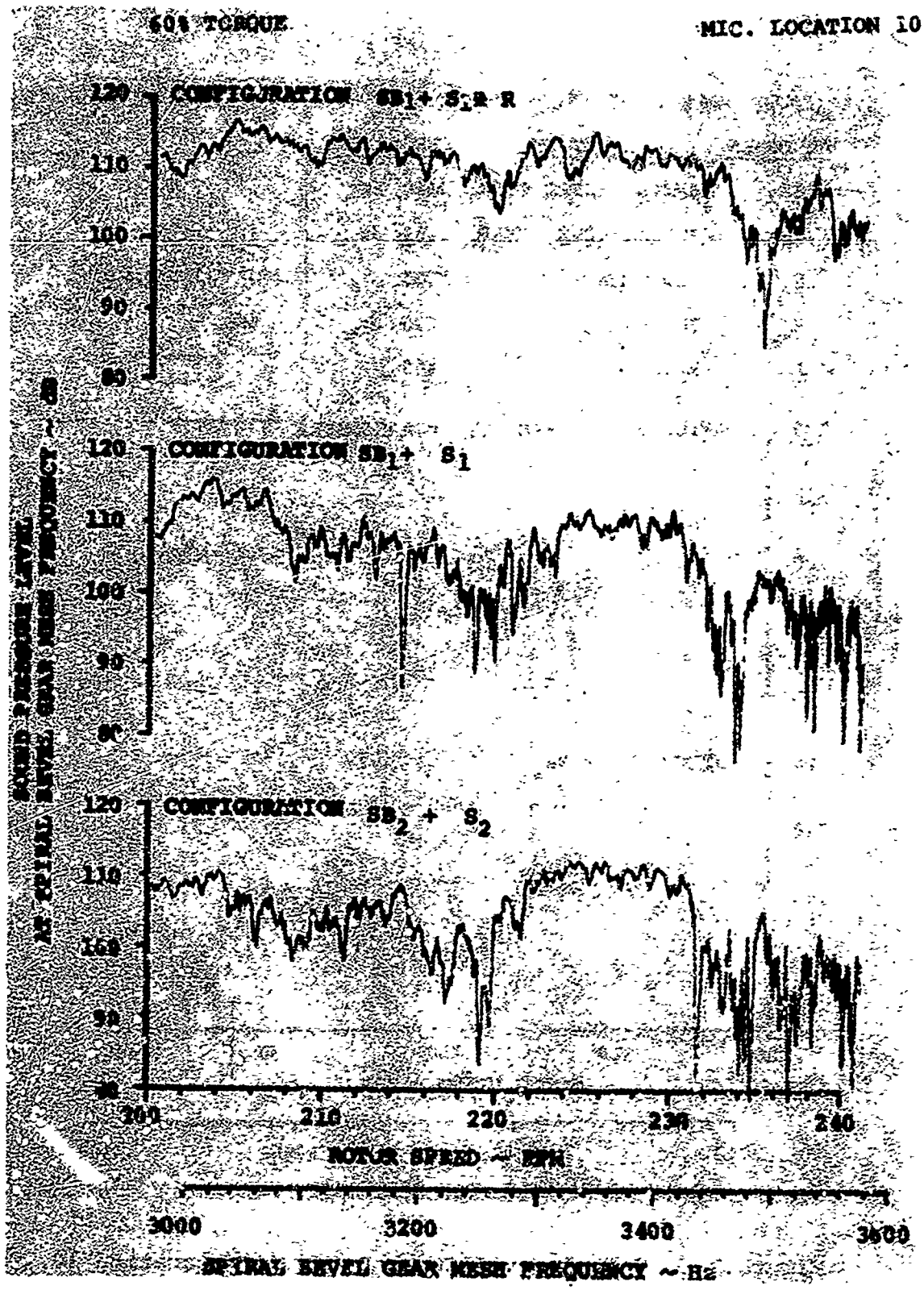

Figure 69. (Continued)

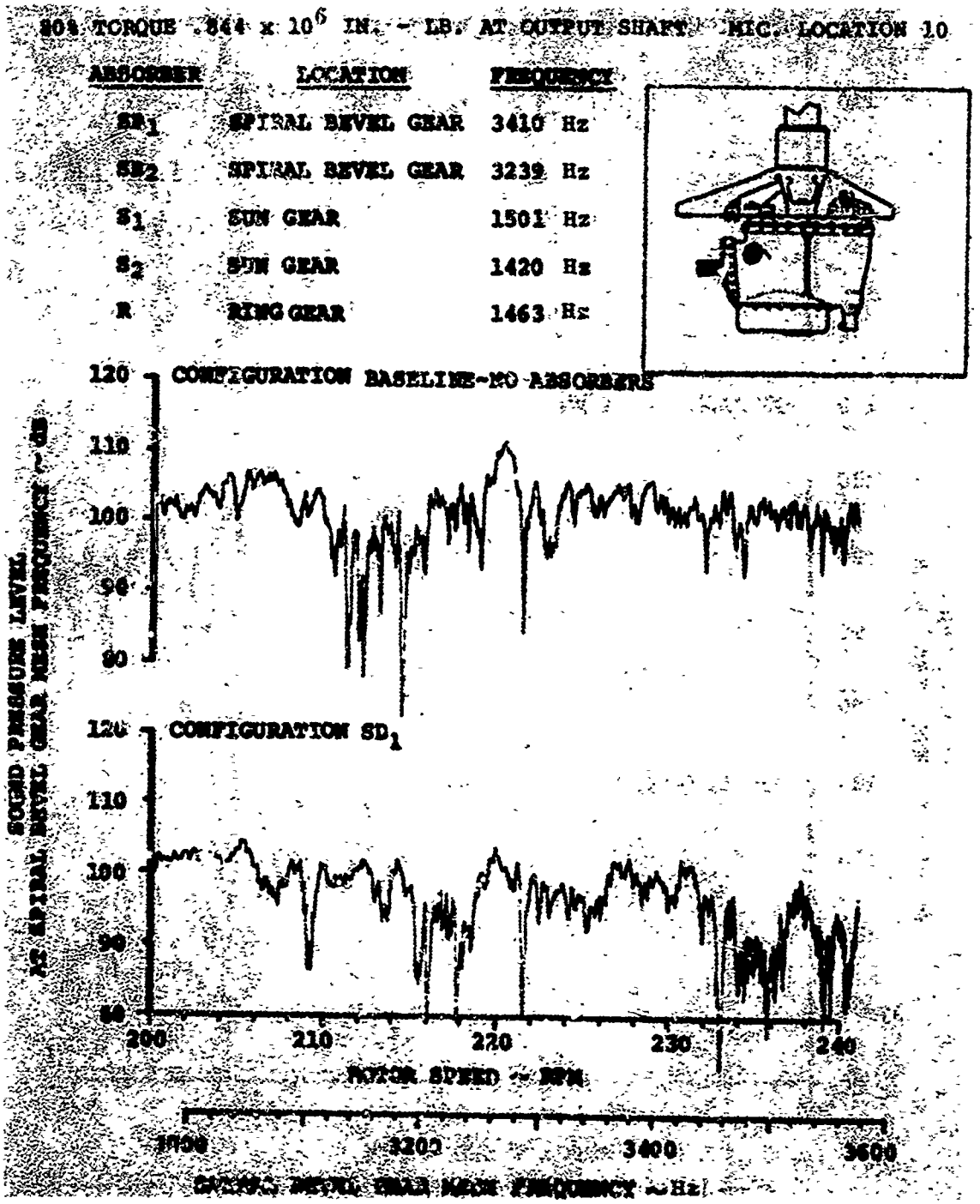

Figure 70. Spiral Bevel Sweep Data, Mic. Location 10, Torque 80%.

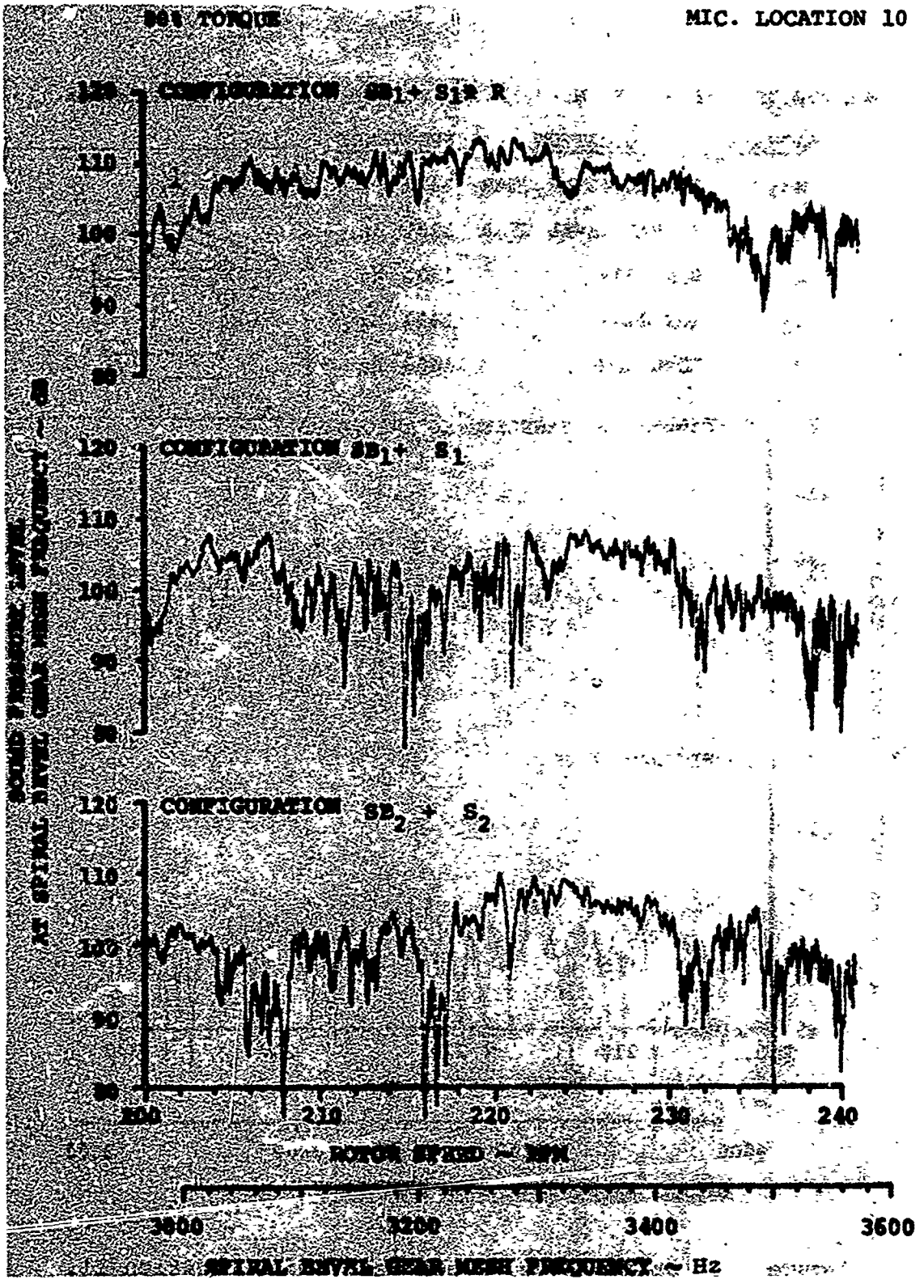

Figure 70. (Continued)

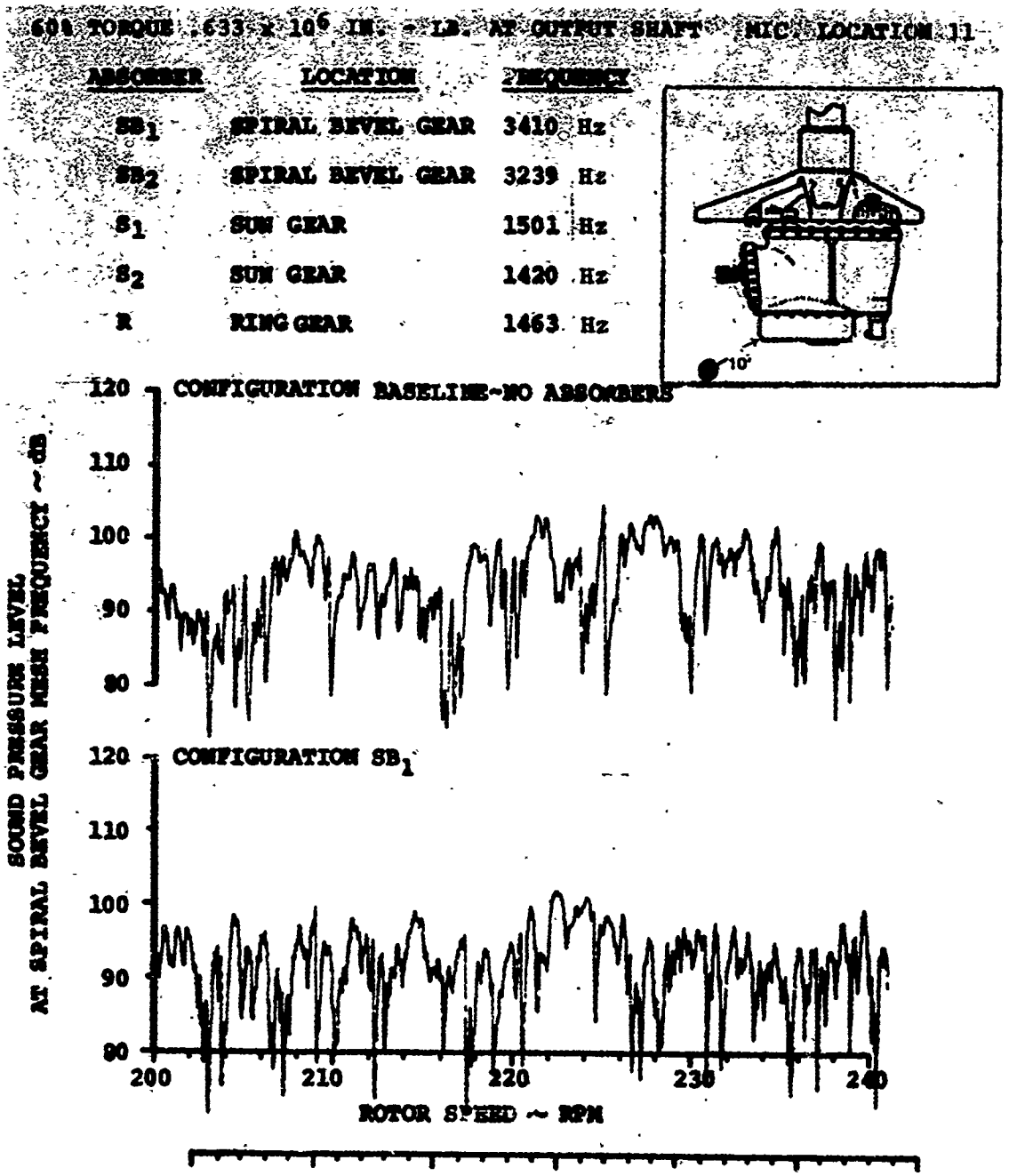

Figure 71. Spiral Bevel Sweep Data, Mic. Location 11, Torque 60%.

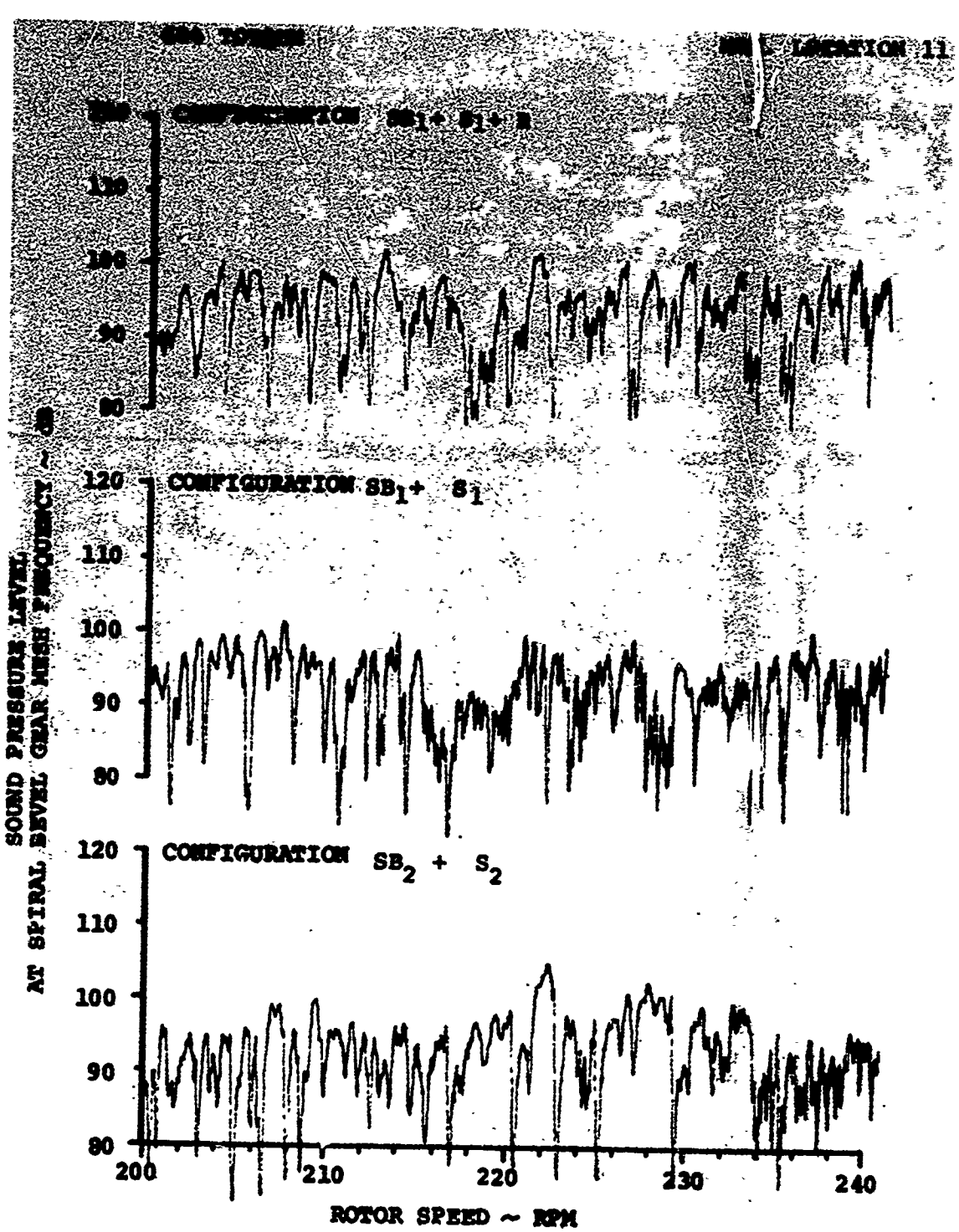

Figure 71. (Continued)

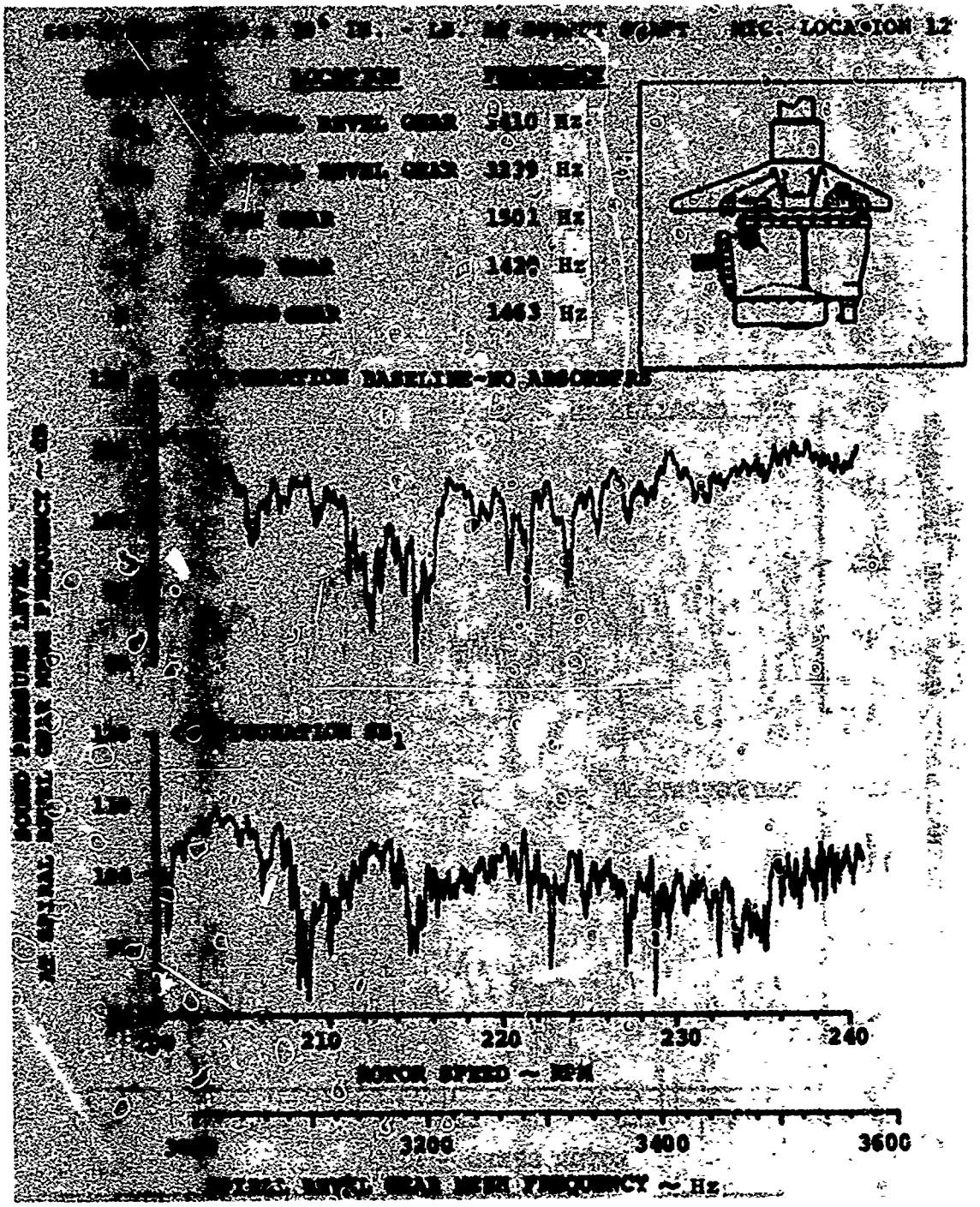

Figure 72. Spiral Bevel Sweep Data, Mic. Location 12, Torque 60%.

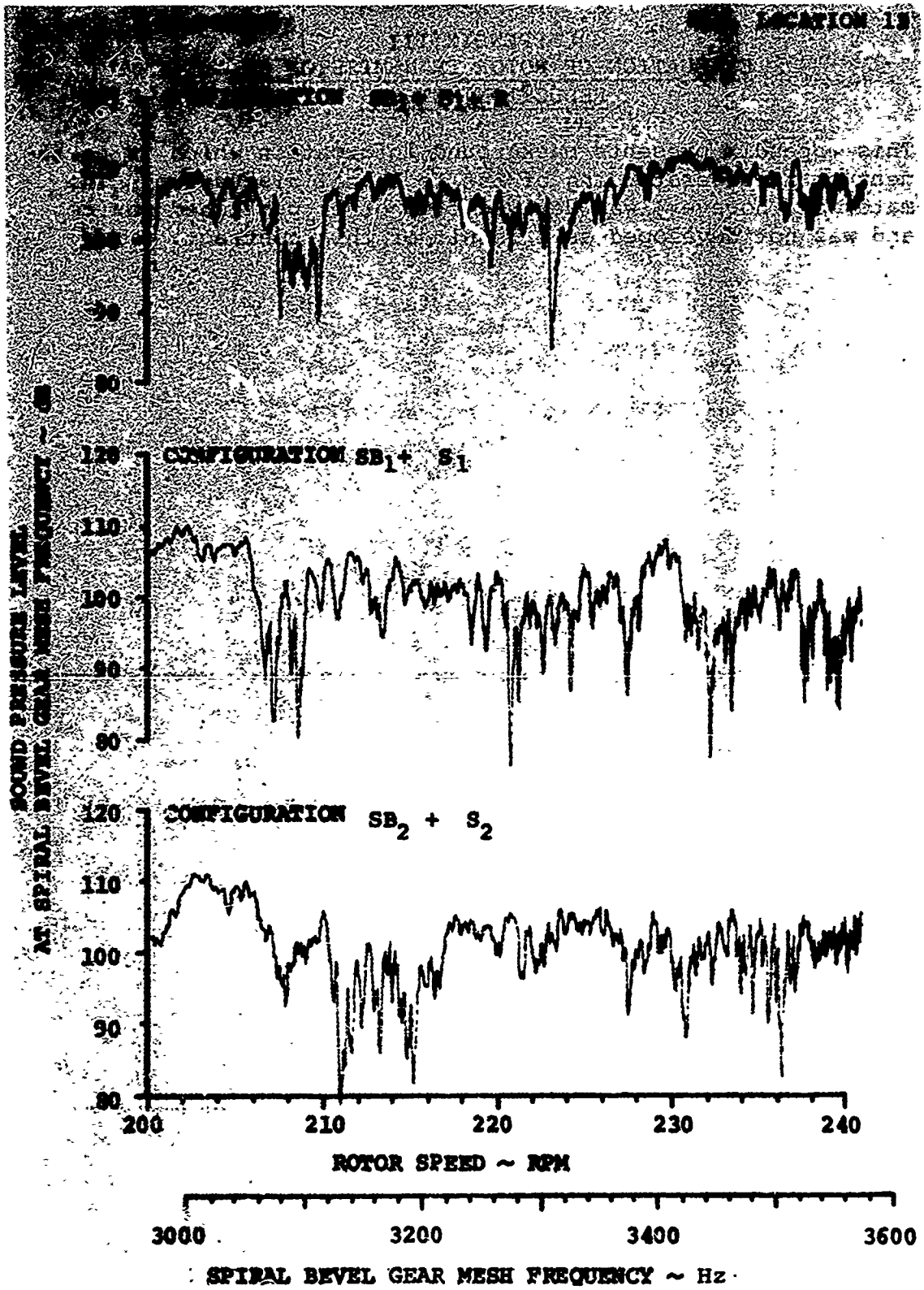

Figure 72. (Continued)

APPENDIX III
EVALUATION OF ROTOR TRANSMISSION SOUND REDUCTION METHODS

This appendix presents background information which is pertinent to an understanding of the technical discussion. The material, however, was derived from other published sources and was not developed as a result of this contract.

The efficient reduction of aircraft interior noise in terms of weight and serviceability of the treatment employed is dependent on an understanding of how noise is generated and then how it propagates to the ear of a person within the cabin. Conventional methods for reducing cabin noise have relied upon soft or limp blankets fastened to frames and bulkheads as a total acoustical treatment; if even a small part of this treatment is removed for inspection or for equipment cooling purposes, a substantial part of the acoustic integrity of the treatment is lost. Because of the high sound levels generated by the rotor drive system components, particularly the rotor transmissions and combining gearboxes, removal of any of the critical blankets means that crew members or passengers lose much of the protection that the treatment was designed to afford them. In view of the inevitable requirements for occasional or continuous blanket removal in an operational helicopter, it is apparent that substantial amounts of the noise reduction should be provided by elements other than cabin blankets, either by direct reduction of source levels, tightly fitting acoustic enclosures at the gearboxes, acoustical attenuation applied directly to the cases, or other procedures for achieving losses in noise transmission such as isolation from structure and structural damping. This section contains a discussion of the propagation of rotor transmission noise beginning at the surface of the case and how it can be attenuated to achieve desired sound levels.

NOISE PATHS

Rotor transmission sound propagation for a CH-47 helicopter is shown in Figure 73 to illustrate the paths which the noise may take in reaching the ear of an observer within the cabin (similar paths could also be drawn for any other part of the cabin, as well as the cockpit). An important first consideration in the reduction of interior noise is the treatment of noise at the point where it is generated; i.e., gear vibration absorbers (A) or other means for reducing gear excitation forces (several such methods have been presented in other sections of this report). Beginning with the acoustic energy at the gearbox, note that there are two major paths which the noise takes: direct airborne sound radiation (B) and radiation which is transmitted through the aircraft structure beginning at the mounting points of the gearbox (C). The direct airborne radiation shown in Figure 73 can be attenuated initially by an acoustic treatment at the rotor transmission (D). Its purpose is to achieve substantial noise reduction over as small a surface area as possible in order to keep treatment weight at a minimum. The effect which acoustical leaks in the enclosure have on the integrity of the treatment cannot be overemphasized, and this will be discussed in greater detail.

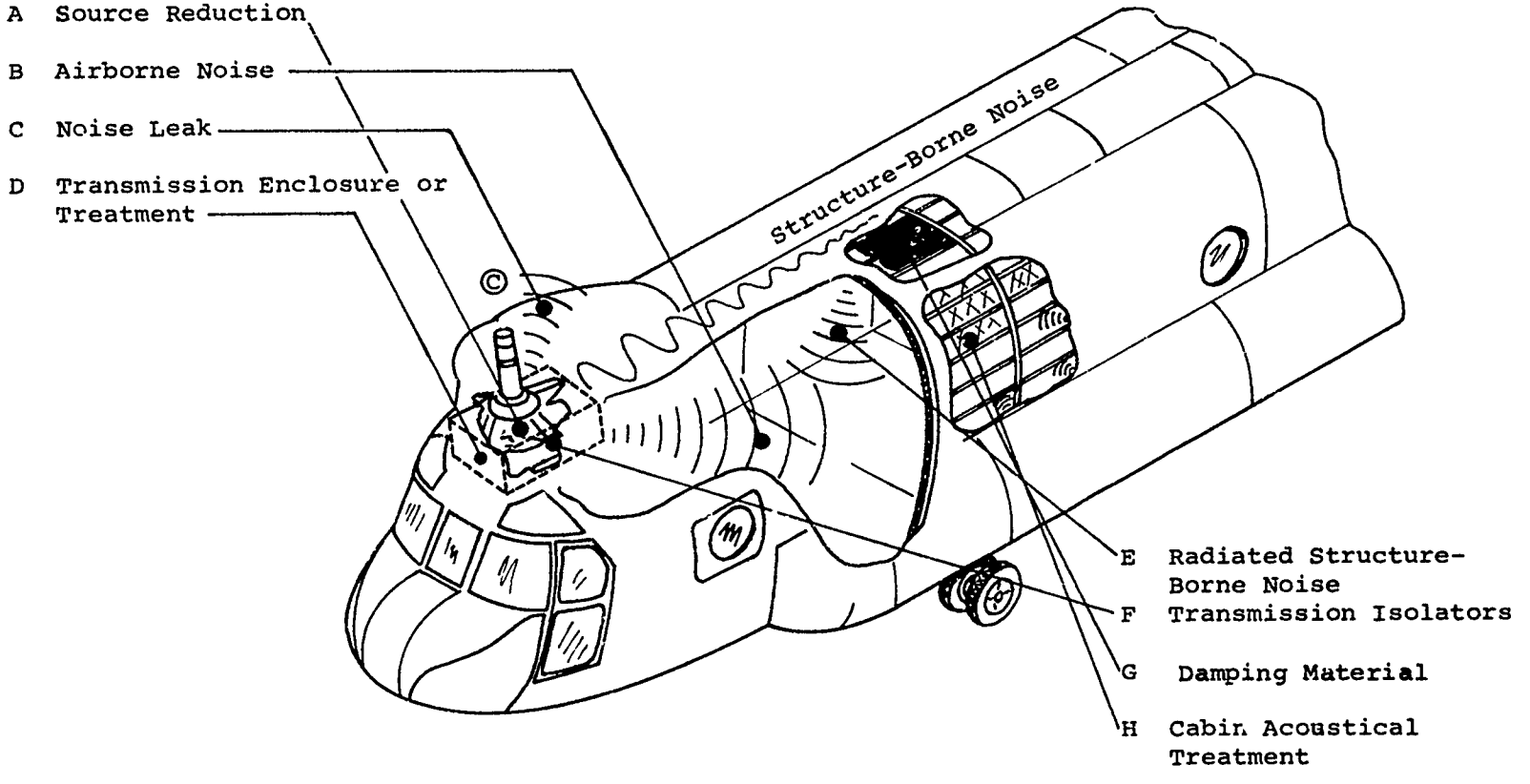

Figure 73. Schematic Of Noise Paths.

Energy transmitted into the airframe (C) and then reradiated by the structure as airborne noise (E) is the second path from the rotor gearbox. This energy can be attenuated by isolating the gearbox from the structure (F), particularly at those frequencies where a substantial portion of the acoustical power is concentrated; i.e., gear mesh frequencies. The vibration of the structure arising from the gearbox excitation can be further attenuated by adding damping to the structure (G). The vibration energy which radiates as airborne noise can be treated by an acoustical treatment which attenuates the level of the wavefront as well as provides sound absorption (H) within the cabin. It will be shown later that without some absorption in the cabin, no noise reduction can be realized.

The method of achieving this noise reduction in terms of using a soft, limp blanket or a hard, durable surfaced composite panel backed with glass fiber, etc., determines the weight associated with the treatment. Estimates for the surface weight of various combinations of acoustical treatments to provide the required noise reduction will be presented and discussed.

DESCRIPTION OF ROTOR TRANSMISSION NOISE PROPAGATION

In order to illustrate the approach to noise control in rotary-wing aircraft, a specific example utilizing the CH-47 helicopter will be used. Figure 74 is a graphic representation of the approach to achieving reductions in interior noise and is a flowchart of the methodology which is presented in this section. Figures 75 (a) and (b) show the noise-reduction requirements for the CH-47 in terms of both airborne and structure-borne noise levels. Measurements were made in an untreated CH-47. Airborne noise was recorded in a diffuse sound field as noted by the similarity of noise levels at Stations 140 and 300. Structure-borne noise measurements were made using a microphone inside a small enclosure which had high transmission loss and absorption properties, and one open side. This open side was placed against the skin panels to obtain a measure of the noise radiating from skin only, while blocking all other noise sources. The success of achieving only skin-radiated noise by this method is dependent, of course, on the ability to shield the microphone from the airborne-radiated noise. Because the enclosure was not large (dimensions were of the order of 1 foot), measured data are presented only at frequencies of 500 Hz and above, and this is adequate for transmission noise. In general, the contribution of the structure-borne noise at these two locations is not large relative to the airborne level.

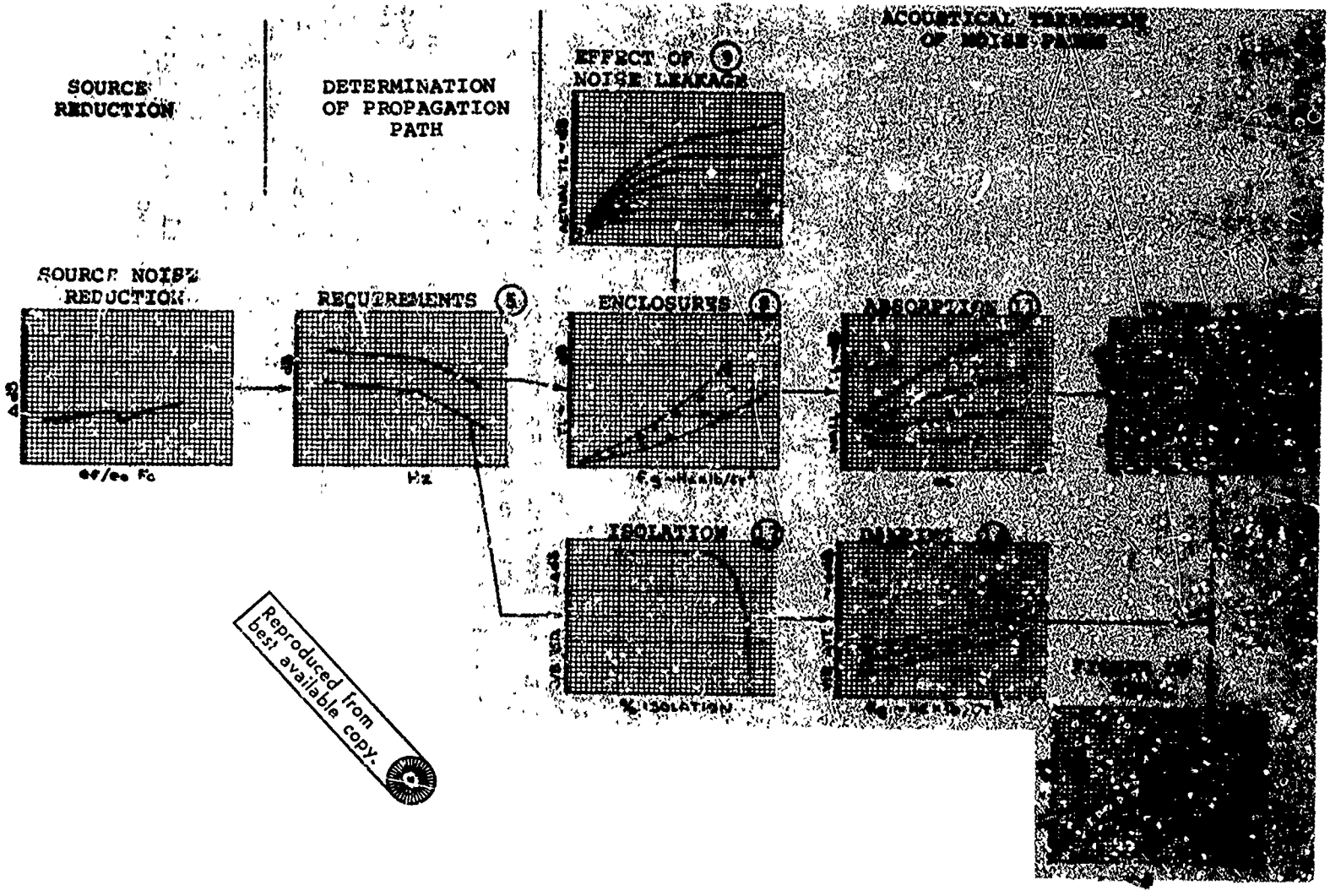

Figure 74. Interior Noise Treatment Flow Diagram.

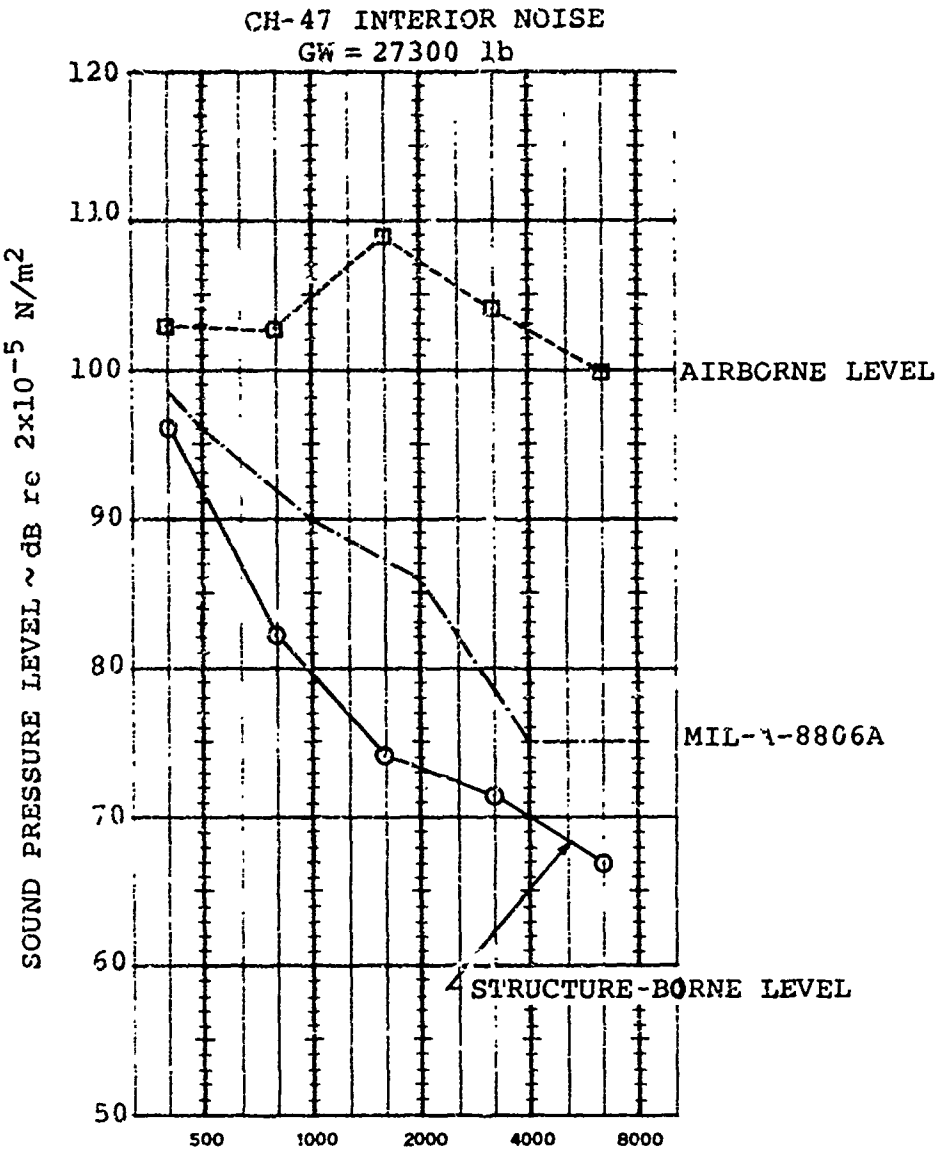

(a) Sta 140

Figure 75. Airborne and Structure-Borne Noise Requirements.

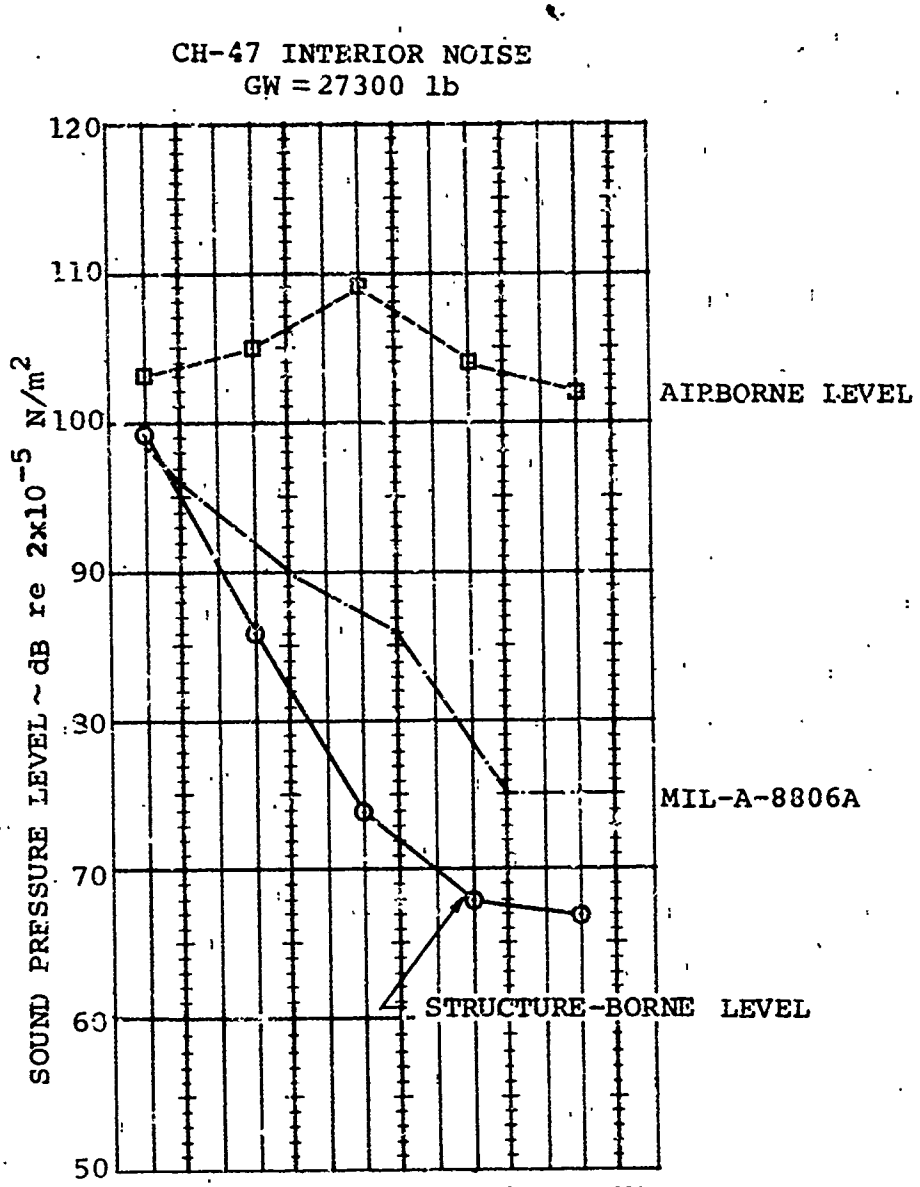

(b) Sta 300

Figure 75. (Continued)

Source Reduction

Reference 2 develops a relationship for sound levels generated by the mechanical energy cycled through the teeth of a meshed set of gears,

$$L = 10 \log \frac{4.94 \times 10^4 (\alpha\beta)}{r^2} f\sum e_o F_o$$

To reduce sound levels, a reduction in the total cycled mechanical energy is required, and a reduction in the energy term, eF, to one-half its initial value $\frac{eF}{e_o F_o} = 0.5$ achieves a 3 dB reduction in sound level. Since there are many sets of gears meshing concurrently in the transmission, the energy ratio in each set must be reduced similarly in order to achieve an overall noise reduction of the entire transmission of 3 dB. Substantial reductions in this energy term are required before a significant noise reduction is realized.

That portion of the mechanical energy which propagates from the transmission after any source noise reduction takes place, then, radiates in two basic paths: airborne and structure-borne. In the CH-47, airborne radiation (as shown in Figure 75) contributes to a greater extent to the noise in the cabin than does structure-borne radiation. This path will be discussed first.

Airborne Radiation

Transmission Case Attenuation

As noted earlier in the discussion, acoustical enclosures of the rotor transmission are thought to be very efficient methods for controlling cabin noise levels since the surface area can be very small relative to the surface area which would be required if the entire cabin had to be treated at the same surface weight density. The drawback of the enclosure is that rotor transmissions generally have a myriad of mechanical shafts and linkages, hydraulic and electrical connections, and accessories which require substantial clearance. However, it is this same clearance which creates "leakage" in the acoustical enclosure which tends to void the effectiveness of the enclosure. Figure 76, for example, illustrates the sound transmission loss achievable with enclosures which are totally sealed around the gearbox and which have no acoustical leakage. In excess of 40 db TL is achievable in the highest region of the frequency/surface weight product.

While an enclosure of the type described has never been fabricated, and therefore no data exists on the minimum amount of leakage which can be achieved, an estimated 5% of the total

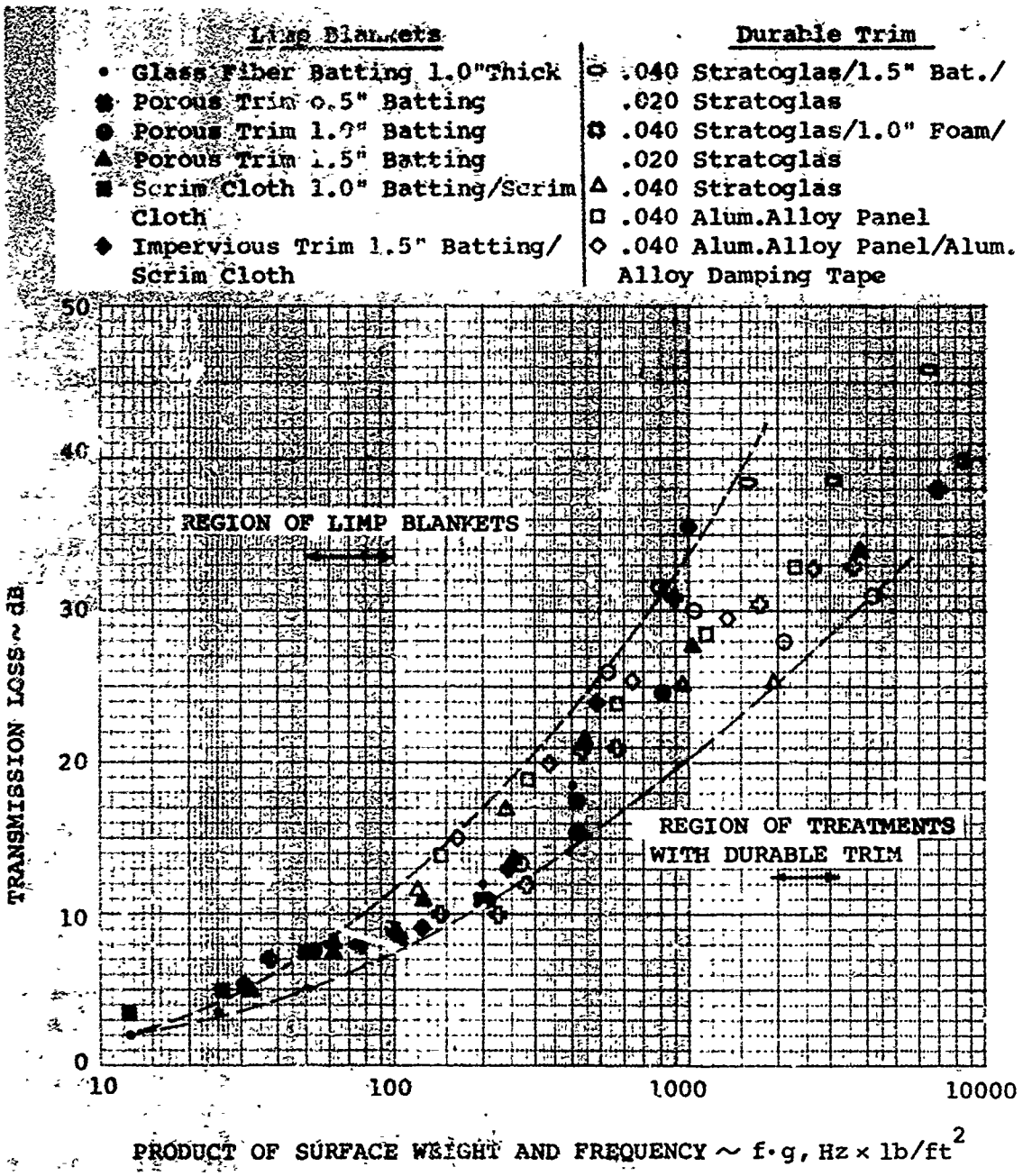

Figure 76. Effect of Transmission Enclosures on Source Attenuation.

surface area may be required to provide the necessary clearance for transmission operation. Figure 77 shows that the attenuation actually achieved for a potential transmission loss of 40 dB and a 95% coverage enclosure (5% leakage area) is on the order of 13-15 dB, rather than the total potential of 40 dB. The relationship plotted in Figure 77 would also indicate that 13-14 dB can be achieved as well with an enclosure whose potential noise reduction is only 20-25 dB. A reduction of 13-14 dB, in itself, would not be sufficient to achieve the requirements for acoustical noise levels in the CH-47; thus additional treatment of the cabin is required.

Substantial improvements in the effective coverage area could be obtained using another concept in transmission noise control involving the application of noise control materials directly to the case itself, either applied externally or combined with the case structure as a sandwich composite. The acoustic losses of the gearbox wall would be increased and the effective leakage area significantly reduced. Materials which have high damping and sound transmission loss, such as energy-absorbing polymers, should be investigated for this purpose.

Noise reduction in excess of that which can be obtained at the transmission requires a general treatment of the cabin which (1) provides the additional sound transmission loss and (2) provides sufficient absorption so that the maximum noise reduction is derived from the transmission loss available. The relationship between transmission loss and sound absorption of the acoustical treatment will be discussed in the following sections.

Cabin Acoustical Treatment

The remaining noise reduction must be obtained from a general cabin soundproofing designed to produce adequate transmission loss (TL) in the frequency ranges of interest. Figure 78 illustrates how this TL may be obtained. The curve for each frequency represents the maximum TL for a given surface weight of the material. Details of the derivation of these curves can be found in Reference 3. The amount of noise reduction which can be derived is a function of both the acoustical absorption and the transmission loss of the treatment. This is illustrated in Figure 79. Note that regardless of the attenuation of the cabin wall, when absorption coefficients approach zero, sound level reductions remain very small, and that only when the absorption coefficients are unity does the noise reduction become equal to the total available attenuation of the cabin wall. It is for this reason that the bare aircraft structure which is highly reflective must be modified to provide substantial acoustical absorption, such that required amounts of noise reduction within the aircraft can be obtained.

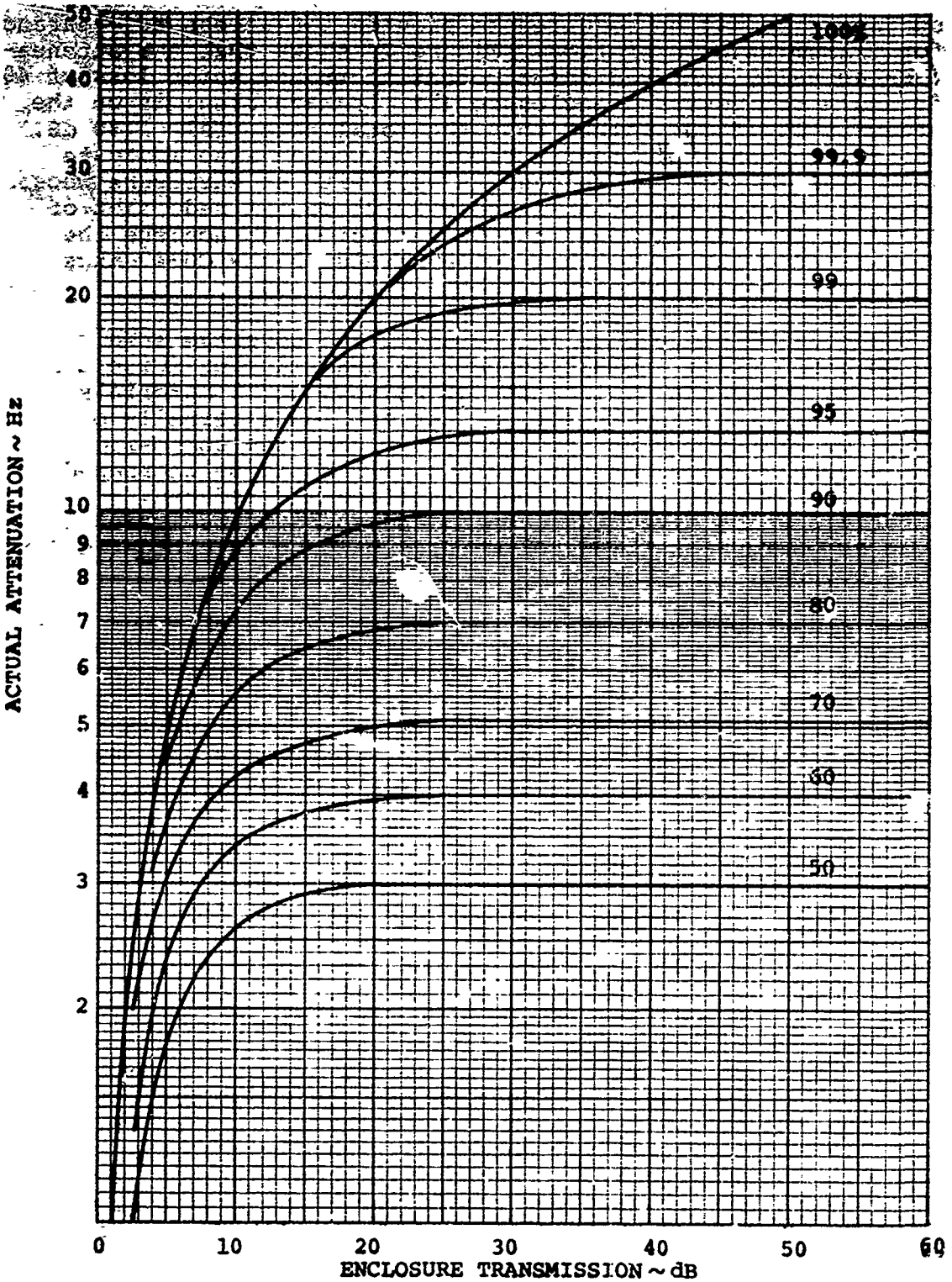

Figure 77. Effect of Enclosure Leakage on Potential Noise Reduction.

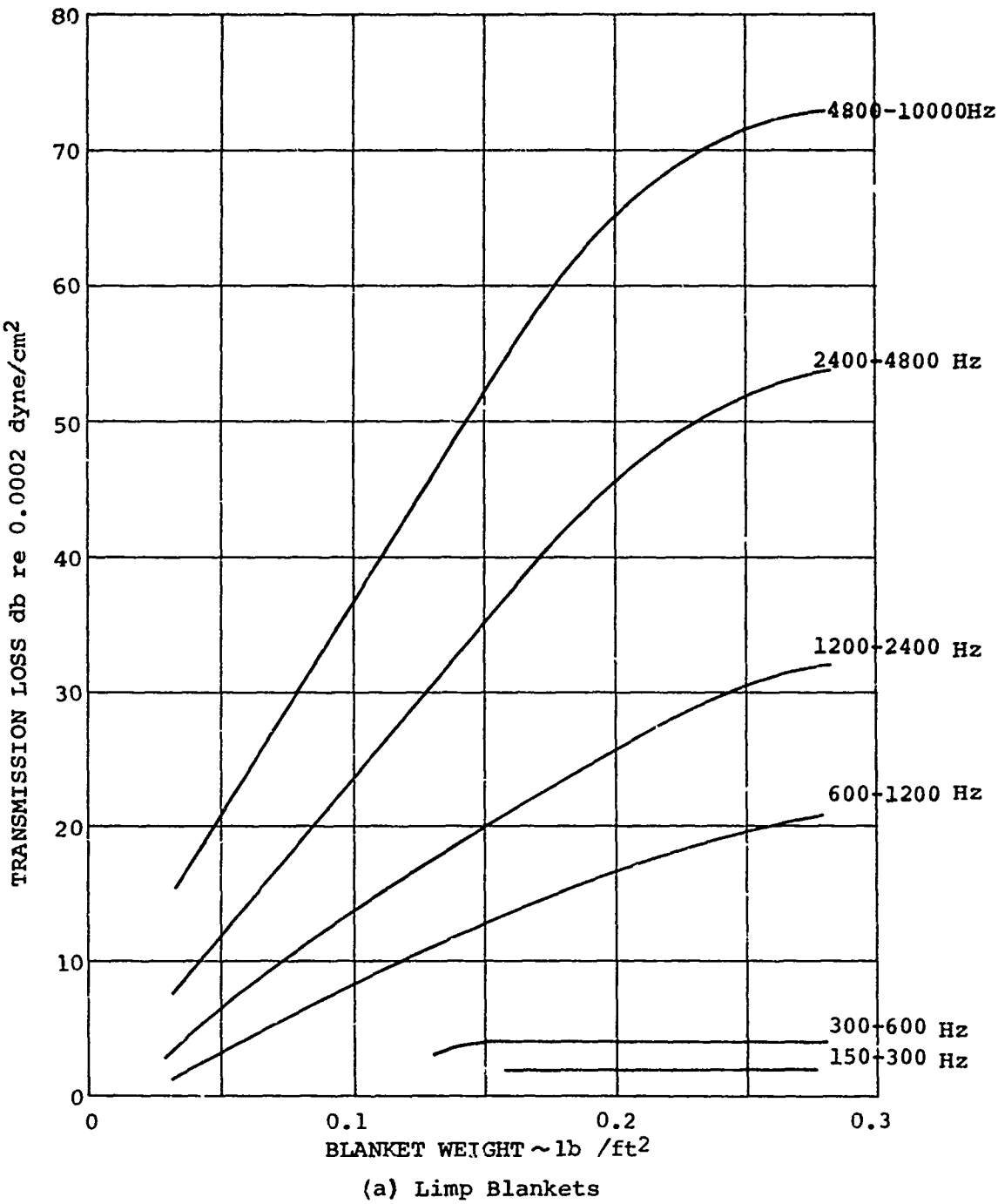

(a) Limp Blankets

Figure 78. Transmission Loss Curves for Acoustical Materials.

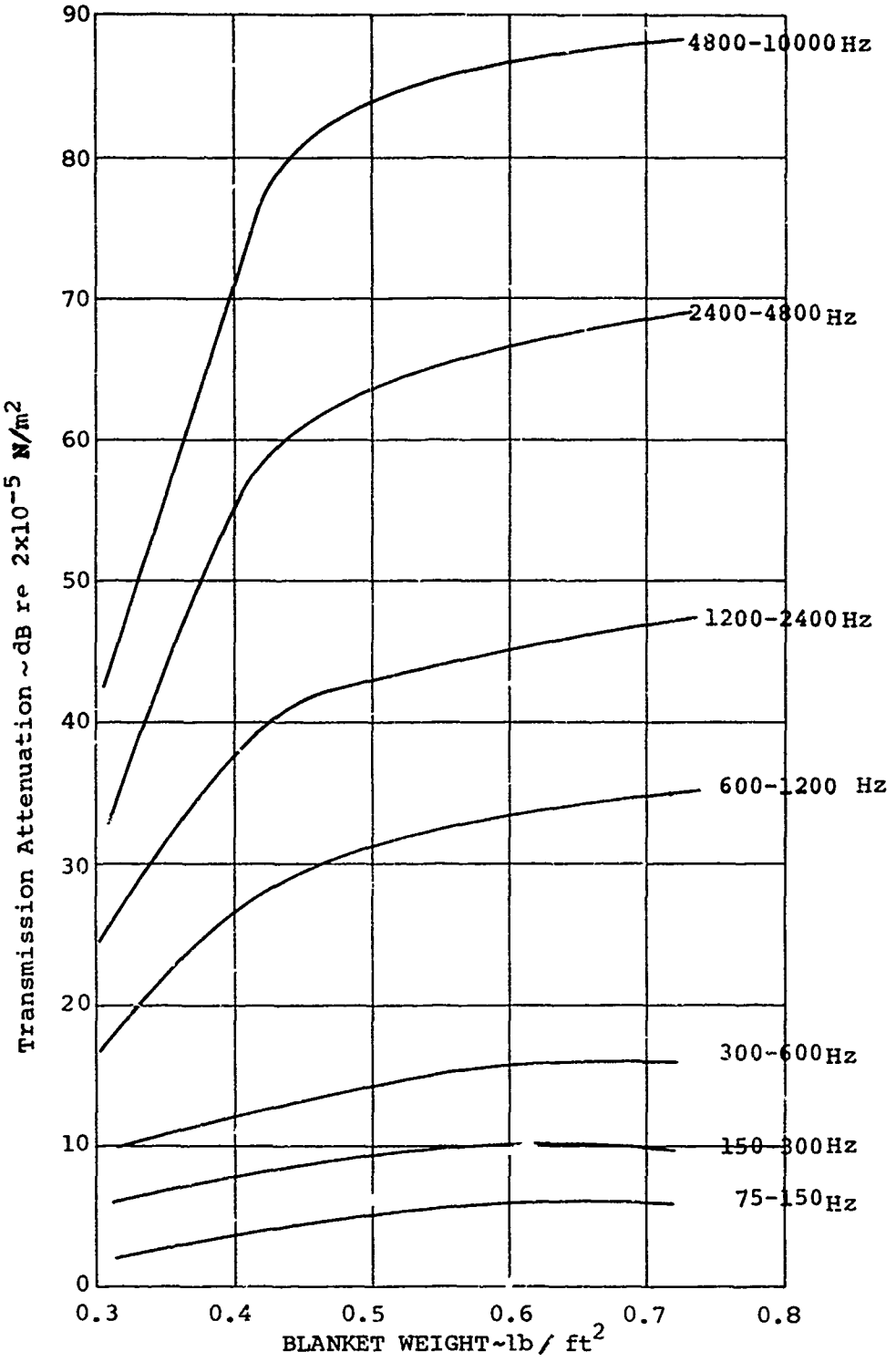

(b) Rigid Panels

Figure 78. (Continued)

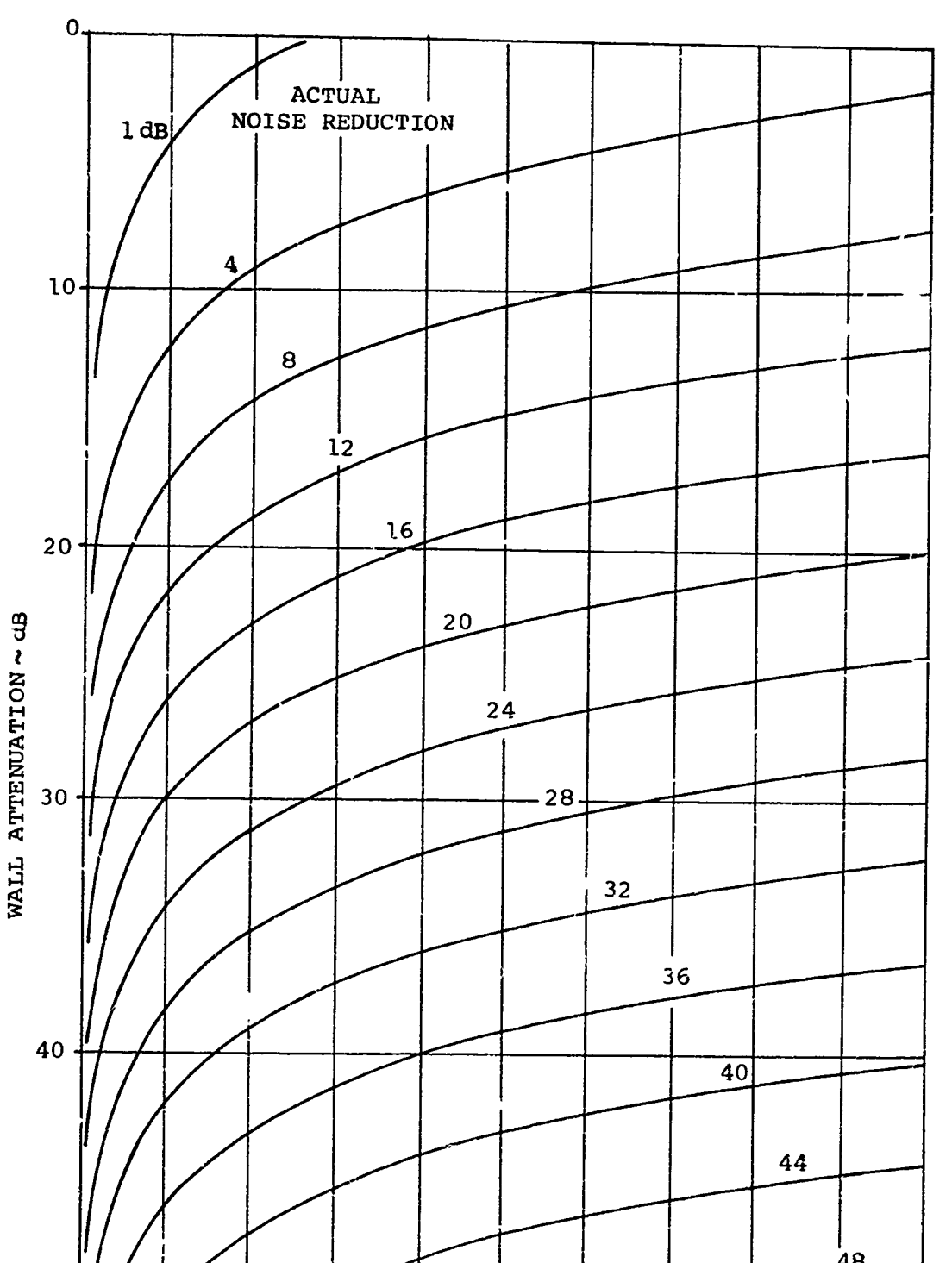

Figure 79. Reduction of Noise in Enclosed Spaces.

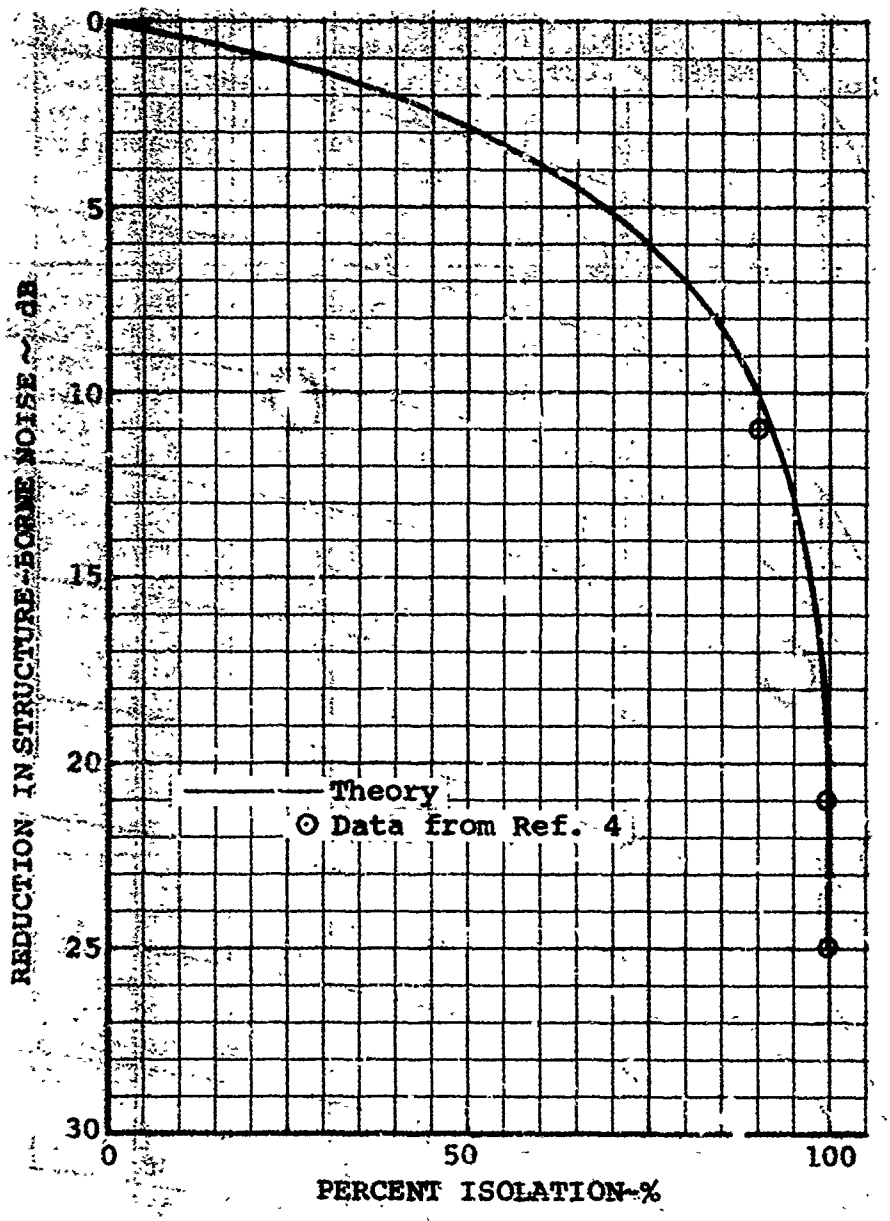

Figure 80. Effect of Structural Isolation on Transmitted Noise

Structure-Borne Noise

The second major path which acoustical energy takes in transmission from the gearboxes to a person's ear is that which radiates as vibration throughout the structure, subsequently to be converted to noise as the motion of the structure couples to the adjacent air. Any reduction in amplitude of the structural noise which can be afforded, either by isolation of the energy source from the airframe to which it is attached or by damping of the structural vibratory loading by materials which absorb energy (for example, constrained layer foils with viscoelastic compounds or unconstrained damping compounds), will reduce the sound amplitude radiated from the airframe and skin panels. Vibration absorbers, either active or passive, or isolators which are tuned to the desired frequency range will also reduce sound amplitudes. Figure 80 illustrates the theoretical effect of isolation of an energy source, such as a rotor transmission, on the potential noise reradiated from the surrounding structure. Although large-magnitude vibration isolation appears attractive, Figure 75 illustrates the relative importance which structure-borne noise may exhibit in generating cabin noise, and it is desirable to have an understanding of the relative contribution of airborne and structure-borne noise prior to commitment to specific vibration isolation requirements.

Damping

Damping of the airframe can be an additional means for achieving reduction of the cabin noise and may provide an effective means for reducing vibration amplitude when the structure is at or near a resonance. Figure 81 illustrates the importance of damped structures particularly at high frequencies. The data were assembled from tests on helicopter structure using constrained layer, viscoelastic damping tape with one, two, and four layers covering 12.5%, 50%, and 100% of the panel area. Figure 82 shows the attenuation of aircraft structure as a function of frequency and was obtained from two aircraft structures: the CH-21 and the CH-46. The CH-21 data were taken by Bolt, Beranek and Newman and reported to Boeing-Vertol[4], and the CH-46 data were obtained as part of a Boeing-Vertol IR&D program.[5] Data trends are similar over the range of frequencies tested. However, the CH-21 data show a marked reduction in the structural attenuation of 8 kHz apparently due to the characteristic of that airframe. If the frequencies associated with the noise radiating from the structure are high or the structure is not near a resonance, a general acoustical treatment may provide a more effective method for achieving noise reduction in the cabin.

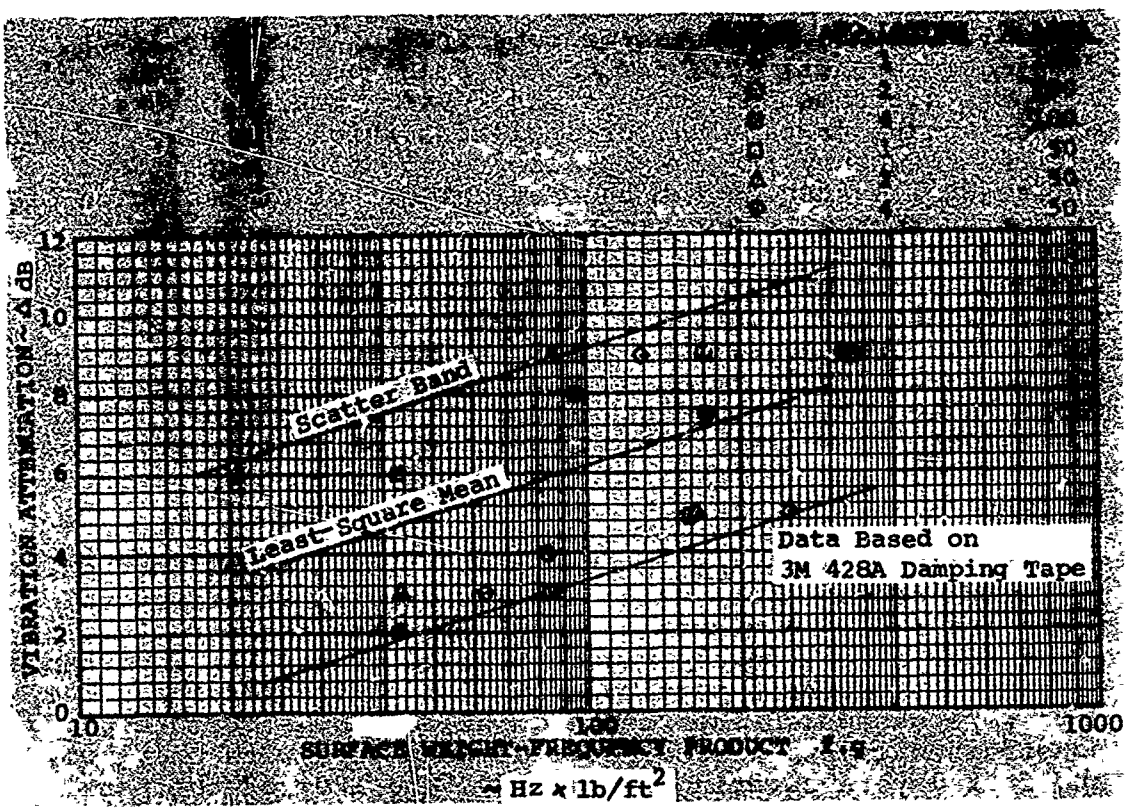

Figure 81. Effect of Damping on Structure-Borne Noise.

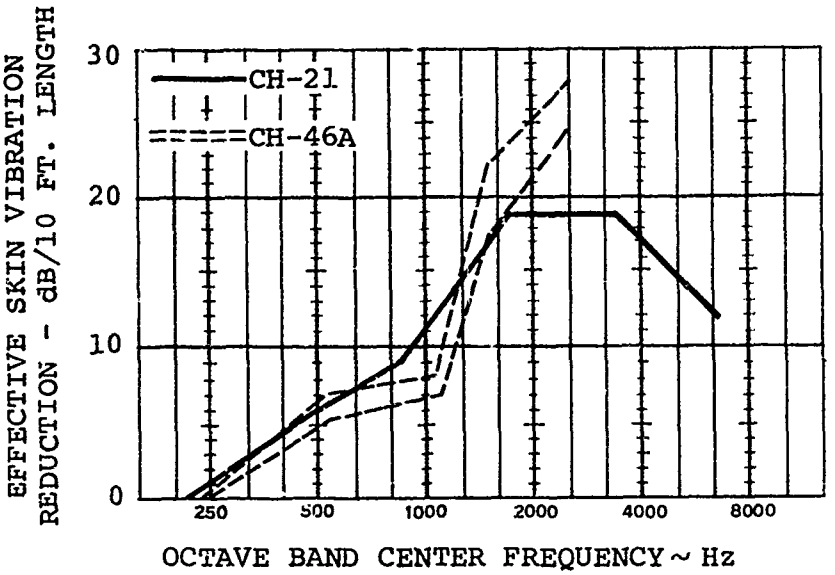

Figure 82. Skin Panel Vibration Attenuation.

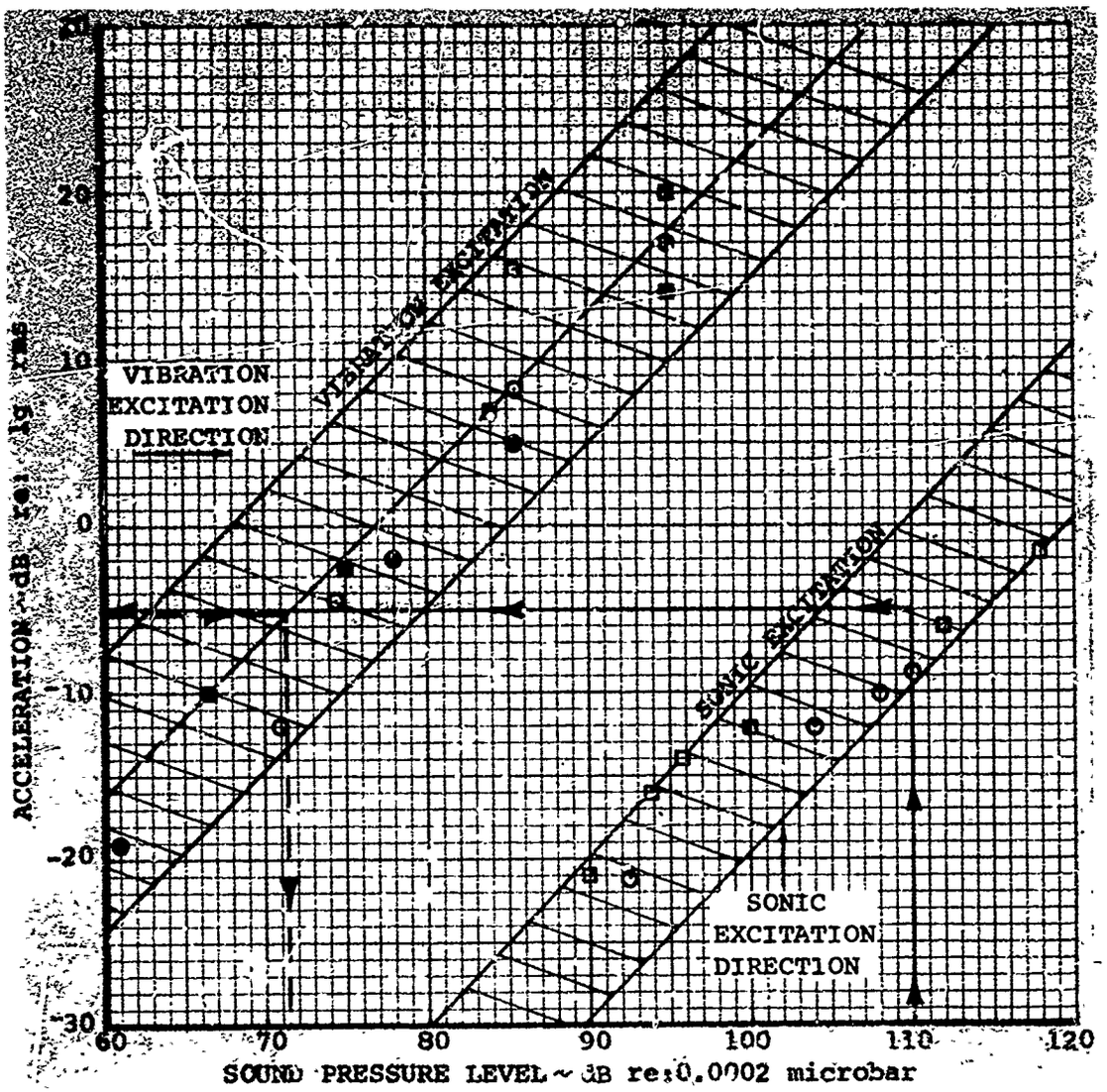

Figure 83. Generation of Noise by Reradiation of Induced Structure-Borne Vibration.

Structure-Borne Noise Due to Airborne Excitation

A third path which gearbox noise takes in propagating to a point within the cabin is that which is initially airborne radiation impinging on the structure and then reradiating as airborne noise. However, Figure 83 shows that this path does not materially contribute to the sound within the cabin. Note that a sound level of 110 dB impinging on a section of fuselage induces a vibration level of -5 db, which then reradiates at a sound level of 71 dB. Figure 83 has been derived from programs on a CH-46 fuselage which measured vibration induced in the sidewall by sonic excitation, and measurements of noise radiated by the sidewall generated by vibration of the structure. The midpoint of the data envelope was used to illustrate the example.

2.3 FIGURE OF MERIT

In a concern for minimum weight, helicopter designers pursue efficiency in all areas of aircraft design. Not the least of these is the weight of material used for soundproofing. To express this efficiency in mathematical terms, several factors must be considered. As early as 1947, Nichols et al[6], suggested a merit factor for acoustical treatments which was defined as

$$n_5/W = \text{Merit Factor}$$

where n_5 = measured attenuation (db) by which soundproofing material or structure exceeds that of a single panel with the same surface density

W = surface density of the total acoustical treatment

This concept has been extended to include all frequency bands of noise, as well as a measure of the acoustical absorption of the soundproofing treatment, and is presented here. It is also desirable to include in the figure of merit a term to describe the durability of the surface of the soundproofing treatment in terms of its serviceability, wear resistance, etc. However, it is difficult to assign a value to this quantity unless it is in terms of abrasion resistance as defined by the method of Reference 7. Because of this inability to express mathematically the durability of a treatment, the figure of merit for acoustical treatments has not included such a term but is defined as

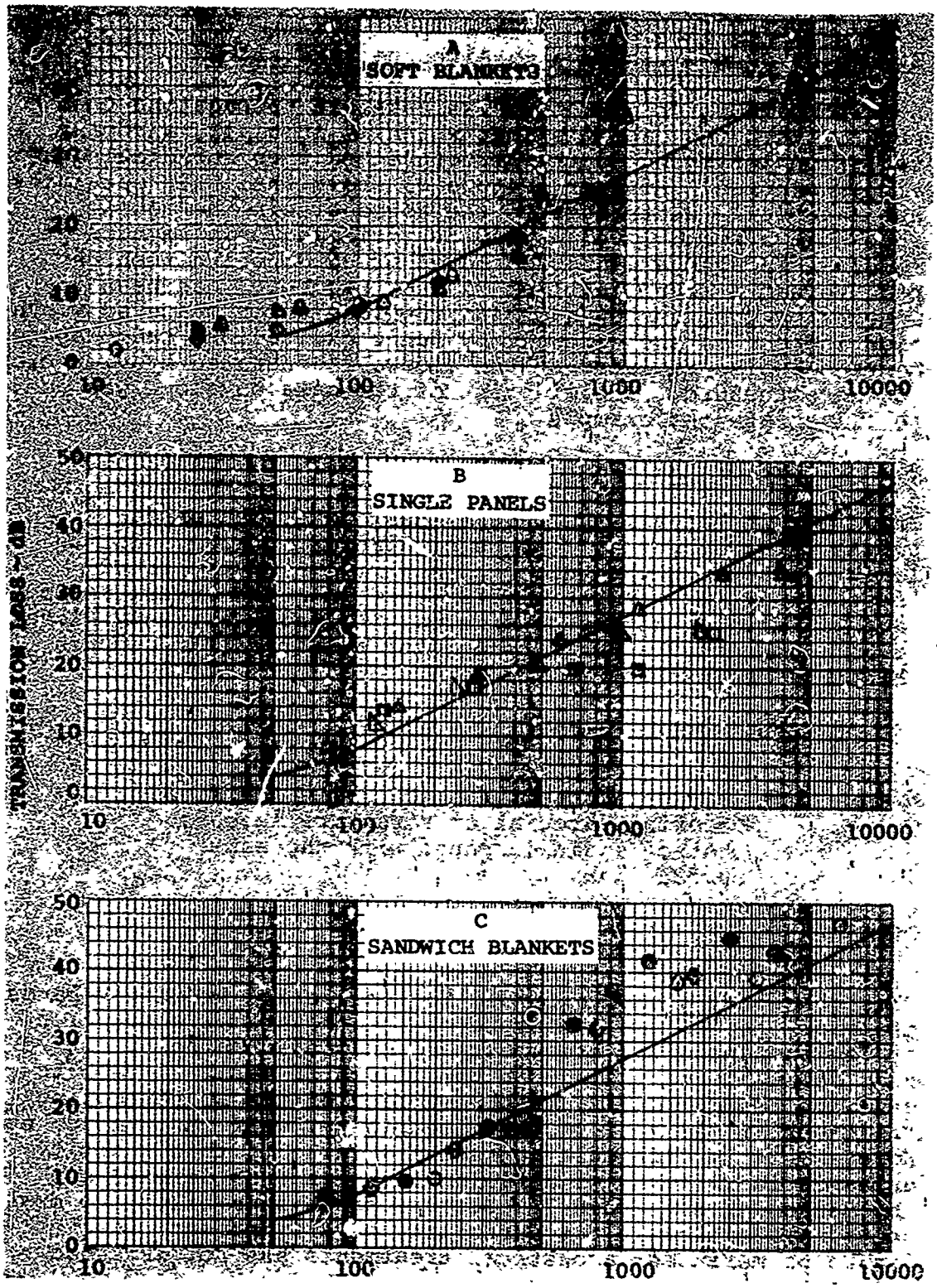

Figure 84. Acoustical Treatment TL Compared With Mass Law.

$$(FM)_{ac} = \frac{\sum_{i=1}^{m} \eta_i}{m} \quad \frac{NRC}{W}$$

where η_i = the variance in the i in frequency band relative to the mass law attenuation for a limp panel of the same surface weight and frequency

m = number of frequency bands

W = surface weight of the treatment, lb/ft^2

NRC = noise reduction coefficient - the average of the absorption coefficients at 500, 1000, 2000, and 4000 Hz.

Several materials evaluated in the Reference 4 program have been examined in terms of this acoustical figure of merit and are tabulated in the following table. Ten samples were used in the evaluation of the figure of merit representing limp blankets, rigid panels, and sandwich composites. The materials which display large positive values of the $(FM)_{ac}$ represent the most acoustically efficient cabin noise treatment since the large values are derived from sound transmission loss characteristics which are consistently better than mass law TL (see Figure 84 as well as noise reduction coefficients which are relatively large; for example, NRC > 0.60). Negative values of the $(FM)_{ac}$ imply sound transmission loss values which are less than those achievable by mass law capability alone. An interesting acoustical material which has already had widespread application to Boeing commercial airplanes is the tuned honeycomb resonator panel. The honeycomb core is tuned as a Helmholtz resonator to a broad range of frequencies and has good sound absorption properties combined with a durable surface. As shown in the table, it has an attractively large figure of merit. As noted previously, the $(FM)_{ac}$ does not include a weighting factor for surface durability, which would show it to be a desirable material for acoustical treatment of military aircraft.

ACOUSTICAL FIGURE OF MERIT						
Sample*	NRC-Noise Reduction Coefficient	Surface Weight (lb/ft^2)	Σn_i i=4 (dB)	$\Sigma n_{i/m}$ (dB)	NRC/W (ft^2/lb)	Figure of Merit $(FM)_{ac}=(\Sigma n_i/m)(NRC/W)$ ($dB.ft^2/lb$)
Limp Blankets						
1" Glass Fiber Batting	0.85	0.050	-1.0	-.167	17.0	-2.85
Porous Trim 1.0" Batting 2 oz/yd^2 Backing	0.60	0.102	-1.0	-.167	5.85	-0.98
Impervious Trim 1.5" Batting Scrim Cloth	0.40	0.124	+15.	+2.5	3.23	+8.1
40 oz/yd^2 Lead Vinyl	0.20	0.278	-17.	-2.85	0.72	-2.04
Sandwiched Materials						
Blanket A** 20 oz/yd^2 Leaded Vinyl Blanket B***	0.85	0.316	+31.	+5.15	2.7	+13.9
Blanket A** 20 oz/yd^2 Leaded Vinyl Blanket B*** 20 oz/yd^2 Leaded Vinyl	0.85	0.466	+19.	+3.16	1.82	+5.75
.040 Stratoglas Blanket B*** .020 Stratoglas	0.20	0.795	+13.	+2.16	0.25	+0.54

ACOUSTICAL FIGURE OF MERIT (continued)

Sample	Noise Reduction Coefficient	Surface Weight (lb/ft^2)	Σ_{n_i} i=4 (dB)	$\Sigma_{n_i/m}$ (dB)	NRC/W (ft^2/lb)	Figure of Merit $(FM)_{ac}=(\Sigma_{n_i}/m)(NRC/W)$ ($dB.ft^2/lb$)
Single Rigid Panels						
0.040 Stratoglas	0.20	0.480	-10.5	-1.75	0.42	-0.73
0.040 Aluminum Alloy Panel	0.05	0.570	+3.5	+0.58	0.087	+0.05
1" Honeycomb Resonator Panel	0.85	0.50		+5.8	1.7	+ 9.85

*Materials listed in layers from interior surface to aircraft structure

**Blanket A, Trim: Porous (MIL-C-7514B) Type III 5.5 oz/yd^2
Vinyl-coated glass cloth
Batting: Glass fiber quilted (+.5 inch thick)
Septum: Lead vinyl, 20 oz/yd^2
Batting: Glass fiber quilted (1.5 inch thick)

***Blanket B, Same as Blanket A but no porous trim cloth

APPENDIX IV
TEST INSTRUMENTATION

This appendix specifies the instrumentation used for data acquisition and analysis.

Instrumentation

The following types of instrumentation were used on this program.

Accelerometers - Endevco Type 222B

Accelerometer Amplifiers - Unholta Dickie "Dial-a-Gain" Type 610RM6-3

Microphone Cartridges - Bruel & Kjaer Type 4131

Microphone Cathode Followers - Bruel & Kjaer Type 2613

Microphone Power Supplies - Bruel & Kjaer Type 2801

Tape Recorder - Ampex Type AR-200, 1", WBFM

Spectrum Analyzer - Federal Scientific "Ubiquitious" Type UA-6.

Calibration curves for one typical accelerometer system and one typical microphone system are presented in Figure 17 of the text. These calibrations were done just prior to the test program. Since the accelerometers were mounted on cubical blocks of aluminum, all mount natural frequencies were much higher than the range of interest and, for all practical purposes, unmeasurable.

The data was analyzed on a Federal Scientific "Ubiquitous" Spectrum Analyzer, Model UA-6. Figure 85 presents the filter characteristic. All data was analyzed over a range of 0-5000 Hz with a bandwidth (β) of 10 Hz.

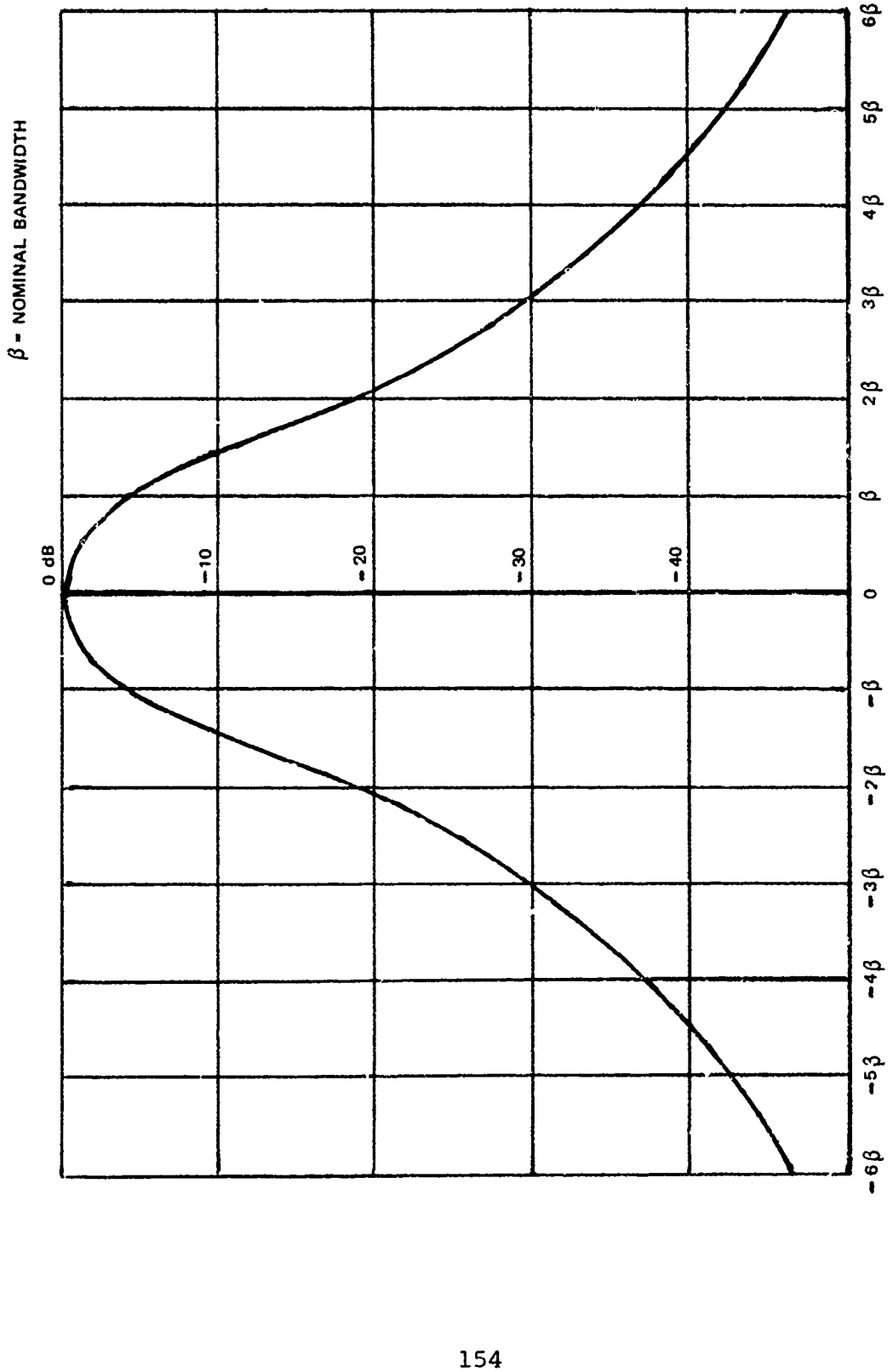

Figure 85. Filter Selectivity.